NATURALITY IN HEEGAARD FLOER HOMOLOGY

by

MICHAEL GARTNER

A DISSERTATION

Presented to the Department of Mathematics
and the Graduate School of the University of Oregon
in partial fulfillment of the requirements
for the degree of
Doctor of Philosopy

December 2019

DISSERTATION APPROVAL PAGE

Student: Michael Gartner

Title: Naturality In Heegaard Floer Homology

This dissertation has been accepted and approved in partial fulfillment of the requirements for the Doctor of Philosopy degree in the Department of Mathematics by:

Robert Lipshitz	Chair
Boris Botvinnik	Core Member
Dan Dugger	Core Member
Ben Elias	Core Member
Katya Hokanson	Institutional Representative

and

Kate Mondloch	Interim Vice Provost and Dean of the Graduate School

Original approval signatures are on file with the University of Oregon Graduate School.

Degree awarded December 2019

DISSERTATION ABSTRACT

Michael Gartner

Doctor of Philosopy

Department of Mathematics

December 2019

Title: Naturality In Heegaard Floer Homology

Let Man_* denote the category of closed, connected, oriented and based 3-manifolds, with basepoint preserving diffeomorphisms between them. We show that the Heegaard Floer invariants yield functors

$$HF^\circ : \mathrm{Man}_* \to \mathrm{Trans}(P(\mathbb{Z}[U]\text{-Mod}))$$

to the category of transitive systems in the projectivized category of $\mathbb{Z}[U]$-modules, whose values agree with the Heegaard Floer invariants defined by Ozsváth and Szabó. In doing so, we will see that these projective functors actually come from a transitive system, in the projectivized homotopy category of chain complexes over $\mathbb{Z}[U]$-Mod, associated to each 3-manifold. This extends work of Juhász, Thurston and Zemke, who showed that there are analogous functors

$$HF^\circ : \mathrm{Man}_* \to \mathbb{F}_2[U]\text{-Mod}$$

coming from the Heegaard Floer invariants. We discuss several applications of these naturality results, and use them to introduce and investigate an invariant of nonorientable 3-manifolds coming from Heegaard Floer Homology. This dissertation includes material that has been submitted for publication.

CURRICULUM VITAE

NAME OF AUTHOR: Michael Gartner

GRADUATE AND UNDERGRADUATE SCHOOLS ATTENDED:

University of Oregon, Eugene, OR
University of California San Diego, San Diego, CA
Columbia University, New York, NY

DEGREES AWARDED:

Doctor of Philosopy, Mathematics, 2019, University of Oregon
Master of Science, Physics, 2014, University of California San Diego
Bachelor of Science, Mathematics and Physics, 2012, Columbia University

AREAS OF SPECIAL INTEREST:

Low Dimensional Topology

PROFESSIONAL EXPERIENCE:

Graduate Employee, University of Oregon, 2016-2019

Graduate Employee, University of California San Diego, 2012-2016

ACKNOWLEDGEMENTS

I thank my graduate advisor Robert Lipshitz for his continuous support, kindness, encouragement and assistance, and for teaching me what I know about low dimensional topology. I also thank him for his help in the preparation of this and other manuscripts.

I thank Keegan Boyle, Daniel Copeland, Mike Enciso, Mike Jackson, Mike Klug, Robert Lipshitz, Jeffrey Musyt, Justin Roberts and many others for sharing with me what has always been my favorite aspect of mathematics: learning from and thinking with other people.

I thank my previous graduate advisor Justin Roberts for introducing me to the beauty of topology and knot theory, encouraging me to pursue my interest in topology, and for sharing a wonderful outlook on what mathematics ought to be about.

I thank all of my friends for being wonderful people and sharing their lives with me.

I thank my family Jeanne, Joe and Sarah for providing endless support and encouragement, both in my academic pursuits and in life in general.

I thank Abby for always being there for me and helping me see the positive side of things, for all of her love and support, and for being herself.

For Abby, Jeanne, Joe and Sarah, whose support and love made this possible and worthwhile.

TABLE OF CONTENTS

LIST OF FIGURES

CHAPTER I

INTRODUCTION

1.1. Non Technical Introduction

Let us begin by musing on some of the basic ideas with which topology is concerned. Mathematicians may prefer (and perhaps should be encouraged) to skip this section.

Topology is a field of mathematics concerned with studying spaces and shapes. It shares many features with and has deep relations to the (perhaps more familiar) field of geometry, though it is often concerned with qualities of a space which do not depend on a particular notion of distance. It turns out that many foundational results about spaces of interest to topologists, as well as techniques which have proved to be most useful in studying these spaces, depend strongly on the dimension of the spaces at hand. In many regards there is a sort of phase transition in topology at dimension 4, and the techniques which have proved to be most useful, and certainly most popular, are drastically different in the two regimes. Low dimensional topology is the study of spaces with dimension less than or equal to 4.

One of the central goals of low dimensional topology is to understand a particular class of spaces known as *manifolds*. These are spaces which locally resemble the Euclidean spaces we are familiar with from our waking lives. For example, a thin shoelace can be modeled as a 1 dimensional manifold, since an ant walking along it might be tricked into thinking there are precisely two directions in which it could walk: forward and backward. Such

an ant would see the shoelace as resembling a small portion of a straight, infinite line, i.e. as resembling the 1 dimensional Euclidean space. Of course, a physical string would have some thickness, so it would be reasonable to object that this description is not a perfect model.

As another example, consider the surface of the earth. This could be modeled as a 2 dimensional manifold: an ant walking on its surface would look at the ground immediately surrounding them to see a two dimensional plane resembling the two dimensional Euclidean plane. An astute ant might realize that while they may be convinced that their immediate, local surroundings resemble 2 dimensional Euclidean space, they should not conclude that the entire surface of the earth must also resemble it. This point lies at the heart of the interest in mathematics of the study of manifolds. Manifolds are locally familiar from our everyday experience, and are locally amenable to calculations, but nonetheless can have large scale, nontrivial structure, such as the sphere-like structure of the surface of the earth.

As a final example, the physical space we inhabit seems to be well modeled by a 3 dimensional manifold. Regardless of where you are on earth or in space, locally it seems there is a 3 dimensional Euclidean space of directions in which you can move: front/back, up/down and left/right. Someone might justly argue that in fact time is another independent direction in which we move, so perhaps it is better to say that our space is well modeled by a 4 dimensional manifold. This line of reasoning is one of the first principles of our current understanding of large scale gravity. Some

examples of manifolds and their local structure are displayed in Figure 1 below.

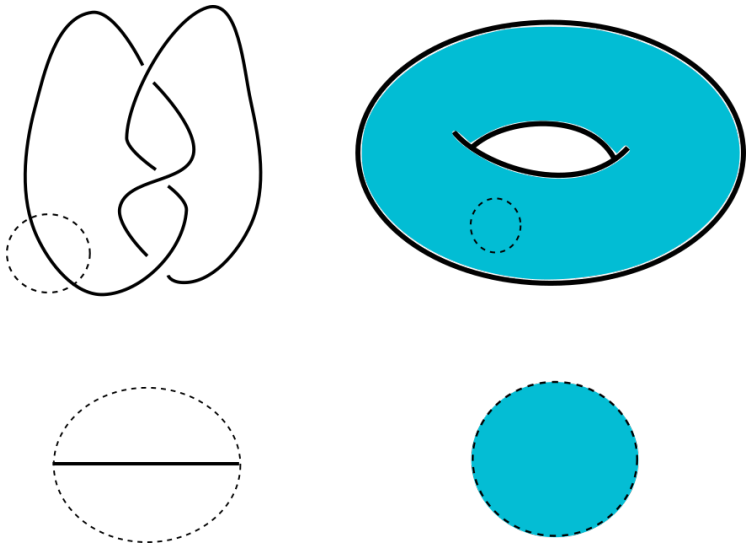

FIGURE 1 An example of a 1-manifold and a 2-manifold. On the top are the spaces in question, along with a local region in each indicated inside the dashed circles. On the bottom are depictions of the Euclidean spaces which model immediate surroundings of the local region.

There are many types of questions about manifolds which are asked and addressed in the study of low dimensional topology. To give a flavor for these questions, here are a few:

1. Can we enumerate or list all manifolds of a given dimension?

2. How can we distinguish different manifolds? (e.g. how can we tell whether the large scale structure of the earth resembles a sphere, a donut, a piece of paper, or none of these? One answer: Fly a spaceship around it and take pictures.)

3. How can we distinguish different manifolds using *intrinsic* information? (e.g. no spaceships, only measurements we can make from on the surface of the earth.)

4. How do spaces interact with other spaces contained within them?

5. How does one do calculus on a manifold?

6. Are there inequivalent ways to do calculus on a given manifold?

To end our discussion and segue into more precise mathematics, we note that one way to address questions 2 and 3 (and often inform many other questions simultaneously) is to come up with an *invariant* of manifolds. This is an assignment of a mathematical object to every manifold which has the property that if two manifolds are the same (i.e. equivalent in an appropriate sense), then the mathematical objects they are assigned are also the same. The most obvious utility of an invariant is in addressing questions 2 and 3: if your invariant assigns two different objects to two manifolds, then the manifolds must also be distinct. In this dissertation, we will for the most part be concerned with the study of a particular invariant of 3 manifolds known as Heegaard Floer Homology. This invariant takes the form of an assignment of an algebraic object to each 3 dimensional manifold, and as we shall discuss in more detail, it has been studied extensively and shown to have deep consequences. In particular, it can be used to address all of the questions mentioned above, as well as many others.

1.2. Mathematical Setting

We now assume background in mathematics and topology, and provide an outline of some context for our main results. The Heegaard Floer invariants associated to closed, oriented 3-manifolds were defined in the work of Ozsváth and Szabó [1]. There it was shown that to each such 3-manifold,

one can associate an isomorphism class of $\mathbb{Z}[U]$-module. Furthermore, cobordisms between 3-manifolds were shown to induce maps between the invariants [2]. However, there was a gap in the proof of the naturality of these maps. Showing that these invariants are natural with respect even to diffeomorphisms is subtle, and involves detailed consideration of the dependence of the invariants on the choices of Heegaard data, basepoints and embeddings of Heegaard diagrams involved in their construction.

These subtleties were studied extensively by Juhász, Thurston and Zemke in [3]. There they explicated a particular type of loop of Heegaard moves, simple handleswaps, which previous work did not preclude from potentially yielding monodromy in the Heegaard Floer invariants. Moves analogous to these simple handleswap moves were previously studied in detail and suggested as possible candidates for loops with monodromy in the work of Sarkar (e.g. in [4]). Through a careful analysis of a space of embedded Heegaard diagrams, Juhász, Thurston and Zemke exhausted all possible monodromies and obstructions to the Heegaard Floer assignments being natural with respect to diffeomorphisms, and were then able to provide a minimal set of requirements which could be checked to verify such naturality. They then checked that these requirements are satisfied for all variants of Heegaard Floer homology with coefficients in $\mathbb{F}_2$. By building on the work in [2] and [3], Zemke established in [5] that the cobordism maps defined in [2] are in fact natural (over $\mathbb{F}_2$) with respect to composition of cobordisms (when the cobordisms are appropriately decorated with graphs).

In this dissertation we explain the necessary modifications that must be made to obtain naturality with respect to diffeomorphisms of all variants

of Heegaard Floer homology, but with coefficients in $\mathbb{Z}$. The most immediate goal of our work is simply to fill a gap in the literature. We hope this will be useful both as a resource for non-experts who aim to understand Heegaard Floer homology itself, and as groundwork which can be used to better understand other invariants associated with Heegaard Floer homology. For example, the contact invariants defined in [6] have proved to be extremely effective in detecting subtle contact properties, and both their definition and many of their applications require the ability to nail down particular elements in the modules HF°, and the ability to effectively compare two such elements in the same module. We also note that the results in [3] and the analogous integral results presented here are necessary steps for establishing naturality of the integral Heegaard Floer invariants with respect to cobordisms.

A secondary goal of our work is to utilize naturality of the Heegaard Floer invariants with respect to diffeomorphisms over $\mathbb{Z}$ to obtain new applications of the invariants. We use our results to extend a construction known as Involutive Heegaard Floer homology to the integral setting, and also use them to introduce and investigate an for nonorientable 3-manifolds arising from Heegaard Floer homology.

1.3. Statement of Main Results

In order to study naturality of many flavors of Heegaard Floer homology and Knot Floer homology simultaneously, Juhász, Thurston and Zemke work with sutured 3-manifolds. They consider a graph $\mathcal{G}$ which encodes the combinatorial structure of a space of sutured Heegaard diagrams

related by certain Heegaard moves. Roughly, the vertices of $\mathcal{G}$ correspond to isotopy diagrams of sutured manifolds, and between any two such isotopy diagrams there are edges which describe whether they are related by any of the standard Heegaard moves, or additionally whether they are related by a diffeomorphism. The graph $\mathcal{G}$ contains many sutured isotopy diagrams which are not relevant to the consideration of closed 3-manifolds, so in considering the closed 3-manifold invariants HF° attention is restricted to a subgraph $\mathcal{G}(\mathcal{S}_{\text{man}})$. This is the full subgraph of $\mathcal{G}$ whose vertices consist only of those isotopy diagrams representing sutured manifolds which can be constructed from a closed 3-manifold in a prescribed way. Since we are only concerned with results regarding closed 3-manifolds in this dissertation, we will minimize the role of sutured manifolds, and phrase our results in terms of a graph which is isomorphic to $\mathcal{G}(\mathcal{S}_{\text{man}})$ which we denote by $\mathcal{G}_{\text{man}}$. This graph has vertices corresponding to isotopy diagrams of closed, pointed 3-manifolds, where the isotopies are required to be supported away from the basepoint. Edges in $\mathcal{G}_{\text{man}}$ correspond to stabilizations, diffeomorphisms and sequences of handleslides.

To study naturality using these graphs, we consider the two notions of a *Heegaard invariant* introduced in [3]. The first, a *weak Heegaard invariant* valued in a category $\mathcal{C}$, is simply a morphism of graphs from $\mathcal{G}_{\text{man}}$ to $\mathcal{C}$ under which all edges in the domain get mapped to isomorphisms. In this language, we can summarize one of the invariance results shown in [1] as stating that the morphisms of graphs

$$HF^\circ : G_{\text{man}} \to \mathcal{C}$$

for $\mathcal{C} = \mathbb{Z}[U]$-Mod or $\mathcal{C} = \mathbb{F}_2[U]$-Mod determined by Heegaard Floer homology are weak Heegaard invariants. The second notion, that of a *strong Heegaard invariant*, serves as a minimal set of conditions which are needed to ensure that a weak Heegaard invariant yields a natural invariant of the underlying 3-manifolds; precisely, the authors show that the image of a strong Heegaard invariant $HF^\circ : G_{\text{man}} \to \mathcal{C}$, when appropriately restricted, forms a transitive system in $\mathcal{C}$. This step occupies a majority of the work in the paper, and none of the results in this step depend on the target category $\mathcal{C}$. The authors then prove that, in the case when $\mathcal{C} = \mathbb{F}_2[U]$-Mod, such a transitive system yields a functor

$$HF^\circ : \text{Man}_* \to \mathbb{F}_2[U]\text{-Mod}.$$

Finally, they establish that $HF^\circ : G_{\text{man}} \to \mathbb{F}_2[U]$-Mod is in fact a strong Heegaard invariant, completing their proof that the invariants HF° yield functors from Man_* to $\mathbb{F}_2[U]$-Mod.

Our main goal here is to establish similar results for $\mathcal{C} = P(\mathbb{Z}[U]\text{-Mod})$, the quotient category obtained from $\mathbb{Z}[U]$-Mod by the relation $f \sim -f$ for all $f \in \text{Hom}_{\mathbb{Z}[U]\text{-Mod}}$. Said simply, we want to show that naturality holds over $\mathbb{Z}$, up to a sign. We will consider a category $\text{Trans}(P(\mathbb{Z}[U]\text{-Mod}))$ of transitive systems in $P(\mathbb{Z}[U]\text{-Mod})$, and our main result will be:

Theorem 1.3.1. *There are functors*

$$\widehat{HF}, HF^-, HF^+, HF^\infty : \mathit{Man}_* \to \mathit{Trans}(P(\mathbb{Z}[U]\text{-}\mathit{Mod}))$$

whose values on a based 3-manifold (Y, z) are isomorphic to the modules defined in [1]. Furthermore, isotopic diffeomorphisms have the same image under HF°.

Remark 1.3.2. The finite rank variant HF_{red} of Heegaard Floer homology defined in [1, Definition 4.7] arises as a suitable quotient (or submodule) of $HF^{\pm}$, and Theorem 1.3.1 implies that this variant also yields a functor $HF_{\mathrm{red}} : \mathrm{Man}_* \to \mathrm{Trans}(P(\mathbb{Z}[U]\text{-Mod}))$.

We will import wholesale the logical structure of [3] used to prove the analog of Theorem 1.3.1 appearing there. It will therefore suffice to show that $HF^\circ : \mathcal{G}_{\mathrm{man}} \to P(\mathbb{Z}[U]\text{-Mod})$ is a strong Heegaard invariant. We will in fact show something slightly stronger. Let $\mathrm{Kom}(\mathbb{Z}[U]\text{-Mod})$ denote the homotopy category of chain complexes over $\mathbb{Z}[U]$-Mod, and, as described above, let $P(\mathrm{Kom}(\mathbb{Z}[U]\text{-Mod}))$ denote the projectivization of this category. Finally, let $\mathrm{Trans}(P(\mathrm{Kom}(\mathbb{Z}[U]\text{-Mod})))$ denote the category of transitive systems in $P(\mathrm{Kom}(\mathbb{Z}[U]\text{-Mod}))$. We will unpack the precise meaning of these categories in Section 2.5. A majority of the paper will be occupied with showing:

Theorem 1.3.3. *The morphisms*

$$\widehat{CF}, CF^-, CF^+, CF^\infty : \mathcal{G}_{man} \to \mathit{Trans}(P(\mathit{Kom}(\mathbb{Z}[U]\text{-}\mathit{Mod})))$$

are strong Heegaard invariants.

While proving Theorem 1.3.3 we will show the analogous result holds on the level of homology:

Corollary 1.3.4. *The morphisms*

$$\widehat{HF}, HF^-, HF^+, HF^\infty : \mathcal{G}_{man} \to P(\mathbb{Z}[U]\text{-}Mod)$$

are strong Heegaard invariants.

We will establish Theorem 1.3.3 in Sections 2.8 and 2.9. We will also obtain from Theorem 1.3.3 the following statement about the constituent chain complexes.

Corollary 1.3.5. *Given a closed, connected, oriented and based 3-manifold (Y, z) and a Spin^c-structure $\mathfrak{s}$ over Y, the $\mathbb{Z}[U]$-module chain complexes $CF^\circ(\mathcal{H}, \mathfrak{s})$, ranging over all strongly $\mathfrak{s}$-admissible embedded Heegaard diagrams $\mathcal{H}$ for (Y, z), fit into a transitive system of homotopy equivalences in $P(Kom(\mathbb{Z}[U]\text{-}Mod))$ with respect to the maps induced by sequences of pointed handleslides, stabilizations, isotopies, and diffeomorphisms of Heegaard surfaces which are isotopic to the identity in Y.*

Remark 1.3.6. The Heegaard Floer invariants arise as direct sums of invariants

$$HF^\circ(Y, z) = \bigoplus_{\mathfrak{s} \in \mathrm{Spin}^c(Y)} HF^\circ(Y, z, \mathfrak{s})$$

associated to triples $(Y, z, \mathfrak{s})$ for $\mathfrak{s} \in \mathrm{Spin}^c(Y)$. All of the main results have refined statements regarding these invariants of $(Y, z, \mathfrak{s})$. Theorem 1.3.3, Corollary 1.3.4 and Corollary 1.3.5 also depend on choices of coherent orientation systems, which we omit from the statements here. For now, we note that all of the results above hold in particular for the Heegaard Floer chain complexes defined with respect to the canonical coherent orientation

systems constructed in [7]. The precise conditions required of the coherent orientation systems implicitly appearing in the results above will be specified in Definition 2.7.9.

1.4. Organization of the Dissertation

In Chapter II we address our naturality results for Heegaard Floer homology. We begin in Section 2.2 by recalling the definition and setting of Heegaard Floer homology. In Section 2.3 we recall the notion of sutured 3-manifolds and sutured Heegaard diagrams, as all of the results in [3] are phrased in this setting. We discuss a correspondence between sutured and closed 3-manifolds, and use the correspondence to translate a graph of sutured diagrams central to setting of [3] into an equivalent graph of closed diagrams which we use throughout the remainder of the paper. In Section 2.4 we introduce and rephrase the notions of weak and strong Heegaard invariants defined in [3]. Section 2.5 deals with setting up the algebraic framework in which our main results are phrased, and in particular includes the definitions of the projectivizations and categories of transitive systems appearing in Theorems 1.3.1 and 1.3.3. In Section 2.6, we deduce Theorem 1.3.1 and Corollary 1.3.5 from Theorem 1.3.3 and Corollary 1.3.4. In Sections 2.7 and 2.8 we recall the constructions involved in defining the integral Heegaard Floer chain complexes, and establish that these constructions yield suitably defined weak Heegaard invariants. In Section 2.8, we check that these weak Heegaard invariants satisfy all but one of the axioms required of a strong Heegaard invariant. Finally, in Section 2.9 we

carry out the main work and establish that these weak Heegaard invariants also satisfy the last axiom, known as simple handleswap invariance.

In Chapter III we describe an application of our naturality results to involutive Heegaard Floer homoloy, as well as potential generalizations to stronger naturality results and lines of future work which we expect to be useful.

In Chapter IV we discuss potential applications to studying nonorientable 3-manifolds using Heegaard Floer Homology. We begin by describing a notion of Heegaard splittings and Heegaard diagrams for nonorientable manifolds, and proving some existence results for such things. We then introduce a bilinear form coming from Heegaard Floer homology asociated to nonorientable 3-manifolds, and study its properties. Finally, we give examples and outline future lines of questioning.

We note that Sections 1.3, Sections 2.1-2.9 and Chapter III of this dissertation have been submitted for publication.

CHAPTER II

NATURALITY OF HEEGAARD FLOER HOMOLOGY

The Heegaard Floer invariants associated to closed, oriented 3-manifolds were defined in the work of Ozsváth and Szabó [1]. These invariants take the form of an isomorphism class of $\mathbb{Z}[U]$-module assigned to each such 3-manifold. To describe the construction of the invariants and our results, we first recall some notions regarding decompositions of 3-manifolds into elementary pieces. The work in this chapter has been submitted for publication to the Journal of Topology.

2.1. Background on Heegaard Splittings

A 3-*dimensional handlebody* is a compact 3-manifold with boundary, H, which contains a collection of disjoint, properly embedded disks

$$\{(D_i, \partial D_i) \hookrightarrow (H, \partial H)\}$$

such that cutting H along the collection of disks yields a 3-ball. The *genus of a handlebody* is the genus of the surface ∂H. An example of a handlebody is depicted in Figure 2.

A *Heegaard splitting* of a closed, connected 3-manifold Y is a decomposition

$$Y = H_1 \cup_\Sigma H_2,$$

where H_1 and H_2 are handlebodies glued by a diffeomorphism along their common boundary surface Σ. We say a Heegaard splitting is a *genus* g

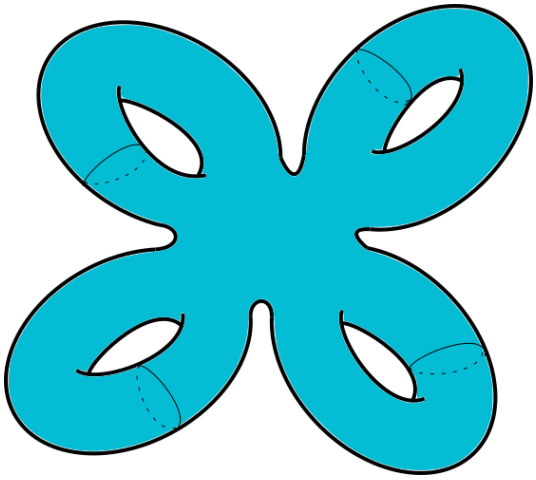

FIGURE 2 A 3-dimensional, genus 4 Handlebody, with one possible system of disks indicated.

Heegaard spliting if the genus of Σ is g. For example, consider two copies of a genus 1 handlebody (i.e. two copies of a solid torus). Let us call a curve on the boundary surface of the handlebody which bounds a disk within the handlebody a *meridian*, and any other curve which intersects a meridian transversally in a single point a *longitude*. Then by glueing two copies of the solid torus along their boundary by a diffeomorphism which identifies a meridian with a longitude, we obtain a Heegaard splitting for S^3. If we instead identify the two handlebodies along their boundaries by a diffeomorphism which identifies the two meridians and the two longitudes, we obtain a Heegaard splitting for $S^1 \times S^2$. These examples are depicted in Figure 3.

A classical theorem in smooth topology asserts that every closed, connected, oriented 3-manifold admits a Heegaard splitting [8]. This can be seen by considering a piecewise-linear structure on Y and taking H_1 to be a regular neighborhood of the 1-skeleton and H_2 to be a regular neighborhood of the corresponding dual graph, or via Morse theory by considering a

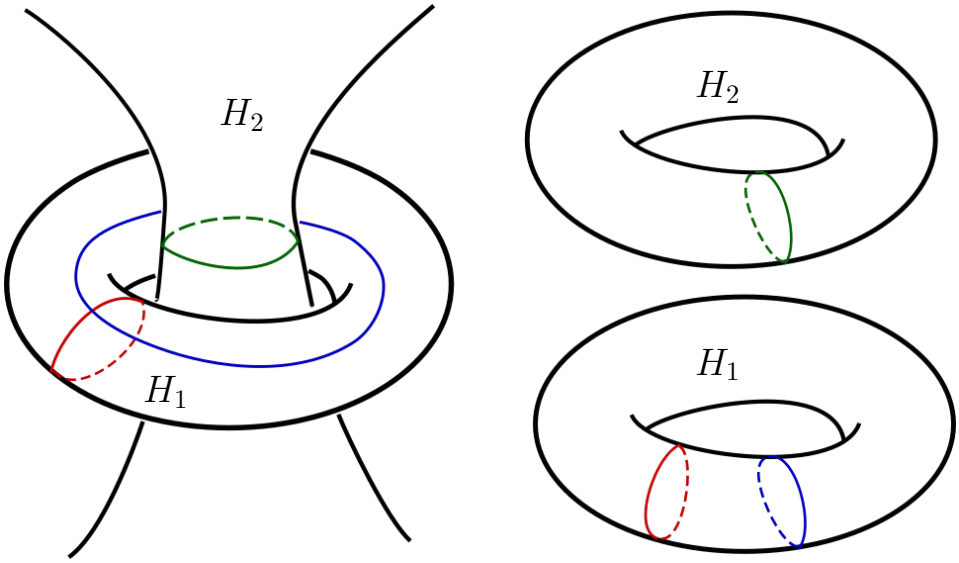

FIGURE 3 Two schematics for genus 1 Heegaard splittings: on the left is a splitting of S^3, and on the right is a splitting for $S^1 \times S^2$. Meridians on H_1 are depicted in red, while meridians on H_2 are depicted in green. In each case, we glue the handlebodies along their boundary by the evident diffeomorphism which carries the green curve to the blue curve.

CW decomposition of Y coming from a Morse function. In fact, a given 3-manifold will admit many different Heegaard splittings. For example, given a genus g splitting $Y = H_1 \cup_\Sigma H_2$, one can construct a genus $g+1$ splitting for the same 3-manifold as follows. We say an arc γ properly embedded in H_2 is an *unknotted arc* if there is an embedded disk D in H_2 such that ∂D is the union of a single arc α on ∂H_2 and the interior of the arc γ. Then one can choose any unknotted arc properly embedded in the handlebody (H_2, Σ) connecting two points on Σ and attach a tube to Σ along this arc to obtain a surface Σ', and a genus $g+1$ Heegaard splitting $Y = H_1' \cup_{\Sigma'} H_2'$. An example of this process is depicted in Figure 4.

We call the process exhibited in this example *stabilization* of a Heegaard splitting. Singer showed that any two Heegaard splittings for

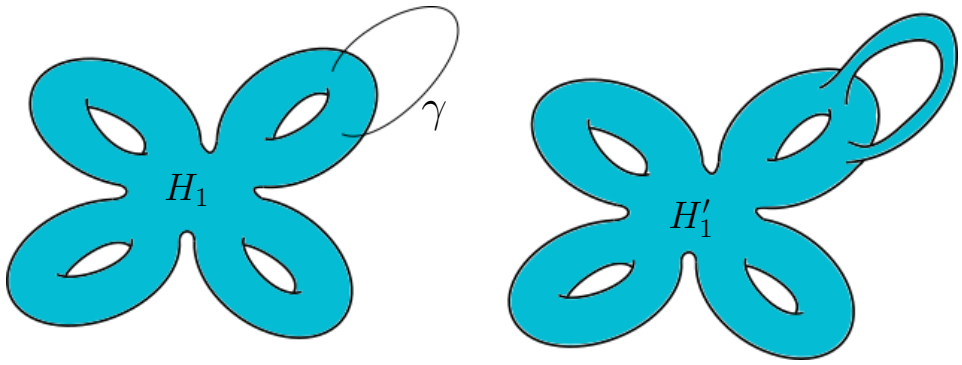

FIGURE 4 A depiction of the stabilization process. On the left is a genus 4 handlebody which we imagine embedded in a genus 4 Heegaard splitting, and an unknotted arc γ properly embedded in the complement of H_1. On the right is the result H_1' of attaching a solid tube along this arc to obtain a new splitting with genus increased by 1.

the same 3-manifold become isotopic after stabilizing each splitting some number of times:

Theorem 2.1.1. *[8] Let $Y = H_1 \cup H_2$ and $Y = H_1' \cup H_2'$ be two Heegaard splittings for the same 3-manifold. Then the k-fold stabilization of the first splitting is diffeomorphic to the k'-fold stabilization of the second splitting for some k and k'.*

This implies that any well-defined assignment of algebraic objects to diffeomorphism classes of Heegaard splittings which is invariant under stabilization is in fact an invariant of closed, oriented 3-manifolds. As we will now describe, the construction of the Heegaard Floer invariants arises in this way.

To explain how this occurs, we first describe a framework for encoding the data of a Heegaard splitting using curves and surfaces. Given a handlebody H with $\partial H = \Sigma$ a genus g surface, the collection of properly embedded disks $\{D_i \hookrightarrow H\}$ specifies a collection of closed embedded curves

$\{\alpha_i : \partial D_i \hookrightarrow \Sigma\}$ in the boundary surface. Since H is a handlebody, these curves bound pairwise disjoint, properly embedded disks in H, and removing the curves from Σ yields a sphere with punctures. Given any collection of closed embedded curves $\{\gamma_i\}_{i=1,\dots,g}$ in the genus g surface $\Sigma = \partial H$ satisfying

1. The curves γ_i are disjoint in Σ.
2. The curves γ_i bound pairwise disjoint, properly embedded disks in H.
3. $\Sigma \setminus (\gamma_1 \cup \ldots \cup \gamma_g)$ is connected.

we will say the collection $\{\gamma_i\}$ is an *attaching set for* H. Given any collection of closed embedded curves $\{\gamma_i\}_{i=1,\dots,g}$ in a genus g surface Σ which satisfy conditions (1) and (3), we will say the collection is an (abstract) *attaching set in* Σ. Let $Y = H_1 \cup_\Sigma H_2$ be a genus g Heegaard splitting. We will say a collection of closed, embedded curves $(\Sigma, \alpha_1, \dots, \alpha_g, \beta_1, \dots, \beta_g)$ is a *Heegaard diagram* for the splitting $Y = H_1 \cup_\Sigma H_2$ if $\{\alpha_i\}$ form an attaching set for H_1 and $\{\beta_i\}$ form an attaching set for H_2. For example, the two splittings depicted in Figure 3 above can be represented by the Heegaard diagrams depicted in Figure 5.

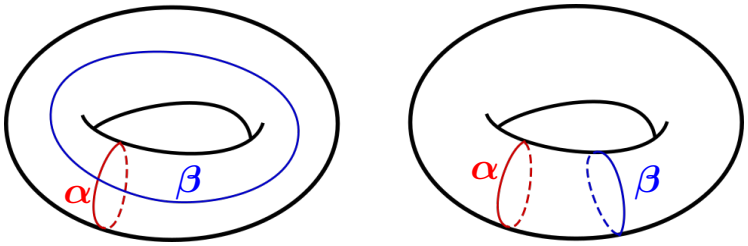

FIGURE 5 Heegaard diagrams for the splittings of S^3 and $S^1 \times S^2$ depicted in Figure 3.

We note that the correspondence between Heegaard splittings and Heegaard diagrams representing them is not a bijection. While an abstract

Heegaard diagram specifies a diffeomorphism class of Heegaard splitting and thus a diffeomorphism class of 3-manifold, even a fixed class of Heegaard splitting admits many Heegaard diagrams (as can be easily seen, for example, by performing small isotopies on the embedded curves defining any diagram compatible with a given splitting). However, any two diagrams for the same 3-manifold are related by a sequence of basic moves on diagrams, namely *isotopies*, *handleslides*, and *stabilizations*. We now discuss each of these moves.

Given two attaching sets in a surface Σ, we say they are *related by an isotopy* if the two sets of attaching curves are related by an isotopy for which the curves remain disjoint throughout the isotopy.

Given an attaching set $\{\gamma_i\}$ in a genus g surface Σ, fix an arc δ in Σ whose endpoints are on γ_1 and γ_2, and whose interior is disjoint from all of the γ_i. A small tubular neighborhood of $\gamma_1 \cup \gamma_2 \cup \delta$ in Σ then has three boundary components $\gamma_1' \cup \gamma_2' \cup \delta'$, where γ_1' and γ_2' are isotopic to γ_1 and γ_2 respectively. We say the attaching set $\{\delta', \gamma_2, \gamma_3, \ldots, \gamma_g\}$ obtained by replacing γ_1 with δ' is an attaching set obtained from $\{\gamma_1, \gamma_2, \gamma_3 \ldots, \gamma_g\}$ by *handlesliding* γ_1 *over* γ_2 . In this situation we will also say the attaching sets are *related by a handleslide*. Note that this definition is equivalent to saying that δ' is obtained by handlesliding γ_1 over γ_2 if δ', γ_1 and γ_2 cobound a pair of pants embedded in $\Sigma \setminus (\gamma_3 \cup \ldots \cup \gamma_g)$.

We will say two Heegaard diagrams $(\Sigma, \alpha_1, \ldots, \alpha_g, \beta_1, \ldots, \beta_g)$ and $(\Sigma, \alpha_1', \ldots, \alpha_g', \beta_1', \ldots, \beta_g')$ are related by a sequence of isotopies (resp. sequence of handleslides) if the attaching sets $(\alpha_1, \ldots, \alpha_g)$ and $(\alpha_1', \ldots, \alpha_g')$ are related by isotopies (resp. handleslides) and the attaching sets

$(\beta_1, \ldots, \beta_g)$ and $(\beta'_1, \ldots, \beta'_g)$ are related by isotopies (resp. handleslides). An example of two Heegard diagrams related by an isotopy is depicted in Figure 6. An example of two Heegaard diagrams related by a handleslide is depicted in Figure 7.

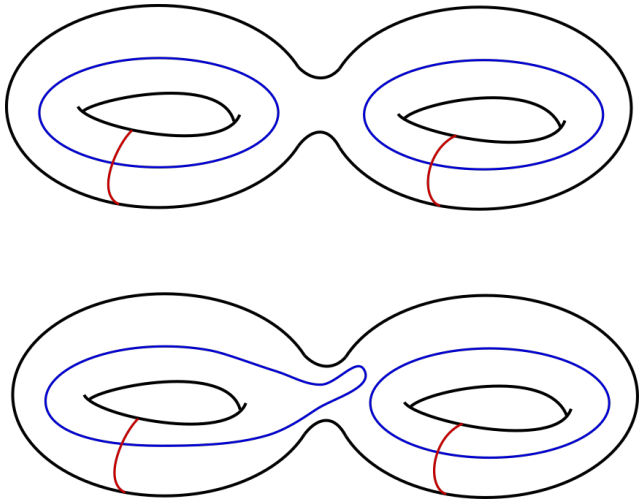

FIGURE 6 Two Heegaard diagrams related by an isotopy.

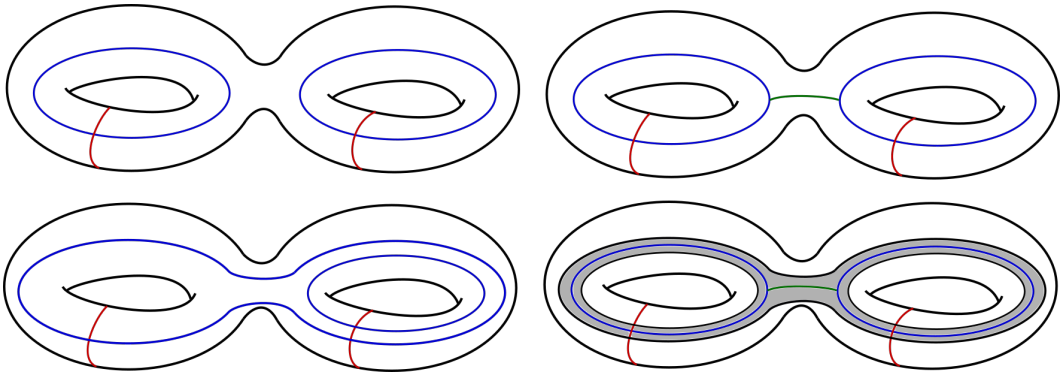

FIGURE 7 The figures on the left are Heegaard diagrams related by a handleslide. In the top right, an arc connecting two curves in one of the original attaching sets is depicted in green. In the bottom right, a pair of pants specified by this arc is shaded in gray. The result of the handleslide is obtained by replacing one of the curves in the original attaching set with the third boundary component of this pair of pants.

We now state a key result which relates different attaching sets for the same handlebody. Reidemeister and Singer showed (See [9] or [10] for modern descriptions of this result):

Theorem 2.1.2 ([8], [11])**.** *Any two attaching sets* $(\Sigma, \alpha_1, \ldots, \alpha_g)$ *and* $(\Sigma, \alpha'_1, \ldots, \alpha'_g)$ *for a handlebody* H *are related by a sequence of isotopies and handleslides.*

If a Heegaard surface Σ is endowed with a choice of basepoint z, we further refine the above definitions and say two Heegaard diagrams on Σ are related by *pointed isotopies* or *pointed handleslides* if the processes described above can be carried out in the complement of the basepoint. Given two choices of basepoint on a Heegaard surface for a fixed splitting, we will say two diagrams on the surface are related by a sequence of pointed isotopies and pointed handleslides if the curves in the diagrams can be related as above, while also allowing isotopy of the basepoint. In this case, we require that the isotopies of attaching curves and handleslides of attaching curves remain disjoint from the basepoint throughout the entire isotopy of the basepoint. Then one can also show that any two choices of basepoint on the same diagram are related by pointed Heegaard moves, according to the following result.

Theorem 2.1.3. *[1] Given a Heegaard diagram* $(\Sigma, \alpha_1, \ldots, \alpha_g, \beta_1, \ldots, \beta_g)$ *and basepoints* $z, z' \in \Sigma \setminus (\alpha_1 \cup \alpha_2 \cup \ldots \cup \alpha_g \cup \beta_1 \cup \beta_2 \ldots \cup \beta_g)$*, the Heegaard diagrams* $(\Sigma, \alpha_1, \ldots, \alpha_g, \beta_1, \ldots, \beta_g, z)$ *and* $(\Sigma, \alpha_1, \ldots, \alpha_g, \beta_1, \ldots, \beta_g, z')$ *are related by a sequence of pointed handleslides and pointed isotopies.*

Finally, we describe the stabilization move on a Heegaard diagram. Given a genus g Heegaard diagram $(\Sigma, \alpha_1, \ldots, \alpha_g, \beta_1, \ldots, \beta_g)$ for a genus

g Heegaard splitting $Y = H_1 \cup_\Sigma H_2$, we may form a new diagram $(\Sigma \# T, \alpha_1, \ldots, \alpha_g, \alpha_{g+1}\beta_1, \ldots, \beta_g, \beta_{g+1})$ by taking the connect sum of Σ with the genus 1 surface T, and introducing two new closed curves α_{g+1} and β_{g+1} which are contained in T and intersect transverally in a single point. This new diagram is genus $g+1$, and is compatible with the Heegaard splitting obtained from the original diagram by stabilizing it in the sense previously described. Stabilization of a diagram is depicted in Figure 8 (compare Figure 4).

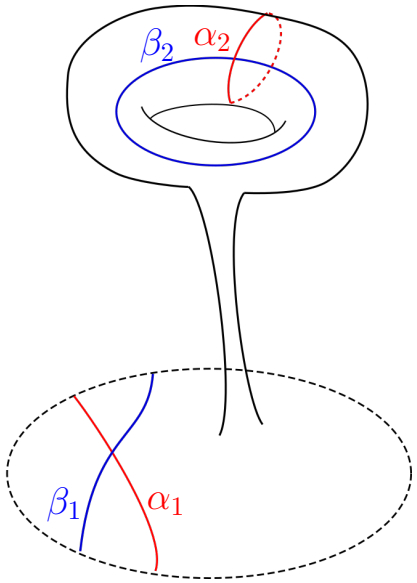

FIGURE 8 A region of the Heegaard diagram $(\Sigma_1, \boldsymbol{\alpha}_1, \boldsymbol{\beta}_1)$ is depicted in the dashed circle, with two attaching curves $\alpha_1 \in \boldsymbol{\alpha}_1$ and $\beta_1 \in \boldsymbol{\beta}_1$. The standard genus 1 diagram for S^3 has been attached via a connect sum to the this region, resulting in the stabilized diagram.

The key observation is then that any two pointed Heegaard diagrams for the same 3-manifold become diffeomorphic after applying a sequence of pointed isotopies, pointed handleslides and stabilizations:

Theorem 2.1.4. *[1] Any two pointed Heegaard diagrams* $(\Sigma, \boldsymbol{\alpha}, \boldsymbol{\beta}, z)$ *and* $(\Sigma', \boldsymbol{\alpha}', \boldsymbol{\beta}', z')$ *representing the same* 3*-manifold become diffeomorphic after applying a finite sequence of pointed Heegaard moves.*

This follows from Theorem 2.1.1, Theorem 2.1.2 and Theorem 2.1.3. From this observation it follows that any assignment of algebraic data to pointed Heegaard diagrams which is invariant under pointed isotopies, pointed handleslides and stabilizations is an invariant of closed, oriented 3-manifolds. In the next subsection we will provide a brief overview of how Heegaard Floer homology arises in this way.

2.2. Background on Heegaard Floer Homology

Heegaard Floer homology is an invariant of closed, connected, oriented 3-manifolds introduced by Ozsváth and Szabó in [1]. In this section, we provide a sketch of the construction of the invariant. We will omit many details, and refer the reader to the original source [1] for a more detailed description of the technical ingredients that go into the construction. We will also recall more of the technical background that will be necessary to prove our main results in Section 2.7. We concern ourselves here with the simplest variant of Heegaard Floer homology, which is denoted $\widehat{HF}$.

Heegaard Floer homology is defined with respect to a Heegaard diagram for a 3-manifold. Fix a genus g based Heegaard diagram

$$\mathcal{H} = (\Sigma, \boldsymbol{\alpha} = (\alpha_1, \alpha_2, \ldots, \alpha_g), \boldsymbol{\beta} = (\beta_1, \beta_2, \ldots, \beta_g), z)$$

for a closed, connected, oriented and based 3-manifold (Y, z). We begin by considering the symmetric product

$$\mathrm{Sym}^g(\Sigma) := (\Sigma \times \cdots \times \Sigma)/S_g,$$

which is the quotient of the g-fold product of Σ with itself by the action of the symmetric group which permutes the factors of the product. Despite the fact that the symmetric group action is not free, $\mathrm{Sym}^g(\Sigma)$ is in fact a smooth manifold (where the smooth structure depends on a choice of complex structure j on Σ). One can also show that this choice of complex structure j on Σ induces a complex structure $J := \mathrm{Sym}^g(j)$ on $\mathrm{Sym}^g(\Sigma)$. Fixing such complex structures j and J, one considers the tori

$$\alpha_1 \times \alpha_2 \times \cdots \times \alpha_g, \;\; \beta_1 \times \beta_2 \times \cdots \times \beta_g \subset \Sigma \times \cdots \times \Sigma$$

and their images in the symmetric product $\mathrm{Sym}^g(\Sigma)$. We denote their images in the symmetric product by $\mathbb{T}_{\boldsymbol{\alpha}}$ and $\mathbb{T}_{\boldsymbol{\beta}}$ respectively. It can be shown that the induced tori $\mathbb{T}_{\boldsymbol{\alpha}}$ and $\mathbb{T}_{\boldsymbol{\beta}}$ are totally real with respect to the induced almost complex structure J. The Heegaard Floer homology is then defined as a variation of Lagrangian intersection Floer homology, as defined by Floer in [12], applied to these tori. We will now sketch this process and illustrate some of the details in a few examples.

First, we note that Heegaard Floer homology is the homology of a chain complex. To define the chain complex, one must in fact fix some additional data related to the fixed Heegaard diagram $\mathcal{H}$. In addition to the Heegaard diagram $\mathcal{H}$, the complex structure j on Σ, and the induced

complex structure J on $\mathrm{Sym}^g(\Sigma)$, one must also fix a choice of generic path J_s of almost complex structures on $\mathrm{Sym}^g(\Sigma)$, which satisfies $J_{s=0} = J$ and an additional technical condition which we ignore for the purposes of this introduction (see [1]). We will also require that our Heegaard diagram $\mathcal{H} = (\Sigma, \boldsymbol{\alpha}, \boldsymbol{\beta}, z)$ satisfy a certain admissibility criterion. We postpone a precise discussion of this admissibility criterion to Section 2.7. For now, we just note that it is shown in [1] that every closed, connected, oriented and based 3-manifold admits a Heegaard diagram which is appropriately admissible, so admissibility is never an obstruction to applying the construction to a 3-manifold to obtain a Heegaard Floer chain complex.

For an admissible Heegaard diagram, the chain complex, denoted by $\widehat{CF}_{J_s}(\mathcal{H})$ (or by $\widehat{CF}(\mathcal{H})$ or $\widehat{CF}(Y)$ when the dependence on the additional data is understood), is freely generated as an abelian group by the intersection points $\mathbb{T}_{\boldsymbol{\alpha}} \cap \mathbb{T}_{\boldsymbol{\beta}}$. We note that an intersection point $\boldsymbol{x} \in \mathbb{T}_{\boldsymbol{\alpha}} \cap \mathbb{T}_{\boldsymbol{\beta}}$ is just an unordered g-tuple of intersection points $\{x_1, x_2, \ldots, x_g\}$ between $\boldsymbol{\alpha}$ and $\boldsymbol{\beta}$ in Σ such that each α_i and β_j contains exactly one of the x_k. The differential will count pseudo-holomorphic disks in the symmetric product, as we now explain.

Given two intersection points $\boldsymbol{x}, \boldsymbol{y} \in \mathbb{T}_{\boldsymbol{\alpha}} \cap \mathbb{T}_{\boldsymbol{\beta}}$, we begin by considering Whitney disks in $\mathrm{Sym}^g(\Sigma)$ connecting $\boldsymbol{x}$ to $\boldsymbol{y}$. Let $D = [0,1] \times \mathbb{R} \subset \mathbb{C}$ denote the infinite strip in the complex plane, $D_L = \{0\} \times \mathbb{R}$ denote the left part of the boundary, and $D_R = \{1\} \times \mathbb{R}$ denote the right part of the boundary. We write $z = s + ti$ for coordinates on D, and interchangeably refer to D as a disk or a strip. A *Whitney disk* u from $\boldsymbol{x}$ to $\boldsymbol{y}$ is a smooth map $u : D \to \mathrm{Sym}^g(\Sigma)$ satisfying:

1. $\lim_{t\to-\infty} u(s+ti) = \boldsymbol{x}$.

2. $\lim_{t\to\infty} u(s+ti) = \boldsymbol{y}$.

3. $u(D_L) \subset \mathbb{T}_{\boldsymbol{\beta}}$.

4. $u(D_R) \subset \mathbb{T}_{\boldsymbol{\alpha}}$.

A schematic of a Whitney disk is given in Figure 9. We caution the reader that a Whitney disk as just defined is a map to $\mathrm{Sym}^g(\Sigma)$, so our schematic which indicates the image as a disk in the plane is misleading for $g > 1$.

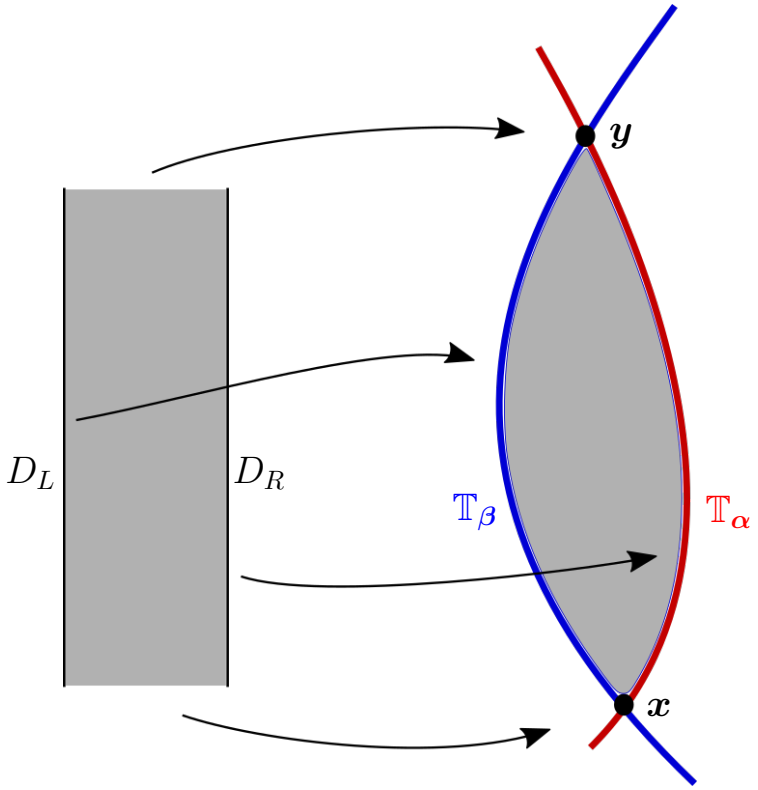

FIGURE 9 A schematic of a Whitney disk from $\boldsymbol{x}$ to $\boldsymbol{y}$.

Given two intersection points $\boldsymbol{x}, \boldsymbol{y} \in \mathbb{T}_{\boldsymbol{\alpha}} \cap \mathbb{T}_{\boldsymbol{\beta}}$, we let $\pi_2(\boldsymbol{x}, \boldsymbol{y})$ denote the set of homotopy classes of Whitney disks connecting $\boldsymbol{x}$ to $\boldsymbol{y}$. Given such a homotopy class $\phi \in \pi_2(\boldsymbol{x}, \boldsymbol{y})$, we denote by $\mathcal{M}_{J_s}(\phi)$ the parametrized

moduli space of J_s-holomorphic disks in the class ϕ:

$$\mathcal{M}_{J_s}(\phi) = \{u \in \phi | \frac{du}{ds} + J_s \frac{du}{dt} = 0\}.$$

We note that $\mathcal{M}_{J_s}(\phi)$ comes equipped with an $\mathbb{R}$-action coming from vertical translations on the strip (the automorphisms of the strip fixing the ends and preserving the boundary components). To define the differential we want to count certain types of pseudo-holomorphic disks which are unparametrized, so we will consider

$$\widehat{\mathcal{M}_{J_s}}(\phi) := \mathcal{M}_{J_s}(\phi)/\mathbb{R},$$

the quotient of the parametrized moduli space with respect to this $\mathbb{R}$-action.

To finish defining the differential, we need to make use of the Maslov index of a pseudo-holomorphic disk with Lagrangian boundary conditions. Given a homotopy class of Whitney disks ϕ, the unparametrized moduli space $\mathcal{M}_{J_s}(\phi)$ may or may not be a smooth manifold. In fact, the moduli space $\mathcal{M}_{J_s}(\phi)$ can be viewed as the zero set of a bundle section $\overline{\partial}$, and using well-known results about transversality in infinite dimensional settings it is smooth whenever this section $\overline{\partial}$ is transverse to the zero section. The Maslov index $\mu(\phi)$ is the expected dimension of $\mathcal{M}_{J_s}(\phi)$, and corresponds to the Fredholm index of the linearized (Fredholm) operator determined by the differential $D(\overline{\partial})$ of $\overline{\partial}$. When the moduli space is transversely cut out by the section $\overline{\partial}$, the Maslov index agrees with the dimension of the resulting smooth manifold. We will need the following result to state the definition of the differential.

Theorem 2.2.1. *[1] There is a choice of almost complex structure data J_s such that for any homotopy class of Whitney disk ϕ with $\mu(\phi) = 1$, the unparametrized moduli space $\widehat{\mathcal{M}_{J_s}}(\phi)$ is a compact, oriented, 0-dimensional manifold.*

Let $\mu(\phi)$ denote the Maslov index of the class ϕ, and let $n_z(\phi)$ denote the algebraic intersection number of ϕ with $\{z\} \times \mathrm{Sym}^{g-1}(\Sigma)$. The Maslov index yields a well defined relative cyclic grading on the generators of $\widehat{CF}(\mathcal{H})$ defined above, via the formula

$$\mathrm{gr}(\boldsymbol{x}, \boldsymbol{y}) = \mu(\phi) - 2n_z(\phi)$$

where ϕ is any homotopy class of Whitney disk $\phi \in \pi_2(\boldsymbol{x}, \boldsymbol{y})$.

Finally, the differential

$$\partial : \widehat{CF}(\mathcal{H}) \to \widehat{CF}(\mathcal{H})$$

is defined by the formula

$$\partial(\boldsymbol{x}) = \sum_{\{\boldsymbol{y} \in \mathbb{T}_{\boldsymbol{\alpha}} \cap \mathbb{T}_{\boldsymbol{\beta}}\}} \sum_{\{\phi \in \pi_2(\boldsymbol{x}, \boldsymbol{y}) | \mu(\phi) = 1, n_z(\phi) = 0\}} \#\widehat{\mathcal{M}_{J_s}}(\phi) \cdot \boldsymbol{y}$$

A few words are in order about terms appearing in the differential, and the well-defintion of this construction. By Theorem 2.2.1, for a suitable choice of complex structure data J_s the unparametrized moduli spaces $\widehat{\mathcal{M}_{J_s}}(\phi)$ appearing in the sum in the differential are compact, oriented, 0-manifolds. Furthermore, by work of Gromov and Ozsváth and Szabó, the unparametrized moduli space $\bigcup_{\phi | \mu(\phi)=1} \widehat{\mathcal{M}_{J_s}(\phi)}$ will in this case be

a compact 0-manifold so long as the Heegaard diagram is admissible, so the sum appearing in the differential is finite. It turns out that the moduli spaces can all be oriented, and the symbol $\#\widehat{\mathcal{M}_{J_s}}(\phi)$ indicates the signed count of this collection of oriented points with respect to some implicitly chosen orientations. These remarks justify the fact that the boundary operator given above is a well defined map. Finally, as shown in [1] using well-known glueing results about the moduli spaces in question, this operator also satisfies $\partial^2 = 0$ (assuming certain technical conditions are satisfied) and thus yields the structure of a chain complex on $\widehat{CF}(\mathcal{H})$. We will discuss more of the technical details of this construction in later sections.

We now turn towards describing a few examples to illustrate the construction of the Heegaard Floer chain complex in practice, and to illustrate some of the difficulties that immediately arise when one tries to calculate the differentials involved. Before doing so, we introduce some results which are convenient for analyzing Whitney disks in $\mathrm{Sym}^g(\Sigma)$, and which will be useful in our calculations.

Definition 2.2.2. Given a Heegaard diagram $\mathcal{H} = (\Sigma, \boldsymbol{\alpha}, \boldsymbol{\beta})$, let $D_1, \ldots, D_k$ denote the closures of the connected components of $\Sigma \setminus (\boldsymbol{\alpha} \cup \boldsymbol{\beta})$. Fix points $p_i \subset D_i$ which miss the curves $\boldsymbol{\alpha}$ and $\boldsymbol{\beta}$. Given a homotopy class of Whitney disk ϕ, the *domain of* ϕ is the formal linear combination:

$$D(\phi) = \sum_{i=1}^{k} n_{p_i}(\phi) D_i.$$

We regard domains as being two chains in $C_2(\Sigma)$. Any homotopy class of Whitney disk $\phi \in \pi_2(\boldsymbol{x}, \boldsymbol{y})$ specifies a two chain $D(\phi)$ by the construction defined above, and in fact it is possible to determine when such a two chain comes from a homotopy class of Whitney disk:

Lemma 2.2.3. *[13] Fix a Heegaard diagram $\mathcal{H} = (\Sigma, \boldsymbol{\alpha}, \boldsymbol{\beta})$ with connected components D_i as above. Given intersection points $\boldsymbol{x} = \{x_1, \ldots, x_g\}, \boldsymbol{y} = \{y_1, \ldots, y_g\} \in \mathbb{T}_{\boldsymbol{\alpha}} \cap \mathbb{T}_{\boldsymbol{\beta}}$, and a linear combination*

$$D = \sum_i c_i D_i,$$

we say D is a domain from $\boldsymbol{x}$ to $\boldsymbol{y}$ if the boundary of D restricted to the curves $\boldsymbol{\alpha}$ consists of curves from $\boldsymbol{x}$ to $\boldsymbol{y}$, while the boundary of D restricted to the curves $\boldsymbol{\beta}$ consists of curves from $\boldsymbol{y}$ to $\boldsymbol{x}$. Then if $g(\Sigma) > 1$, any domain D from $\boldsymbol{x}$ to $\boldsymbol{y}$ is the domain of a homotopy class of Whitney disk $\phi \in \pi_2(\boldsymbol{x}, \boldsymbol{y})$.

Next, we note a crucial lemma which provides a low dimensional model for holomorphic disks in symmetric products of surfaces.

Lemma 2.2.4. *[1] Given a homotopy class $\phi \in \pi_2(\boldsymbol{x}, \boldsymbol{y})$ and a holomorphic representative $u \in \mathcal{M}(\phi)$, there is a Riemann surface S, a holomorphic g-fold branched covering space $u_D : S \to D$ and a holomorphic map $u_\Sigma : S \to \Sigma$ such that for each $p \in D$,*

$$u(p) = u_\Sigma(u_D^{-1}(p)).$$

Furthermore, this is one direction of a bijective correspondence:

$$\{\textit{holomorphic disks } u : D \to \textit{Sym}^g(\Sigma)\} \leftrightarrow \left\{ \begin{array}{l} \begin{array}{ccc} S & \xrightarrow{u_\Sigma} & \Sigma \\ \textit{diagrams} \quad \downarrow{\scriptstyle u_D} & & \\ D & & \end{array} \\ \\ \textit{where } S \textit{ is a Riemann surface,} \\ u_\Sigma \textit{ and } u_D \textit{ are holomorphic,} \\ \textit{and } u_D \textit{ is a } g\textit{-fold branched cover} \end{array} \right\}$$

Finally, we provide some facts which are extremely useful for calculating the Maslov index. To do so, we first introduce a few more definitions. Let $\phi \in \pi_2(\boldsymbol{x}, \boldsymbol{y})$ be a homotopy class of Whitney disk, and consider the domain $D(\phi)$. For $x_i \in \boldsymbol{x}$, let $n_{x_i}(\phi)$ be the average of the coefficients of the four cells adjacent to x_i appearing in $D(\phi)$, and $n_{\boldsymbol{x}}(\phi) = \sum_i n_{x_i}$. Define $n_{\boldsymbol{y}}(\phi)$ by the analogous formula. Finally, the Euler measure of the domain $D = D(\phi)$ is given by the formula

$$e(D) := \chi(D) + a/4 - b/4$$

where $\chi(D)$ is the Euler characteristic, a is the number of 270° corners in D, and b is the number of 90° corners in D. The Euler measure is additive in the sense that $e(\sum_i D_i) = \sum_i e(D_i)$.

Lipshitz proved the following combinatorial formula which can be used to calculate the Maslov index of holomorphic disks.

Theorem 2.2.5. *[14] Given a homotopy class of Whitney disks* $\phi \in \pi_2(\boldsymbol{x}, \boldsymbol{y})$*, the Maslov index* $\mu(\phi)$ *is given by the formula*

$$\mu(\phi) = e(\phi) + n_{\boldsymbol{x}}(\phi) + n_{\boldsymbol{y}}(\phi).$$

A straightforward application shows that this implies:

Corollary 2.2.6. *If* ϕ*,* ϕ' *are two homotopy classes of Whitney disks with domains related by* $D(\phi) = D(\phi') + k \cdot \Sigma$ *then* $\mu(\phi) = \mu(\phi') + 2k$*.*

We are now ready to investigate some examples.

Example 2.2.7. The simplest example is the chain complex associated with the "standard" genus 1 pointed diagram $\mathcal{H}$ for S^3 depicted in Figure 10. In such a genus 1 case, we have $\mathrm{Sym}^1(\Sigma) = \Sigma$ and $\mathbb{T}_{\boldsymbol{\alpha}} \cap \mathbb{T}_{\boldsymbol{\beta}} = \boldsymbol{\alpha} \cap \boldsymbol{\beta}$. The $\boldsymbol{\alpha}$ and $\boldsymbol{\beta}$ curve intersect transversely in a single intersection point which we denote $\boldsymbol{x}$. We thus have

$$\widehat{CF}(\mathcal{H}) = \mathbb{Z}\langle \boldsymbol{x} \rangle.$$

The differential must be zero, since the differential is degree -1 and $\mathrm{gr}(\boldsymbol{x}, \boldsymbol{x}) = 0$, so we have:

$$\widehat{HF}(S^3) \cong \mathbb{Z}.$$

Example 2.2.8. Next we consider the diagram $\mathcal{H}$ for S^3 depicted in Figure 11. This can be obtained from the diagram in Figure 10 by an isotopy of the blue attaching curve. In this case, there are three intersection points $\boldsymbol{x}, \boldsymbol{y}, \boldsymbol{z} \in \mathbb{T}_{\boldsymbol{\alpha}} \cap \mathbb{T}_{\boldsymbol{\beta}}$, so as an abelian group the chain complex is given by:

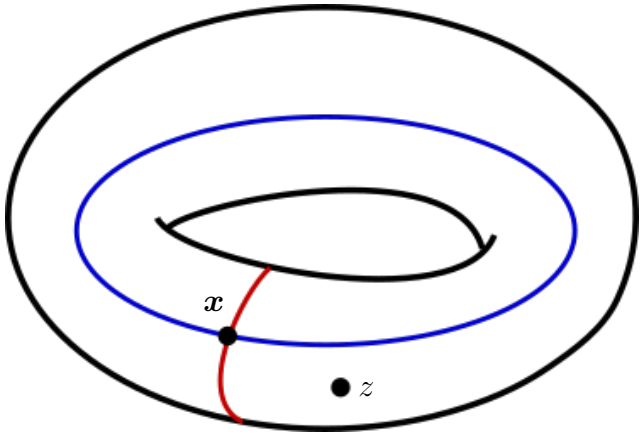

FIGURE 10 A pointed diagram for S^3. The chain complex is generated by the single intersection point $\boldsymbol{x}$, and there can be no differentials.

$$\widehat{CF}(\mathcal{H}) = \mathbb{Z}\langle \boldsymbol{x}, \boldsymbol{y}, \boldsymbol{z} \rangle = \mathbb{Z} \oplus \mathbb{Z} \oplus \mathbb{Z}.$$

To understand the differential, we make the following observations. First, there are precisely three components of $\Sigma \setminus (\boldsymbol{\alpha} \cup \boldsymbol{\beta})$. Any disk being counted in the differential must have a domain which misses the basepoint, so we may disregard the region containing z. There remain two regions, both of which are bigons. The evident homotopy classes of Whitney disks from $\boldsymbol{x}$ to $\boldsymbol{y}$ and from $\boldsymbol{z}$ to $\boldsymbol{y}$ (shaded in gray in Figure 11) each admit holomorphic maps from a disk with the appropriate boundary conditions; by the Riemann mapping theorem, both of these regions are biholomorphically equivalent to the unit disk (or the domain of a Whitney disk), and such biholomorphisms can easily be adjusted to ensure the necessary boundary conditions hold.

Moreover, we may conclude that these homotopy classes each admit a unique holomorphic representative (up to the $\mathbb{R}$-action) as follows. Given two holomorphic disks u_1 and u_2 with the appropriate boundary conditions,

we may arrange for them to agree at a third point on the boundary of their domains by applying an appropriate vertical translation. Then $u_1 \circ u_2^{-1}$ is an automorphism of the unit disk with three fixed points on the boundary. By standard results in complex analysis, such a map must be the identity.

Both of these disks can also be shown to have Maslov index 1. For example, by Theorem 2.2.5, the top domain has index $\mu(\phi) = e(\phi) + n_{\boldsymbol{x}} + n_{\boldsymbol{y}} = e(\phi) + 1/4 + 1/4$. The Euler measure is given by $e(\phi) = \chi + a/4 - b/4 = 1 + 0 - 2/4 = 1/2$. Thus $\mu(\phi) = 1$. We thus conclude that $\partial \boldsymbol{x} = \pm \boldsymbol{y}$ and $\partial \boldsymbol{z} = \pm \boldsymbol{y}$. If the signs of these two differentials are opposite, we have

$$\widehat{HF}(S^3) \cong \widehat{HF}(\mathcal{H}) = \mathbb{Z}\langle \boldsymbol{x} + \boldsymbol{z} \rangle = \mathbb{Z}$$

as desired, and if the signs are the same we have

$$\widehat{HF}(S^3) \cong \widehat{HF}(\mathcal{H}) = \mathbb{Z}\langle \boldsymbol{x} - \boldsymbol{z} \rangle = \mathbb{Z}$$

as desired.

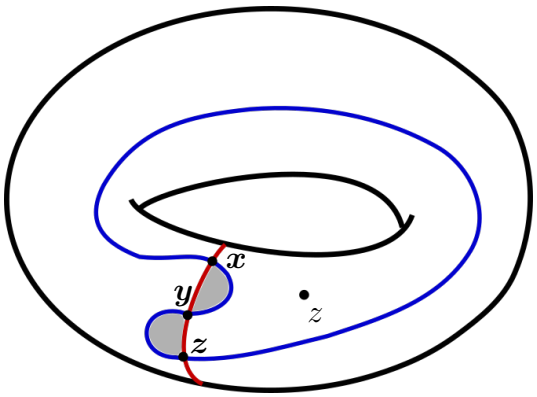

FIGURE 11 Another pointed diagram for S^3. The chain complex is generated by the intersection points $\boldsymbol{x}$, $\boldsymbol{y}$ and $\boldsymbol{z}$. Disks from $\boldsymbol{x}$ to $\boldsymbol{y}$ and from $\boldsymbol{z}$ to $\boldsymbol{y}$ are shaded in gray.

The genus 1 examples discussed above are misleading for several reasons. In general, calculating the differential for a higher genus Heegaard diagram is a difficult business, since counting holomorphic representatives of homotopy classes of Whitney disks can be complicated. We end our brief introduction to the Heegaard Floer invariants with a genus 2 example which illustrates some of these complications.

Example 2.2.9. We consider the genus 2 pointed Heegaard diagram $\mathcal{H}$ shown in Figure 12 below. This is again a diagram representing S^3. It can be obtained from the standard genus 1 diagram depicted in Figure 10 by first stablizing the diagram, then performing a handleslide on the resulting diagram, and finally performing an isotopy on this resulting diagram.

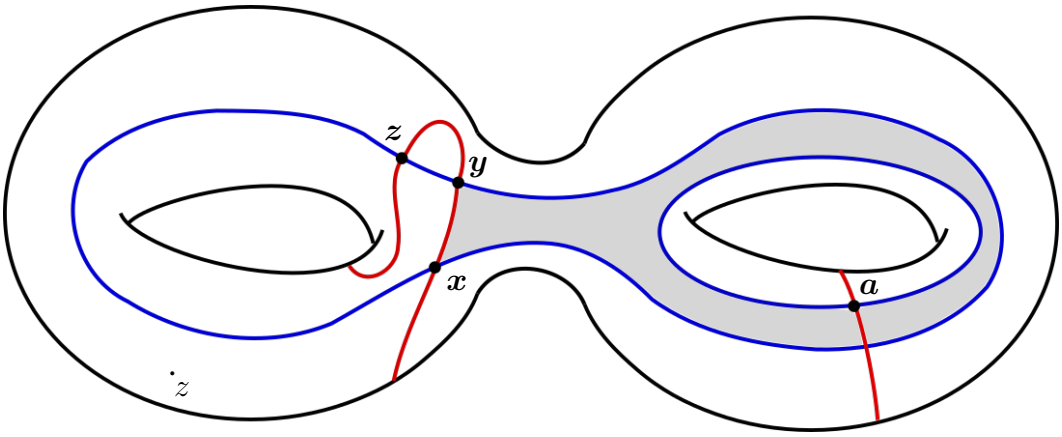

FIGURE 12 Yet another pointed diagram for S^3. The chain complex is generated by the intersection points $\boldsymbol{x} \times \boldsymbol{a}$, $\boldsymbol{y} \times \boldsymbol{a}$ and $\boldsymbol{z} \times \boldsymbol{a}$. A domain D which supports a holomorphic disk is shaded in gray.

In this case, generators of the complex $\widehat{CF}(\mathcal{H})$ are given by the points of $\mathbb{T}_{\boldsymbol{\alpha}} \cap \mathbb{T}_{\boldsymbol{\beta}} \subset \mathrm{Sym}^2(\Sigma)$. Such points correspond to unordered tuples $\{x_1, x_2\}$ of intersection points x_i in Σ between the curves $\boldsymbol{\alpha}$ and $\boldsymbol{\beta}$. These unordered tuples must furthermore satisfy the condition that every curve

α_j in $\boldsymbol{\alpha}$ contains exactly one x_i, and every β_j in $\boldsymbol{\beta}$ contains exactly one x_i. Abusing notation, we will denote the unordered tuple $\{x_1, x_2\} \in \mathrm{Sym}^2(\Sigma)$ by $x_1 \times x_2$. In the case at hand, we have precisely three intersection points $\boldsymbol{x} \times \boldsymbol{a}, \boldsymbol{y} \times \boldsymbol{a}, \boldsymbol{z} \times \boldsymbol{a} \in \mathbb{T}_{\boldsymbol{\alpha}} \cap \mathbb{T}_{\boldsymbol{\beta}}$, and the Heegaard Floer chain complex is generated as:

$$\widehat{CF}(\mathcal{H}) = \mathbb{Z}\langle \boldsymbol{x} \times \boldsymbol{a}, \boldsymbol{y} \times \boldsymbol{a}, \boldsymbol{z} \times \boldsymbol{a} \rangle = \mathbb{Z} \oplus \mathbb{Z} \oplus \mathbb{Z}.$$

There are again three connected components of $\Sigma \setminus (\boldsymbol{\alpha} \cup \boldsymbol{\beta})$. Since we aim to count holomorphic disks in classes ϕ with $n_z(\phi) = 0$, we focus attention on the two components that do not contain the basepoint.

Consider the region homeomorphic to a disk situated between $\boldsymbol{y}$ and $\boldsymbol{z}$. By the same argument used in the previous example, it can be shown that there is a unique holomorphic disk u in Σ connecting $\boldsymbol{y}$ to $\boldsymbol{z}$, up to vertical translation in the source. Such a disk gives rise to a holomorphic Whitney disk $u' : D \to \mathrm{Sym}^2(\Sigma)$ from $\boldsymbol{y} \times \boldsymbol{a}$ to $\boldsymbol{z} \times \boldsymbol{a}$ via $u'(p) = \{u(p), \boldsymbol{a}\}$, and in fact this is the unique unparametrized holomorphic Whitney disk in this homotopy class. One can show it has Maslov index 1, so we have a unique index 1 holomorphic disk from $\boldsymbol{y} \times \boldsymbol{a}$ to $\boldsymbol{z} \times \boldsymbol{a}$.

Next, we consider the connected component of $\Sigma \setminus (\boldsymbol{\alpha} \cup \boldsymbol{\beta})$ indicated in gray in Figure 12. This is a domain from $\boldsymbol{y} \times \boldsymbol{a}$ to $\boldsymbol{x} \times \boldsymbol{a}$, so by Lemma 2.2.3 it is the domain of some homotopy class of Whitney disk from $\boldsymbol{y} \times \boldsymbol{a}$ to $\boldsymbol{x} \times \boldsymbol{a}$. We claim that this domain admits exactly one holomorphic disk representative. To argue that this is the case, we will use Lemma 2.2.4.

Consider the annulus specified by the shaded domain, and perform a cut of length l from the intersection point $\boldsymbol{a}$ into the annulus along the

red curve in $\boldsymbol{\alpha}$. This yields a region biholomorphic to the complex annulus A depicted in the top right of Figure 13 below. We denote by $\boldsymbol{a}_1$ and $\boldsymbol{a}_2$ the two points in the cut annulus corresponding to the original intersection point $\boldsymbol{a}$. By Lemma 2.2.4, any holomorphic disk u in the homotopy class in question will give rise to a branched double cover $u_D : A \to D$ satisfying $u_D(\boldsymbol{a}_1) = u_D(\boldsymbol{y}) = i$ and $u_D(\boldsymbol{a}_2) = u_D(\boldsymbol{x}) = -i$. Such a branched double cover will be the quotient of the annulus A under a holomorphic covering involution which preserves $\{\boldsymbol{x}, \boldsymbol{a}_1\}$ and $\{\boldsymbol{y}, \boldsymbol{a}_2\}$, and exchanges the red curves on the two boundary components (see Figure 13). Such an involution can only exist if the angles determined by the two red arcs are the same, and in this case there is a unique such involution [1, Lemma 9.3]. By analyzing the Gromov limits of the sequence of annuli obtained as the cut length varies from 0 to 1, one can show that there is algebraically a single cut length for which the images of the red curves on the uniformized annulus will have the same conformal angle. This can presumably also be shown using a classical conformal invariant, such as extremal length. We thus conclude that there is algebraically one cut length l for which the annulus branch double covers the disk (for a branched double cover with the appropriate boundary conditions). By Lemma 2.2.4, this implies that the signed count of holomorphic disks representing the annular shaded domain is precisely one.

Finally, one can show that the holomorphic disk u just described has Maslov index 1, using Theorem 2.2.5. The domain $D(u)$ has Euler characteristic $\chi = 0$, two 90° corners, and zero 270° corners, thus the Euler

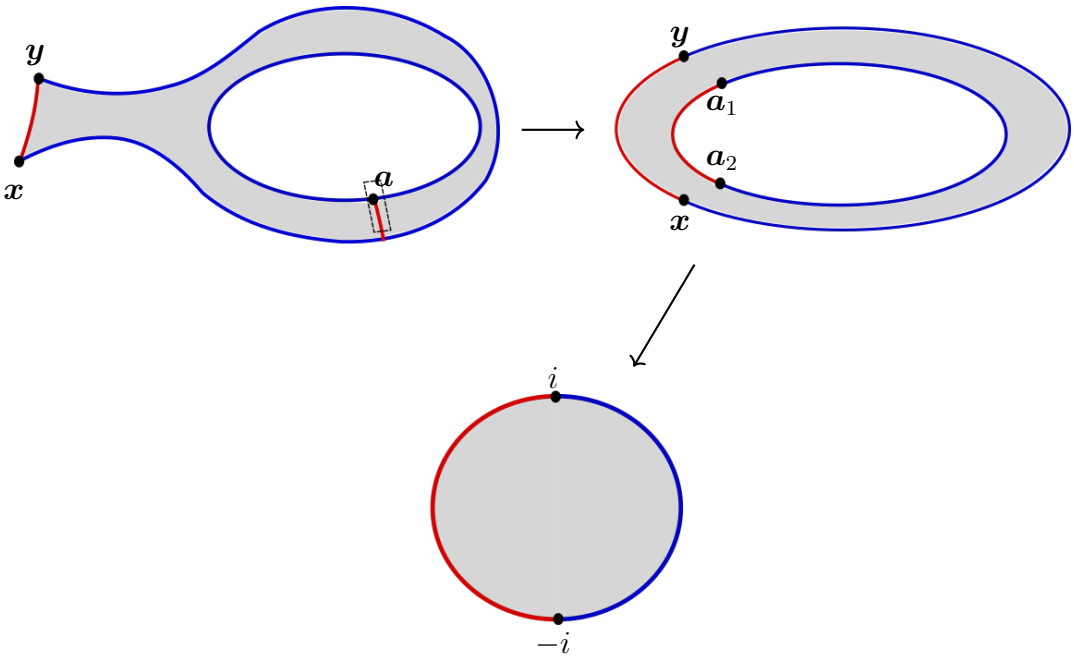

FIGURE 13 The annular domain under consideration is depicted in the top left. We cut along the red curve in the dotted box to obtain an annulus biholomorphic to the standard annulus in the top right. There is a unique cut length for which this annulus admits an involution exchanging the red arcs on the two boundary components. Such an involution gives rise to a branched double cover of the disk.

measure is

$$e(D) = 0 - 2/4 = -1/2.$$

The average multiplicities at the intersection points in question are given by

$$n_{\boldsymbol{y}\times\boldsymbol{a}}(u) = 1/4 + 2/4 = 3/4$$

and

$$n_{\boldsymbol{x}\times\boldsymbol{a}}(u) = 1/4 + 2/4 = 3/4.$$

Thus by Theorem 2.2.5 we have $\mu(u) = -1/2 + 3/2 = 1$. Thus there is a unique index 1 disk from $\boldsymbol{y} \times \boldsymbol{a}$ to $\boldsymbol{x} \times \boldsymbol{a}$.

To finish computing the form of the differential on this chain complex, we would need to analyze the possible orientations of the moduli spaces of disks just discussed. Since we postpone a careful treatment of these orientations until later, we just note here that for any possible orientations, the resulting chain complex will yield the Heegaard Floer homology of S^3 that we computed in the previous examples, as desired. For example, if consideration of orientations showed that:

$$\partial(\boldsymbol{y} \times \boldsymbol{a}) = \boldsymbol{x} \times \boldsymbol{a} + \boldsymbol{z} \times \boldsymbol{a}.$$

then we would obtain

$$\widehat{HF}(\mathcal{H}) = \frac{\mathbb{Z}\langle \boldsymbol{x} \times \boldsymbol{a}, \boldsymbol{z} \times \boldsymbol{a} \rangle}{\mathbb{Z}\langle \boldsymbol{x} \times \boldsymbol{a} + \boldsymbol{z} \times \boldsymbol{a} \rangle} \cong \mathbb{Z}.$$

The computations for other possible orientations are analagous.

2.3. Background on Sutured Manifolds

In order to introduce notation and terminology for the remainder of the dissertation, we give a quick summary of some relevant background on sutured manifolds and Heegaard diagrams. The discussion in this section follows [3]. To unify the approach, the results in [3] are most often phrased in terms of sutured manifolds. Since we are interested here in the closed variants of Heegaard Floer homology, we will set up some background in order to be able to rephrase the results we use from [3] in language more typically used for the closed invariants. We hope this section will serve as a dictionary for the interested reader referencing results we cite from [3].

To begin, we will briefly sketch the necessary background on sutured manifolds and the relation to the closed 3 manifolds of interest to us here. We will then describe the notion of sutured diagrams for sutured manifolds, and see how moves on them relate to the typical Heegaard moves one considers on Heegaard diagrams for closed 3 manifolds. Next we will recall the definition of the graph of sutured isotopy diagrams $\mathcal{G}(\mathcal{S}_{\text{man}})$ introduced in Section I, and describe an isomorphism to a graph $\mathcal{G}_{\text{man}}$ of closed isotopy diagrams which we will consider instead of $\mathcal{G}(\mathcal{S}_{\text{man}})$ throughout the remainder of the dissertation. We refer the reader to [3, Section 2.1] for a more detailed treatment of all of the background in this section.

Sutured Manifolds

In this dissertation a sutured manifold will always refer to the following notion.

Definition 2.3.1. A *sutured manifold* (M, γ) is a compact, connected, oriented 3 manifold M with boundary ∂M, along with a specification of the following data:

1. A collection $\gamma \subset \partial M$ of pairwise disjoint annuli in the boundary of M
2. For each annulus in the collection, an oriented simple closed curve contained in the interior of the annulus, which is homologically nontrivial in the annulus. We call the union of these curves *sutures*, and denote them by $s(\gamma)$.
3. A choice of orientation on each component of $R(\gamma) = \partial M \setminus \text{int}(\gamma)$ which agrees with the orientation on $s(\gamma)$.

We denote by $R^+(\gamma) \subset R(\gamma)$ those components for which the orientation agrees with that of ∂M induced by the orientation on M, and by $R^-(\gamma) \subset R(\gamma)$ those components for which the orientation is the opposite of that of ∂M induced by the orientation on M.

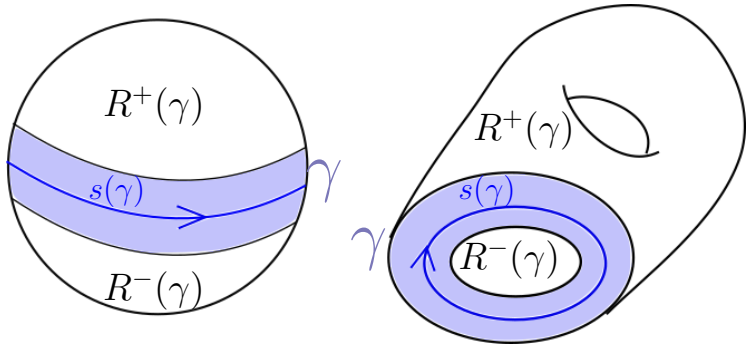

FIGURE 14 Sutured manifold structures on B^3 and $\Sigma \times I$, where Σ is a torus with a disk removed.

Remark 2.3.2. The definition here is less general than the standard definition in the literature, i.e. that introduced by Gabai in [15, Definition 2.6]. In particular, we dismiss here the possibility of toroidal sutures on the boundary.

Remark 2.3.3. We will say a sutured manifold (M, γ) is *proper* if M has no closed components and every boundary component contains at least one suture (i.e. $\pi_0(\gamma) \to \pi_0(\partial M)$ is surjective). In this case, the data of M and γ satisfying the first two conditions in Definition 2.3.1 uniquely specifies orientations on the components of $R(\gamma)$ which give (M, γ) the structure of a sutured manifold. Throughout this dissertation, all sutured manifolds will be assumed to be proper unless otherwise stated.

Sutured Diagrams

We now describe the notion of Heegaard diagrams for sutured manifolds. Throughout the dissertation we will need to keep track of the distinction between genuine Heegaard diagrams, which carry a fixed, concrete set of attaching curves, and isotopy diagrams, in which only the isotopy class of the attaching curves are recorded. We begin with some definitions.

Definition 2.3.4. Given a compact, oriented surface Σ with boundary, we say a one dimensional smooth submanifold $\boldsymbol{\delta} \subset \text{int}(\Sigma)$ is an *attaching set in* Σ if every connected component of $\Sigma \setminus \boldsymbol{\delta}$ contains at least one component of $\partial\Sigma$. For any attaching set $\boldsymbol{\delta}$ in Σ, we denote by $[\boldsymbol{\delta}]$ the isotopy class of the submanifold $\boldsymbol{\delta}$.

Definition 2.3.5. A *sutured diagram* $(\Sigma, \boldsymbol{\alpha}, \boldsymbol{\beta})$ is a compact surface with boundary, Σ, together with two attaching sets $\boldsymbol{\alpha}$ and $\boldsymbol{\beta}$. If $(\Sigma, \boldsymbol{\alpha}, \boldsymbol{\beta})$ is a sutured diagram, we call the data $(\Sigma, [\boldsymbol{\alpha}], [\boldsymbol{\beta}])$ a *sutured isotopy diagram.*

To describe the relationship between sutured diagrams and sutured manifolds, we first describe how a single attaching set gives rise to a sutured manifold.

Definition 2.3.6. A sutured manifold (M, γ) is called a *sutured compression body* if either

1. There is an attaching set $\boldsymbol{\delta}$ in $R^+(\gamma)$ such that compressing $R^+(\gamma)$ inside M along $\boldsymbol{\delta}$ yields a surface which is isotopic to $R^-(\gamma)$ relative to $s(\gamma)$

   or

2. There is an attaching set $\boldsymbol{\delta}$ in $R^-(\gamma)$ such that compressing $R^-(\gamma)$ inside M along $\boldsymbol{\delta}$ yields a surface which is isotopic to $R^+(\gamma)$ relative to $s(\gamma)$

In either case we say that $\boldsymbol{\delta}$ is an attaching set for the sutured compression body (M, γ).

To any attaching set in a surface Σ, we can associate a sutured compression body as follows.

Definition 2.3.7. Given an attaching set $\boldsymbol{\delta}$ in Σ, let $C(\boldsymbol{\delta}) = (M, \gamma)$ be the sutured compression body given by the following data. Let M be the 3 manifold with boundary obtained from $\Sigma \times I$ by attaching 3 dimensional two handles along $\boldsymbol{\delta} \times \{1\} \subset \Sigma \times \{1\}$, let $\gamma = \partial\Sigma \times I$, and let the sutures be given by $s(\gamma) = \partial\Sigma \times \{\frac{1}{2}\}$. We write $C^-(\boldsymbol{\delta}) = R^-(M, \gamma) = \Sigma \times \{0\}$ and $C^+(\boldsymbol{\delta}) = R^+(M, \gamma) = \partial C(\boldsymbol{\delta}) \setminus (C^-(\boldsymbol{\delta}) \cup \gamma)$.

This can be verified to be a sutured compression body by taking the attaching set required in Definition 2.3.6 to be $\boldsymbol{\delta}' := \boldsymbol{\delta} \times \{0\} \subset C^-(\boldsymbol{\delta})$. By construction, compressing $R^-(\gamma)$ along the attaching curve $\boldsymbol{\delta}$ then yields a surface which is isotopic to $R^+(\gamma)$. See Figure 15 for a depiction of this construction.

Definition 2.3.8. Given two attaching sets $\boldsymbol{\delta}$ and $\boldsymbol{\delta}'$ in Σ, we will say they are *compression equivalent*, and write $\boldsymbol{\delta} \sim \boldsymbol{\delta}'$, if the corresponding compression bodies are equivalent in the following sense: there is a diffeomorphism $d : C(\boldsymbol{\delta}) \to C(\boldsymbol{\delta}')$ such that $d|_{C^-(\boldsymbol{\delta})} = \mathrm{id}$. This relation is well defined on isotopy classes, so we will also write $[\boldsymbol{\delta}] \sim [\boldsymbol{\delta}']$ to indicate compression equivalence of isotopy classes.

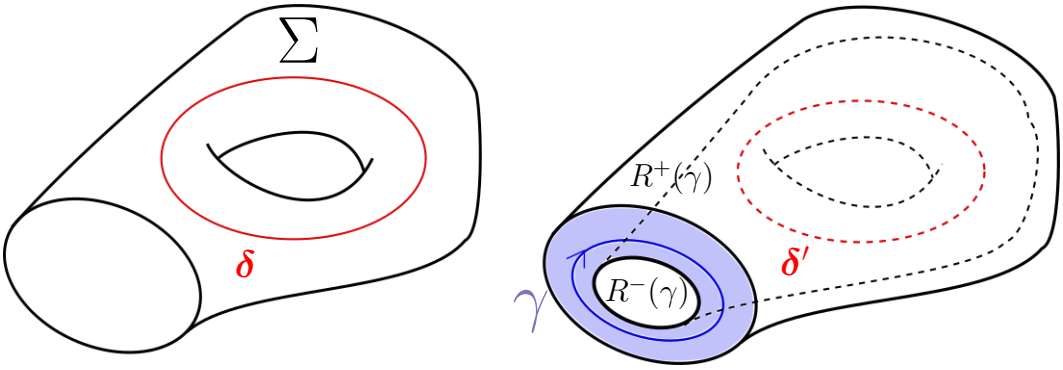

FIGURE 15 The construction of a sutured compression body from a surface Σ with an attaching set $\boldsymbol{\delta}$. On the left is a torus Σ with a disk removed, and an attaching set $\boldsymbol{\delta}$. On the right is the sutured manifold $C(\boldsymbol{\delta})$. The attaching set $\boldsymbol{\delta}'$ in $C^-(\boldsymbol{\delta})$ is a parallel copy of $\boldsymbol{\delta}$ living on $\Sigma \times \{0\}$. Compressing $C^-(\boldsymbol{\delta})$ along it yields a punctured sphere which is isotopic to $C^+(\boldsymbol{\delta})$ relative to the suture $s(\boldsymbol{\gamma})$

Remark 2.3.9. The sutured compression body $C(\boldsymbol{\delta})$ satisfies $\chi(C^+(\boldsymbol{\delta})) = \chi(C^-(\boldsymbol{\delta})) + 2|\boldsymbol{\delta}|$, where $|\boldsymbol{\delta}|$ is the number of connected components in the attaching set $\boldsymbol{\delta}$. Thus if two attaching sets $\boldsymbol{\delta}$ and $\boldsymbol{\delta}'$ are compression equivalent, $\boldsymbol{\delta} \sim \boldsymbol{\delta}'$, then in fact the attaching sets must have the same number of components: $|\boldsymbol{\delta}| = |\boldsymbol{\delta}'|$.

We note that the notion of compression equivalence of attaching sets in a surface Σ corresponds precisely to the notion of sequences of handleslide equivalences of attaching sets in typical Heegaard diagrams.

Definition 2.3.10. Fix two simple closed curves δ and δ'' in a surface Σ, and an embedded closed arc γ in Σ whose endpoints are on δ and δ'' respectively, and whose interior is disjoint from $\delta \cup \delta''$. Then a small neighborhood of $\delta \cup \delta'' \cup \gamma$ in Σ has three boundary components, one isotopic to δ, one isotopic to δ'' and one given by a third curve we denote by δ'. We say δ' is obtained by *handlesliding* δ over δ'' in Σ, or that δ and δ' are *related by a handleslide*.

Given two attaching sets $\boldsymbol{\delta}$ and $\boldsymbol{\delta}'$ in Σ, we say they are *related by a handleslide* if there are two components $\delta_1, \delta_2 \subset \boldsymbol{\delta}$ such that one can handleslide δ_1 over δ_2 along an arc whose interior is disjoint from all of $\boldsymbol{\delta}$ to obtain the curve δ_1', and $(\boldsymbol{\delta} \setminus \delta_1) \cup \delta_1' = \boldsymbol{\delta}'$.

Given two isotopy classes of attaching sets $A = [\boldsymbol{\delta}]$ and $A = [\boldsymbol{\delta}']$, we say they are related by a handleslide if they can be represented by attaching sets which are.

Lemma 2.3.11. *[3, Lemma 2.11] Fix two attaching sets $\boldsymbol{\delta}$ and $\boldsymbol{\delta}'$ in a surface Σ. If $\boldsymbol{\delta}$ and $\boldsymbol{\delta}'$ are related by a handleslide, then $\boldsymbol{\delta} \sim \boldsymbol{\delta}'$. Conversely, if $\boldsymbol{\delta} \sim \boldsymbol{\delta}'$ then $[\boldsymbol{\delta}]$ and $[\boldsymbol{\delta}']$ are related by a sequence of handleslides.*

We are now ready to state the definition of an *embedded sutured diagram* for a sutured manifold (M, γ).

Definition 2.3.12. [3, Definition 2.13] Let (M, γ) be a sutured manifold. We will say that the sutured diagram $(\Sigma, \boldsymbol{\alpha}, \boldsymbol{\beta})$ is an *embedded sutured diagram for* (M, γ) if:

1. Σ is an embedded oriented surface $\Sigma \subset M$ such that $\partial\Sigma = s(\gamma)$ as oriented manifolds.

2. The components in the collection $\boldsymbol{\alpha}$ bound disjoint discs in M on the negative side of Σ, and the components in the collection $\boldsymbol{\beta}$ bound disjoint discs in M on the positive side of Σ.

3. Compressing Σ along $\boldsymbol{\alpha}$ yields a surface which is isotopic to $R^-(\gamma)$ relative to γ

4. Compressing Σ along $\boldsymbol{\beta}$ yields a surface which is isotopic to $R^+(\gamma)$ relative to γ.

We say an isotopy sutured diagram (Σ, A, B) is an *embedded isotopy diagram for* (M, γ) if there is an embedded sutured diagram $(\Sigma, \boldsymbol{\alpha}, \boldsymbol{\beta})$ for (M, γ) with $A = [\boldsymbol{\alpha}]$ and $B = [\boldsymbol{\beta}]$.

We note that as in the case of Heegaard splittings, all sutured manifolds (M, γ) admit embedded sutured diagrams for (M, γ) ([3, Lemma 2.14]). Conversely, from any (abstract) sutured diagram one can construct a sutured manifold for which the sutured diagram is in fact an embedded sutured diagram (via the same sort of construction mentioned for compression bodies earlier, but applied now to both attaching sets). This construction yields a well defined diffeomorphism type of sutured manifold which only depends on the underlying abstract isotopy diagram. Thus for an abstract isotopy diagram H, we denote by $S(H)$ the diffeomorphism type of sutured manifold arising from this construction.

Moves on Sutured Diagrams

We now discuss the set of moves on sutured diagrams we will be considering throughout this dissertation. They will play a role analogous to that of pointed Heegaard moves on Heegaard diagrams for closed 3-manifolds. In fact, we will make this correspondence more precise in the next subsection.

Definition 2.3.13. Given two isotopy diagrams (Σ_1, A_1, B_1) and (Σ_2, A_2, B_2), we say they are $\boldsymbol{\alpha}$-*equivalent* if $\Sigma_1 = \Sigma_2$, $B_1 = B_2$ and $A_1 \sim A_2$. We say they are $\boldsymbol{\beta}$-*equivalent* if $\Sigma_1 = \Sigma_2$, $A_1 = A_2$ and $B_1 \sim B_2$.

Definition 2.3.14. We say the sutured diagram $(\Sigma_2, \boldsymbol{\alpha}_2, \boldsymbol{\beta}_2)$ is obtained from $(\Sigma_1, \boldsymbol{\alpha}_1, \boldsymbol{\beta}_1)$ by a *stabilization*, or equivalently that $(\Sigma_1, \boldsymbol{\alpha}_1, \boldsymbol{\beta}_1)$ is obtained from $(\Sigma_2, \boldsymbol{\alpha}_2, \boldsymbol{\beta}_2)$ by *destabilization* if:

1. There is a disc $D_1 \subset \Sigma_1$ and a punctured torus $T_2 \subset \Sigma_2$ such that $\Sigma_1 \setminus D_1 = \Sigma_2 \setminus T_2$.

2. $\boldsymbol{\alpha}_1 = \boldsymbol{\alpha}_2 \cap (\Sigma_2 \setminus T_2)$

3. $\boldsymbol{\beta}_1 = \boldsymbol{\beta}_2 \cap (\Sigma_2 \setminus T_2)$

4. $\boldsymbol{\alpha}_2 \setminus \boldsymbol{\alpha}_1 := \alpha_2$ and $\boldsymbol{\beta}_2 \setminus \boldsymbol{\beta}_1 := \beta_2$ are simple closed curves in T_2 which intersect transversely in a single point.

   A schematic of such a stabilized diagram is depicted in Figure 16.

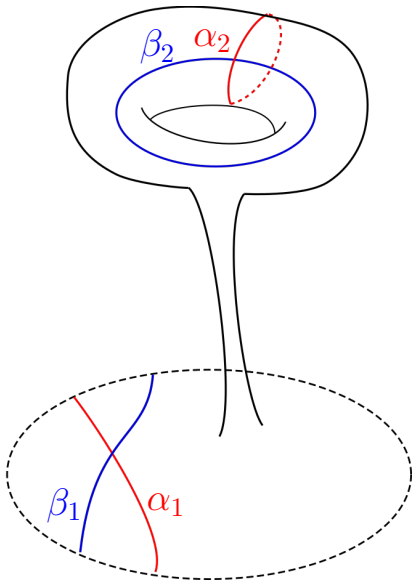

FIGURE 16 A region of the Heegaard diagram $(\Sigma_1, \boldsymbol{\alpha}_1, \boldsymbol{\beta}_1)$ is depicted in the dashed circle, with two attaching curves $\alpha_1 \in \boldsymbol{\alpha}_1$ and $\beta_1 \in \boldsymbol{\beta}_1$. The standard genus 1 diagram for S^3 has been attached via a connect sum to the this region, resulting in the stabilized diagram $(\Sigma_2, \boldsymbol{\alpha}_2, \boldsymbol{\beta}_2)$.

Given isotopy diagrams H_1 and H_2, we say they are related by a stabilization/destabilization if these conditions hold for some representatives of the isotopy classes of attaching sets.

Definition 2.3.15. Let $H_1 = (\Sigma_1, A_1, B_1)$ and $H_2 = (\Sigma_2, A_2, B_2)$ be isotopy diagrams for sutured manifolds. A *diffeomorphism of isotopy diagrams* $d : H_1 \to H_2$ is an orientation preserving diffeomorphism $d : \Sigma_1 \to \Sigma_2$ such that $d(A_1) = A_2$ and $d(B_1) = B_2$. Here for an isotopy class A_1 of an attaching set on Σ_1, we mean by $d(A_1)$ the isotopy class $[d(\boldsymbol{\alpha})]$ for some representative $\boldsymbol{\alpha}$ of A_1.

As we will describe in Section , sutured manifolds representing the same 3-manifold can always be connected by a sequence of the aforementioned moves.

A Correspondence Between Closed and Sutured Manifolds

Since our goal in this dissertation is to ultimately establish facts about the Heegaard Floer invariants for closed 3 manifolds, we now describe how we can move between sutured and closed manifolds in the cases of interest. We will need to understand certain properties of this correspondence to ensure that the techniques used to obtain functoriality in [3] which we import can be applied to the closed setting of interest here.

First, suppose (M, γ) is a sutured manifold, with $\partial M \cong S^2$ and a single suture $s(\gamma)$. Then one can take the quotient $Y = M/S^2$ to obtain a closed, oriented 3-manifold. The fact that $\partial M \cong S^2$ ensures this operation is a topological manifold, and the fact that we are in dimension 3 ensures this operation can be smoothed uniquely. We view the result as a based

3-manifold (Y, p), with basepoint p given by the equivalence class of the boundary, $p = [\partial M]$.

Conversely, given any closed, connected, oriented and based 3-manifold (Y, p), and an oriented two dimensional subspace $V \subset T_pM$, one can construct a sutured manifold $(Y(p, V), \gamma)$ with boundary S^2 and a single suture $s(\gamma)$. To describe the construction, we recall the following notion of a spherical blow up. We only sketch the idea of the construction and refer the reader to [16] for a precise formulation of the definition.

Definition 2.3.16. Given a 3-manifold M, and an embedded submanifold $L \subset M$, denote the normal bundle of L in M by $N(L)$, and the corresponding sphere bundle by $S(N(L))$. Then the *spherical blowup of M along L* is the 3-manifold with boundary obtained by replacing x for each $x \in L$ with the fiber $S(N(L))_x$. We denote this blow up by $\mathrm{Bl}_L M$. Equivalently, it is the 3 manifold $M \setminus \mathrm{int}(D(N(L)))$, where $D(N(L))$ is the unit disc bundle of $N(L)$.

With this in hand, we construct a sutured manifold from a closed one as follows.

Definition 2.3.17. Fix a closed, connected, oriented 3 manifold Y, a basepoint $p \in Y$, and an oriented two plane $V \subset T_pY$. The oriented two plane V specifies an oriented curve $s(\gamma) \subset \partial(\mathrm{Bl}_pY) \cong S^2$. We denote by $(Y(p, V), \gamma)$ the sutured manifold with underlying 3-manifold $Y(p, V) = \mathrm{Bl}_pY$, $s(\gamma)$ the curve specified by V, and γ a small tubular neighborhood of $s(\gamma)$ in $\partial(\mathrm{Bl}_pY) \cong S^2$.

Since the suture data in this construction is defined using only the data Y, p, and V, we will denote both the resulting 3-manifold with boundary and the sutured manifold by $Y(p, V)$.

Remark 2.3.18. The sutured manifolds $Y(p, V)$ arising from this construction have boundary S^2 and a single suture.

Graphs of Heegaard Diagrams

Following [3, Definition 2.22], construct a directed graph $\mathcal{G}$ as follows. The class of vertices, $|\mathcal{G}|$, of $\mathcal{G}$ is given by the class of isotopy diagrams of sutured manifolds. Given two isotopy diagrams $H_1, H_2 \in |\mathcal{G}|$, the oriented edges from H_1 to H_2 come in four flavors

$$\mathcal{G}(H_1, H_2) = \mathcal{G}_\alpha(H_1, H_2) \cup \mathcal{G}_\beta(H_1, H_2) \cup \mathcal{G}_{\text{stab}}(H_1, H_2) \cup \mathcal{G}_{\text{diff}}(H_1, H_2).$$

Here

1. $\mathcal{G}_\alpha(H_1, H_2)$ consists of a single edge if the diagrams are $\boldsymbol{\alpha}$-equivalent.
2. $\mathcal{G}_\beta(H_1, H_2)$ consists of a single edge if the diagrams are $\boldsymbol{\beta}$-equivalent.
3. $\mathcal{G}_{\text{stab}}(H_1, H_2)$ consists of a single edge if the diagrams are related by a stabilization or destabilization.
4. $\mathcal{G}_{\text{diff}}(H_1, H_2)$ consists of a collection of edges, with one edge for each diffeomorphism between the isotopy diagrams.

We denote by $\mathcal{G}_\alpha, \mathcal{G}_\beta, \mathcal{G}_{\text{stab}}$ and $\mathcal{G}_{\text{diff}}$ the subgraphs of $\mathcal{G}$ arising from only considering the corresponding edges on the class of vertices $|\mathcal{G}|$.

We can now state precisely the following analog of the Reidemeister Singer theorem for sutured manifolds (applied to sutured *diagrams*) alluded to earlier:

Proposition 2.3.19. *[3, Proposition 2.23] Two isotopy diagrams H_1, $H_2 \in |\mathcal{G}|$ can be connected by an oriented path in $\mathcal{G}$ if and only if they define diffeomorphic sutured manifolds.*

Remark 2.3.20. By the definition of $\mathcal{G}$, if there is an unoriented path from H_1 to H_2 then there is also an oriented path from H_1 to H_2.

Given any set $\mathcal{S}$ of diffeomorphism types of sutured manifolds, denote by $\mathcal{G}(\mathcal{S})$ the full subgraph of $\mathcal{G}$ spanned by those isotopy diagrams H for which $S(H) \in \mathcal{S}$. For our purposes, the case of interest will be $\mathcal{S} = \mathcal{S}_{\text{man}}$. This is the set of diffeomorphism types of sutured manifolds which arise as $[Y(p, V)]$, where (Y, p) is a closed, oriented, based 3-manifold, and $V \subset T_pY$ is an oriented 2-plane.

Thus the vertices of $\mathcal{G}(\mathcal{S}_{\text{man}})$ correspond to isotopy diagrams H for sutured manifolds which arise as $Y(p, V)$ for a closed, oriented 3-manifold Y. Given an actual (rather than isotopy) sutured diagram $\mathcal{H} = (\Sigma, \boldsymbol{\alpha}, \boldsymbol{\beta})$ for such a 3-manifold $Y(p, V)$, the boundary of the Heegaard surface Σ is S^1, so it can be quotiented to a point to obtain a closed surface $\overline{\Sigma}$ and a pointed Heegaard diagram $\overline{\mathcal{H}} = (\overline{\Sigma}, \boldsymbol{\alpha}, \boldsymbol{\beta}, z)$ for Y, where the basepoint z is given by the equivalence class of the image of the boundary of Σ under the quotient. Under this correspondence, isotopies of attaching curves in the sutured diagram $\mathcal{H}$ yield *pointed* isotopies (i.e. isotopies which do not cross the basepoint z) of attaching curves in $\overline{\mathcal{H}}$. Thus a sutured

isotopy diagram H specifies a pointed isotopy diagram $\overline{H}$. It is clear that diffeomorphisms of sutured isotopy diagrams $d : H_1 \to H_2$ as in Definition 2.3.15 correspond bijectively to pointed diffeomorphisms of pointed isotopy diagrams $d : \overline{H_1} \to \overline{H_2}$. It also is immediate that stabilizations of sutured isotopy diagrams correspond to stabilizations of pointed isotopy diagrams. By Lemma 2.3.11, two sutured isotopy diagrams $H_1 = (\Sigma, \boldsymbol{\alpha}_1, \boldsymbol{\beta}_1)$ and $H_2 = (\Sigma, \boldsymbol{\alpha}_2, \boldsymbol{\beta}_2)$ are $\boldsymbol{\alpha}$-equivalent if and only if the curves $\boldsymbol{\alpha}_1$ and $\boldsymbol{\alpha}_2$ are related by a sequence of handleslides in the pointed isotopy diagrams $\overline{H_1}$ and $\overline{H_1}$, where the handleslides never cross the basepoint. The analogous statement holds for $\boldsymbol{\beta}$-equivalent sutured isotopy diagrams. Since these sorts of equivalences will play a prominent role throughout the dissertation, we introduce terminology introduced in [2] to describe them:

Definition 2.3.21. Given two closed, pointed Heegaard diagrams $\mathcal{H}_1 = (\Sigma, \boldsymbol{\alpha}_1, \boldsymbol{\beta}_1, z)$ and $\mathcal{H}_2 = (\Sigma, \boldsymbol{\alpha}_2, \boldsymbol{\beta}_2, z)$ we say they are *strongly equivalent* if they are related by a sequence of isotopies and handleslides which do not cross the basepoint. If the diagrams are related by a sequence of isotopies, and handleslides which occur only among the $\boldsymbol{\alpha}$ curves, we say the diagrams are *strongly $\boldsymbol{\alpha}$-equivalent*. If the diagrams are related by a sequence of isotopies, and handleslides which occur only among the $\boldsymbol{\beta}$ curves, we say the diagrams are *strongly $\boldsymbol{\beta}$-equivalent*.

Let $\mathcal{G}_{\text{man}}$ be the oriented graph with vertices given by pointed isotopy Heegaard diagrams of closed, connected 3 manifolds, and with the edges from an isotopy diagram H_1 to an isotopy diagram H_2 given by

$$\mathcal{G}_{\text{man}}(H_1, H_2) = \mathcal{G}^{\alpha}_{\text{man}}(H_1, H_2) \cup \mathcal{G}^{\beta}_{\text{man}}(H_1, H_2) \cup \mathcal{G}^{\text{stab}}_{\text{man}}(H_1, H_2) \cup \mathcal{G}^{\text{diff}}_{\text{man}}(H_1, H_2)$$

where

1. $\mathcal{G}^{\alpha}_{\text{man}}(H_1, H_2)$ consists of a single edge if the diagrams are strongly $\boldsymbol{\alpha}$-equivalent.

2. $\mathcal{G}^{\beta}_{\text{man}}(H_1, H_2)$ consists of a single edge if the diagrams are strongly $\boldsymbol{\beta}$-equivalent.

3. $\mathcal{G}^{\text{stab}}_{\text{man}}(H_1, H_2)$ consists of a single edge if the diagrams are related by a stabilization or destabilization.

4. $\mathcal{G}^{\text{diff}}_{\text{man}}(H_1, H_2)$ consists of a collection of edges, with one edge for each pointed diffeomorphism between the isotopy diagrams.

We provide a sketch of a piece of the graph $\mathcal{G}_{\text{man}}$ in Figure 17 below. The following analog of Proposition 2.3.19 holds in the closed and pointed setting:

Proposition 2.3.22. *[1, Proposition 7.1] Two isotopy diagrams H_1, $H_2 \in |\mathcal{G}_{man}|$ can be connected by an oriented path in $\mathcal{G}_{man}$ if and only if they define diffeomorphic pointed manifolds.*

The preceding arguments specify an isomorphism of graphs

$$T : \mathcal{G}(\mathcal{S}_{\text{man}}) \to \mathcal{G}_{\text{man}} \tag{2.1}$$

which we will use implicitly in the remainder of the dissertation to rephrase certain results from [3] in terms of $\mathcal{G}_{\text{man}}$.

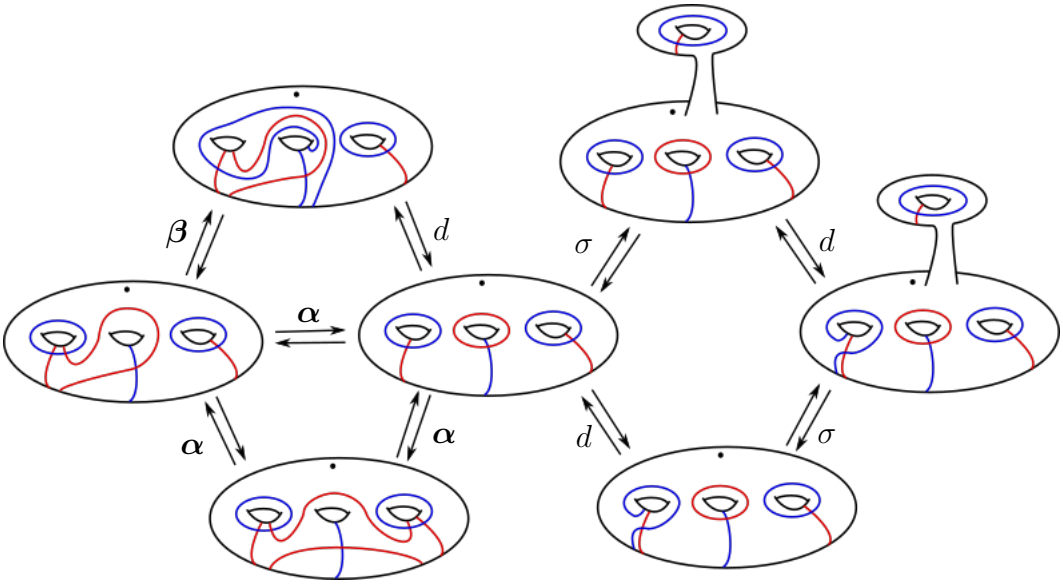

FIGURE 17 An illustration of a small subgraph in $\mathcal{G}_{\text{man}}$. The vertices are isotopy diagrams, which in the picture are depicted by particular Heegaard diagrams representing the isotopy class. We label each pair of edges with $\boldsymbol{\alpha}, \boldsymbol{\beta}, \sigma$ or d according to whether the given pair of edges corresponds to a strong $\boldsymbol{\alpha}$-equivalence, a strong $\boldsymbol{\beta}$-equivalence, a stabilization/destabilization pair, or a diffeomorphism pair respectively. We use the convention that on each Heegaard diagram the collection of red attaching curves is denoted $\boldsymbol{\alpha}$ while the collection of blue attaching curves is denoted $\boldsymbol{\beta}$.

2.4. Heegaard Invariants

We now make precise two notions of what one might mean by a Heegaard invariant of closed 3-manifolds. For the interested reader's convenience, we note that the definitions originally given in [3] apply to sutured manifolds and the graph $\mathcal{G}(\mathcal{S}_{\text{man}})$. Instead, we state here the equivalent definitions phrased in terms of closed manifolds and the graph $\mathcal{G}_{\text{man}}$.

Suppose we produce some assignment of algebraic objects to Heegaard diagrams (the vertices of the graph $\mathcal{G}_{\text{man}}$), and an assignment of maps between these algebraic objects to each Heegaard move between two

diagrams (the edges of $\mathcal{G}_{\text{man}}$). Given Proposition 2.3.22, the minimal requirement we should ask of such an assignment to obtain an invariant of the underlying 3-manifold is for edges in $\mathcal{G}_{\text{man}}$ to be assigned isomorphisms. Given any category $\mathcal{C}$, we have:

Definition 2.4.1. [3, Compare Definition 2.24] A *weak Heegaard invariant of closed* 3*-manifolds* is a morphism of graphs $F : \mathcal{G}_{\text{man}} \to \mathcal{C}$ for which $F(e)$ is an isomorphism for all edges $e \in \mathcal{G}_{\text{man}}$.

Of course, this level of invariance was established for Heegaard Floer homology at the outset.

Theorem 2.4.2 ([1])**.** *The morphisms*

$$\widehat{HF}, HF^-, HF^+, HF^\infty : \mathcal{G}_{man} \to \mathbb{F}_2[U]\text{-}Mod$$

and

$$\widehat{HF}, HF^-, HF^+, HF^\infty : \mathcal{G}_{man} \to \mathbb{Z}[U]\text{-}Mod$$

are weak Heegaard invariants of closed 3*-manifolds.*

The above results also immediately yield

Corollary 2.4.3. *The morphisms*

$$HF^\circ : \mathcal{G}_{man} \to P(\mathbb{Z}[U]\text{-}Mod)$$

are weak Heegaard invariants of closed 3*-manifolds.*

In Section 2.7 we will recall the definition of these morphisms of graphs precisely. In particular, since the vertices of $\mathcal{G}_{\text{man}}$ are isotopy diagrams, we

will need to explain the meaning of $HF^\circ(H)$ when H is an isotopy diagram rather than a particular Heegaard diagram representing the isotopy class.

Remark 2.4.4. For the reader referencing the corresponding results stated in [3], we note that in [3, Theorem 2.26], Theorem 2.4.2 is instead phrased as "$HF^\circ : \mathcal{G}(\mathcal{S}_{\text{man}}) \to \mathbb{F}_2[U]$-Mod are weak Heegaard invariants". Of course, as they were originally defined HF° are invariants assigned to closed, pointed Heegaard diagrams; the meaning of $HF^\circ(H)$ for H a sutured isotopy diagram in this statement is interpreted as follows. Recall that vertices of $\mathcal{G}(\mathcal{S}_{\text{man}})$ correspond to isotopy diagrams H of sutured manifolds which arise as $Y(p, V)$ for a closed, oriented 3-manifold Y. Given an actual sutured diagram $\mathcal{H} = (\Sigma, \boldsymbol{\alpha}, \boldsymbol{\beta})$ (not up to isotopy) for such a 3-manifold $Y(p, V)$, the boundary of the Heegaard surface Σ is S^1, so it can be capped off with a disk to obtain a closed surface $\overline{\Sigma}$ and a pointed Heegaard diagram $\overline{\mathcal{H}} = (\overline{\Sigma}, \boldsymbol{\alpha}, \boldsymbol{\beta}, z)$ for Y, where the basepoint z is chosen to lie in the disk. Thus given a sutured diagram $\mathcal{H}$ representing the isotopy diagram H, we define $CF^\circ(\mathcal{H}) := CF^\circ(\overline{\mathcal{H}})$. Finally, we will describe how the collection $\{CF^\circ(\mathcal{H})\}$ gives rise to $CF^\circ(H)$ in Section . Equivalently, using the isomorphism of graphs T specified in Equation (2.1), the definitions above will amount to defining $HF^\circ(H) := HF^\circ(T(H))$ for H a sutured isotopy diagram.

Let Man_* be the category whose class of objects consists of closed, connected, oriented and based 3-manifolds, and whose morphisms are basepoint preserving diffeomorphisms. In [1] and [2], significant progress was made towards showing that the weak Heegaard invariants in the theorem above can in fact be assembled into functors from Man_* to $\mathbb{F}_2[U]$-Mod.

However, there was a gap in the proof. In [3], the authors carefully analyzed the dependence of such a result on the nature of embedded (versus abstract) Heegaard diagrams, and basepoints, and set up a framework which allowed them to finish this program. To do so, they introduced a stronger notion of a Heegaard invariant which we now describe.

To begin, we introduce some terminology for particular subgraphs in $\mathcal{G}_{\text{man}}$ (or more generally in $\mathcal{G}$) which will serve as minimal data on which this new notion of invariance will rely.

Definition 2.4.5. [3, Definition 2.29] A *distinguished rectangle* is a subgraph of $\mathcal{G}_{\text{man}}$ of the form

$$\begin{array}{ccc} H_1 & \xrightarrow{e} & H_2 \\ \downarrow{\scriptstyle f} & & \downarrow{\scriptstyle g} \\ H_3 & \xrightarrow{h} & H_4 \end{array}$$

which satisfies one of the following conditions:

1. The arrows e and h are strong $\boldsymbol{\alpha}$-equivalences, and the arrows f and g are strong $\boldsymbol{\beta}$-equivalences.

2. The arrows e and h are either both strong $\boldsymbol{\alpha}$-equivalences or both strong $\boldsymbol{\beta}$-equivalences, and the arrows f and g are stabilizations.

3. The arrows e and h are either both strong $\boldsymbol{\alpha}$-equivalences or both strong $\boldsymbol{\beta}$-equivalences, and the arrows f and g are diffeomorphisms. Furthermore, $f = g$ (Note in this case $\Sigma_1 = \Sigma_2$, and $\Sigma_3 = \Sigma_4$, so this requirement makes sense).

4. All of the arrows e, f, g and h are stabilizations. Furthermore, there are disjoint disks $D_1, D_2 \subset \Sigma_1$ and disjoint punctured tori $T_1, T_2 \subset \Sigma_4$ such that $\Sigma_1 \setminus (D_1 \cup D_2) = \Sigma_4 \setminus (T_1 \cup T_2)$, $\Sigma_2 = (\Sigma_1 \setminus D_1) \cup T_1$, and $\Sigma_3 = (\Sigma_1 \setminus D_2) \cup T_2$.

5. The arrows e and h are stabilizations, and the arrows f and g are diffeomorphisms. Furthermore, the diffeomorphism g is an extension of the diffeomorphism f in the following sense. There are disks $D_1 \subset \Sigma_1$, $D_3 \subset \Sigma_3$ and punctured tori $T_2 \subset \Sigma_2$, $T_4 \subset \Sigma_4$ such that $\Sigma_1 \setminus D_1 = \Sigma_2 \setminus T_2$, $\Sigma_3 \setminus D_3 = \Sigma_4 \setminus T_4$, $f(D_1) = D_2$, $g(T_3) = T_4$ and $f|_{\Sigma_1 \setminus D_1} = g|_{\Sigma_2 \setminus T_2}$.

We illustrate cases 4 and 5 schematically in Figures 18 and 19 below.

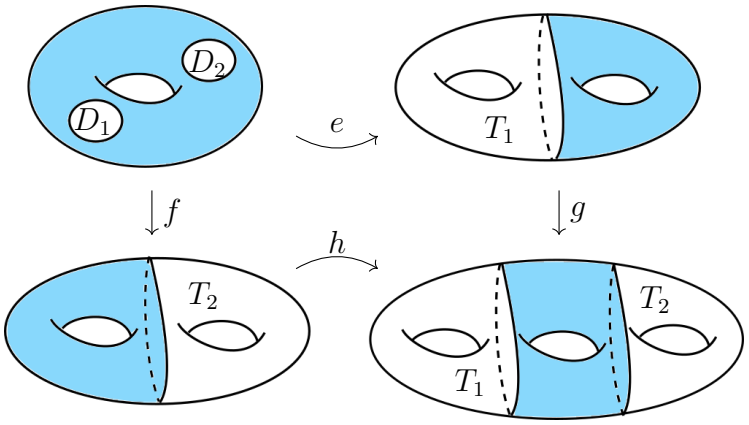

FIGURE 18 A schematic illustrating case 4 in the definition of a distinguished rectangle. The blue regions indicate the identifications specified in case 4. For ease of visualization, we suppress the attaching curve data in the initial diagram and in the stabilizations.

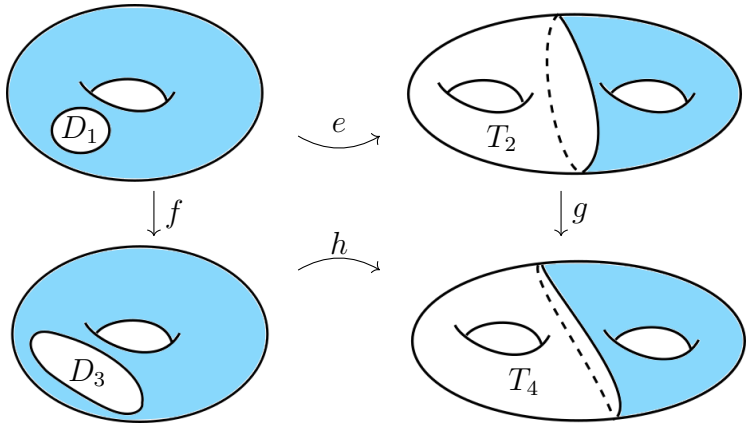

FIGURE 19 A schematic illustrating case 5 in the definition of a distinguished rectangle. The blue regions indicate the identifications of the regions specified in case 5. For ease of visualization, we suppress the attaching curve data in each diagram.

Definition 2.4.6. [3, Definition 2.31] A *simple handleswap* is a subgraph of $\mathcal{G}_{\text{man}}$ of the form

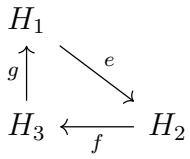

such that:

1. The isotopy diagrams H_i are given by $H_i = (\Sigma \# \Sigma_0, [\boldsymbol{\alpha}_i], [\boldsymbol{\beta}_i])$, where Σ_0 is a genus two surface.

2. e is a strong $\boldsymbol{\alpha}$-equivalence, f is a strong $\boldsymbol{\beta}$-equivalence, and g is a diffeomorphism.

3. In the punctured genus two surface $P = (\Sigma \# \Sigma_0) \setminus \Sigma$, the above triangle is equivalent to the triangle in Figure 20 in the following sense. There are diffeomorphisms from $P \cap H_i$ to the green discs labeled H_i in the figure, such that the image of the α curves are the red circles in

the figures, and the image of the β curves are the blue circles in the figures.

4. The diagrams H_1, H_2 and H_3 are identical when restricted to Σ.

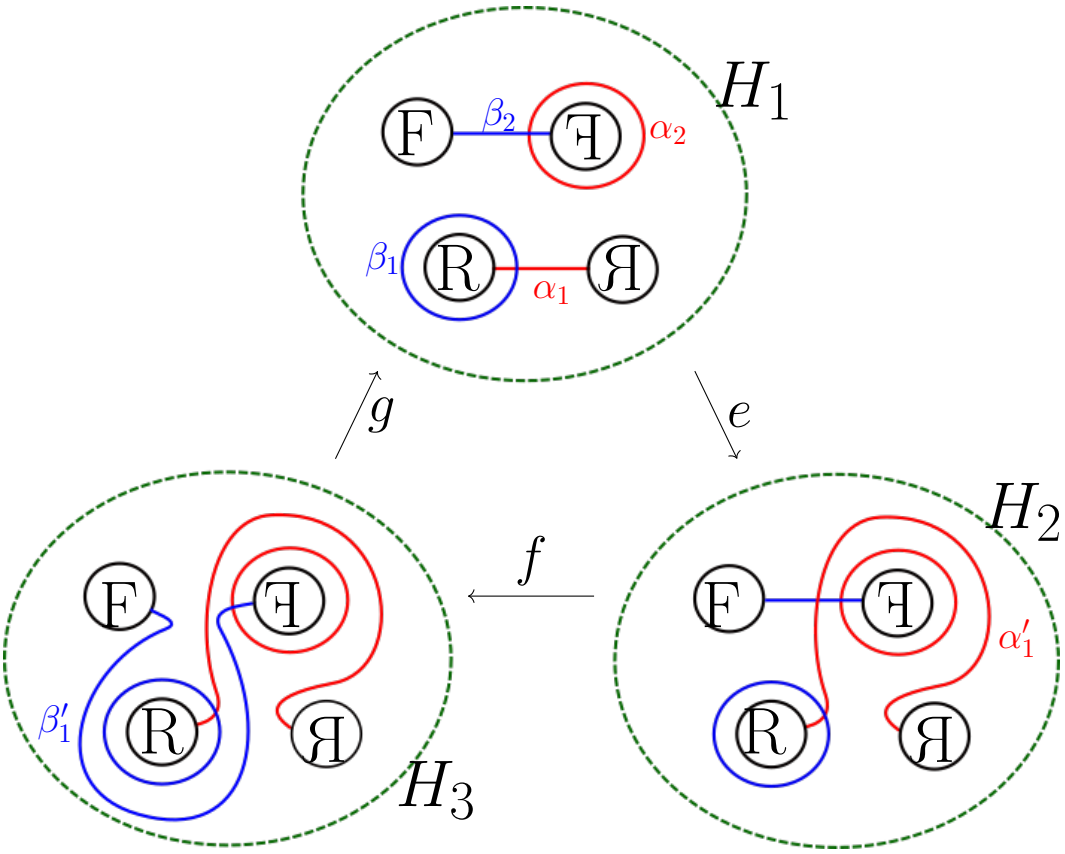

FIGURE 20 The standard simple handleswap.

With these notions in hand, the stronger sense of invariance we will ask of our Heegaard invariants is as follows.

Definition 2.4.7. [3, Definition 2.32] A *strong Heegaard invariant of closed 3-manifolds* is a weak Heegaard invariant $F : \mathcal{G}_{\text{man}} \to \mathcal{C}$ that additionally satisfies the following axioms:

1. **Functoriality**: The restriction of F to $\mathcal{G}^{\alpha}_{\text{man}}$, $\mathcal{G}^{\beta}_{\text{man}}$ and $\mathcal{G}^{\text{diff}}_{\text{man}}$ are functors to $\mathcal{C}$. If $e : H_1 \to H_2$ is a stabilization and $e' : H_2 \to H_1$ is the corresponding destabilization, then $F(e') = F(e)^{-1}$.

2. **Commutativity**: For every distinguished rectangle in $\mathcal{G}_{\text{man}}$,

$$\begin{array}{ccc} H_1 & \xrightarrow{e} & H_2 \\ \downarrow{\scriptstyle f} & & \downarrow{\scriptstyle g} \\ H_3 & \xrightarrow{h} & H_4 \end{array}$$

   we have $F(g) \circ F(e) = F(h) \circ F(f)$.

3. **Continuity**: If $H \in |\mathcal{G}_{\text{man}}|$ and $e \in \mathcal{G}^{\text{diff}}_{\text{man}}(H, H)$ is a diffeomorphism isotopic to Id_{Σ}, then $F(e) = \text{Id}_{F(H)}$.

4. **Handleswap Invariance**: For every simple handleswap in $\mathcal{G}_{\text{man}}$,

$$\begin{array}{ccc} H_1 & & \\ {\scriptstyle g}\uparrow & \searrow^{e} & \\ H_3 & \xleftarrow[f]{} & H_2 \end{array}$$

   we have $F(g) \circ F(f) \circ F(e) = \text{Id}_{F(H_1)}$.

As we will summarize in Section 2.6, it was shown in [3] that for any weak Heegaard invariant the axioms required above are sufficient to ensure the images of the invariant, when restricted to a particular subgraph of $\mathcal{G}_{\text{man}}$ whose vertices represent a fixed 3-manifold, form a transitive system in the given category. For certain categories $\mathcal{C}$, this in turn is enough to ensure

that the assignments of the invariants can be understood as a functor from an appropriate category of 3-manifolds.

2.5. Transitive Systems

In this section we describe the algebraic framework which will be necessary to phrase our projective functoriality results. To begin with, we recall the following fundamental notions.

Definition 2.5.1. A *directed set* $(I, \leq)$ is a set I together with a reflexive and transitive binary relation $\leq$, such that for every pair of elements $a, b \in I$ there is an element $c \in I$ with $a \leq c$ and $b \leq c$.

Definition 2.5.2. Let $\mathcal{C}$ be a category, and $(I, \leq)$ be a directed set. Given a collection of objects $\{O_i\}$ in $\mathcal{C}$ indexed by I, and a collection of morphisms $\{f_{i,j} : O_i \to O_j\}$ for all $i, j \in I$ with $i \leq j$, we say the collections are a *transitive system in $\mathcal{C}$ (indexed by I)* if they satisfy:

1. $f_{i,i} = \mathrm{Id}_{O_i}$
2. $f_{i,k} = f_{j,k} \circ f_{i,j}$

We also have the following notion of morphisms between transitive systems:

Definition 2.5.3. Given two transitive systems $T_1 = \{I_1, \leq, \{O_i\}, \{f_{i,j}\}\}$ and $T_2 = \{I_2, \leq, \{P_i\}, \{g_{i,j}\}\}$ in a category $\mathcal{C}$, a *morphism of transitive systems* $(M, \{n_i\})$ from T_1 to T_2 consists of a map of directed sets $M : I_1 \to I_2$ and a collection of morphisms $\{n_i : O_i \to P_{M(i)}\}$ in $\mathcal{C}$ such that for all

$i, j \in I_1$ with $i \leq j$ the squares

$$\begin{array}{ccc} O_i & \xrightarrow{n_i} & P_{M(i)} \\ \downarrow{\scriptstyle f_{i,j}} & & \downarrow{\scriptstyle g_{M(i),M(j)}} \\ O_j & \xrightarrow{n_j} & P_{M(j)} \end{array}$$

commute in $\mathcal{C}$. We denote the resulting category of transitive systems in $\mathcal{C}$ by Trans($\mathcal{C}$).

Finally, given a transitive system in Trans($\mathcal{C}$) indexed by J, we obtain what one might call a two dimensional transitive system. Such a two dimensional transitive system naturally has the structure of a transitive system in $\mathcal{C}$ indexed by $I \times J$, where $(i, j) \leq (i', j')$ if and only if $i \leq i'$ and $j \leq j'$.

We now explain how these notions will arise in the context of our results. We will begin by considering the category Kom($\mathbb{Z}[U]$-Mod), the homotopy category of chain complexes of $\mathbb{Z}[U]$-modules. To each pointed isotopy diagram H, corresponding to a vertex of $\mathcal{G}_{\text{man}}$, we will assign a transitive system $CF^-(H) \in$ Trans(Kom($\mathbb{Z}[U]$-Mod)). To a diffeomorphism, strong $\boldsymbol{\alpha}$-equivalence, strong $\boldsymbol{\beta}$-equivalence, or stabilization between two such isotopy diagrams H_1 and H_2 we will associate a morphism of transitive systems from $CF^-(H_1)$ to $CF^-(H_2)$. Together, these assignments will yield a morphism of graphs

$$CF^- : \mathcal{G}_{\text{man}} \to \text{Trans}(\text{Kom}(\mathbb{Z}[U]\text{-Mod})).$$

This morphism of graphs may not be a strong Heegaard invariant. We will however be able to establish that this morphism of graphs satisfies the axioms required of a strong Heegaard invariant up to an overall sign in each of the axioms (2), (3) and (4) appearing Definition 2.4.7.

Equivalently, we will phrase this result in terms of an appropriate projectivization. Recall that given any category $\mathcal{C}$, with an equivalence relation $\sim$ on every hom set which furthermore respects composition, we may form the quotient category $\mathcal{C} = \mathcal{C}/\sim$. This is the category whose objects are those of $\mathcal{C}$, and whose morphisms are equivalence classes of morphisms with respect to $\sim$. Given an additive category $\mathcal{C}$, we define the *projectivization of* $\mathcal{C}$, $P(\mathcal{C})$, to be the quotient category of $\mathcal{C}$ with respect to the relation $f \sim -f$ for all morphisms f. The last statement in the preceding paragraph is then given precisely by the following statement: considering now the category of transitive systems in the projectivized homotopy category, $\mathrm{Trans}(P(\mathrm{Kom}(\mathbb{Z}[U]\text{-Mod})))$, we will show that the morphism of graphs above yields a strong Heegaard invariant

$$CF^- : \mathcal{G}_{\mathrm{man}} \to \mathrm{Trans}(P(\mathrm{Kom}(\mathbb{Z}[U]\text{-Mod}))).$$

Remark 2.5.4. While the proliferation of transitive systems may seem undesirable, we were unable to produce another framework in which our naturality results could be phrased. There appear to be two issues that arise if one tries to use the same framework developed in [3] to phrase our projective results.

The first issue comes from the fact that the statement in Theorem 1.3.3 is concerned with the Floer chain complexes. If one wanted to dispense

with the category of transitive systems appearing in that statement, one would need to assign a *single* chain complex $CF^\circ(H)$ of $\mathbb{Z}[U]$-modules to an isotopy diagram H. As we will recall in the next section, what the Heegaard Floer construction actually produces for each isotopy diagram H is a transitive system of chain homotopy equivalences between chain complexes of $\mathbb{Z}[U]$-modules. In general, it is not clear how one should define an object like a colimit of such a transitive system of chain complexes to obtain a single chain complex. We note that it seems likely that this issue is in fact a non-issue, for the following reason. We expect our transitive system of chain homotopy equivalences is homotopy coherent in the sense of [17], which if true would allow one to define a single chain complex $CF^\circ(H)$ via a homotopy colimit. Indeed, that our transitive systems are homotopy coherent in this sense seems likely to follow from the results in [18].

However, even if one could assign to each isotopy diagram a single chain complex $CF^\circ(H)$, there is another key obstruction to phrasing Theorem 1.3.1 without the use of transitive systems. In the proof of Theorem 1.3.1, which will be given in Section 2.6, we will associate to each closed, pointed 3-manifold a transitive system in $P(\mathbb{Z}[U]\text{-Mod})$. The author is unaware of a notion of a colimit in $P(\mathbb{Z}[U]\text{-Mod})$ which would allow Theorem 1.3.1 to be stated without transitive systems, in such a way that it is also not merely reduced to a statement about the $\mathbb{F}_2$ invariants.

2.6. Projective Naturality from Strong Heegaard Invariants

In this section we prove Theorem 1.3.1 assuming Corollary 1.3.4, which we will prove in turn in Section 2.8. Our argument will follow the

same logical structure as that used to prove the analogous result over $\mathbb{F}_2$ appearing in [3, Theorem 1.5]. We provide the argument here for the reader's convenience, but note that the scheme is essentially the same.

In [3] Juhász, Thurston and Zemke show that the images of any strong Heegaard invariant, appropriately restricted, fit into a transitive system. To make this precise, we introduce a few more definitions.

Definition 2.6.1. Suppose H_1 and H_2 are embedded isotopy diagrams for a closed, oriented, pointed 3-manifold (Y, z), with Heegaard surfaces $\iota_1, \iota_2 : (\Sigma_1, z), (\Sigma_2, z) \hookrightarrow (Y, z)$. We say a diffeomorphism of isotopy diagrams $d : H_1 \to H_2$ is *isotopic to the identity in* M if $\iota_2 \circ d : \Sigma_1 \to (Y, z)$ is isotopic to $\iota_1 : \Sigma_1 \to (Y, z)$ relative to the basepoint.

Definition 2.6.2. Given (Y, z), let $(\mathcal{G}_{\text{man}})_{(Y,z)}$ be the following subgraph of $\mathcal{G}_{\text{man}}$ whose vertices are embedded isotopy diagrams for (Y, z). The edges $e \in (\mathcal{G}_{\text{man}})_{(Y,z)}(H_1, H_2)$ between two isotopy diagrams again come in four flavors:

$$(\mathcal{G}_{\text{man}})_{(Y,z)}(H_1, H_2) = \mathcal{G}^{\alpha}_{\text{man}}(H_1, H_2) \cup \mathcal{G}^{\beta}_{\text{man}}(H_1, H_2) \cup \mathcal{G}^{\text{stab}}_{\text{man}}(H_1, H_2) \cup (\mathcal{G}^{\text{diff}}_{\text{man}})^0(H_1, H_2)$$

Here $\mathcal{G}^{\alpha}_{\text{man}}$, $\mathcal{G}^{\beta}_{\text{man}}$ and $\mathcal{G}^{\text{stab}}_{\text{man}}$ are the same collections as in the definition of $\mathcal{G}_{\text{man}}$, while $(\mathcal{G}^{\text{diff}}_{\text{man}})^0(H_1, H_2)$ consists of one edge for each element in the set of diffeomorphisms from H_1 to H_2 which are isotopic to the identity in M.

With these notions in hand, we have a stronger version of Proposition 2.3.22 which applies now to embedded diagrams for some fixed (Y, z):

Proposition 2.6.3. *[3, Proposition 2.36] Given (Y, z), any two vertices in the graph $(\mathcal{G}_{man})_{(Y,z)}$ can be connected by an oriented path in $(\mathcal{G}_{man})_{(Y,z)}$.*

The salient feature of a strong Heegaard invariant, F, is that the the isomorphisms $F(e)$ associated to edges e in $(\mathcal{G}_{\text{man}})_{(Y,z)}$ fit into a transitive system. This follows from the fact that the isomorphism associated to a path depends only on the endpoints:

Theorem 2.6.4 (Theorem 2.38 in [3])**.** *Let $F : \mathcal{G}_{man} \to \mathcal{C}$ be a strong Heegaard invariant. Given two isotopy diagrams $H, H' \in |(\mathcal{G}_{man})(Y, z)|$ and any two oriented paths η and ν in $(\mathcal{G}_{man})(Y, z)$ from H to H', we have*

$$F(\eta) = F(\nu)$$

Now, for any two isotopy diagrams H, H' and an oriented path η from H to H', we can define the map $F_{H,H'} = F(\eta)$.

Corollary 2.6.5 (Corollary 2.41 in [3])**.** *Suppose that $H, H', H'' \in |(\mathcal{G}_{man})_{(Y,z)}|$. Then*

$$F_{H,H''} = F_{H',H''} \circ F_{H,H'}$$

These results should provide some intuitive justification for the appearance of the notion of a strong Heegaard invariant. At the very least, the notion is enough to ensure such invariants fit into a transitive system. In particular, applying Corollary 2.6.5 to the strong Heegaard invariants

$$CF^\circ : \mathcal{G}_{\text{man}} \to \text{Trans}(P(\text{Kom}(\mathbb{Z}[U]\text{-Mod})))$$

of Theorem 1.3.3 immediately yields Corollary 1.3.5. We now show that this transitivity is also enough for the functoriality ends we seek in Theorem 1.3.1.

Proof of Theorem 1.3.1. Assuming Corollary 1.3.4, the Heegaard Floer invariants

$$HF^\circ : \mathcal{G}_{\text{man}} \to P(\mathbb{Z}[U]\text{-Mod})$$

are strong Heegaard invariants. Let $\mathbf{Man}_*$ be the category of closed, connected, oriented, and based 3-manifolds with based diffeomorphisms. Using the strong Heegaard invariants above, we can obtain functors:

$$HF_1^\circ : \mathbf{Man}_* \to \text{Trans}(P(\mathbb{Z}[U]\text{-Mod}))$$

as follows. Given a manifold $(Y, z) \in \text{Ob}(\mathbf{Man}_*)$, Corollary 2.6.5 ensures that the modules $HF^\circ(H)$ for isotopy diagrams $H \in |(\mathcal{G}_{\text{man}})_{(Y,z)}|$, along with the isomorphisms $HF^\circ_{H,H'}$, form a transitive system. We denote this transitive system by $HF_1^\circ(Y, z) \in \text{Trans}(P(\mathbb{Z}[U]\text{-Mod}))$.

To a pointed diffeomorphism $\phi : (Y, z) \to (Y', z')$, the functor HF_1° will assign a morphism of transitive systems

$$HF_1^\circ(\phi) : HF_1^\circ(Y, z) \to HF_1^\circ(Y', z')$$

defined as follows. Given any isotopy diagram $H = (\Sigma, A, B, z)$ for (Y, z), let $\phi_H = \phi|_\Sigma$ and H' be the isotopy diagram $\phi(H)$ for (Y', z'). By virtue of being a strong Heegaard invariant, HF° associates a morphism $HF^\circ(\phi_H) : HF^\circ(H) \to HF^\circ(H')$ in $P(\mathbb{Z}[U]\text{-Mod})$ to any such diffeomorphism of isotopy

diagrams ϕ_H. The collection of morphisms $\{\phi_H\}$ for $H \in |(\mathcal{G}_{\text{man}})_{(Y,z)}|$ will thus yield a collection of morphisms $\{HF^\circ(\phi_H)\}$. We claim that this collection of morphisms is in fact a morphism of transitive systems

$$HF_1^\circ(\phi) : HF_1^\circ(Y,z) \to HF_1^\circ(Y',z')$$

as desired. According to Definition 2.5.3, we must check that for any path of edges γ in $(\mathcal{G}_{\text{man}})_{(Y,z)}$ from H_1 to H_2, we have $HF^\circ(\phi_{H_2}) \circ HF^\circ(\gamma) = HF^\circ(\gamma') \circ HF^\circ(\phi_{H_1})$, for some path γ' in $(\mathcal{G}_{\text{man}})_{(Y',z')}$ from H_1' to H_2'. If γ is given by the path of edges

$$D_0 \xrightarrow{e_1} D_1 \xrightarrow{e_2} \cdots \xrightarrow{e_{n-1}} D_{n-1} \xrightarrow{e_n} D_n$$

in $(\mathcal{G}_{\text{man}})_{(Y,z)}$ from $D_0 = H_1$ to $D_n = H_2$, we pick out a path γ' in $(\mathcal{G}_{\text{man}})_{(Y',z')}$ from H_1' to H_2' given by

$$D_0' \xrightarrow{e_1'} D_1' \xrightarrow{e_2'} \cdots \xrightarrow{e_{n-1}'} D_{n-1} \xrightarrow{e_n'} D_n'$$

as follows. We define the intermediate isotopy diagrams in the path γ' by $D_i' = \phi(D_i)$. If the edge e_i is given by a strong $\boldsymbol{\alpha}$-equivalence, a strong $\boldsymbol{\beta}$-equivalence, or a (de)stabilization, we let $e_{i'}$ denote the corresponding strong $\boldsymbol{\alpha}$-equivalence, strong $\boldsymbol{\beta}$-equivalence, or (de)stabilization. If e_i corresponds to a diffeomorphism $e_i : D_{i-1} \to D_i$ isotopic to the identity, we set $e_i' = \phi_{D_i} \circ e_i \circ \phi_{D_{i-1}}^{-1}$. We then have a subgraph in $\mathcal{G}_{\text{man}}$ given by

$$\begin{array}{ccccccccc} D_0 & \xrightarrow{e_1} & D_1 & \xrightarrow{e_2} & \cdots & \xrightarrow{e_{n-1}} & D_{n-1} & \xrightarrow{e_n} & D_n \\ \downarrow{\scriptstyle \phi_{H_1}} & & \downarrow{\scriptstyle \phi_{D_1}} & & & & \downarrow{\scriptstyle \phi_{D_{n-1}}} & & \downarrow{\scriptstyle \phi_{H_2}} \\ D_0' & \xrightarrow{e_1'} & D_1' & \xrightarrow{e_2'} & \cdots & \xrightarrow{e_{n-1}'} & D_{n-1} & \xrightarrow{e_n'} & D_n' \end{array}$$

The condition that needs to be verified is that the image under HF° of the outer rectangle in this subgraph commutes. By construction of the path γ', each small square in the diagram is either a distinguished rectangle (recall Definition 2.4.7) or a commuting square of diffeomorphisms. Commutativity of the large rectangle now follows by virtue of HF° being a strong Heegaard invariant. Since the restriction of HF° to $\mathcal{G}_{\text{man}}^{\text{diff}}$ is a functor, the image under HF° of the commuting square of diffeomorphisms also commutes. Since the image under HF° of any distinguished rectangle also commutes, we thus see that the morphism of transitive systems

$$HF_1^\circ(\phi) : HF_1^\circ(Y, z) \to HF_1^\circ(Y', z')$$

associated to a pointed diffeomorphism ϕ is well defined.

The assignments above thus define the functor HF_1°; we note that composition of morphisms in $\mathbf{Man}_*$ are respected under HF_1° because HF° is a strong Heegaard invariant, and in particular must be a functor when restricted to $\mathcal{G}_{\text{man}}^{\text{diff}}$ (see Axiom 1 in Definition 1.3.4).

Finally, we note that isotopic diffeomorphisms in $\mathbf{Man}_*$ induce identical maps under HF_1°. To see this, suppose $\phi : (Y, z) \to (Y, z)$ is isotopic to $\text{Id}_{(Y,z)}$, and fix an isotopy diagram $H = (\Sigma, A, B, z)$ for (Y, z). Then $\phi_H = \phi|_H$ is isotopic to Id_H and $H' = \phi(H) = H$, so by virtue

of HF° being a strong Heegaard invariant we must have $HF^\circ(\phi_H) = \mathrm{Id}_{HF^\circ(H)}$. Thus $HF_1^\circ(\phi)$ is the map of transitive systems defined by the data $\{HF^\circ(\phi_H) = \mathrm{Id}_{HF^\circ(H)}\}$ for $H \in (\mathcal{G}_{\mathrm{man}})_{(Y,z)}$, and is thus an identity morphism in Trans($P(\mathbb{Z}[U]$-Mod)).

□

2.7. Heegaard Floer Homology as a Weak Heegaard Invariant

In this section we very briefly recall numerous maps defined on the Heegaard Floer chain complexes, and then use these maps to define the underlying morphisms of graphs of the strong Heegaard invariants appearing in Theorem 1.3.3. For the most part we just seek to establish notation in the first few subsections, and refer the reader to [1], [14] and [3] for detailed descriptions of the constructions involved in the definitions appearing there.

For concreteness and ease of notaton, we will phrase the results in this section in terms of CF^-, however we note that the definitions vary in a cosmetic way, and analogous results hold, for all of the variants CF°. In particular, the proof of Theorem 1.3.3 for CF° will follow by the same arguments given here for CF^-. In fact, one could also obtain the results for the other variants directly from those we prove, as $\widehat{CF}, CF^+$ and CF^∞ can all be obtained by taking suitable tensor products with CF^- and quotients thereof.

Finally, we note at the outset that we will use $\sim$ to indicate homotopic chain maps.

Spin Structures and Strong Admissibility

We must first address the fact that while the graph $\mathcal{G}_{\text{man}}$ that we have been considering thus far contains arbitrary Heegaard diagrams, the Heegaard Floer chain complexes defined in [1] are defined only with respect to certain *admissible* diagrams. Since we will focus on the case of CF^- in this section, the admissibility we will need is given by the notion of *strong admissibility*, which we now summarize.

We begin by recalling the setting of Heegaard Floer homology, and the role of Spin^c structures in the construction of the Heegaard Floer chain complexes. This discussion is an elaboration of that in Section 2.2, in which we will both provide more details and emphasize the role of Spin^c-structures, admissibility, and orientation systems. Given a genus g based Heegaard diagram

$$\mathcal{H} = (\Sigma, \boldsymbol{\alpha} = (\alpha_1, \alpha_2, \ldots, \alpha_g), \boldsymbol{\beta} = (\beta_1, \beta_2, \ldots, \beta_g), z)$$

for a closed, connected, oriented and based 3-manifold (Y, z), one considers the tori

$$\mathbb{T}_{\boldsymbol{\alpha}} = \alpha_1 \times \alpha_2 \cdots \times \alpha_g, \;\; \mathbb{T}_{\boldsymbol{\beta}} = \beta_1 \times \beta_2 \cdots \times \beta_g$$

in the symmetric product $\text{Sym}^g(\Sigma) := (\Sigma \times \cdots \Sigma)/S_g$. A choice of complex structure on Σ induces an almost complex structure on $\text{Sym}^g(\Sigma)$, and with respect to such an induced structure the tori $\mathbb{T}_{\boldsymbol{\alpha}}$ and $\mathbb{T}_{\boldsymbol{\beta}}$ are totally real. The Heegaard Floer homology is then defined as a variation of Lagrangian intersection Floer homology applied to these tori. To define the chain

complexes one must fix a complex structure j on Σ, and a choice of generic path J_s of almost complex structures on $\mathrm{Sym}^g(\Sigma)$ through $\mathrm{Sym}^g(j)$ (see [1]).

The basepoint z induces a map

$$s_z : \mathbb{T}_{\boldsymbol{\alpha}} \cap \mathbb{T}_{\boldsymbol{\beta}} \to \mathrm{Spin}^c(Y)$$

which associates to each intersection point a Spin^c-structure. One first defines a chain complex

$$CF^-(\mathcal{H}, \mathfrak{s})$$

which is freely generated as an abelian group by $[\boldsymbol{x}, i]$, for $\boldsymbol{x} \in \mathbb{T}_{\boldsymbol{\alpha}} \cap \mathbb{T}_{\boldsymbol{\beta}}$ with $s_z(\boldsymbol{x}) = \mathfrak{s}$ and for $i \in \mathbb{Z}$ with $i < 0$. Given two intersection points $\boldsymbol{x}, \boldsymbol{y} \in \mathbb{T}_{\boldsymbol{\alpha}} \cap \mathbb{T}_{\boldsymbol{\beta}}$, we let $\pi_2(\boldsymbol{x}, \boldsymbol{y})$ denote the set of homtopy classes of Whitney disks connecting $\boldsymbol{x}$ to $\boldsymbol{y}$ in $\mathrm{Sym}^g(\Sigma)$, with the usual boundary conditions. Given a homotopy class $\phi \in \pi_2(\boldsymbol{x}, \boldsymbol{y})$, we denote by $\mathcal{M}_{J_s}(\phi)$ the moduli space of J_s-holomorphic disks in the class ϕ, and write $\widehat{\mathcal{M}_{J_s}}(\phi) = \mathcal{M}_{J_s}(\phi)/\mathbb{R}$ for the quotient with respect to the $\mathbb{R}$-action coming from the translation action on the disks. We let $\mu(\phi)$ denote the Maslov index of the class ϕ, and let $n_z(\phi)$ denote the algebraic intersection number of ϕ with $z \times \mathrm{Sym}^{g-1}(\Sigma)$. We then have a well defined relative grading on the generators defined above, given by the formula

$$\mathrm{gr}([\boldsymbol{x}, i], [\boldsymbol{y}, j]) = \mu(\phi) - 2n_z(\phi) + 2i - 2j,$$

where ϕ is any class $\phi \in \pi_2(\boldsymbol{x}, \boldsymbol{y})$. Finally, the differential

$$\partial : CF^-(\mathcal{H}, \mathfrak{s}) \to CF^-(\mathcal{H}, \mathfrak{s})$$

is defined by the formula

$$\partial([\boldsymbol{x},i]) = \sum_{\{\boldsymbol{y}\in\mathbb{T}_{\boldsymbol{\alpha}}\cap\mathbb{T}_{\boldsymbol{\beta}}|s_z(\boldsymbol{y})=\mathfrak{s}\}} \sum_{\{\phi\in\pi_2(\boldsymbol{x},\boldsymbol{y})|\mu(\phi)=1\}} \#\widehat{\mathcal{M}_{J_s}}(\phi)\cdot[\boldsymbol{y},i-n_z(\phi)].$$

There is an action of the polynomial ring $\mathbb{Z}[U]$ on the complex $CF^-(\mathcal{H},\mathfrak{s})$, where

$$U\cdot[\boldsymbol{x},i] = [\boldsymbol{x},i-1]$$

decreases the relative grading by 2. We will always consider $CF^-(\mathcal{H},\mathfrak{s})$ as a complex of $\mathbb{Z}[U]$-modules. Finally, the total chain complex associated to $\mathcal{H}$ then splits by definition as

$$CF^-(\mathcal{H}) = \bigoplus_{\mathfrak{s}\in\mathrm{Spin}^c(Y)} CF^-(\mathcal{H},\mathfrak{s}).$$

Given a Spin^c structure $\mathfrak{s}$, we call a pointed Heegaard diagram $\mathfrak{s}$-*realized* if there is an intersection point $\boldsymbol{x}\in\mathbb{T}_{\boldsymbol{\alpha}}\cap\mathbb{T}_{\boldsymbol{\beta}}$ with $s_z(\boldsymbol{x})=\mathfrak{s}$. We note that for any $\mathfrak{s}\in\mathrm{Spin}^c(Y,z)$ there is an $\mathfrak{s}$-realized pointed Heegaard diagram for (Y,z) by [1, Lemma 5.2].

The chain complex $CF^-(\mathcal{H},\mathfrak{s})$ can in fact only be defined for Heegaard diagrams $\mathcal{H}=(\Sigma,\boldsymbol{\alpha},\boldsymbol{\beta},z)$ which satisfy an admissibility hypothesis. Given $\mathfrak{s}\in\mathrm{Spin}^c(Y)$, we say the diagram $\mathcal{H}$ is *strongly* $\mathfrak{s}$*-admissible* if every nontrivial periodic domain D on $\mathcal{H}$ satisfying $\langle c_1(\mathfrak{s}),H(D)\rangle = 2n \geq 0$ has some coefficient that is greater than n. Here $H(D)\in H_2(Y;\mathbb{Z})$ is the homology class naturally associated to the periodic domain D. It turns out that this notion of admissibility is enough to ensure that differential ∂ given above consists of a finite sum and is well defined on $CF^-(\mathcal{H},\mathfrak{s})$, and to

ensure that it in fact yields a chain complex. It is shown in [1, Lemma 5.4] that given any $\mathfrak{s} \in \mathrm{Spin}^c(Y)$, there is an $\mathfrak{s}$-realized, strongly $\mathfrak{s}$-admissible pointed diagram for (Y, z).

To define triangle maps on the Floer chain complexes, we will need an analogous notion of admissibility for Heegaard triple diagrams. A pointed triple diagram $\mathcal{T} = (\Sigma, \boldsymbol{\alpha}, \boldsymbol{\beta}, \boldsymbol{\gamma}, z)$ specifies a 4-manifold with boundary, which we denote by $X_{\boldsymbol{\alpha},\boldsymbol{\beta},\boldsymbol{\gamma}}$. Given now a Spin^c-structure $\mathfrak{s}$ on $X_{\boldsymbol{\alpha},\boldsymbol{\beta},\boldsymbol{\gamma}}$, denote by $\mathfrak{s}_{\boldsymbol{\alpha},\boldsymbol{\beta}}$ the restriction of $\mathfrak{s}$ to the boundary component $Y_{\boldsymbol{\alpha},\boldsymbol{\beta}}$. We will say the triple diagram $\mathcal{T}$ is *strongly $\mathfrak{s}$-admissible* if any triply periodic domain D which is the sum of doubly periodic domains,

$$D = D_{\boldsymbol{\alpha},\boldsymbol{\beta}} + D_{\boldsymbol{\beta},\boldsymbol{\gamma}} + D_{\boldsymbol{\alpha},\boldsymbol{\gamma}}$$

and which furthermore satisfies

$$\langle c_1(\mathfrak{s}_{\boldsymbol{\alpha},\boldsymbol{\beta}}), H(D_{\boldsymbol{\alpha},\boldsymbol{\beta}})\rangle + \langle c_1(\mathfrak{s}_{\boldsymbol{\beta},\boldsymbol{\gamma}}), H(D_{\boldsymbol{\beta},\boldsymbol{\gamma}})\rangle + \langle c_1(\mathfrak{s}_{\boldsymbol{\alpha},\boldsymbol{\gamma}}), H(D_{\boldsymbol{\alpha},\boldsymbol{\gamma}})\rangle = 2n \geq 0$$

has some coefficient greaer than n. It is shown in [1, Lemma 8.11] that given any pointed triple diagram $\mathcal{T}$ and a Spin^c structure $\mathfrak{s}$ on $X_{\boldsymbol{\alpha},\boldsymbol{\beta},\boldsymbol{\gamma}}$, there is a pointed triple diagram isotopic to $\mathcal{T}$ which is strongly $\mathfrak{s}$-admissible.

Orientation Systems

Coherent Orientation Systems of Disks

We recall that to define the differential on the Heegaard Floer chain complexes with coefficients in $\mathbb{Z}$, one must perform signed counts of the

points in certain moduli spaces of psuedo-holomorphic disks. To do so, one must ensure that on a pointed Heegaard diagram $\mathcal{H} = (\Sigma, \boldsymbol{\alpha}, \boldsymbol{\beta}, z)$ the moduli spaces of holomorphic disks in a homotopy class $A \in \pi_2(\boldsymbol{x}, \boldsymbol{y})$, which we denote by $\mathcal{M}^A$ or $\mathcal{M}(A)$, are orientable. By [1, Proposition 3.10] (or[14, Proposition 6.3] for the reader more comfortable in the cylindrical setting), these moduli spaces are orientable whenever they are smoothly cut out. There this is shown by trivializing the determinant line bundle $\mathcal{L}$ of the virtual index bundle of the linearized $\bar{\partial}$-equation defining the moduli space in question, so when necessary we will specify our orientations by specifying sections of these determinant line bundles.

In order for these orientations to allow for the structure of a chain complex on the Heegaard Floer chain modules, we actually need somewhat more: we want the moduli spaces for different homotopy classes of disks to be oriented coherently. To make this precise, Ozsváth and Szabó used the notion of a *coherent orientation system* for the moduli spaces of holomorphic disks in a Heegaard diagram $\mathcal{H} = (\Sigma, \boldsymbol{\alpha}, \boldsymbol{\beta}, z)$. Such an orientation system consists of a collection $\mathfrak{o}_{\mathcal{H}} = \mathfrak{o}_{\boldsymbol{\alpha},\boldsymbol{\beta}} := \{\mathfrak{o}^A_{\boldsymbol{\alpha},\boldsymbol{\beta}}\}$ of sections $\mathfrak{o}^A_{\boldsymbol{\alpha},\boldsymbol{\beta}}$ of the determinant line bundle $\mathcal{L}$ over all possible homotopy classes of disks $A \in \pi_2(\boldsymbol{x}, \boldsymbol{y})$ (ranging over all $\boldsymbol{x}, \boldsymbol{y} \in \mathbb{T}_{\boldsymbol{\alpha}} \cap \mathbb{T}_{\boldsymbol{\beta}}$). Roughly, the coherence condition amounts to requiring that these sections are compatible with a process of glueing holomorphic disks together. We refer the reader to [1] for the precise definition of the coherence condition, or to Section where we will formulate a precise version of the notion in the cylindrical setting. For our purposes in this section, we just recall the fact that every pointed Heegaard diagram equipped with complex structure data achieving transversality

admits a coherent orientation system by [1, Remarks following Definition 3.12].

Coherent Orientation Systems of Triangles

Given a pointed Heegaard triple diagram $\mathcal{T} = (\Sigma, \boldsymbol{\alpha}, \boldsymbol{\beta}, \boldsymbol{\gamma}, z)$, we also note that moduli spaces of holomorphic triangles in a homotopy class ψ, which we denote by $\mathcal{M}^{\psi}$ or $\mathcal{M}(\psi)$, are also orientable when they are smoothly cut out, by [1, Section 8.2] (or [14, Proposition 10.3]). Given a collection $\mathfrak{o}_{\mathcal{T}} := \{\mathfrak{o}_{\boldsymbol{\alpha},\boldsymbol{\beta},\boldsymbol{\gamma}}, \mathfrak{o}_{\boldsymbol{\alpha},\boldsymbol{\beta}}, \mathfrak{o}_{\boldsymbol{\beta},\boldsymbol{\gamma}}, \mathfrak{o}_{\boldsymbol{\alpha},\boldsymbol{\gamma}}\}$, where $\mathfrak{o}_{\boldsymbol{\alpha},\boldsymbol{\beta},\boldsymbol{\gamma}}$ is a collection of sections of the determinant line bundle over all homotopy classes of triangles, and $\mathfrak{o}_{\boldsymbol{\alpha},\boldsymbol{\beta}}$, $\mathfrak{o}_{\boldsymbol{\beta},\boldsymbol{\gamma}}$, and $\mathfrak{o}_{\boldsymbol{\alpha},\boldsymbol{\gamma}}$ are collections of sections of the determinant line bundle over all homotopy classes of disks in the respective double diagrams, we will consider a related notion of coherence (see [1, Definition 8.6]). Roughly, the coherence condition here will amount to the requirement that each collection of orientations of the moduli spaces of strips on the respective double diagrams are coherent, and that all possible pregluings of triangles with strips satisfy the analogous glueing condition (this coherence condition will also be spelled out precisely in Section). The existence of such coherent orientation systems is guaranteed by the following result.

Lemma 2.7.1. *[1, Lemma 8.7] Fix a pointed Heegaard triple diagram $(\Sigma, \boldsymbol{\alpha}, \boldsymbol{\beta}, \boldsymbol{\gamma}, z)$, and let $\mathfrak{s}$ be a Spin^c structure on $X_{\boldsymbol{\alpha},\boldsymbol{\beta},\boldsymbol{\gamma}}$ whose restriction to each boundary component is realized by an intersection point in the corresponding Heegaard diagram. Then for any coherent orientation systems $\mathfrak{o}_{\boldsymbol{\alpha},\boldsymbol{\beta}}$ and $\mathfrak{o}_{\boldsymbol{\beta},\boldsymbol{\gamma}}$ for two of the boundary components, there exists at least one*

coherent orientation system $\mathfrak{o}_{\boldsymbol{\alpha},\boldsymbol{\gamma}}$ *for the remaining boundary component and a coherent orientation system* $\mathfrak{o}_{\boldsymbol{\alpha},\boldsymbol{\beta},\boldsymbol{\gamma}}$ *such that the entire collection of orientations is coherent.*

Change of Almost Complex Structures

Next, we recall the dependence of the construction of the Heegaard Floer invariants on the choices of almost complex structures involved. The definition of the Heegaard Floer chain complex associated to a pointed Heegaard diagram $(\Sigma, \boldsymbol{\alpha}, \boldsymbol{\beta}, z)$ in fact requires a choice of complex structure j on Σ, and a generic path of almost complex structures $J_s \subset \mathcal{U}$ on $\mathrm{Sym}^g(\Sigma)$ going through the structure $\mathrm{Sym}^g(j)$ induced by j. Here g is the genus of Σ and $\mathcal{U}$ is a particular contractible set of almost complex structures specified by Ozsváth and Szabó in [1, Theorem 3.15 and Section 4.1]. Given a strongly $\mathfrak{s}$-admissible pointed Heegaard diagram $\mathcal{H} = (\Sigma, \boldsymbol{\alpha}, \boldsymbol{\beta}, z)$, a coherent orientation $\mathfrak{o}$ on $\mathcal{H}$, and two choices of such almost complex structure data (j, J_s) and (j', J'_s), there is a chain homotopy equivalence

$$\Phi_{J_s \to J'_s} : CF^-_{J_s}(\Sigma, \boldsymbol{\alpha}, \boldsymbol{\beta}, z, \mathfrak{s}, \mathfrak{o}) \to CF^-_{J'_s}(\Sigma, \boldsymbol{\alpha}, \boldsymbol{\beta}, z, \mathfrak{s}, \mathfrak{o}).$$

These equivalences fit into a transitive system in the homotopy category of chain complexes of $\mathbb{Z}[U]$-modules, in the sense that $\Phi_{J_s \to J_s} \sim \mathrm{id}_{CF^-(\Sigma,\boldsymbol{\alpha},\boldsymbol{\beta})}$ and $\Phi_{J'_s \to J''_s} \circ \Phi_{J_s \to J'_s} \sim \Phi_{J_s \to J''_s}$. This is shown in [2, Lemma 2.11]. We denote this transitive system in the homotopy category of complexes of $\mathbb{Z}[U]$-modules by

$$CF^-(\Sigma, \boldsymbol{\alpha}, \boldsymbol{\beta}, z, \mathfrak{s}, \mathfrak{o}).$$

Of course we also obtain from the maps $\Phi_{J_s \to J_s'}$ a transitive system of isomorphisms on homology. We will denote the colimit of the $\mathbb{Z}[U]$-modules $HF^-_{J_s}(\Sigma, \boldsymbol{\alpha}, \boldsymbol{\beta}, z, \mathfrak{s}, \mathfrak{o})$ with respect to this transitive system by

$$HF^-(\Sigma, \boldsymbol{\alpha}, \boldsymbol{\beta}, z, \mathfrak{s}, \mathfrak{o}).$$

Triangle Maps and Continuation Maps

Given a pointed Heegaard triple diagram $\mathcal{T} = (\Sigma, \boldsymbol{\alpha}, \boldsymbol{\beta}, \boldsymbol{\gamma}, z)$ which is strongly $\mathfrak{s}$-admissible for a Spin^c structure $\mathfrak{s}$ on $X_{\boldsymbol{\alpha},\boldsymbol{\beta},\boldsymbol{\gamma}}$, as well as a coherent orientation system $\mathfrak{o}_{\boldsymbol{\alpha},\boldsymbol{\beta},\gamma}$ compatible with coherent orientation systems $\mathfrak{o}_{\boldsymbol{\alpha},\boldsymbol{\beta}}$, $\mathfrak{o}_{\boldsymbol{\beta},\boldsymbol{\gamma}}$ and $\mathfrak{o}_{\boldsymbol{\alpha},\boldsymbol{\gamma}}$, there are $\mathbb{Z}[U]$-module chain maps

$$\mathcal{F}_{\boldsymbol{\alpha},\boldsymbol{\beta},\boldsymbol{\gamma}} : CF^-_{J_s}(\boldsymbol{\alpha}, \boldsymbol{\beta}, \mathfrak{s}_{\boldsymbol{\alpha},\boldsymbol{\beta}}, \mathfrak{o}_{\boldsymbol{\alpha},\boldsymbol{\beta}}) \otimes_{\mathbb{Z}[U]} CF^-_{J_s}(\boldsymbol{\beta}, \boldsymbol{\gamma}, \mathfrak{s}_{\boldsymbol{\beta},\boldsymbol{\gamma}}, \mathfrak{o}_{\boldsymbol{\beta},\boldsymbol{\gamma}}) \to CF^-_{J_s}(\boldsymbol{\alpha}, \boldsymbol{\gamma}, \mathfrak{s}_{\boldsymbol{\alpha},\boldsymbol{\gamma}}, \mathfrak{o}_{\boldsymbol{\alpha},\boldsymbol{\gamma}})$$

defined in [1, Theorem 8.12]. Here we have suppressed the dependence of this map on the spin^c-structure $\mathfrak{s}$, the coherent orientation system $\mathfrak{o}_{\boldsymbol{\alpha},\boldsymbol{\beta},\boldsymbol{\gamma}}$ and the basepoint z in our notation. Put simply, these chain maps count pseudoholomorpic triangles on the triple diagram. In fact, the homotopy class of the chain map $F_{\boldsymbol{\alpha},\boldsymbol{\beta},\boldsymbol{\gamma}}$ does not depend on the choice of almost complex structure data. More precisely, for two choices of almost complex structure data the maps above commute up to homotopy with the change of almost complex structure maps, by [1, Proposition 8.13]. Thus with respect to the transitive systems $CF^-(\Sigma, \boldsymbol{\alpha}, \boldsymbol{\beta}, z, \mathfrak{s}, \mathfrak{o})$, the map $F_{\boldsymbol{\alpha},\boldsymbol{\beta},\boldsymbol{\gamma}}$ is a morphism in Trans(Kom($\mathbb{Z}[U]$-Mod)), i.e. a morphism between two transitive systems

in the homotopy category of $\mathbb{Z}[U]$ modules. We denote this morphism by

$$\mathcal{F}_{\boldsymbol{\alpha},\boldsymbol{\beta},\boldsymbol{\gamma}} : CF^-(\boldsymbol{\alpha},\boldsymbol{\beta},\mathfrak{s}_{\boldsymbol{\alpha},\boldsymbol{\beta}},\mathfrak{o}_{\boldsymbol{\alpha},\boldsymbol{\beta}})\otimes_{\mathbb{Z}[U]} CF^-(\boldsymbol{\beta},\boldsymbol{\gamma},\mathfrak{s}_{\boldsymbol{\beta},\boldsymbol{\gamma}},\mathfrak{o}_{\boldsymbol{\beta},\boldsymbol{\gamma}}) \to CF^-(\boldsymbol{\alpha},\boldsymbol{\gamma},\mathfrak{s}_{\boldsymbol{\alpha},\boldsymbol{\gamma}},\mathfrak{o}_{\boldsymbol{\alpha},\boldsymbol{\gamma}})$$

We also obtain induced maps of $\mathbb{Z}[U]$-modules:

$$\mathcal{F}_{\boldsymbol{\alpha},\boldsymbol{\beta},\boldsymbol{\gamma}} : HF^-(\boldsymbol{\alpha},\boldsymbol{\beta},\mathfrak{s}_{\boldsymbol{\alpha},\boldsymbol{\beta}},\mathfrak{o}_{\boldsymbol{\alpha},\boldsymbol{\beta}})\otimes_{\mathbb{Z}[U]} HF^-(\boldsymbol{\beta},\boldsymbol{\gamma},\mathfrak{s}_{\boldsymbol{\beta},\boldsymbol{\gamma}},\mathfrak{o}_{\boldsymbol{\beta},\boldsymbol{\gamma}}) \to HF^-(\boldsymbol{\alpha},\boldsymbol{\gamma},\mathfrak{s}_{\boldsymbol{\alpha},\boldsymbol{\gamma}},\mathfrak{o}_{\boldsymbol{\alpha},\boldsymbol{\gamma}})$$

The triangle maps above allow one to define maps associated to handleslides. To describe the handleslide maps, we first recall the following fact.

Lemma 2.7.2. *[1, Lemma 9.4 and Section 9.1] (cf. [3, Lemma 9.2]) Let $(\Sigma,\boldsymbol{\beta},\boldsymbol{\gamma}',z)$ be a pointed genus g Heegaard diagram such that $\boldsymbol{\gamma}'$ can be obtained from $\boldsymbol{\beta}$ by performing a sequence of handleslides among the curves in $\boldsymbol{\beta}$. Then the diagram represents $\#^g(S^1\times S^2)$. There is a unique Spin^c structure $\mathfrak{s}_0 \in$ Spin$^c(\#^g(S^1\times S^2))$ such that $c_1(\mathfrak{s}_0)=0$, and upon performing a particular small Hamiltonian isotopy of $\boldsymbol{\gamma}'$ (specified in [1]) to obtain $(\Sigma,\boldsymbol{\beta},\boldsymbol{\gamma},z)$ one can ensure this new diagram is strongly $\mathfrak{s}_0$-admissible. Furthermore, there is a choice of coherent orientation system $\mathfrak{o}_{\boldsymbol{\beta},\boldsymbol{\gamma}}$ on this diagram such that in the highest nontrivial relative homological grading $HF^-(\Sigma,\boldsymbol{\beta},\boldsymbol{\gamma},z,\mathfrak{s}_0,\mathfrak{o}_{\boldsymbol{\beta},\boldsymbol{\gamma}})$ is isomorphic to $\mathbb{Z} =: \langle\theta_{\boldsymbol{\beta},\boldsymbol{\gamma}}\rangle$ for a generator we denote $\theta_{\boldsymbol{\beta},\boldsymbol{\gamma}}$.*

Remark 2.7.3. For such a diagram, we can also identify a particular intersection point $\theta_{\boldsymbol{\beta},\boldsymbol{\gamma}} \in CF^-(\Sigma,\boldsymbol{\beta},\boldsymbol{\gamma},z,\mathfrak{s}_0,\mathfrak{o}_{\boldsymbol{\beta},\boldsymbol{\gamma}})$ representing this element of homology. Indeed, the strongly admissible diagram referred to in the lemma statement yields a chain complex whose rank is the same as that

of its homology, and which has a unique intersection point realizing $\mathfrak{s}_0$ in the maximal relative grading.

Given a strongly $\mathfrak{s}$-admissible triple diagram $(\Sigma, \boldsymbol{\alpha}, \boldsymbol{\beta}, \boldsymbol{\gamma}, z)$ with $\boldsymbol{\gamma}$ related to $\boldsymbol{\beta}$ as in the statement of Lemma 2.7.2, we will write

$$\Psi^{\boldsymbol{\alpha}}_{\boldsymbol{\beta}\to\boldsymbol{\gamma}} := F_{\boldsymbol{\alpha},\boldsymbol{\beta},\boldsymbol{\gamma}}(\cdot\otimes\theta_{\boldsymbol{\beta},\boldsymbol{\gamma}}) : CF^-(\Sigma, \boldsymbol{\alpha}, \boldsymbol{\beta}, z, \mathfrak{s}_{\boldsymbol{\alpha},\boldsymbol{\beta}}, \mathfrak{o}_{\boldsymbol{\alpha},\boldsymbol{\beta}}) \to CF^-(\Sigma, \boldsymbol{\alpha}, \boldsymbol{\gamma}, z, \mathfrak{s}_{\boldsymbol{\alpha},\boldsymbol{\gamma}}, \mathfrak{o}_{\boldsymbol{\alpha},\boldsymbol{\gamma}})$$

Here we have used an arbitrary coherent orientation system $\mathfrak{o}_{\boldsymbol{\alpha},\boldsymbol{\beta}}$ and the coherent orientation system $\mathfrak{o}_{\boldsymbol{\beta},\boldsymbol{\gamma}}$ of Lemma 2.7.2, and enlarged them to a coherent orientation system $\mathfrak{o}_{\boldsymbol{\alpha},\boldsymbol{\beta},\boldsymbol{\gamma}}$ to define this map. That this enlargement can be done is ensured by Lemma 2.7.1. Similarly if instead $\boldsymbol{\beta}$ is related to $\boldsymbol{\alpha}$ as in the statement of Lemma 2.7.2, we will write

$$\Psi^{\boldsymbol{\alpha}\to\boldsymbol{\beta}}_{\boldsymbol{\gamma}} := F_{\boldsymbol{\beta},\boldsymbol{\alpha},\boldsymbol{\gamma}}(\theta_{\boldsymbol{\beta},\boldsymbol{\alpha}}\otimes\cdot) : CF^-(\Sigma, \boldsymbol{\alpha}, \boldsymbol{\gamma}, z, \mathfrak{s}_{\boldsymbol{\alpha},\boldsymbol{\gamma}}, \mathfrak{o}_{\boldsymbol{\alpha},\boldsymbol{\gamma}}) \to CF^-(\Sigma, \boldsymbol{\beta}, \boldsymbol{\gamma}, z, \mathfrak{s}_{\boldsymbol{\beta},\boldsymbol{\gamma}}, \mathfrak{o}_{\boldsymbol{\beta},\boldsymbol{\gamma}})$$

These can be thought of as maps on the Floer invariants associated to (small variations of) sequences of handleslides on diagrams. These maps are in fact homotopy equivalences according to the following result:

Lemma 2.7.4. *[1, Theorem 9.5 and Section 9.1]*

1. *If $(\Sigma, \boldsymbol{\alpha}, \boldsymbol{\beta}, \boldsymbol{\gamma}, z)$ is a strongly $\mathfrak{s}$-admissible triple diagram and $\boldsymbol{\beta}$ is related to $\boldsymbol{\gamma}$ as in the statement of Lemma 2.7.2, then $\Psi^{\boldsymbol{\alpha}}_{\boldsymbol{\beta}\to\boldsymbol{\gamma}}$ is a chain homotopy equivalence.*

2. *Furthermore, such equivalences are transitive: for two triples satisfying the conditions above we have*

$$\Psi^{\boldsymbol{\alpha}}_{\boldsymbol{\beta}\to\boldsymbol{\gamma}} \sim \Psi^{\boldsymbol{\alpha}}_{\boldsymbol{\delta}\to\boldsymbol{\gamma}} \circ \Psi^{\boldsymbol{\alpha}}_{\boldsymbol{\beta}\to\boldsymbol{\delta}}.$$

3. *The analogous results hold for the maps induced by changing the $\boldsymbol{\alpha}$ curves.*

There are also maps associated to special Hamiltonian isotopies of diagrams [1, Proof of Theorem 7.3]. Given strongly $\mathfrak{s}$-admissible diagrams $(\Sigma, \boldsymbol{\alpha}, \boldsymbol{\beta}, z)$ and $(\Sigma, \boldsymbol{\alpha}', \boldsymbol{\beta}', z)$ and an exact Hamiltonian isotopy ϕ_t on (Σ, ω) taking $\boldsymbol{\alpha}$ to $\boldsymbol{\alpha}'$ and $\boldsymbol{\beta}$ to $\boldsymbol{\beta}'$, which furthermore never crosses the basepoint, each coherent orientation system $\mathfrak{o}_{\boldsymbol{\alpha},\boldsymbol{\beta}}$ for the first diagram determines a unique coherent orientation system $\mathfrak{o}_{\boldsymbol{\alpha}',\boldsymbol{\beta}'}$ for the second. With respect to these orientation systems there is an induced chain homotopy equivalence

$$\Gamma^{\boldsymbol{\alpha}\to\boldsymbol{\alpha}'}_{\boldsymbol{\beta}\to\boldsymbol{\beta}'} : CF^-(\Sigma, \boldsymbol{\alpha}, \boldsymbol{\beta}, z, \mathfrak{s}, \mathfrak{o}_{\boldsymbol{\alpha},\boldsymbol{\beta}}) \to CF^-(\Sigma, \boldsymbol{\alpha}', \boldsymbol{\beta}', z, \mathfrak{s}, \mathfrak{o}_{\boldsymbol{\alpha}',\boldsymbol{\beta}'})$$

which we call a continuation map associated to the Hamiltonian isotopy ϕ_t. We will also use the notation

$$\Gamma^{\boldsymbol{\alpha}\to\boldsymbol{\alpha}'}_{\boldsymbol{\beta}} = \Gamma^{\boldsymbol{\alpha}\to\boldsymbol{\alpha}'}_{\boldsymbol{\beta}\to\boldsymbol{\beta}}$$

and

$$\Gamma^{\boldsymbol{\alpha}}_{\boldsymbol{\beta}\to\boldsymbol{\beta}'} = \Gamma^{\boldsymbol{\alpha}\to\boldsymbol{\alpha}}_{\boldsymbol{\beta}\to\boldsymbol{\beta}'}$$

By [2, Lemma 2.12], these equivalences compose naturally under concatenation of isotopies in the sense that

$$\Gamma_{\boldsymbol{\beta}}^{\boldsymbol{\alpha}\to\boldsymbol{\alpha}''} \sim \Gamma_{\boldsymbol{\beta}}^{\boldsymbol{\alpha}'\to\boldsymbol{\alpha}''} \circ \Gamma_{\boldsymbol{\beta}}^{\boldsymbol{\alpha}\to\boldsymbol{\alpha}'}$$

and

$$\Gamma_{\boldsymbol{\beta}\to\boldsymbol{\beta}'}^{\boldsymbol{\alpha}\to\boldsymbol{\alpha}'} \sim \Gamma_{\boldsymbol{\beta}'}^{\boldsymbol{\alpha}\to\boldsymbol{\alpha}'} \circ \Gamma_{\boldsymbol{\beta}\to\boldsymbol{\beta}'}^{\boldsymbol{\alpha}} \sim \Gamma_{\boldsymbol{\beta}\to\boldsymbol{\beta}'}^{\boldsymbol{\alpha}'} \circ \Gamma_{\boldsymbol{\beta}}^{\boldsymbol{\alpha}\to\boldsymbol{\alpha}'}.$$

Furthermore, by their definition in [1, Proof of Theorem 7.3], they satisfy $\Gamma_{\boldsymbol{\beta}\to\boldsymbol{\beta}}^{\boldsymbol{\alpha}\to\boldsymbol{\alpha}} = \mathrm{id}_{CF^-(\Sigma,\boldsymbol{\alpha},\boldsymbol{\beta},z,\mathfrak{s},\mathfrak{o}_{\boldsymbol{\alpha},\boldsymbol{\beta}})}$.

As suggested by the notation, we note that while the continuation map is a priori associated to a Hamiltonian isotopy between the isotopic attaching curves, in the cases of interest for us its chain homotopy class will actually be independent of the choice of isotopy. To see this, we recall:

Lemma 2.7.5. *[1, Lemma 9.1 and Section 9.1] Let $(\Sigma, \boldsymbol{\beta}, \boldsymbol{\beta}', z)$ be a pointed diagram such that each curve β_i' in $\boldsymbol{\beta}'$ is obtained from the curve β_i in $\boldsymbol{\beta}$ by performing a small Hamiltonian isotopy which introduces two transverse intersection points between β_i and β_i', and no intersection points between β_i' and β_j for $j \neq i$. Then the diagram represents $\#^g(S^1 \times S^2)$. There is a unique Spin^c structure $\mathfrak{s}_0 \in$ Spin$^c(\#^g(S^1 \times S^2))$ such that $c_1(\mathfrak{s}_0) = 0$, and the diagram $(\Sigma, \boldsymbol{\beta}, \boldsymbol{\beta}', z)$ is strongly $\mathfrak{s}_0$-admissible. Furthermore, there is a choice of coherent orientation system $\mathfrak{o}_{\boldsymbol{\beta},\boldsymbol{\beta}'}$ on this diagram such that in the highest nontrivial relative homological grading $HF^-(\Sigma, \boldsymbol{\beta}, \boldsymbol{\beta}', z, \mathfrak{s}_0, \mathfrak{o}_{\boldsymbol{\beta},\boldsymbol{\beta}'})$ is isomorphic to $\mathbb{Z} =: \langle \theta_{\boldsymbol{\beta},\boldsymbol{\beta}'} \rangle$ for a generator we denote $\theta_{\boldsymbol{\beta},\boldsymbol{\beta}'}$.*

Using the generator $\theta_{\boldsymbol{\beta},\boldsymbol{\beta}'}$ we have an analogous triangle map to that defined above, which is also shown to be an equivalence:

Lemma 2.7.6. *[1, Theorem 9.8 and Section 9.1] If $(\Sigma, \boldsymbol{\alpha}, \boldsymbol{\beta}, \boldsymbol{\beta}', z)$ is a strongly $\mathfrak{s}$-admissible triple diagram and $\boldsymbol{\beta}'$ is related to $\boldsymbol{\beta}$ as in the statement of Lemma 2.7.5 by a sufficiently small isotopy, then*

$$F_{\boldsymbol{\alpha},\boldsymbol{\beta},\boldsymbol{\beta}'}(\cdot \otimes \theta_{\boldsymbol{\beta},\boldsymbol{\beta}'}) : CF^-(\Sigma, \boldsymbol{\alpha}, \boldsymbol{\beta}, z, \mathfrak{s}_{\boldsymbol{\alpha},\boldsymbol{\beta}}, \mathfrak{o}_{\boldsymbol{\alpha},\boldsymbol{\beta}}) \to CF^-(\Sigma, \boldsymbol{\alpha}, \boldsymbol{\beta}', z, \mathfrak{s}_{\boldsymbol{\alpha},\boldsymbol{\beta}'}, \mathfrak{o}_{\boldsymbol{\alpha},\boldsymbol{\beta}'})$$

is a chain homotopy equivalence.

Furthermore, we have

Lemma 2.7.7. *[14, Proposition 11.4] If the triple diagram $(\Sigma, \boldsymbol{\alpha}, \boldsymbol{\beta}, \boldsymbol{\beta}', z)$ is strongly $\mathfrak{s}$-admissible and $\boldsymbol{\beta}'$ is related to $\boldsymbol{\beta}$ as in the statement of Lemma 2.7.5 by a sufficiently small isotopy, then the continuation map associated to any Hamiltonian isotopy ϕ_t between $\boldsymbol{\beta}$ and $\boldsymbol{\beta}'$ satisfies*

$$\Gamma^{\boldsymbol{\alpha}}_{\boldsymbol{\beta}\to\boldsymbol{\beta}'} \sim F_{\boldsymbol{\alpha},\boldsymbol{\beta},\boldsymbol{\beta}'}(\cdot \otimes \theta_{\boldsymbol{\beta},\boldsymbol{\beta}'})$$

We thus see that the continuation maps associated to small Hamiltonian isotopies of the attaching curves are independent of the choice of isotopy.

Finally, we introduce notation for a composition of triangle maps and continuation maps associated to strong $\boldsymbol{\alpha}$-equivalences and strong $\boldsymbol{\beta}$-equivalences.

Definition 2.7.8. [2, Section 2 and Lemma 2.13] Given two strongly $\mathfrak{s}$-admissible diagrams $(\Sigma, \boldsymbol{\alpha}_1, \boldsymbol{\beta}_1, z)$ and $(\Sigma, \boldsymbol{\alpha}_2, \boldsymbol{\beta}_2, z)$ which are strongly equivalent, one can construct another pointed diagram $(\Sigma, \boldsymbol{\alpha}'_1, \boldsymbol{\beta}'_1, z)$ such that:

1. $\boldsymbol{\alpha}'_1$ and $\boldsymbol{\beta}'_1$ are obtained respectively from $\boldsymbol{\alpha}_1$ and $\boldsymbol{\beta}_1$ by special isotopies.

2. $\boldsymbol{\alpha}_2$ and $\boldsymbol{\beta}_2$ are obtained respectively from $\boldsymbol{\alpha}'_1$ and $\boldsymbol{\beta}'_1$ by (small variations of) sequences of handleslides as in Lemma 2.7.2.

3. The quadruple diagram $(\Sigma, \boldsymbol{\alpha}'_1, \boldsymbol{\beta}'_1, \boldsymbol{\alpha}_2, \boldsymbol{\beta}_2)$ is strongly $\mathfrak{s}$-admissible for the unique Spin^c-structure on $X_{\boldsymbol{\alpha}'_1, \boldsymbol{\beta}'_1, \boldsymbol{\alpha}_2, \boldsymbol{\beta}_2}$ which restricts to $\mathfrak{s}$ on $Y_{\boldsymbol{\alpha}'_1, \boldsymbol{\beta}_2}$ and $\mathfrak{s}_0$ on $Y_{\boldsymbol{\alpha}'_1, \boldsymbol{\alpha}_2}$ and $Y_{\boldsymbol{\beta}'_1, \boldsymbol{\beta}_2}$.

We define a map,

$$\Phi^{\boldsymbol{\alpha}_1 \to \boldsymbol{\alpha}_2}_{\boldsymbol{\beta}_1 \to \boldsymbol{\beta}_2}(\cdot, \mathfrak{s}) : CF^-(\Sigma, \boldsymbol{\alpha}_1, \boldsymbol{\beta}_1, z, \mathfrak{s}) \to CF^-(\Sigma, \boldsymbol{\alpha}_2, \boldsymbol{\beta}_2, z, \mathfrak{s})$$

associated to two such strongly equivalent diagrams by the formula:

$$\Phi^{\boldsymbol{\alpha}_1 \to \boldsymbol{\alpha}_2}_{\boldsymbol{\beta}_1 \to \boldsymbol{\beta}_2}(\cdot, \mathfrak{s}) = \Psi^{\boldsymbol{\alpha}_2}_{\boldsymbol{\beta}'_1 \to \boldsymbol{\beta}_2} \circ \Psi^{\boldsymbol{\alpha}'_1 \to \boldsymbol{\alpha}_2}_{\boldsymbol{\beta}'_1} \circ \Gamma^{\boldsymbol{\alpha}_1 \to \boldsymbol{\alpha}'_1}_{\boldsymbol{\beta}_1 \to \boldsymbol{\beta}'_1}.$$

We will sometimes use the notation

$$\Phi^{\boldsymbol{\alpha}}_{\boldsymbol{\beta} \to \boldsymbol{\beta}'} = \Phi^{\boldsymbol{\alpha} \to \boldsymbol{\alpha}}_{\boldsymbol{\beta} \to \boldsymbol{\beta}'}$$

and

$$\Phi^{\boldsymbol{\alpha} \to \boldsymbol{\alpha}'}_{\boldsymbol{\beta}} = \Phi^{\boldsymbol{\alpha} \to \boldsymbol{\alpha}'}_{\boldsymbol{\beta} \to \boldsymbol{\beta}}.$$

The Weak Heegaard Floer Invariants

Using the previous two subsections, we are now in position to define the value on vertices of the morphism of graphs

$$CF^- : \mathcal{G}_{\text{man}} \to \text{Trans}(P(\text{Kom}(\mathbb{Z}[U]\text{-Mod})))$$

which will partially define the weak invariants underlying the maps in Theorem 1.3.3. In doing so, we will also define the value on vertices of the morphism of graphs

$$HF^- : \mathcal{G}_{\text{man}} \to P(\mathbb{Z}[U]\text{-Mod})$$

appearing in Corollary 1.3.4.

Definition 2.7.9. Fix some pointed isotopy diagram $H = (\Sigma, A, B, z)$ (corresponding to a vertex in $\mathcal{G}_{\text{man}}$) representing the pointed 3-manifold (Y, z). For $\mathfrak{s} \in \text{Spin}^c(Y)$, let

$$\text{Admiss}_{(\Sigma,A,B,z)}(\mathfrak{s}) = \{\text{strongly } \mathfrak{s}\text{-admissible diagrams } (\Sigma, \boldsymbol{\alpha}, \boldsymbol{\beta}, z) | [\boldsymbol{\alpha}] = A, [\boldsymbol{\beta}] = B\}$$

be the set of strongly $\mathfrak{s}$-admissible diagrams representing H. By [1, Proofs of Lemma 5.2 and Lemma 5.4], this is nonempty for all $\mathfrak{s} \in \text{Spin}^c(Y)$. Choose any diagram $\mathcal{H} = (\Sigma, \boldsymbol{\alpha}, \boldsymbol{\beta}, z) \in \text{Admiss}_{(\Sigma,A,B,z)}(\mathfrak{s})$, and fix a coherent orientation system $\mathfrak{o}_{\boldsymbol{\alpha},\boldsymbol{\beta}}$ on it. By [1, Lemma 7.3], the transitive system $CF^-(\Sigma, \boldsymbol{\alpha}, \boldsymbol{\beta}, z, \mathfrak{s}, \mathfrak{o}_{\boldsymbol{\alpha},\boldsymbol{\beta}})$ can be used along with the continuation maps Γ to induce coherent orientation systems for all strongly $\mathfrak{s}$-admissible diagrams representing the isotopy diagram H. Then by [2, Lemma

2.12], the transitive systems $CF^-(\Sigma, \boldsymbol{\alpha}, \boldsymbol{\beta}, z, \mathfrak{s}, \mathfrak{o}_{\boldsymbol{\alpha},\boldsymbol{\beta}})$ ranging over all $(\Sigma, \boldsymbol{\alpha}, \boldsymbol{\beta}, z) \in \mathrm{Admiss}_{(\Sigma,A,B,z)}(\mathfrak{s})$ fit into a transitive system (of morphisms between transitive systems) with respect to the continuation maps $\Gamma^{\boldsymbol{\alpha}\to\boldsymbol{\alpha}'}_{\boldsymbol{\beta}\to\boldsymbol{\beta}'}$. We can therefore define a single transitive system (see Section 2.5) in $\mathrm{Kom}(\mathbb{Z}[U]\text{-Mod})$, which we denote by

$$CF^-(H, \mathfrak{s}).$$

Finally, we define the value of the weak Heegaard invariant CF^- on the isotopy diagram H by

$$CF^-(H) = \bigoplus_{\mathfrak{s}\in \mathrm{Spin}^c(Y)} CF^-(H, \mathfrak{s}).$$

Passing to homology, we obtain instead that the $\mathbb{Z}[U]$-modules $HF^-(\Sigma, \boldsymbol{\alpha}, \boldsymbol{\beta}, z, \mathfrak{s}, \mathfrak{o}_{\boldsymbol{\alpha},\boldsymbol{\beta}})$ for $(\Sigma, \boldsymbol{\beta}, \boldsymbol{\alpha}, z) \in \mathrm{Admiss}_{(\Sigma,A,B,z)}(\mathfrak{s})$ fit into a transitive system of isomorphisms with respect to the continuation maps. We denote the colimit of this transitive system by

$$HF^-(H, \mathfrak{s})$$

and define

$$HF^-(H) = \bigoplus_{\mathfrak{s}\in \mathrm{Spin}^c(Y)} HF^-(H, \mathfrak{s}).$$

We now proceed to fix the data of the underlying coherent orientation systems we will use to define $CF^-(H')$ for all other isotopy diagrams H' in $\mathcal{G}_{\mathrm{man}}$. First consider the path component of $\mathcal{G}_{\mathrm{man}}$ containing the fixed isotopy diagram H chosen above. We note that by Proposition 2.3.22, the

collection of vertices in this path component corresponds to the collection of all isotopy diagrams representing the fixed 3-manifold (Y, z). Given another isotopy diagram H' in this path component, choose a sequence of edges γ in $(\mathcal{G}_{\text{man}})_{(Y,z)}$ from H to H'. For any diagrams $\mathcal{H} \in H$ and $\mathcal{H}'$ in H', the constructions described in the previous subsections yield a composition of maps associated to γ on the underlying chain complexes:

$$CF^-(\gamma) : CF^-(\mathcal{H}) \to CF^-(\mathcal{H}').$$

Here the sequence of maps $CF^-(\gamma)$ of course depends on our previously fixed choice of coherent orientation system for $\mathcal{H}$; we described in the previous subsections how each of the possible constituent maps in the composition $CF^-(\gamma)$ induces a coherent orientation system on the target given a coherent orientation system on the domain, and it is this induced orientation system that we fix on $\mathcal{H}'$. One can check that this induced orientation on $\mathcal{H}'$ is independent of the choice of path γ using [3, Proof of Theorem 2.38 and Remark 2.39], by verifying the commutativity of the induced orientations occurring in each of the five types of distinguished rectangle, and in a simple handleswap. We thus see that our specification of the coherent orientation systems $\mathfrak{o}_{\boldsymbol{\alpha},\boldsymbol{\beta}}$ on all diagrams $\mathcal{H}$ representing H actually yields a choice of coherent orientation systems for all diagrams in the same path component as H. Repeating this entire procedure for all path components in $\mathcal{G}_{\text{man}}$, we have thus defined

$$CF^-(H) = \bigoplus_{\mathfrak{s} \in \text{Spin}^c(Y)} CF^-(H, \mathfrak{s})$$

and

$$HF^-(H) = \bigoplus_{\mathfrak{s}\in \mathrm{Spin}^c(Y)} HF^-(H,\mathfrak{s})$$

for all isotopy diagrams H in $\mathcal{G}_{\mathrm{man}}$.

Remark 2.7.10. We interpret the role of coherent orientations in the definition above loosely as follows. If one fixes any Heegaard diagram for a 3-manifold, there are numerous inequivalent choices of for a coherent orientation system (in fact there are $2^{b_1(Y)}$ such choices, see [1, Lemma 4.16]). The above definition just says one should fix whichever choice they prefer, and then take care to use the maps induced by the standard Heegaard moves (or diffeomorhisms isotopic to the identity) to carry this choice around when considering different Heegaard diagrams for the same 3-manifold.

To finish defining the weak Heegaard invariants, we need to associate isomorphisms to all edges in $\mathcal{G}_{\mathrm{man}}$. We begin by assigning maps to edges corresponding to strong $\boldsymbol{\alpha}$-equivalences and strong $\boldsymbol{\beta}$-equivalences.

Definition 2.7.11. Given two strongly $\boldsymbol{\alpha}$-equivalent isotopy diagrams $H_1 = (\Sigma, A, B, z)$, $H_2 = (\Sigma, A', B, z) \in |\mathcal{G}_{\mathrm{man}}|$ representing (Y, z), and $\mathfrak{s} \in \mathrm{Spin}^c(Y)$, fix strongly $\mathfrak{s}$-admissible diagrams $(\Sigma, \boldsymbol{\alpha}, \boldsymbol{\beta}, z)$ and $(\Sigma, \boldsymbol{\alpha}', \boldsymbol{\beta}, z)$ representing them. As above, this is possible by [1, Section 5]. Then by [2, Theorem 2.3 and Lemma 2.13], the chain homotopy equivalences $\Phi_{\boldsymbol{\beta}}^{\boldsymbol{\alpha}\to\boldsymbol{\alpha}'}$ fit into a morphism of transitive systems between the transitive systems $CF^-(H,\mathfrak{s})$ appearing in Definition 2.7.9. Thus for the edge $e \in \mathcal{G}^{\boldsymbol{\alpha}}_{\mathrm{man}}(H_1, H_2)$ corresponding to the strong $\boldsymbol{\alpha}$-equivalence, we can associate this collection of chain homotopy equivalences (or equivalently, this collection of isomorphisms

in Kom($\mathbb{Z}[U]$-Mod)) to obtain a morphism

$$\Phi_e := \Phi_B^{A \to A'} : CF^-(H_1) \to CF^-(H_2)$$

We note that such a collection of chain homotopy equivalences is precisely the notion of an isomorphism in Trans(Kom($\mathbb{Z}[U]$-Mod)). We define the chain homotopy equivalences associated to a strong $\boldsymbol{\beta}$-equivalence analogously.

To finish defining the weak Heegaard invariants, we assign isomorphisms to stablizations and diffeomorphisms in the next two subsections.

Stabilization Maps

We recall maps on the Heegaard Floer chain complexes which can be associated to stabilizations (in the sense of Definition 2.3.14). Given a strongly $\mathfrak{s}$-admissible diagram $\mathcal{H} = (\Sigma, \boldsymbol{\alpha}, \boldsymbol{\beta}, z)$ and a stablization thereof, $\mathcal{H}' = (\Sigma \# \Sigma_0, \boldsymbol{\alpha}', \boldsymbol{\beta}', z)$, each coherent orientation system $\mathfrak{o}$ on $\mathcal{H}$ induces a coherent orientation system $\mathfrak{o}'$ on $\mathcal{H}'$. With respect to these orientation systems, there is a $\mathbb{Z}[U]$-equivariant chain isomorphism

$$\sigma_{\mathcal{H} \to \mathcal{H}'} : CF^-_{J_s}(\Sigma, \boldsymbol{\alpha}, \boldsymbol{\beta}, z, \mathfrak{s}, \mathfrak{o}) \to CF^-_{J'_s(T)}(\Sigma \# \Sigma_0, \boldsymbol{\alpha}', \boldsymbol{\beta}', z, \mathfrak{s}, \mathfrak{o}')$$

defined for sufficiently large values of a parameter T. This is established in [1, Theorems 10.1 and 10.2].

The curves $\boldsymbol{\alpha}' \cup \boldsymbol{\beta}'$ are obtained as the disjoint union of $\boldsymbol{\alpha} \cup \boldsymbol{\beta}$ along with a pair of closed curves α', β' contained in Σ_0 which intersect

transversally in a single point we will denote by c. We can identify the intersection points in the two diagrams above by assigning to an intersection point $\boldsymbol{x} \in \mathbb{T}_{\boldsymbol{\alpha}} \cap \mathbb{T}_{\boldsymbol{\beta}}$ the intersection point $\sigma_{\mathcal{H}\to\mathcal{H}'}(\boldsymbol{x}) = \boldsymbol{x} \times c \in \mathbb{T}_{\boldsymbol{\alpha}'} \cap \mathbb{T}_{\boldsymbol{\beta}'}$. Fix complex structures j_Σ on Σ and j_{Σ_0} on Σ_0, and let $j'(T)$ denote the complex structure on $\Sigma\#\Sigma_0$ defined by inserting a neck of length T between (Σ, j_Σ) and (Σ_0, j_{Σ_0}). Then one can associate to a perturbation J_s of $\mathrm{Sym}^g(j_\Sigma)$ on $\mathrm{Sym}^g(\Sigma)$ and a perturbation J_s^0 of j_{Σ_0}, a perturbation $J_s'(T)$ of $\mathrm{Sym}^{g+1}(j'(T))$ on $\mathrm{Sym}^{g+1}(\Sigma\#\Sigma_0)$. The key argument needed to establish the above chain isomorphism then comes in the form of a neck stretching argument which yields the following glueing result: for sufficiently large values of T, a homotopy class of Whitney disk $\phi \in \pi_2(\boldsymbol{x}, \boldsymbol{y})$ on Σ with Maslov index 1, and the corresponding homotopy class $\phi' \in \pi_2(\boldsymbol{x} \times c, \boldsymbol{y} \times c)$ on $\Sigma\#\Sigma_0$ with Maslov index 1, there is an identificaton of moduli spaces $\mathcal{M}_{J_s}(\phi) \cong \mathcal{M}_{J_s'(T)}(\phi')$. From this it follows readily that the above map is a $\mathbb{Z}[U]$-equivariant chain isomorphism.

Definition 2.7.12. Given *isotopy* diagrams H and H', with H' obtained from H via a stabilization, we can associate a morphism of transitive systems

$$\sigma_{H\to H'} : CF^-(H) \to CF^-(H')$$

as follows. Fixing any Spin^c-structure $\mathfrak{s}$, strongly $\mathfrak{s}$-admissible representatives $\mathcal{H}$ and $\mathcal{H}'$ which realize the stabilization, and almost complex structure data on $\mathcal{H}$, there is some choice of almost complex structure data on $\mathcal{H}'$ for which the stabilization ismorphism is defined. As described in [2, Lemma 2.15], the stabilization maps $\sigma_{\mathcal{H}\to\mathcal{H}'}$ commute with the change of almost complex structure maps, and with the strong equivalence maps. This

implies that the chain isomorphisms $\{\sigma_{\mathcal{H}\to\mathcal{H}'}\}$, when the complex structures are chosen so that they are defined, satisfy the commutativity requirements required of a morphism of transitive systems as in Definition 2.5.3. We can complete this partially defined morphism of transitive systems for other choices of complex structure data by declaring the stabilization map $\sigma_{\mathcal{H}\to\mathcal{H}'}$ to be computed for allowable complex structure data, followed by the appropriate change of almost complex structure homotopy equivalence $\Phi_{J_s\to J_s'}$. We define the morphism of transitive systems associated to the corresponding destablization to be the inverse of $\sigma_{H\to H'}$.

On the level of homology, we obtain via the colimit construction in Definition 2.7.9 canonical isomorphisms $i_{\mathcal{H}} : HF^-(\mathcal{H}) \to HF^-(H)$ and $i_{\mathcal{H}'} : HF^-(\mathcal{H}') \to HF^-(H')$. We set $\sigma_{H\to H'} = i_{\mathcal{H}'} \circ \sigma_{\mathcal{H}\to\mathcal{H}'} \circ i_{\mathcal{H}}^{-1}$ for any choice of such $\mathcal{H}$, $\mathcal{H}'$. This is independent of the choice of diagrams $\mathcal{H}$ and $\mathcal{H}'$ by the aforementioned result [2, Lemma 2.15]

Diffeomorphism Maps

Finally, we need to discuss how diffeomorphisms of Heegaard surfaces lead to maps on the associated chain complexes. We use the following definition:

Definition 2.7.13. [3, Definition 9.23] Fix a strongly $\mathfrak{s}$-admissible diagram $(\Sigma, \boldsymbol{\alpha}, \boldsymbol{\beta}, z)$, with $|\boldsymbol{\alpha}| = |\boldsymbol{\beta}| = k$. Let j be an almost complex structure on Σ, and J_s be a perturbation of the almost complex structure $\mathrm{Sym}^k(j)$ on $\mathrm{Sym}^k(\Sigma)$. Let $\mathfrak{o}$ be a coherent orientation system on the diagram. Fix a diffeomorphism $d : \Sigma \to \Sigma'$, and set $d(\boldsymbol{\alpha}) = \boldsymbol{\alpha}'$, $d(\boldsymbol{\beta}) = \boldsymbol{\beta}'$. We define an associated map as follows. First, the almost complex structure j

and perturbation J_s can be conjugated via the differential of d to obtain $j' = d_*(j)$ on Σ and $J'_s = d_*(J_s)$ a perturbation of $d_*(j)$ on $\mathrm{Sym}^k(\Sigma')$. The diffeomorphism d provides an identification between periodic classes $\pi_2(\boldsymbol{x}, \boldsymbol{x}) \cong \pi_2(\boldsymbol{x}', \boldsymbol{x}')$ for $\boldsymbol{x} \in \mathbb{T}_{\boldsymbol{\alpha}} \cap \mathbb{T}_{\boldsymbol{\beta}}$ and $\boldsymbol{x}' \in \mathbb{T}_{\boldsymbol{\alpha}'} \cap \mathbb{T}_{\boldsymbol{\beta}'}$. We use this identification to push forward the coherent orientation system $\mathfrak{o}$ to obtain an induced orientation system $\mathfrak{o}'$. This yields a chain isomorphism

$$d_{J_s, J'_s} : CF^-_{J_s}(\Sigma, \boldsymbol{\alpha}, \boldsymbol{\beta}, z, \mathfrak{s}, \mathfrak{o}) \to CF^-_{J'_s}(\Sigma', \boldsymbol{\alpha}', \boldsymbol{\beta}', z', d(\mathfrak{s}), \mathfrak{o}')$$

as can be seen easily by a direct argument pushing forward all intersection points, and holomorphic discs connecting two such, via d. We note that the change of complex structure maps commute with the maps d_{J_s, J'_s} (by a direct check), so there is also an induced map of transitive systems

$$d_* : CF^-(\Sigma, \boldsymbol{\alpha}, \boldsymbol{\beta}, z, \mathfrak{s}) \to CF^-(\Sigma', \boldsymbol{\alpha}', \boldsymbol{\beta}', z', d(\mathfrak{s}))$$

Finally, by Lemma 2.7.7 and [3, Lemma 9.24] the maps d_* commute with the maps $\Gamma^{\boldsymbol{\alpha} \to \boldsymbol{\alpha}'}_{\boldsymbol{\beta} \to \boldsymbol{\beta}'}$ appearing in Definition 2.7.9. Thus by using the continuation maps the maps d_* can be extended to a morphism of the transitive systems in Definition 2.7.9

$$d_* : CF^-(H, \mathfrak{s}) \to CF^-(H', d(\mathfrak{s}))$$

where $H = (\Sigma, [\boldsymbol{\alpha}], [\boldsymbol{\beta}], z)$ and $H' = (\Sigma', [\boldsymbol{\alpha}'], [\boldsymbol{\beta}'], z')$.

On the level of homology, the above definitions give a well defined map of the $\mathbb{Z}[U]$-modules in Definition 2.7.9,

$$d_* : HF^-(H, \mathfrak{s}) \to HF^-(H', d(\mathfrak{s})).$$

2.8. Heegaard Floer Homology as a Strong Heegaard Invariant

In the previous section we recalled the definition of the weak Heegaard invariants

$$CF^- : \mathcal{G}_{\text{man}} \to \text{Trans}(P(\text{Kom}(\mathbb{Z}[U]\text{-Mod})))$$

and

$$HF^- : \mathcal{G}_{\text{man}} \to P(\mathbb{Z}[U]\text{-Mod})$$

underlying the strong Heegaard invariants appearing in Theorem 1.3.3 and Corollary 1.3.4 respectively. To establish Theorem 1.3.3 we need to check the four axioms required of a strong Heegaard invariant in Definition 2.4.7.

The proofs of axioms 1 and 2 given in [3, Section 9.2, pg 131] for $\mathbb{F}_2[U]$-Mod apply almost directly to establish axioms 1 and 2 for CF^- and HF^- as Heegaard invariants valued in $\text{Trans}(P(\text{Kom}(\mathbb{Z}[U]\text{-Mod})))$ and $P(\mathbb{Z}[U]\text{-Mod})$ respectively, as we now summarize for CF^-.

For axiom 1, the functoriality of CF^- restricted to $\mathcal{G}^{\alpha}_{\text{man}}$ and $\mathcal{G}^{\beta}_{\text{man}}$ follows from Lemma 2.7.4 and [2, Theorem 2.3]. The functoriality of CF^- restricted to $\mathcal{G}^{\text{diff}}_{\text{man}}$ is immediate from Definition 2.7.13. Finally, for a stabilization e and the corresponding destabilization e', $CF^-(e') = CF^-(e)^{-1}$ by Definition 2.7.12.

For axiom 2, we need to establish that the images under CF^- of distinguished rectangles in $\mathcal{G}_{\text{man}}$ (recall Definition 2.4.5) form commuting rectangles. For a rectangle of type 1, commutativity follows from Lemma 2.7.4 and [2, Theorem 2.3]. For a rectangle of type 2, commutativity follows from [2, Lemma 2.15]. For a rectangle of type 3, commutativity follows from [3, Lemma 9.24]. Finally, rectangles of type 4 and 5 can be seen to commute by directly applying the arguments in [3, pg. 131].

We now investigate axiom 3. Let $H = (\Sigma, A, B, z) \in |\mathcal{G}_{\text{man}}|$ be an isotopy diagram, $d : H \to H$ a diffeomorphism of isotopy diagrams which is isotopic to Id_Σ, and $d_* := CF^-(e)$ where $e \in \mathcal{G}^{\text{diff}}_{\text{man}}(H, H)$ is the edge corresponding to d. We need to show $d_* = \text{Id}_{CF^-(H)}$ as morphisms of transitive systems in $P(\text{Kom}(\mathbb{Z}[U]\text{-Mod}))$. We adapt and restate the argument given in [3, Proposition 9.27] in order to explain why it can be applied to the case of (projective) integral coefficients. We show the following result.

Theorem 2.8.1. *Let $(\Sigma, \boldsymbol{\alpha}, \boldsymbol{\beta}, z)$ be a strongly $\mathfrak{s}$-admissible diagram. Suppose that $d : \Sigma \to \Sigma$ is a diffeomorphism isotopic to Id_Σ, and let $\boldsymbol{\alpha}' = d(\boldsymbol{\alpha})$ and $\boldsymbol{\beta}' = d(\boldsymbol{\beta})$. Let $\mathfrak{o}_{\boldsymbol{\alpha},\boldsymbol{\beta}}$ be a coherent orienation system on $(\Sigma, \boldsymbol{\alpha}, \boldsymbol{\beta}, z)$ and $\mathfrak{o}_{\boldsymbol{\alpha}',\boldsymbol{\beta}'}$ be the coherent orientation system on $(\Sigma, \boldsymbol{\alpha}', \boldsymbol{\beta}', z)$ induced by d. Then with respect to these orienation systems, we have*

$$d_* = \pm\Gamma^{\boldsymbol{\alpha}\to\boldsymbol{\alpha}'}_{\boldsymbol{\beta}\to\boldsymbol{\beta}'} : HF^-(\Sigma, \boldsymbol{\alpha}, \boldsymbol{\beta}, z, \mathfrak{s}, \mathfrak{o}_{\boldsymbol{\alpha},\boldsymbol{\beta}}) \to HF^-(\Sigma, \boldsymbol{\alpha}', \boldsymbol{\beta}', z', \mathfrak{s}, \mathfrak{o}_{\boldsymbol{\alpha}',\boldsymbol{\beta}'})$$

Furthermore, as maps

$$d_*, \pm\Gamma^{\boldsymbol{\alpha}\to\boldsymbol{\alpha}'}_{\boldsymbol{\beta}\to\boldsymbol{\beta}'} : CF^-(\Sigma, \boldsymbol{\alpha}, \boldsymbol{\beta}, z, \mathfrak{s}, \mathfrak{o}_{\boldsymbol{\alpha},\boldsymbol{\beta}}) \to CF^-(\Sigma, \boldsymbol{\alpha}', \boldsymbol{\beta}', z', \mathfrak{s}, \mathfrak{o}_{\boldsymbol{\alpha}',\boldsymbol{\beta}'})$$

d_* is chain homotopic to one of $\pm\Gamma^{\boldsymbol{\alpha}\to\boldsymbol{\alpha}'}_{\boldsymbol{\beta}\to\boldsymbol{\beta}'}$.

In fact, this theorem will establish axiom (3) in Definition 2.4.7 for the weak Heegaard invariants CF^- and HF^- above. Since d is isotopic to Id_Σ by hypothesis, we have $\boldsymbol{\alpha}'$ is isotopic to $\boldsymbol{\alpha}$ and $\boldsymbol{\beta}'$ is isotopic to $\boldsymbol{\beta}$, so $H := (\Sigma, [\boldsymbol{\alpha}], [\boldsymbol{\beta}], z) = (\Sigma, [\boldsymbol{\alpha}'], [\boldsymbol{\beta}'], z')$. The induced map of transitive systems $d_* : CF^-(H) \to CF^-(H)$ defined in Definition 2.7.13 is then computed by extending the following map by conjugation with the continuation maps:

$$CF^-(\Sigma, \boldsymbol{\alpha}, \boldsymbol{\beta}, z, \mathfrak{o}_{\boldsymbol{\alpha},\boldsymbol{\beta}}) \xrightarrow{d_*} CF^-(\Sigma, \boldsymbol{\alpha}', \boldsymbol{\beta}', z, \mathfrak{o}_{\boldsymbol{\alpha}',\boldsymbol{\beta}'}) \xrightarrow{\Gamma^{\boldsymbol{\beta}'\to\boldsymbol{\beta}}_{\boldsymbol{\alpha}'\to\boldsymbol{\alpha}}} CF^-(\Sigma, \boldsymbol{\alpha}, \boldsymbol{\beta}, z, \mathfrak{o}_{\boldsymbol{\alpha},\boldsymbol{\beta}}).$$

Since $\Gamma^{\boldsymbol{\beta}'\to\boldsymbol{\beta}}_{\boldsymbol{\alpha}'\to\boldsymbol{\alpha}} \sim (\Gamma^{\boldsymbol{\beta}\to\boldsymbol{\beta}'}_{\boldsymbol{\alpha}\to\boldsymbol{\alpha}'})^{-1}$ and $d_* \sim \pm\Gamma^{\boldsymbol{\beta}\to\boldsymbol{\beta}'}_{\boldsymbol{\alpha}\to\boldsymbol{\alpha}'}$ by Theorem 2.8.1, we see that $d_* : CF^-(H) \to CF^-(H)$ is the extension of a map $CF^-(\Sigma, \boldsymbol{\alpha}, \boldsymbol{\beta}, z, \mathfrak{o}_{\boldsymbol{\alpha},\boldsymbol{\beta}}) \to CF^-(\Sigma, \boldsymbol{\alpha}, \boldsymbol{\beta}, z, \mathfrak{o}_{\boldsymbol{\alpha},\boldsymbol{\beta}})$ which is homotopic to plus or minus the identity. Thus we see that $d_* = \mathrm{Id}_{CF^-(H)}$ as morphisms in $\mathrm{Trans}(P(\mathrm{Kom}(\mathbb{Z}[U]\text{-Mod})))$.

Proof of Theorem 2.8.1. Since d is isotopic to id_Σ, we may decompose it into a composition of diffeomorphisms d_i on some diagrams $\mathcal{H}_i = (\Sigma, \boldsymbol{\alpha}_i, \boldsymbol{\beta}_i)$, such that each d_i is Hamiltonian isotopic to id_Σ for some symplectic form ω_i on Σ, and the diagrams satisfy the intersection properties $|\alpha \cap d_i(\alpha)| = |\beta \cap d_i(\beta)| = 2$ for all $\alpha \in \boldsymbol{\alpha}_{i-1}$ and $\beta \in \boldsymbol{\beta}_{i-1}$. As described in [3, Proposition 9.27], it will suffice to prove the result for such a d_i. So let d_t for $t \in \mathbb{R}$ be a Hamiltonian isotopy which is independent of t for $t \in (-\infty, 0]$ and $t \in [1, \infty)$, and which connects id_Σ to a diffeomorphism d of $\mathcal{H} = (\Sigma, \boldsymbol{\alpha}, \boldsymbol{\beta})$. Throughout the proof, we will use the notation $d_t(\boldsymbol{\alpha}) = \boldsymbol{\alpha}_t$, $d_t(\boldsymbol{\beta}) = \boldsymbol{\beta}_t$, and use primes to indicate the values of various quantities at $t = 1$.

Fix the data of a complex structure j on Σ and a perturbation J_s of $\mathrm{Sym}^k(j)$ on $\mathrm{Sym}^k(\Sigma)$, and for $t \in \mathbb{R}$ let $j_t = (d_t)_*(j)$ and $J_{s,t} = (\mathrm{Sym}^k(d_t))_*(J_s)$. As described in the sections above, there are numerous chain maps on the Heegaard Floer chain complexes we can associate with the isotopy d_t and this induced almost complex structure data. We will be concerned here with the following three:

1. We can change the almost complex structure on $\mathrm{Sym}^k(\Sigma)$ from $J_s = J_{s,0}$ to $J'_s = J_{s,1}$, while leaving the attaching curves unchanged, and consider the induced map

$$\Phi_{J_s \to J'_s} : CF^-_{J_s}(\Sigma, \boldsymbol{\alpha}, \boldsymbol{\beta}, z, \mathfrak{o}_{\boldsymbol{\alpha},\boldsymbol{\beta}}) \to CF^-_{J'_s}(\Sigma, \boldsymbol{\alpha}, \boldsymbol{\beta}, z, \mathfrak{o}_{\boldsymbol{\alpha},\boldsymbol{\beta}}).$$

   We recall here that this map is defined (in [1]) by counting Maslov index 0 discs $u : [0,1] \times \mathbb{R} \to \mathrm{Sym}^k(\Sigma)$ connecting some $\boldsymbol{x} \in \mathbb{T}_{\boldsymbol{\alpha}} \cap \mathbb{T}_{\boldsymbol{\beta}}$ to some $\boldsymbol{y} \in \mathbb{T}_{\boldsymbol{\alpha}} \cap \mathbb{T}_{\boldsymbol{\beta}}$, which satisfy $u(0,t) \in \boldsymbol{\alpha}$, $u(1,t) \in \boldsymbol{\beta}$ and $du/ds + J_{s,t}(du/dt) = 0$.

2. We can leave the almost complex structures (j, J_s) fixed, and consider the effect on the Floer complex of altering only the attaching curves via the map

$$\Gamma^{\boldsymbol{\beta} \to \boldsymbol{\beta}'}_{\boldsymbol{\alpha} \to \boldsymbol{\alpha}'} : CF^-_{J_s}(\Sigma, \boldsymbol{\alpha}, \boldsymbol{\beta}, z, \mathfrak{o}_{\boldsymbol{\alpha},\boldsymbol{\beta}}) \to CF^-_{J_s}(\Sigma, \boldsymbol{\alpha}', \boldsymbol{\beta}', z, \mathfrak{o}_{\boldsymbol{\alpha}',\boldsymbol{\beta}'})$$

   associated to the Hamiltonian isotopy d_t. In this case, the map is defined by counting Maslov index 0 discs u connecting some $\boldsymbol{x} \in \mathbb{T}_{\boldsymbol{\alpha}} \cap \mathbb{T}_{\boldsymbol{\beta}}$ to some $\boldsymbol{y} \in \mathbb{T}_{\boldsymbol{\alpha}'} \cap \mathbb{T}_{\boldsymbol{\beta}'}$ as above, but with dynamic

boundary conditions $u(0,t) \in \boldsymbol{\alpha}_t$, $u(1,t) \in \boldsymbol{\beta}_t$, and which satisfy $du/ds + J_s(du/dt) = 0$.

3. We define a new sort of continuation map associated with d_t,

$$\Gamma_{d_t} : CF^-_{J_s}(\Sigma, \boldsymbol{\alpha}, \boldsymbol{\beta}, z, \mathfrak{o}_{\boldsymbol{\alpha},\boldsymbol{\beta}}) \to CF^-_{J'_s}(\Sigma, \boldsymbol{\alpha}', \boldsymbol{\beta}', z, \mathfrak{o}_{\boldsymbol{\alpha}',\boldsymbol{\beta}'})$$

which combines the ideas from the previous two. This map is defined to count Maslov index 0 discs u which connect some $\boldsymbol{x} \in \mathbb{T}_{\boldsymbol{\alpha}} \cap \mathbb{T}_{\boldsymbol{\beta}}$ to some $\boldsymbol{x}' \in \mathbb{T}_{\boldsymbol{\alpha}'} \cap \mathbb{T}_{\boldsymbol{\beta}'}$, have dynamic boundary conditions $u(0,t) \in \boldsymbol{\alpha}_t$, $u(1,t) \in \boldsymbol{\beta}_t$, and which satisfy $du/ds + J_{s,t}(du/dt) = 0$. We will denote the set of homotopy classes of Whitney disks (not necessarily $J_{s,t}$-holomorphic) satisfying the boundary conditions above by $\pi_2^{d_t}(\boldsymbol{x}, \boldsymbol{x}')$, and for $\phi \in \pi_2^{d_t}(\boldsymbol{x}, \boldsymbol{x}')$ we will denote the moduli space of $J_{s,t}$-holomorphic maps representing ϕ by $\mathcal{M}^{d_t}(\phi)$.

We claim that the third map in the list above is in fact chain homotopic to the map d_{J_s,J'_s} from Definition 2.7.13. To see this, we first explain that if a diffeomorphism (which we also indicate by d, as an abuse of notation) $d : \Sigma \to \Sigma$ isotopic to the identity (via an isotopy d_t) is sufficiently close to Id_Σ, then the map defined in case (3) above satisfies $\Gamma_{d_t} = d_{J_s,J'_s}$ as chain maps. Indeed, by taking d to be a sufficiently small perturbation of Id_Σ, we may ensure the isotopy d_t is arbitrarily close to being constant in t. For an isotopy which is constant in t, the definition of the continuation map in (3) above counts Maslov index 0 disks with fixed boundary conditions which are J_s-holomorphic. The only such maps are constant maps. Thus, by Gromov compactness, if the isotopy d_t is sufficiently close to being constant,

the Maslov index 0 solutions to the equation appearing in the definition of Γ_{d_t} will be close enough to constant disks to ensure that Γ_{d_t} will be a nearest point map.

Next we note that the definition of Γ_{d_t} depends on a choice of coherent orientation system for the moduli spaces $\mathcal{M}^{d_t}(\phi)$. As explained in [1, Proof of Proposition 7.3], when $\pi_2^{d_t}(\boldsymbol{x}, \boldsymbol{x}') \neq 0$ a single homotopy class $\phi \in \pi_2^{d_t}(\boldsymbol{x}, \boldsymbol{x}') \cong \mathbb{Z}$ yields via glueing an identification between periodic classes $\pi_2(\boldsymbol{x}, \boldsymbol{x}) \cong_\phi \pi_2(\boldsymbol{x}', \boldsymbol{x}')$ on the two diagrams, and a choice of orientation for $\mathcal{M}^{d_t}(\phi)$ then yields an identification between coherent orientation systems on the two diagrams. Thus given a coherent orientation system $\mathfrak{o}_{\boldsymbol{\alpha},\boldsymbol{\beta}}$ on $(\Sigma, \boldsymbol{\alpha}, \boldsymbol{\beta})$, and an orientation on $\mathcal{M}^{d_t}(\phi)$, we obtain an induced orientation $\mathfrak{o}_{\boldsymbol{\alpha}',\boldsymbol{\beta}'}$ on $(\Sigma, \boldsymbol{\alpha}', \boldsymbol{\beta}')$ with respect to which the map is defined. We claim that we may arrange for this induced orientation to agree with that induced by $d_{J_s,J_s'}$. Indeed, fix for each $\boldsymbol{x} \in \mathbb{T}_{\boldsymbol{\alpha}} \cap \mathbb{T}_{\boldsymbol{\beta}}$ a homotopy class $\phi_{\boldsymbol{x}} \in \pi_2^{d_t}(\boldsymbol{x}, \boldsymbol{x}')$. We can choose orientations on all such $\mathcal{M}^{d_t}(\phi_{\boldsymbol{x}})$ freely such that Γ_{d_t} is the positive nearest point map (with the generator corresponding to an intersection point being taken to the positive generator corresponding to the nearest intersection point after the isotopy is performed), and then extend these choices to a coherent system. The coherent orientation $\mathfrak{o}_{\boldsymbol{\alpha}',\boldsymbol{\beta}'}$ on $(\Sigma, \boldsymbol{\alpha}', \boldsymbol{\beta}', z')$ induced by Γ_{d_t} that results will then be the same as that induced by $d_{J_s,J_s'}$, as we now explain. Fix $\boldsymbol{x}, \boldsymbol{y} \in \mathbb{T}_{\boldsymbol{\alpha}} \cap \mathbb{T}_{\boldsymbol{\beta}}$ and let $\boldsymbol{x}' = d(\boldsymbol{x})$ and $\boldsymbol{y}' = d(\boldsymbol{y})$ be the corresponding interesection points in $\mathbb{T}_{\boldsymbol{\alpha}'} \cap \mathbb{T}_{\boldsymbol{\beta}'}$. Given a homotopy class $\psi \in \pi_2(\boldsymbol{x}, \boldsymbol{y})$ and a positively oriented Whitney disk u from $\boldsymbol{x}$ to $\boldsymbol{y}$ in the class ψ, the orientation system induced by $d_{J_s,J_s'}$ will positively orient the corresponding

disk $d(u)$ representing the class $d(\psi) \in \pi_2(\boldsymbol{x}', \boldsymbol{y}')$ (see Definition 2.7.13). We need to show that the disk $d(u)$ is also positively oriented in the orientation system induced by Γ_{d_t}. As described above, the orientation on $d(u)$ induced by Γ_{d_t} is specified as follows. We consider representative disks v_1 and v_2 for the classes $\phi_{\boldsymbol{x}} \in \pi_2^{d_t}(\boldsymbol{x}, \boldsymbol{x}')$ and $\phi_{\boldsymbol{y}} \in \pi_2^{d_t}(\boldsymbol{y}, \boldsymbol{y}')$, which we may assume are both positively oriented by the choice we made for orientatations on $\mathcal{M}^{d_t}(\phi_{\boldsymbol{x}})$ and $\mathcal{M}^{d_t}(\phi_{\boldsymbol{y}})$. We then consider the glued disk $v_2 \natural u \natural \overline{v_1}$. Since an orientation has been specified on each constituent disk and our system is coherent, this glued disk also has a specified orientation, which is positive given our choices. Finally, we note that this disk is identified with $d(u)$ under the identification between coherent orientation systems in the two diagrams, and thus $d(u)$ must also be oriented positively. We thus see that both maps induce the same coherent orientation system on the target and both take the form of the positive nearest point map, so $\Gamma_{\phi_t} = \phi_{J_s, J_s'}$.

Finally, we can decompose our original diffeomorphism d : $(\Sigma, \boldsymbol{\alpha}_0, \boldsymbol{\beta}_0) \to (\Sigma, \boldsymbol{\alpha}_1, \boldsymbol{\beta}_1)$ into a sequence of diffeomorphisms $d^1, d^2, \cdots, d^N$, where $d^i : (\Sigma, \boldsymbol{\alpha}_{(i-1)/N}, \boldsymbol{\beta}_{(i-1)/N}) \to (\Sigma, \boldsymbol{\alpha}_{i/N}, \boldsymbol{\beta}_{i/N})$ and each d^i is isotopic to Id_Σ via isotopies d_t^i. For sufficiently large N, we can ensure that the continuation map $\Gamma_{d_t^i}$ associated to each consitituent isotopy satisfies

$$\Gamma_{d_t^i} = (d^i)_{J_{s,(i-1)/N}, J_{s,i/N}}$$

by the argument in the preceding paragraphs. Furthermore, by inserting long necks one can see that the composition of the corresponding

continuation maps is homotopic to the original continuation map:

$$\Gamma_{d_t} \sim \left(\Gamma_{d_t^N} \circ \cdots \circ \Gamma_{d_t^1} \right).$$

Since

$$d_{J_s,J_s'} = d^N_{J_{s,(N-1)/N},J_{s,1}} \circ \cdots \circ d^1_{J_{s,0},J_{s,1/N}}$$

we thus see that $d_{J_s,J_s'} \sim \Gamma_{d_t}$, which establishes the claim.

Using Definition 2.7.13 we have $d_* = \Phi_{J_s' \to J_s} \circ d_{J_s,J_s'}$. Thus to complete the proof it will in fact suffice to show that $\Phi_{J_s' \to J_s} \circ d_{J_s,J_s'} \sim \pm\Gamma^{\alpha\to\alpha'}_{\beta\to\beta'}$, or, since $d_{J_s,J_s'} \sim \Gamma_{d_t}$ and $\Phi^{-1}_{J_s' \to J_s} \sim \Phi_{J_s \to J_s'}$, to show that

$$\Gamma_{d_t} \sim \pm\Phi_{J_s \to J_s'} \circ \Gamma^{\alpha\to\alpha'}_{\beta\to\beta'}. \tag{2.2}$$

To see that equation (2.2) is true, we consider the following generalized notion of a continuation map, of which each of the three maps involved are a special case. Consider a Hamiltonian isotopy ϕ_t and a generic two parameter family of almost complex structures $K_{s,t}$ on $\mathrm{Sym}^k(\Sigma)$ which are perturbations of $\mathrm{Sym}^k(k_t)$ where k_t is a one parameter family of complex structures on Σ. Here we assume for convenience as above that this data is independent of t for $t \in (-\infty, 0]$ and $t \in [1, \infty)$. We set $\boldsymbol{\alpha}_t = \phi_t(\boldsymbol{\alpha})$ and $\boldsymbol{\beta}_t = \phi_t(\boldsymbol{\beta})$. Given such data we can associate the *continuation map with respect to* $(\phi_t, K_{s,t})$:

$$\Gamma_{(\phi_t,K_{s,t})} : CF^-_{K_{s,0}}(\Sigma, \boldsymbol{\alpha}_0, \boldsymbol{\beta}_0) \to CF^-_{K_{s,1}}(\Sigma, \boldsymbol{\alpha}_1, \boldsymbol{\beta}_1) \tag{2.3}$$

by counting Maslov index 0 discs u connecting some $\boldsymbol{x} \in \mathbb{T}_{\boldsymbol{\alpha}_0} \cap \mathbb{T}_{\boldsymbol{\beta}_0}$ to some $\boldsymbol{y} \in \mathbb{T}_{\boldsymbol{\alpha}_1} \cap \mathbb{T}_{\boldsymbol{\beta}_1}$, with dynamic boundary conditions $u(0,t) \in \boldsymbol{\alpha}_t$, $u(1,t) \in \boldsymbol{\beta}_t$, and which satisfy

$$\frac{du}{ds} + K_{s,t}(\frac{du}{dt}) = 0.$$

The maps $\Gamma_{d_t}, \Phi_{J_s \to J'_s}$ and $\Gamma^{\alpha \to \alpha'}_{\beta \to \beta'}$ above are then the continuation maps with respect to the data $(d_t, J_{s,t})$, $(\mathrm{id}_\Sigma, J_{s,t})$ and $(d_t, J_{s,0})$ respectively. Furthermore, since the homotopy classes of such continuation maps are natural under concatenation and rescaling of the ϕ_t and $K_{s,t}$ by [2, Lemma 2.12] (see also the argument below), the composite $\Phi_{J_s \to J'_s} \circ \Gamma^{\alpha \to \alpha'}_{\beta \to \beta'}$ is homotopic to the continuation map defined with respect to the data

$$(d_{t,1}, J_{s,t,1}) := \begin{cases} (d_{2t}, J_{s,0}) & t \in [0, 1/2] \\ (\mathrm{id}_\Sigma, J_{s,2t-1}) & t \in [1/2, 1]. \end{cases}$$

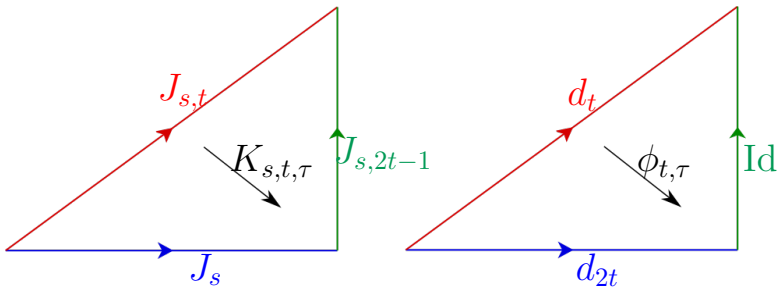

FIGURE 21 A schematic of the complex structure and isotopy data defining the continuation maps Γ_{d_t} and (a continuation map homotopic to) $\Phi_{J_s \to J'_s} \circ \Gamma^{\boldsymbol{\alpha} \to \boldsymbol{\alpha}'}_{\boldsymbol{\beta} \to \boldsymbol{\beta}'}$, and the homotopies between the two sets of data. The data defining Γ_{d_t} is represented by the top edges of the two triangles, while the data defining $\Phi_{J_s \to J'_s} \circ \Gamma^{\boldsymbol{\alpha} \to \boldsymbol{\alpha}'}_{\boldsymbol{\beta} \to \boldsymbol{\beta}'}$ is represented by the bottom edges followed by the vertical edges.

Consider now two Hamiltonian isotopies $\phi_{t,0}$ and $\phi_{t,1}$ with $\phi_{0,0} = \phi_{0,1} = \mathrm{id}_\Sigma$ and $\phi_{1,0} = \phi_{1,1}$, and two generic two parameter families $K_{s,t,0}$ and $K_{s,t,1}$

with $K_{s,0,0} = K_{s,0,1}$ and $K_{s,1,0} = K_{s,1,1}$. We will complete the proof by showing that a generic homotopy $h = (\phi_{t,\tau}, K_{s,t,\tau})$ between $(\phi_{t,0}, K_{s,t,0})$ and $(\phi_{t,1}, K_{s,t,1})$ induces a chain homotopy between $\Gamma_{(\phi_{t,0},K_{s,t,0})}$ and $\pm\Gamma_{(\phi_{t,1},K_{s,t,1})}$. In particular, equation (2.2) will follow, as the data $(d_t, J_{s,t})$ used to define $\Gamma_{d_t,J_{s,t}} =: \Gamma_{d_t}$ is homotopic to the data $(d_{t,1}, J_{s,t,1})$ used to define $\Gamma_{d_{t,1},J_{s,t,1}} \sim \Phi_{J_s \to J'_s} \circ \Gamma^{\alpha\to\alpha'}_{\beta\to\beta'}$.

Fixing τ, let $\pi_2^\tau(\boldsymbol{x}, \boldsymbol{y})$ denote the homotopy classes of discs u which connect $\boldsymbol{x}$ to $\boldsymbol{y}$, and which satisfy the boundary conditions $u(0,t) \in \phi_{t,\tau}(\boldsymbol{\alpha})$, $u(1,t) \in \phi_{t,\tau}(\boldsymbol{\beta})$. Given a homotopy class $\phi \in \pi_2^\tau(\boldsymbol{x}, \boldsymbol{y})$, we denote by $\mathcal{M}_\tau(\phi)$ the moduli space of discs in the class ϕ satisfying

$$\frac{du}{ds} + K_{s,t,\tau}(\frac{du}{dt}) = 0$$

We note that for fixed τ, the definition of the continuation map with respect to $(\phi_{t,\tau}, K_{s,t,\tau})$ given above can be restated succinctly as counting Maslov index 0 discs in the moduli spaces $\mathcal{M}_\tau(\phi)$. For any τ, the homotopy h induces an identification between homotopy classes of discs $\pi_2^0(\boldsymbol{x}, \boldsymbol{y}) \cong \pi_2^\tau(\boldsymbol{x}, \boldsymbol{y})$. Using this identification, we may define for each $\phi \in \pi_2^0(\boldsymbol{x}, \boldsymbol{y})$ the moduli space

$$\mathcal{M}^h(\phi) = \bigcup_{\tau\in I} \mathcal{M}_\tau(\phi) \times \{\tau\} \tag{2.4}$$

For a generic choice of homotopy h, this is a manifold of dimension $\mu(\phi) + 1$. We use this moduli space to define a chain homotopy $H^h : CF^-_{K_{s,0}}(\Sigma, \boldsymbol{\alpha}_0, \boldsymbol{\beta}_0) \to CF^-_{K_{s,1}}(\Sigma, \boldsymbol{\alpha}_1, \boldsymbol{\beta}_1)$ between $\Gamma_{(\phi_{t,0},K_{s,t,0})}$ and $\Gamma_{(\phi_{t,1},K_{s,t,1})}$ associated with the homotopy h. For $\boldsymbol{x} \in \mathbb{T}_{\boldsymbol{\alpha}} \cap \mathbb{T}_{\boldsymbol{\beta}}$ we set

$$H^h([\boldsymbol{x}, i]) = \sum_{\boldsymbol{y} \in \mathbb{T}_{\boldsymbol{\alpha}_1} \cap \mathbb{T}_{\boldsymbol{\beta}_1}} \sum_{\substack{\phi \in \pi_2^0(\boldsymbol{x}, \boldsymbol{y}) \\ \mu(\phi) = -1}} \#(\mathcal{M}^h(\phi))[\boldsymbol{y}, i - n_p(\phi)].$$

To see that this is a chain homotopy, we will consider the ends of the moduli spaces $\mathcal{M}^h(\psi)$ for ψ with Maslov index $\mu(\psi) = 0$. Since such spaces $\mathcal{M}^h(\psi)$ are smooth 1 dimensional manifolds for generic choices of almost complex structure data, and since they are orientable, the signed count of the ends is zero for any choice of orientation.

The ends can be partitioned into three types: those corresponding to $\tau = 0$, those corresponding to $\tau = 1$, and those corresponding to strips breaking off for values $0 < \tau < 1$. For the ends corresponding to $\tau = 0$, the contribution to the count of the ends is given by the count of the zero dimensional moduli space $\#\mathcal{M}_{\tau=0}(\psi)$. Modulo signs, this is precisely the count occurring in the definition of $\Gamma_{(\phi_{t,0}, K_{s,t,0})}$. For $\tau = 1$, the contribution to the count of the ends is similarly given by $\#\mathcal{M}_{\tau=1}(\psi)$, which is the count occurring in the definition of $\Gamma_{(\phi_{t,1}, K_{s,t,1})}$, modulo signs. We will discuss the signed contributions below. Finally, the ends corresponding to strip breaking come from the space

$$\left(\coprod_{\substack{\phi * \phi' = \psi \\ \mu(\phi) = 0, \mu(\phi') = 1}} \mathcal{M}^h(\phi) \times \widehat{\mathcal{M}}(\phi') \right) \coprod \left(\coprod_{\substack{\phi' * \phi = \psi \\ \mu(\phi) = 0, \mu(\phi') = 1}} \widehat{\mathcal{M}}(\phi') \times \mathcal{M}^h(\phi) \right)$$

Supposing the orientations on the moduli spaces $\mathcal{M}^h$ are chosen to be coherent with respect to preglueings of strips, the count of the terms in the first parentheses is precisely the count occurring in the composition

$\partial_0^- \circ H^h$, while the count of the terms in the second parentheses is precisely the count occurring in $H^h \circ (\partial_1)^-$. Here ∂_0^- indicates the differential on $CF^-_{K_{s,0}}(\Sigma, \boldsymbol{\alpha}_0, \boldsymbol{\beta}_0)$ and $(\partial_1)^-$ indicates the differential on $CF^-_{K_{s,1}}(\Sigma, \boldsymbol{\alpha}_1, \boldsymbol{\beta}_1)$.

Finally, we note that we may arrange for the spaces $\mathcal{M}^h(\phi)$ to be coherently oriented such that the total signed count of the ends of $\mathcal{M}^h(\psi)$ is given by

$$0 = \Gamma_{(\phi_{t,0}, K_{s,t,0})} - \Gamma_{(\phi_{t,1}, K_{s,t,1})} - ((\partial_1)^- \circ H^h + H^h \circ \partial_0^-)$$

Indeed, we have

$$\mathcal{M}^h(\psi) = \bigcup_{\tau \in I} \mathcal{M}_\tau(\psi) \times \{\tau\} = \{(u, \tau) \in C^\infty(I \times \mathbb{R}, \mathrm{Sym}^k(\Sigma)) \times I | u \in \mathcal{M}_\tau(\psi)\} \tag{2.5}$$

so for each homotopy class ψ we may choose orientations on $\mathcal{M}_{\tau=0}(\psi)$ fitting together coherently, and obtain induced orientations on the spaces $\mathcal{M}^h(\psi)$ via the product structure in equation (2.5). Such an induced orientation will enjoy the property that the restrictions to the ends at $\tau = 0$ and $\tau = 1$ yield the counts $-\#\mathcal{M}_{\tau=0}(\psi)$ and $+\#\mathcal{M}_{\tau=1}(\psi)$ respectively. We omit the technical details of this argument, and refer the interested reader to the proof of Lemma 2.9.13, where an analogous argument dealing with holomorphic triangles is spelled out in detail. We have thus shown that a generic homotopy $h = (\phi_{t,\tau}, K_{s,t,\tau})$ between $(\phi_{t,0}, K_{s,t,0})$ and $(\phi_{t,1}, K_{s,t,1})$ induces a chain homotopy between $\Gamma_{(\phi_{t,0}, K_{s,t,0})}$ and $\pm\Gamma_{(\phi_{t,1}, K_{s,t,1})}$.

Finally, we note that since the homotopy h is constant in τ for $t = 0$ and $t = 1$, the chain homotopy H^h, defined with respect to the orientations on $\mathcal{M}^h(\phi)$ specified above, is a chain homotopy between the continuation

maps

$$\Gamma_{(\phi_{t,0},K_{s,t,0})}, \Gamma_{(\phi_{t,1},K_{s,t,1})} : CF^-_{K_{s,0,0}=K_{s,0,1}}(\Sigma, \boldsymbol{\alpha}_0, \boldsymbol{\beta}_0, z, \mathfrak{o}_{\boldsymbol{\alpha}_0,\boldsymbol{\beta}_0}) \to CF^-_{K_{s,1,0}=K_{s,1,1}}(\Sigma, \boldsymbol{\alpha}_1, \boldsymbol{\beta}_1, z, \mathfrak{o}_{\boldsymbol{\alpha}_1,\boldsymbol{\beta}_1})$$

defined with respect to the same coherent orientation systems on their domains, and the same coherent orientation systems on their targets. In particular, in the case of interest (i.e. equation (2.2)) we may choose orientations on $\mathcal{M}_{\tau=0} = \mathcal{M}^{d_t}$ so that $d_{J_s,J'_s} \sim \Gamma_{d_t}$ (which we established is possible earlier), which together with the above remarks establishes equation (2.2). This completes the proof of the theorem. □

Finally, we relegate the proof of axiom 4, simple handleswap invariance, to Section 2.9 below. Given a simple handleswap in $\mathcal{G}_{\text{man}}$,

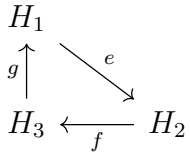

we will show that the composition of the induced maps in the category of transitive systems in the projectivized homotopy category yields the identity. We recall from Definition 2.4.6 that here $H_i = (\Sigma \# \Sigma_0, \boldsymbol{\alpha}_i, \boldsymbol{\beta}_i)$ are isotopy diagrams, e is a strong $\boldsymbol{\alpha}$-equivalence, f is a strong $\boldsymbol{\beta}$-equivalence, and g is a diffeomorphism of isotopy diagrams.

Theorem 2.8.2 (cf. Theorem 9.30 in [3])**.** *Let $(\{H_i\}, e, f, g)$ be data defining a simple handleswap as above. For the weak Heegaard invariants CF° defined in Definition 2.7.9, the induced maps $g_* := CF^\circ(g)$, $\Phi_e := CF^\circ(e)$,*

and $\Phi_f := CF^\circ(f)$ *satisfy*

$$g_* \circ \Phi_f \circ \Phi_e = Id_{CF^-(H_1)}$$

Thus the weak Heegaard invariants $CF^\circ : \mathcal{G}_{man} \to$ *Trans*$(P($*Kom*$(\mathbb{Z}[U]$*-Mod*$)))$ *satisfy simple handleswap invariance.*

Corollary 2.8.3. *The weak Heegaard invariants* $HF^- : \mathcal{G}_{man} \to P(\mathbb{Z}[U]$*-Mod*$)$ *satisfy simple handleswap invariance.*

Theorem 2.8.2 and Corollary 2.8.3 will establish Theorem 1.3.3 and Corollary 1.3.4, which by Section 2.6 also establishes Theorem 1.3.1.

2.9. Simple Handleswap Invariance

In this section we prove Theorem 2.8.2. The key result which will need to be established is the integral analog of a triangle count proved in [3, Proposition 9.31]. We will consider the pointed genus two Heegaard triple diagram $\mathcal{T}_0$ shown in Figure 22 (compare the diagrams in Figure 20). Given any triple diagram $\mathcal{T}$ we will show that triangle maps on the stabilized diagram $\mathcal{T}\#\mathcal{T}_0$, endowed with a sufficiently stretched neck, are determined by triangle maps on the unstabilized diagram $\mathcal{T}$.

We now fix some notation regarding the intersection points in the triple diagram $\mathcal{T}_0 = (\Sigma, \boldsymbol{\alpha}'_0, \boldsymbol{\alpha}_0, \boldsymbol{\beta}_0, p_0)$. We write $\mathbb{T}_{\boldsymbol{\alpha}_0} \cap \mathbb{T}_{\boldsymbol{\beta}_0} = \{\boldsymbol{a}\}$, $\mathbb{T}_{\boldsymbol{\alpha}'_0} \cap \mathbb{T}_{\boldsymbol{\beta}_0} = \{\boldsymbol{b}\}$, and $\mathbb{T}_{\boldsymbol{\alpha}'_0} \cap \mathbb{T}_{\boldsymbol{\alpha}_0} = \{\theta_1^+\theta_2^+, \theta_1^+\theta_2^-, \theta_1^-\theta_2^+, \theta_1^-\theta_2^-\}$. Here the intersection points $\theta_1^\pm \in \alpha'_1 \cap \alpha_1$ and $\theta_2^\pm \in \alpha'_2 \cap \alpha_2$ are those labeled in Figure 22. We write $\boldsymbol{\Theta} := \theta_1^+\theta_2^+$. We will show:

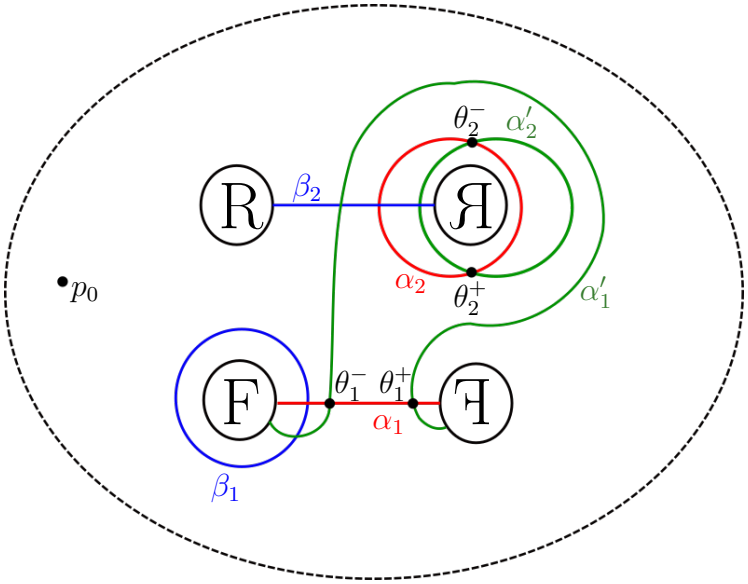

FIGURE 22 The pointed triple diagram $\mathcal{T}_0$, with the curves $\boldsymbol{\alpha}_0' = (\alpha_1', \alpha_2')$, $\boldsymbol{\alpha}_0 = (\alpha_1, \alpha_2)$, $\boldsymbol{\beta}_0 = (\beta_1, \beta_2)$, and the θ intersection points, labeled.

Proposition 2.9.1. *(compare [3, Proposition 9.31]) Fix a strongly $\mathfrak{s}$-admissible Heegaard triple $\mathcal{T} = (\Sigma, \boldsymbol{\alpha}', \boldsymbol{\alpha}, \boldsymbol{\beta}, p)$, and consider the diagram $\mathcal{T}\#\mathcal{T}_0$, where $\mathcal{T}_0 = (\Sigma, \boldsymbol{\alpha}_0', \boldsymbol{\alpha}_0, \boldsymbol{\beta}_0, p_0)$ is the diagram in Figure 22 and the connect sum is taken at the basepoints p and p_0. Then for a generic and sufficiently stretched almost complex structure there is a coherent orientation system $\mathfrak{o}_{\mathcal{T}_0}$ on $\mathcal{T}_0$, which together with any coherent orientation system $\mathfrak{o}_{\mathcal{T}}$ on $\mathcal{T}$ induces a coherent orientation system $\mathfrak{o}_{\mathcal{T}\#\mathcal{T}_0}$ on $\mathcal{T}\#\mathcal{T}_0$. Furthermore, with respect to these orientations,*

$$\mathcal{F}_{\mathcal{T}\#\mathcal{T}_0}((\boldsymbol{x} \times \boldsymbol{\Theta}) \otimes (\boldsymbol{y} \times \boldsymbol{a}), \mathfrak{s}) = \pm \mathcal{F}_{\mathcal{T}}(\boldsymbol{x} \otimes \boldsymbol{y}, \mathfrak{s}) \times \boldsymbol{b}$$

for any $\boldsymbol{x} \in \mathbb{T}_{\boldsymbol{\alpha}'} \cap \mathbb{T}_{\boldsymbol{\alpha}}$ and $\boldsymbol{y} \in \mathbb{T}_{\boldsymbol{\alpha}} \cap \mathbb{T}_{\boldsymbol{\beta}}$.

In fact when we prove handleswap invariance the diagram $\mathcal{T}_0$ and the triangle count just stated will be relevant only to the consideration

of the strong $\boldsymbol{\alpha}$-equivalence involved in the statement. We will need an analogous result which pertains to the strong $\boldsymbol{\beta}$-equivalence map occurring in the statement. We now state the precise result we will need for this. Let $\mathcal{T}_0' = (\Sigma_0, \boldsymbol{\alpha}_0', \boldsymbol{\beta}_0, \boldsymbol{\beta}_0', p_0)$ denote the pointed genus two triple diagram shown in Figure 23, where $\boldsymbol{\alpha}_0' = \{\alpha_1', \alpha_2'\}$, $\boldsymbol{\beta}_0' = \{\beta_1, \beta_2\}$ and $\boldsymbol{\beta}_0' = \{\beta_1', \beta_2'\}$ (again compare the diagrams in Figure 20).

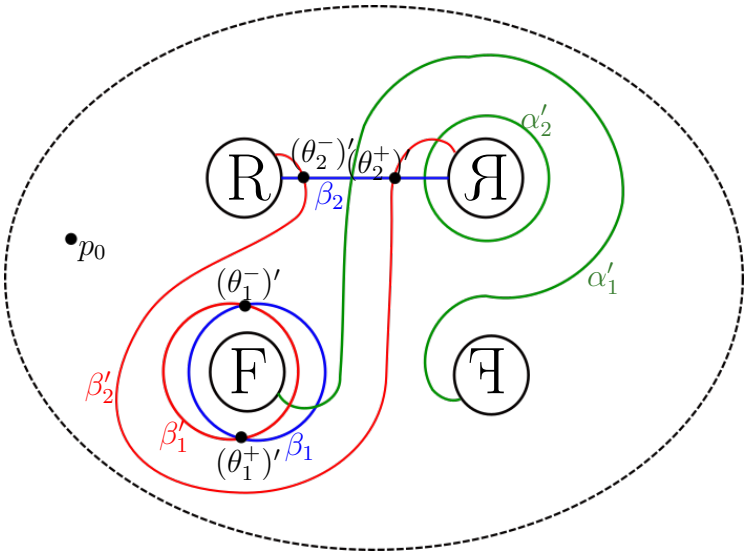

FIGURE 23 The pointed triple diagram $\mathcal{T}_0'$, with the curves $\boldsymbol{\alpha}_0' = (\alpha_1', \alpha_2')$, $\boldsymbol{\beta}_0 = (\beta_1, \beta_2)$, and $\boldsymbol{\beta}_0' = (\beta_1', \beta_2')$, and the θ' intersection points, labeled.

We further fix the following notation for intersection points in the diagram: we let $\mathbb{T}_{\boldsymbol{\alpha}_0'} \cap \mathbb{T}_{\boldsymbol{\beta}_0} = \{\mathbf{b}\}$, $\mathbb{T}_{\boldsymbol{\alpha}_0'} \cap \mathbb{T}_{\boldsymbol{\beta}_0'} = \{\mathbf{c}\}$, and $\boldsymbol{\Theta}'$ denote the generator in $\mathbb{T}_{\boldsymbol{\beta}_0} \cap \mathbb{T}_{\boldsymbol{\beta}_0'}$ with the highest relative grading. Let $\mathcal{T}' = (\Sigma, \boldsymbol{\alpha}', \boldsymbol{\beta}, \boldsymbol{\beta}', p)$ be another pointed Heegaard triple, and consider the diagram $\mathcal{T}' \# \mathcal{T}_0'$, where the connect sum is taken at the basepoints p and p_0. Then we will have an analogous triangle count:

Proposition 2.9.2. *(compare [3, Proposition 9.32]) Fix a strongly $\mathfrak{s}$-admissible Heegaard triple $\mathcal{T}' = (\Sigma, \boldsymbol{\alpha}', \boldsymbol{\beta}, \boldsymbol{\beta}', p)$, and consider the diagram*

$\mathcal{T}'\#\mathcal{T}_0'$ as above. Then for a generic and sufficiently stretched almost complex structure there is a coherent orientation system $\mathfrak{o}_{\mathcal{T}_0'}$ on $\mathcal{T}_0'$, which together with any coherent orientation system $\mathfrak{o}_{\mathcal{T}'}$ on $\mathcal{T}'$ induces a coherent orientation system $\mathfrak{o}_{\mathcal{T}'\#\mathcal{T}_0'}$ on $\mathcal{T}'\#\mathcal{T}_0'$. Furthermore, with respect to these orientations,

$$\mathcal{F}_{\mathcal{T}'\#\mathcal{T}_0'}((\boldsymbol{x}\times\boldsymbol{b})\otimes(\boldsymbol{y}\times\boldsymbol{\Theta}'),\mathfrak{s}) = \pm\mathcal{F}_{\mathcal{T}'}(\boldsymbol{x}\otimes\boldsymbol{y},\mathfrak{s})\times\boldsymbol{c}$$

for any $\boldsymbol{x}\in\mathbb{T}_{\boldsymbol{\alpha}'}\cap\mathbb{T}_{\boldsymbol{\beta}}$ and $\boldsymbol{y}\in\mathbb{T}_{\boldsymbol{\beta}}\cap\mathbb{T}_{\boldsymbol{\beta}'}$.

We will prove Proposition 2.9.1 in the following subsection. Since a nearly identical proof can be used to establish Proposition 2.9.2, we omit the proof of that result. We now assume Propositions 2.9.1 and 2.9.2 and use them to establish Theorem 2.8.2.

Proof of Theorem 2.8.2. We consider a simple handleswap (H_1, H_2, H_3, e, f, g) as in Definition 2.4.6. We first note that to prove the statement about transitive systems appearing in Theorem 2.8.2, it will suffice to find representatives $\mathcal{H}_1$, $\mathcal{H}_2$, and $\mathcal{H}_3$ for the isotopy diagrams, and show that for these representatives we have

$$g_*\circ\Phi_f\circ\Phi_e = \pm\mathrm{Id}_{CF^-(\mathcal{H}_1)}$$

in Kom($\mathbb{Z}[U]$-Mod), or equivalently

$$g_*\circ\Phi_f\circ\Phi_e = \mathrm{Id}_{CF^-(\mathcal{H}_1)}$$

in $P(\mathrm{Kom}(\mathbb{Z}[U]\text{-Mod}))$. Indeed, since each of the maps Φ_e, Φ_f, and g_* above are contained in the morphisms Φ_e, Φ_f and g_* of the transitive systems $CF^-(H)$, by the results in Sections 2.7 and 2.8, this monodromy relation will automatically yield corresponding monodromy relation for all such triangles.

Let $\mathcal{H}_1 = (\Sigma\#\Sigma_0, \boldsymbol{\alpha}_1, \boldsymbol{\beta}_2)$ be a representative for the first isotopy diagram in the collection of data specifying the simple handleswap. By definition, $\mathcal{H}_1$ decomposes as $\mathcal{H}\#\mathcal{H}_0$, where $\mathcal{H} = (\Sigma, \boldsymbol{\alpha}, \boldsymbol{\beta})$ and $\mathcal{H}_0 = (\Sigma_0, \boldsymbol{\alpha}_0, \boldsymbol{\beta}_0)$ are as in Figure 20 ($\mathcal{H}_0$ here is what we were denoting by $P \cap \mathcal{H}_1$ in Definition 2.4.6).

Fix two new curves $\boldsymbol{\alpha}_0'$ on Σ_0 which are related to $\boldsymbol{\alpha}_0$ as in the diagram $\mathcal{T}_0$ in the statement of Proposition 2.9.1. Fix also a collection of curves $\boldsymbol{\alpha}'$ on Σ which are obtained by performing a small Hamiltonian isotopy on the curves in $\boldsymbol{\alpha}$. The second isotopy diagram H_2 can then be represented as $H_2 = (\Sigma\#\Sigma_0, \boldsymbol{\alpha}' \cup \boldsymbol{\alpha}_0', \boldsymbol{\beta} \cup \boldsymbol{\beta}_0)$, and the morphism associated to the strong $\boldsymbol{\alpha}$-equivalence e is given by the triangle map $\Phi_e := \Psi^{\boldsymbol{\alpha}\cup\boldsymbol{\alpha}_0 \to \boldsymbol{\alpha}'\cup\boldsymbol{\alpha}_0'}_{\boldsymbol{\beta}\cup\boldsymbol{\beta}_0}$. We note that our choices of representatives for the isotopy diagrams H_1 and H_2 ensure that the strong equivalence map of Definition 2.7.8 applied to these representatives is computed using only a single triangle map, as opposed to a composition of triangle maps and continuation maps. As in the notation of Proposition 2.9.1, we set $\mathbb{T}_{\boldsymbol{\alpha}_0} \cap \mathbb{T}_{\boldsymbol{\beta}_0} = \{\boldsymbol{a}\}$ and $\mathbb{T}_{\boldsymbol{\alpha}_0'} \cap \mathbb{T}_{\boldsymbol{\beta}_0} = \{\boldsymbol{b}\}$.

We then have for any $\boldsymbol{y} \times \boldsymbol{a} \in \mathbb{T}_{\boldsymbol{\alpha} \cup \boldsymbol{\alpha}_0} \cap \mathbb{T}_{\boldsymbol{\beta} \cup \boldsymbol{\beta}_0}$:

$$\begin{aligned}
\Phi_e(\boldsymbol{y} \times \boldsymbol{a}) &= \Psi^{\boldsymbol{\alpha} \cup \boldsymbol{\alpha}_0 \to \boldsymbol{\alpha}' \cup \boldsymbol{\alpha}_0'}_{\boldsymbol{\beta} \cup \boldsymbol{\beta}_0}(\boldsymbol{y} \times \boldsymbol{a}) \\
&= \mathcal{F}_{\boldsymbol{\alpha}' \cup \boldsymbol{\alpha}_0', \boldsymbol{\alpha} \cup \boldsymbol{\alpha}_0, \boldsymbol{\beta} \cup \boldsymbol{\beta}_0}(\boldsymbol{\Theta}_{\boldsymbol{\alpha}' \cup \boldsymbol{\alpha}_0', \boldsymbol{\alpha} \cup \boldsymbol{\alpha}_0} \otimes (\boldsymbol{y} \times \boldsymbol{a})) \\
&= \mathcal{F}_{\boldsymbol{\alpha}' \cup \boldsymbol{\alpha}_0', \boldsymbol{\alpha} \cup \boldsymbol{\alpha}_0, \boldsymbol{\beta} \cup \boldsymbol{\beta}_0}((\boldsymbol{\Theta}_{\boldsymbol{\alpha}', \boldsymbol{\alpha}} \times \boldsymbol{\Theta}) \otimes (\boldsymbol{y} \times \boldsymbol{a})) \\
&= \pm \mathcal{F}_{\boldsymbol{\alpha}', \boldsymbol{\alpha}, \boldsymbol{\beta}}(\boldsymbol{\Theta}_{\boldsymbol{\alpha}', \boldsymbol{\alpha}} \times \boldsymbol{y}) \times \boldsymbol{b} \\
&= \pm \Gamma^{\boldsymbol{\alpha} \to \boldsymbol{\alpha}'}_{\boldsymbol{\beta}}(\boldsymbol{y}) \times \boldsymbol{b}
\end{aligned}$$

Here we have used Proposition 2.9.1 in the second to last equality, and Lemma 2.7.7 in the last equality.

We perform the analogous calculation for the strong $\boldsymbol{\beta}$-equivalence. Fix two new curves $\boldsymbol{\beta}_0'$ on Σ_0 which are related to $\boldsymbol{\beta}_0$ as in the diagram $\mathcal{T}_0'$ in the statement of Proposition 2.9.2. Fix also a collection of curves $\boldsymbol{\beta}'$ on Σ which are obtained by performing a small Hamiltonian isotopy on the curves in $\boldsymbol{\beta}$. The third isotopy diagram H_3 can then be represented as $H_3 = (\Sigma \# \Sigma_0, \boldsymbol{\alpha}' \cup \boldsymbol{\alpha}_0', \boldsymbol{\beta}' \cup \boldsymbol{\beta}_0')$, and the morphism associated to the strong $\boldsymbol{\beta}$-equivalence f is given by the triangle map $\Phi_f := \Psi^{\boldsymbol{\alpha}' \cup \boldsymbol{\alpha}_0'}_{\boldsymbol{\beta} \cup \boldsymbol{\beta}_0 \to \boldsymbol{\beta}' \cup \boldsymbol{\beta}_0'}$. As in the notation of Proposition 2.9.2, we set $\mathbb{T}_{\boldsymbol{\alpha}_0'} \cap \mathbb{T}_{\boldsymbol{\beta}_0'} = \{\mathbf{c}\}$. By the same sequence of computations as in the previous case we then have for any

$\boldsymbol{x} \times \boldsymbol{b} \in \mathbb{T}_{\boldsymbol{\alpha}' \cup \boldsymbol{\alpha}'_0} \cap \mathbb{T}_{\boldsymbol{\beta} \cup \boldsymbol{\beta}_0}$:

$$\begin{aligned}
\Phi_f(\boldsymbol{x} \times \boldsymbol{b}) &= \Psi^{\boldsymbol{\alpha}' \cup \boldsymbol{\alpha}'_0}_{\boldsymbol{\beta} \cup \boldsymbol{\beta}_0 \to \boldsymbol{\beta}' \cup \boldsymbol{\beta}'_0}(\boldsymbol{x} \times \boldsymbol{b}) \\
&= \mathcal{F}_{\boldsymbol{\alpha}' \cup \boldsymbol{\alpha}'_0, \boldsymbol{\beta} \cup \boldsymbol{\beta}_0, \boldsymbol{\beta}' \cup \boldsymbol{\beta}'_0}((\boldsymbol{x} \times \boldsymbol{b}) \otimes \boldsymbol{\Theta}_{\boldsymbol{\beta} \cup \boldsymbol{\beta}_0, \boldsymbol{\beta}' \cup \boldsymbol{\beta}'_0}) \\
&= \mathcal{F}_{\boldsymbol{\alpha}' \cup \boldsymbol{\alpha}'_0, \boldsymbol{\beta} \cup \boldsymbol{\beta}_0, \boldsymbol{\beta}' \cup \boldsymbol{\beta}'_0}((\boldsymbol{x} \times \boldsymbol{b}) \otimes (\boldsymbol{\Theta}_{\boldsymbol{\beta}, \boldsymbol{\beta}'} \times \boldsymbol{\Theta})) \\
&= \pm \mathcal{F}_{\boldsymbol{\alpha}', \boldsymbol{\beta}, \boldsymbol{\beta}'}(\boldsymbol{x} \times \boldsymbol{\Theta}_{\boldsymbol{\beta}, \boldsymbol{\beta}'}) \times \boldsymbol{c} \\
&= \pm \Gamma^{\boldsymbol{\alpha}'}_{\boldsymbol{\beta} \to \boldsymbol{\beta}'}(\boldsymbol{x}) \times \boldsymbol{c}
\end{aligned}$$

This time we have used Proposition 2.9.2 in the second to last equality, and again used Lemma 2.7.7 in the last equality.

We note that in the collection of representatives for the isotopy diagrams in a simple handleswap one could leave the $\boldsymbol{\alpha}$ and $\boldsymbol{\beta}$ curves unchanged throughout the handleswap, which would necessitate the diffeomorphism g restricting to the identity on Σ. Here we have altered $\boldsymbol{\alpha}$ and $\boldsymbol{\beta}$ slightly, so that the strong $\boldsymbol{\alpha}$-equivalence and strong $\boldsymbol{\beta}$-equivalence maps could each be computed via a single triangle map Ψ. Since our alteration of the curves $\boldsymbol{\alpha}$ and $\boldsymbol{\beta}$ on Σ came from small Hamiltonian isotopies, we can however still ensure that for our representatives for the handleswap the diffeomorphism g is isotopic to the identity when restricted to Σ. Furthermore, since g is part of a simple handleswap it must satisfy $g(\boldsymbol{\alpha}') = g(\boldsymbol{\alpha})$ and $g(\boldsymbol{\beta}') = g(\boldsymbol{\beta})$. Thus, by definition of the maps induced by diffeomorphisms of diagrams, we have

$$g_*(\boldsymbol{z} \times \boldsymbol{c}) = (g|_\Sigma)_*(\boldsymbol{z}) \times \boldsymbol{a}$$

for all $(\boldsymbol{z} \times \boldsymbol{c}) \in \mathbb{T}_{\boldsymbol{\alpha}' \cup \boldsymbol{\alpha}'_0} \cap \mathbb{T}_{\boldsymbol{\beta}' \cup \boldsymbol{\beta}'_0}$.

Putting these formulas for each of the induced maps together, we find that

$$\begin{aligned} g_* \circ \Phi_f \circ \Phi_e(\boldsymbol{y} \times \boldsymbol{a}) &= \left(g_* \circ \Psi^{\boldsymbol{\alpha}' \cup \boldsymbol{\alpha}'_0}_{\boldsymbol{\beta} \cup \boldsymbol{\beta}_0 \to \boldsymbol{\beta}' \cup \boldsymbol{\beta}'_0} \circ \Psi^{\boldsymbol{\alpha} \cup \boldsymbol{\alpha}_0 \to \boldsymbol{\alpha}' \cup \boldsymbol{\alpha}'_0}_{\boldsymbol{\beta} \cup \boldsymbol{\beta}_0} \right) (\boldsymbol{y} \times \boldsymbol{a}) \\ &= \pm \left((g|_\Sigma)_* \circ \Gamma^{\boldsymbol{\alpha}'}_{\boldsymbol{\beta} \to \boldsymbol{\beta}'} \circ \Gamma^{\boldsymbol{\alpha} \to \boldsymbol{\alpha}'}_{\boldsymbol{\beta}} \right) (\boldsymbol{y}) \times \boldsymbol{a} \end{aligned}$$

Since the restiction of g to Σ is isotopic to the identity, Theorem 2.8.1 ensures

$$(g|_\Sigma)_* \circ \Gamma^{\boldsymbol{\alpha}'}_{\boldsymbol{\beta} \to \boldsymbol{\beta}'} \circ \Gamma^{\boldsymbol{\alpha} \to \boldsymbol{\alpha}'}_{\boldsymbol{\beta}} \sim \pm \mathrm{Id}_{CF^-(\mathcal{H})}$$

We thus have

$$\begin{aligned} g_* \circ \Phi_f \circ \Phi_e &= \pm \left((g|_\Sigma)_* \circ \Gamma^{\boldsymbol{\alpha}'}_{\boldsymbol{\beta} \to \boldsymbol{\beta}'} \circ \Gamma^{\boldsymbol{\alpha} \to \boldsymbol{\alpha}'}_{\boldsymbol{\beta}} \right) \otimes \mathrm{Id}_{CF^-(\mathcal{H}_0)} \\ &\sim \pm \mathrm{Id}_{CF^-(\mathcal{H})} \otimes \mathrm{Id}_{CF^-(\mathcal{H}_0)} \\ &\sim \pm \mathrm{Id}_{CF^-(\mathcal{H}_1)} \end{aligned}$$

which by the remarks at the beginning of the proof completes the argument.

□

Having established the implication (Proposition 2.9.1 and Proposition 2.9.2 $\implies$ Theorem 2.8.2), we now turn towards proving Proposition 2.9.1.

We employ the strategy used in [3] for proving the analog of Proposition 2.9.1 appearing there. We import many results exactly as they are stated there, while in a few cases we make small modifications in order to be able to apply their results. For the reader's convenience we provide

statements of some results from [3], and provide proofs of any imported results which must be modified slightly for our purposes. We also provide sketches of proofs of certain statements from [3] which we do not need to modify, but whose exposition we hope will aid in the readibility of this dissertation.

In the remainder of this section we work in the cylindrical formulation of Heegaard Floer homology introduced by Lipshitz in [14].

Moduli Spaces of Triangles

We begin by recalling some notation and terminology regarding holomormphic triangles in the cylindrical setting of Heegaard Floer homology (see [14]). We denote by Δ the subset of $\mathbb{C}$ shown in Figure 24 below, which has three cylindrical ends modeled on $[0,1] \times [0,\infty)$. We will think of this region as a triangle with its vertices removed. We also introduce in the figure notation we will use to indicate the boundary components and ends of this region.

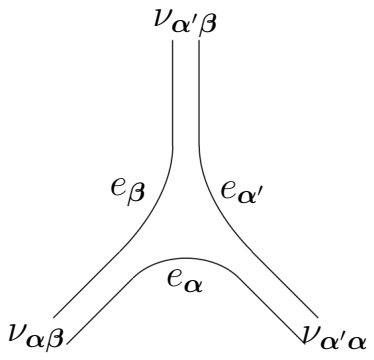

FIGURE 24 The region Δ.

We will consider almost complex structures J on $\Sigma \times \Delta$ which satisfy the following conditions:

($J'1'$) J is tamed by the split symplectic form on $\Sigma \times \Delta$.

($J'2'$) On each component of $\Sigma \setminus (\boldsymbol{\alpha}' \cup \boldsymbol{\alpha} \cup \boldsymbol{\beta})$ there is at least one point at which $J = j_\Sigma \times j_\Delta$.

($J'3'$) On each cylindrical end $\Sigma \times [0,1] \times \mathbb{R}$ of $\Sigma \times \Delta$, there is a 2-plane distribution η on $\Sigma \times [0,1] \times \{0\}$ such that the restriction of ω to η is non-degenerate, J preserves η, and the restriction of J to η is compatible with ω. Furthermore, η is tangent to Σ near $(\Sigma \times \{0,1\} \times \{0\}) \cup (\Sigma \times [0,1] \times \{0\})$.

($J'4'$) The planes $T_d(\{p\} \times \Delta)$ are complex lines of J for all $(p,d) \in \Sigma \times \Delta$.

($J'5'$) There is an open set $U \subset \Delta$ containing $\partial\Delta \setminus \{\nu_{\alpha'\alpha}, \nu_{\alpha\beta}, \nu_{\alpha'\beta}\}$ such that the planes $T_p(\Sigma \times \{d\})$ are complex lines of J for all (p,d) near $(\boldsymbol{\alpha}' \cup \boldsymbol{\alpha} \cup \boldsymbol{\beta}) \times \Delta$ and for all $(p,d) \in \Sigma \times U$.

J-holomorphic curves in $\Sigma \times \Delta$ for almost complex structures J of this sort enjoy the following property.

Lemma 2.9.3 (Lemma 3.1 in [14])**.** *Let J be an almost complex structure on $\Sigma \times \Delta$ that satisfies the axioms $(J'1') - (J'5')$. If $u : S \to \Sigma \times \Delta$ is J-holomorphic and $\pi_\Sigma \circ u$ is nonconstant on a component S_0 of S, then $\pi_\Sigma \circ u|_{S_0}$ is an open map. Furthermore, there are coordinates near any critical point of $\pi_\Sigma \circ u|_{S_0}$ where $\pi_\Sigma \circ u$ takes the form $z \mapsto z^k$ for some $k > 0$.*

In fact, this result follows immediately from [19, Theorem 7.1].

To understand Proposition 2.9.1, we will need to investigate the nature of triangle maps on the diagram $\mathcal{T}\#\mathcal{T}_0$. In the cylindrical setting, the notion of a holomorphic triangle in a Heegaard triple diagram takes the following form.

Definition 2.9.4. Let $\mathcal{T} = (\Sigma, \boldsymbol{\alpha'}, \boldsymbol{\alpha}, \boldsymbol{\beta})$ be a triple diagram, and set $d = |\boldsymbol{\alpha'}| = |\boldsymbol{\alpha}| = |\boldsymbol{\beta}|$. By a *holomorphic triangle in the triple diagram* $\mathcal{T}$ we will mean a (j, J)-holomorphic map $u : S \to \Sigma \times \Delta$ satsifying:

(M1) (S, j) is a (possibly nodal) Riemann surface with boundary and $3d$ punctures on ∂S.

(M2) u is locally nonconstant.

(M3) $u(\partial S) \subset (\boldsymbol{\alpha'} \times e_{\boldsymbol{\alpha'}}) \cup (\boldsymbol{\alpha} \times e_{\boldsymbol{\alpha}}) \cup (\boldsymbol{\beta} \times e_{\boldsymbol{\beta}})$.

(M4) u has finite energy.

(M5) For each $i \in \{1, \ldots, d\}$ and $\sigma \in \{\boldsymbol{\alpha'}, \boldsymbol{\alpha}, \boldsymbol{\beta}\}$, the preimage $u^{-1}(\sigma_i \times e_\sigma)$ consists of exactly one component of the punctured boundary of S.

(M6) As one approaches the punctures of ∂S, the map u converges to a collection of intersection points on the Heegaard triple in the cylindrical ends of $\Sigma \times \Delta$.

We will often ask holomorphic triangles to satisfy the following additional two requirements:

(M7) $\pi_\Delta \circ u$ is nonconstant on each component of S.

(M8) S is smooth, and u is an embedding.

Unless otherwise specified, we will use the term holomorphic triangle to refer to maps satisfying axioms $(M1)-(M6)$, and explicitly note when we are considering curves satisfying the additional axioms $(M7)$ and $(M8)$.

For any homology class ψ of triangles on a Heegaard triple diagram $\mathcal{T}$, we will denote by $\mathcal{M}(\psi)$ the moduli space of holomorphic triangles on $\mathcal{T}$ in the homology class ψ. Given a Riemann surface S, we will indicate by $\mathcal{M}(\psi, S)$ the subspace of $\mathcal{M}(\psi)$ consisting of holomorphic triangles with source S.

To obtain the triangle count we are after on a sufficiently stretched copy of $\mathcal{T}\#\mathcal{T}_0$, we will need to understand compactifications of these moduli spaces of triangles. These compactifications allow for a weaker notion of triangle which we refer to as broken:

Definition 2.9.5. Let $\mathcal{T} = (\Sigma, \boldsymbol{\alpha}', \boldsymbol{\alpha}, \boldsymbol{\beta})$ and d be as above. We say that a collection of (j, J)-holomorphic curves $BT = (u_1, v_1, \ldots, v_n, w_1, \ldots, w_m)$ is a *broken holomorphic triangle on $\mathcal{T}$ representing the homology class ψ* if

(BT1) u_1 is a curve mapping to $\Sigma \times \Delta$ satisfying $(M1)$ and $(M3)-(M6)$.

(BT2) v_i are curves mapping to $\Sigma \times I \times \mathbb{R}$ which satisfy the analogs of $(M1)$ and $(M3)-(M6)$, each representing some homology class of strips in one of the diagrams $(\Sigma, \boldsymbol{\alpha}, \boldsymbol{\alpha}')$, $(\Sigma, \boldsymbol{\alpha}', \boldsymbol{\beta})$ or $(\Sigma, \boldsymbol{\alpha}, \boldsymbol{\beta})$.

(BT3) The w_i are curves from Riemann surfaces with d boundary components and a single puncture on each boundary component, and which map to $\Sigma \times I \times \mathbb{R} \coprod \Sigma \times \Delta$. For each i, the boundary components of the curve w_i all map to a single set of attaching curves.

(BT4) The total homology class of the curves in BT is equal to ψ.

With this notion in hand, we can state the following compactness result which describes the behavior of triangles on $\mathcal{T}\#\mathcal{T}_0$ as we stretch the neck:

Proposition 2.9.6 (Proposition 9.40 in [3]). *Let $\psi\#\psi_0$ be a homology class of triangles on $(\Sigma\#\Sigma_0)\times\Delta$, and u_{T_i} be a sequence of holomorphic triangle representatives for $\psi\#\psi_0$ on $(\Sigma\#\Sigma_0)\times\Delta$, with respect to almost complex structures $J(T_i)$ for neck lengths $T_i\to\infty$. Then there is a subsequence which converges to a triple (U,V,U_0) where U and U_0 are broken holomorphic triangles on $\Sigma\times\Delta$ and $\Sigma_0\times\Delta$ representing ψ and ψ_0 respectively, and V is a collection of holomorphic curves on the neck regions $S^1\times\mathbb{R}\times\Delta$ or $S^1\times\mathbb{R}\times[0,1]\times\mathbb{R}$ which are asymptotic to (possibly multiply covered) Reeb orbits $S^1\times\{d\}$ for $d\in\Delta$ or $d\in[0,1]\times\mathbb{R}$.*

Remark 2.9.7. More precisely, the asymptotic condition on the curves appearing in V in Proposition 2.9.6 above has the following meaning. By a "Reeb orbit" in this context, we mean a periodic orbit γ of the vector field $\dfrac{d}{d\theta}$ on $S^1\times\mathbb{R}\times\Delta$ or $S^1\times\mathbb{R}\times I\times\mathbb{R}$, where θ is the coordinate on S^1. The curves v in V have as sources punctured Riemann surfaces. Let S be a connected component of such a source, q a puncture of S, and $v:S\to S^1\times\mathbb{R}\times\Delta$. Write (θ,r,z) for coordinates on the target. Then v is asymptotic to γ at q if:

1. There is a neighborhood U of q in S and a biholomorphic diffeomorphism $\phi:U\cong S^1\times(0,\infty)$. Write (x,y) for coordinates on $S^1\times(0,\infty)$.

2. $r\circ v\circ\phi^{-1}\to\infty$ as $y\to\infty$

3. $(\theta, z) \circ v \circ \phi^{-1}(x, y) \to \gamma(x)$ as $y \to \infty$ as maps $S^1 \to S^1 \times \Delta$ in $\mathcal{C}^\infty_{\text{loc}}$.

Matched Moduli Spaces and Orientations

Fix a triple diagram $\mathcal{T} = (\Sigma, \boldsymbol{\alpha'}, \boldsymbol{\alpha}, \boldsymbol{\beta})$ and a point $p \in \Sigma \setminus (\boldsymbol{\alpha'} \cup \boldsymbol{\alpha} \cup \boldsymbol{\beta}))$. Let $u : S \to \Sigma \times \Delta$ be a J-holomorphic curve satisfying (M1)-(M6), for some almost complex structure J on $\Sigma \times \Delta$ satisfying $(J'1')$-$(J'5')$. Then u is locally non-constant by condition (M2), so by Lemma 2.9.3 $\pi_\Sigma \circ u$ is an open map on each component of S, and takes the form $z \mapsto z^k$ near any critical point. Thus $(\pi_\Sigma \circ u)^{-1}(p)$ is a finite set of points. Furthermore, using property $(J'4')$ of the almost complex structure J, positivity of complex intersections for J-holomorphic curves (See e.g [19] or [20]) ensures that all intersections between $p \times \Delta$ and the image of u are positive.

We will write $(\pi_\Sigma \circ u)^{-1}(p) = \{x_1, \ldots, x_{n_p(u)}\} \in \text{Sym}^{n_p(u)}(S)$, and define

$$\rho^p(u) := \{\pi_\Delta \circ u(x_1), \ldots, \pi_\Delta \circ u(x_{n_p(u)})\} \in \text{Sym}^{n_p(u)}(\Delta)$$

We remark that our notation involving set braces is somewhat misleading, as there may of course be repetitions among the points x_i in the symmetric product, corresponding to intersection points occuring with positive multiplicity greater than 1.

To understand the triangle count, we will be concerned with holomorphic triangles u for which $\rho^p(u)$ takes prescribed values. As a first step towards understanding the moduli spaces of such triangles, Juhász, Thurston and Zemke show that, for any prescribed value outside the fat diagonal, such a triangle is somewhere injective.

Lemma 2.9.8 (Lemma 9.45 in [3]). *Let $(\Sigma, \boldsymbol{\alpha'}, \boldsymbol{\alpha}, \boldsymbol{\beta}, p)$ be a triple diagram, and $\boldsymbol{d} \in Sym^k(\Delta) \setminus Diag(\Delta)$. If $u : S \to \Sigma \times \Delta$ is a J-holomorphic curve satsifying $(M1) - (M6)$ for an almost complex structure satisfying $(J'1') - (J'5')$, which furthermore has $\rho^p(u) = \boldsymbol{d}$, then every component of u is somewhere injective.*

Fix a Heegaard triple diagram $\mathcal{T} = (\Sigma, \boldsymbol{\alpha}', \boldsymbol{\alpha}, \boldsymbol{\beta}, p)$ and a homology class of triangle ψ, with $n_p(\psi) = k$. Given a subset $X \subset \mathrm{Sym}^k(\Delta)$, we let

$$\mathcal{M}(\psi, S, X) = \{u \in \mathcal{M}(\psi, S) | \rho^p(u) \in X\}$$

and

$$\mathcal{M}(\psi, X) = \{u \in \mathcal{M}(\psi) | \rho^p(u) \in X\}.$$

Using techniques similar to those used in the standard setting, Juhász, Thurston and Zemke prove the following result, which shows that generically these matched moduli spaces are smooth manifolds.

Proposition 2.9.9 (Proposition 9.47 in [3]). *Let $(\Sigma, \boldsymbol{\alpha'}, \boldsymbol{\alpha}, \boldsymbol{\beta})$ be a triple diagram, and fix a point $p \in \Sigma \setminus (\boldsymbol{\alpha'} \cup \boldsymbol{\alpha} \cup \boldsymbol{\beta})$. Suppose $X \subset Sym^k(\Delta)$ for some $k \in \mathbb{N}$ is a nonempty submanifold that does not intersect the fat diagonal. Furthermore, suppose that for every $x \in X$, the k-tuple x has no coordinate in the open set $U \subset \Delta$ from $(J'5')$. Then, for a generic choice of almost complex structure J, the set $\mathcal{M}(\psi, S, X)$ is a smooth manifold of dimension*

$$ind(\psi, S) - codim(X)$$

where $ind(\psi, S)$ denotes the Fredholm index of the linearized $\bar{\partial}$ operator at any representative $u : S \to \Sigma \times \Delta$ for ψ. For $X = Sym^k(\Delta)$, the same statement holds near any curve u that has no component T on which $\pi_\Delta \circ u|_T$ is constant and has image in U, and such that all components of u are somewhere injective.

It will be important for our purposes to note that these moduli spaces are also orientable when they are smoothly cut out, which follows in a straightforward manner from the framework in which the proof of the previous proposition is carried out. We now provide a sketch of the argument.

Lemma 2.9.10. *For J and X satisfying the hypotheses of Proposition 2.9.9, with $X \subset Sym^k(\Delta)$ furthermore assumed to be an orientable submanifold, $\mathcal{M}(\psi, S, X)$ is orientable.*

Proof. Forgetting the matching condition (i.e. taking $X = \mathrm{Sym}^k(\Delta)$) we consider $\mathcal{M}(\psi, S, \mathrm{Sym}^k(\Delta)) = \mathcal{M}(\psi, S)$. By [14, Proposition 6.3 and Section 10.3], whenever this space is transversely cut out it is an orientable smooth manifold.

For the case when $X \neq \mathrm{Sym}^k(\Delta)$, we briefly recall how one can establish the existence of a smooth manifold structure on $\mathcal{M}(\psi, S, X)$, as in the proof of [3, Proposition 9.47]. Consider the map $\rho^p : \mathcal{M}(\psi, S) \to \mathrm{Sym}^k(\Delta)$. To obtain the smooth manifold structure on $\mathcal{M}(\psi, S, X)$, one considers the universal moduli space $\mathcal{M}^\ell_{\mathrm{univ}}(\psi, S)$. This consists of triples (u, j, J), where j is a C^ℓ complex structure on S, J is a C^ℓ almost complex structure on $\Sigma \times \Delta$ satisying conditions $(J'1') - (J'5')$, and u is a (j, J)-holomorphic map $u : S \to \Sigma \times \Delta$ in the homology class ψ, which

furthermore satisfies certain regularity conditions (see [14, pg 968]). It is shown in the proof of Proposition 2.9.9, using the technique of [14, Proposition 3.7], that the universal moduli space $\mathcal{M}^{\ell}_{\text{univ}}(\psi, S)$ is a Banach manifold and the evaluation map $\rho^p : \mathcal{M}^{\ell}_{\text{univ}}(\psi, S) \to \text{Sym}^k(\Delta)$ is a submersion at all triples (u, j, J) for which $\rho^p(u)$ is not in the fat diagonal. Thus for X missing the fat diagonal, the universal matched moduli space $\mathcal{M}^{\ell}_{\text{univ}}(\psi, S, X) := (\rho^p)^{-1}(X)$ is a Banach manifold. One can then apply the Sard-Smale theorem to the Fredholm map $\pi : \mathcal{M}^{\ell}_{\text{univ}}(\psi, S, X) \to \mathcal{J}^{\ell}$ to obtain a regular value $J \in J^{\ell}$ so that $\mathcal{M}^{\ell}(\psi, S, X) = \pi^{-1}(J)$ is a smooth manifold. Finally, one uses an approximating bootstrapping argument to obtain the same result for C^{∞} complex structures. More precisely, one obtains that for a generic choice of J the space $\mathcal{M}(\psi, S)$ is a smooth manifold and the map

$$\rho^p : \mathcal{M}(\psi, S) \to \text{Sym}^k(\Delta)$$

is transverse to X. Thus for X missing the fat diagonal $\mathcal{M}(\psi, S, X) := (\rho^p)^{-1}(X)$ is a smooth manifold.

Fixing $u \in \mathcal{M}(\psi, S, X)$ we have

$$T_u\mathcal{M}(\psi, S) \cong T_u\mathcal{M}(\psi, S, X) \oplus N_u$$

where N is any choice of orthogonal complement. Since $\mathcal{M}(\psi, S)$ is orientable, it will suffice to show N is orientable to establish that

$\mathcal{M}(\psi, S, X)$ is orientable. Since ρ^p is transverse to X, we have

$$d\rho^p(T_u\mathcal{M}(\psi, S)) + T_{\rho^p(u)}X = T_{\rho^p(u)}\mathrm{Sym}^k(\Delta).$$

Since $(d\rho^p)^{-1}(TX) = T\mathcal{M}(\psi, S, X)$, the two equations above yield a direct sum decomposition

$$d\rho^p(N_u) \oplus T_{\rho^p(u)}X \cong T_{\rho^p(u)}\mathrm{Sym}^k(\Delta).$$

Finally, since X and $\mathrm{Sym}^k(\Delta)$ are orientable, and $d\rho^p|_N$ is an ismorphism on each fiber, the last equation establishes orientability of the complement N. Thus $\mathcal{M}(\psi, S, X)$ is orientable, as desired. □

We now turn to an investigation of the behavior of orientations on these moduli spaces. We recall again the notion of coherent orientation systems, and now provide the precise definitions in the cylindrical setting, as we will need them in some of our computations. We begin with the moduli space of holomorphic *strips* in a homology class $A \in \pi_2(\boldsymbol{x}, \boldsymbol{y})$, denoted $\mathcal{M}^A$, on some Heegaard (double) diagram $\mathcal{H} = (\Sigma, \boldsymbol{\alpha}, \boldsymbol{\beta})$. We set $\widehat{\mathcal{M}}^A = \mathcal{M}^A/\mathbb{R}$. As noted above, these moduli spaces are orientable whenever they are smoothly cut out by [14, Proposition 6.3]. There this is shown by trivializing the determinant line bundle of the virtual index bundle of the linearized $\bar{\partial}$-equation. In fact, this line bundle is trivialized over a larger auxiliary space of curves which are not necessarily holomorphic, which we denote by $\mathcal{B}^A$, rather than over $\mathcal{M}^A$. We ask for the trivializations of these determinant lines $\mathcal{L}$ over $\mathcal{B}^A$ to satisfy the following compatibility under glueing.

Definition 2.9.11. Given a Heegaard diagram $\mathcal{H}$, homology classes of strips A, A' which are adjacent on the diagram (i.e. $A \in \pi_2(\boldsymbol{x}, \boldsymbol{y})$, $A' \in \pi_2(\boldsymbol{y}, \boldsymbol{z})$), and maps $u : S \to \Sigma \times I \times \mathbb{R}$ and $u' : S' \to \Sigma \times I \times \mathbb{R}$ representing A and A' respectively, one can preglue the positive corners of u to the negative corners of u' (see [14, Appendix A] for one such construction). In fact, there is a 1 parameter family of such preglueings $(u \natural_r u' : S \natural_r S' \to \Sigma \times I \times \mathbb{R})$ in the class $A+A'$, defined for sufficiently large values of the parameter r . One can show that this map preserves the analogs of $(M1)$, $(M3)$ and $(M4)$ for strips, and the asymptotic conditions one asks of the strips. Denote the collection of maps of the form $S \to \Sigma \times I \times \mathbb{R}$ in a given homology class A which furthermore satisfy $(M1)$, $(M3)$, $(M4)$, and the asymptotic conditions by $\mathcal{B}^A(S)$. We say a choice of orientations for all $\widehat{\mathcal{M}}^A$, specified by a collection of nonvanishing sections $\mathfrak{o}_{\mathcal{H}} = \mathfrak{o}_{\boldsymbol{\alpha},\boldsymbol{\beta}} = \{\mathfrak{o}^A\}$ of $\mathcal{L}$ over all of the $\widehat{\mathcal{M}}^A$, is a *coherent orientation system on* $\mathcal{H}$ if the induced map of determinant lines covering the map $\natural_r : \mathcal{B}^A(S) \times \mathcal{B}^{A'}(S') \times (R, \infty) \to \mathcal{B}^{A+A'}(S \natural_r S')$ satisfies $(\natural_r)_*(\mathfrak{o}^A \times \mathfrak{o}^{A'}) = +\mathfrak{o}^{A+A'}$.

That such coherent orientation systems exist is shown in numerous places. One construction sufficient for our purposes can be found in [14, Section 6].

In the case of holomorphic triangles, the moduli spaces $\mathcal{M}(\psi)$ are also orientable. For a collection of orientations on $\mathcal{M}(\psi)$ for all homology classes ψ of triangles in a triple diagram, we will consider a related notion of coherence.

Definition 2.9.12. Given a Heegaard triple diagram $\mathcal{T}$, we will say a choice of orientations for $\mathcal{M}^{\psi_{\boldsymbol{\alpha},\boldsymbol{\beta}}}$, $\mathcal{M}^{\psi_{\boldsymbol{\beta},\boldsymbol{\gamma}}}$, $\mathcal{M}^{\psi_{\boldsymbol{\alpha},\boldsymbol{\gamma}}}$, and $\mathcal{M}(\psi)$ (for $\psi_{\boldsymbol{\alpha},\boldsymbol{\beta}}$, $\psi_{\boldsymbol{\beta},\boldsymbol{\gamma}}$ and

$\psi_{\boldsymbol{\alpha},\boldsymbol{\gamma}}$ ranging over all classes of strips in the respective double diagrams, and ψ ranging over all classes of triangles in the triple diagram) specified by a collection of sections $\mathfrak{o}_{\mathcal{T}} = \{\mathfrak{o}_{\boldsymbol{\alpha},\boldsymbol{\beta},\boldsymbol{\gamma}}, \mathfrak{o}_{\boldsymbol{\alpha},\boldsymbol{\beta}}, \mathfrak{o}_{\boldsymbol{\beta},\boldsymbol{\gamma}}, \mathfrak{o}_{\boldsymbol{\alpha},\boldsymbol{\gamma}}\}$ is a *coherent orientation system of triangles*, if each collection of orientations of the moduli spaces of strips on the respective double diagrams are coherent, and all possible pregluings of triangles with strips satisfy the analogous glueing condition.

Following [14, Section 6], given a homology class of triangles ψ on the triple diagram $\mathcal{T}$, let $T(\psi)$ denote the space of pairs (u, j), where $u : S \to \Sigma \times \Delta$ is a curve in the class ψ satisfying $(M1)$, $(M3)$ and $(M4)$, and j is a complex structure on S. We declare two such pairs $(u : S \to \Sigma \times \Delta, j)$ and $(u' : S' \to \Sigma \times \Delta, j')$ to be equivalent if there is a biholomorphism $\phi : (S, j) \to (S', j')$ such that the diagram

$$\begin{array}{ccc} S & \xrightarrow{\phi} & S' \\ & {\scriptstyle u}\searrow \quad \swarrow{\scriptstyle u'} & \\ & \Sigma \times \Delta & \end{array} \tag{2.6}$$

commutes. We denote the quotient of $T(\psi)$ by this equivalence relation by $\mathcal{B}(\psi)$.

Let $p : I \to \mathrm{Sym}^k(\Delta)$ be an embedded path missing the fat diagonal. We consider the following moduli spaces of triangles associated to homology classes $\psi_0 \in \pi_2(\boldsymbol{\Theta}, \boldsymbol{a}, \boldsymbol{b})$ in the triple diagram $\mathcal{T}_0$ from Proposition 2.9.1:

$$\mathcal{B}_I^{\psi_0} = \mathcal{B}(\psi_0, p(I)) = \{(u, t) | u \in \mathcal{B}(\psi_0) \text{ and } \rho^p(u) \in p(t) \text{ for some } t \in I\}$$

and

$$\mathcal{B}_t^{\psi_0} = \mathcal{B}(\psi_0, p(t)) = \{u \in \mathcal{B}(\psi_0) \text{ and } \rho^p(u) \in p(t)\}$$

Let $\mathcal{M}_I^{\psi_0} = \mathcal{M}(\psi, p(I))$ and $\mathcal{M}_t^{\psi_0} = \mathcal{M}(\psi, p(t))$ denote the corresponding moduli subspaces of *holomorphic* curves satisfying the same constraints as well as the other conditions required of holomorphic triangles (recall Definition 2.9.4). By Proposition 2.9.9, for a generic choice of almost complex structure on $\Sigma_0 \times \Delta$ the moduli spaces $\mathcal{M}_I^{\psi_0}$ are smooth manifolds of dimension $\mu(\psi_0) - \text{codim}(p(I))$. By Lemma 2.9.18, we have $\mu(\psi_0) = 2n_{p_0}(\psi_0)$, so the expected dimension becomes $2n_{p_0}(\psi_0) - (2k-1)$. In particular, when $k = n_{p_0}(\psi_0)$ the moduli space $\mathcal{M}_I^{\psi_0}$ is a smooth 1 manifold when it is transversely cut out. Similarly, the expected dimension of $\mathcal{M}_t^{\psi_0}$ is 0 when $k = n_{p_0}(\psi_0)$. Finally, we define the spaces

$$\mathcal{M}_I = \coprod_{\substack{\psi_0 \in \pi_2(\boldsymbol{\Theta}, \boldsymbol{a}, \boldsymbol{b}) \\ n_{p_0}(\psi_0) = k}} \mathcal{M}_I^{\psi_0}$$

$$\mathcal{M}_t = \coprod_{\substack{\psi_0 \in \pi_2(\boldsymbol{\Theta}, \boldsymbol{a}, \boldsymbol{b}) \\ n_{p_0}(\psi_0) = k}} \mathcal{M}_t^{\psi_0}$$

$$\mathcal{B}_I = \coprod_{\substack{\psi_0 \in \pi_2(\boldsymbol{\Theta}, \boldsymbol{a}, \boldsymbol{b}) \\ n_{p_0}(\psi_0) = k}} \mathcal{B}_I^{\psi_0}$$

$$\mathcal{B}_t = \coprod_{\substack{\psi_0 \in \pi_2(\boldsymbol{\Theta}, \boldsymbol{a}, \boldsymbol{b}) \\ n_{p_0}(\psi_0) = k}} \mathcal{B}_t^{\psi_0}$$

We provide a schematic of these spaces and their relationships in Figure 25.

We note for the following arguments that by the remarks above $\mathcal{M}_I$ is a smooth manifold of dimension 1 for a generic choice of almost complex structure, and for each t a (potentially different) generic choice of almost complex structure will ensure $\mathcal{M}_t$ is a smooth manifold of dimension 0. We will denote by $\mathfrak{o}_{\mathcal{M}_I}$ and $\mathfrak{o}_{\mathcal{M}_t}$ nowhere zero sections of the bundles $\mathcal{L}_I$ and $\mathcal{L}_t$ respectively, which are the determinant line bundles of the virtual index bundles of the linearized equations defining these moduli spaces. We recall that such sections determine orientations of the moduli spaces.

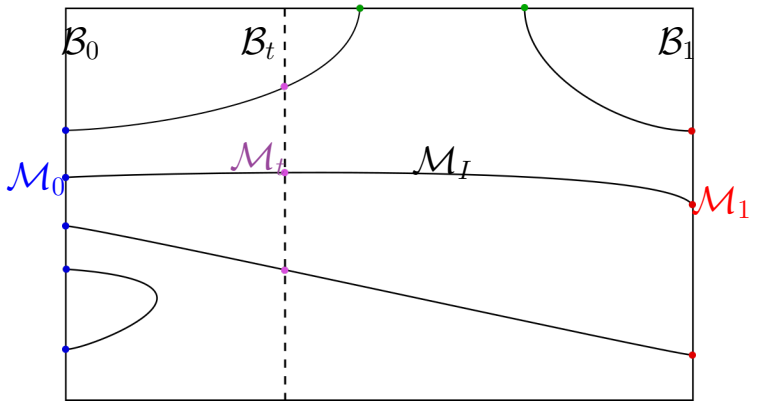

FIGURE 25 A schematic of the space $\mathcal{B}_I$. Vertical slices of the picture such as the vertical dashed line represent the spaces $\mathcal{B}_t$, while the solid curves represent the smooth moduli space $\mathcal{M}_I$. The left and right endpoints on $\mathcal{M}_I$ represent $\mathcal{M}_0$ and $\mathcal{M}_1$ respectively, while the endpoints of $\mathcal{M}_I$ on the top and bottom of the figure represent degenerations of triangles into broken triangles in the compactification.

For arguments appearing later, we want to ensure we can achieve the following intuitively achievable constraints on our orientations:

Lemma 2.9.13. *Let $\mathcal{M}_I$ and $\mathcal{M}_t$ be as above. Then there is a nowhere vanishing section $\mathfrak{o}_{\mathbb{R}}$ of the bundle $\mathcal{M}_I \times \mathbb{R}$, and coherent orientation systems $\mathfrak{o}_{\mathcal{M}_0}$ on $\mathcal{M}_0$, $\mathfrak{o}_{\mathcal{M}_1}$ on $\mathcal{M}_1$, and $\mathfrak{o}_{\mathcal{M}_I}$ on $\mathcal{M}_I$ such that $(\mathfrak{o}_{\mathcal{M}_I})|_{\mathcal{M}_0} = -\mathfrak{o}_{\mathcal{M}_0} \otimes (\mathfrak{o}_{\mathbb{R}}|_{\mathcal{M}_0})$ and $(\mathfrak{o}_{\mathcal{M}_I})|_{\mathcal{M}_1} = \mathfrak{o}_{\mathcal{M}_1} \otimes (\mathfrak{o}_{\mathbb{R}}|_{\mathcal{M}_1})$. Furthermore, given a particular*

coherent orientation system $\mathfrak{o}_{\mathcal{M}_0}$*, there are coherent orientation systems* $\mathfrak{o}_{\mathcal{M}_1}, \mathfrak{o}_{\mathcal{M}_I}$ *and a section* $\mathfrak{o}_{\mathbb{R}}$ *satisfying the same relations.*

Proof. Orientations for $\mathcal{M}_I$ and $\mathcal{M}_t$ can be specified by a trivialization of the determinant line bundle of the virtual index bundle for the corresponding linearized $\bar{\partial}$ equation (See [14, Section 6]). Somewhat less opaquely, this amounts to a trivialization of the determinant line bundle $\mathcal{L}_I := \det(D\bar{\partial}) = \Lambda^{\text{top}}(\ker(D\bar{\partial})) \otimes \Lambda^{\text{top}}(\text{coker}(D\bar{\partial}))$ over $\mathcal{B}_I$, and to a trivialization of the line bundle $\mathcal{L}_0 := \det(D(\bar{\partial}|_{\mathcal{B}_t})) = \Lambda^{\text{top}}(\ker(D(\bar{\partial}|_{\mathcal{B}_t}))) \otimes \Lambda^{\text{top}}(\text{coker}(D(\bar{\partial}|_{\mathcal{B}_t})))$ over $\mathcal{B}_t$.

To describe this process in more detail, we consider the vector bundle $\mathcal{E} = \mathcal{E}^p_{k-1}$ over $\mathcal{B}_I$, whose fiber over u is $L^{p,d}_{k-1}(\Lambda^{0,1}T^*S \otimes_J u^*T(\Sigma \times \Delta))$. For our purposes, it will be sufficient to note that such fibers are the Banach spaces comprised of sections of the bundle $\Lambda^{0,1}T^*S \otimes_J u^*T(\Sigma \times \Delta)$ which satisfy a finite norm regularity condition (see [20, Section 3.2] or [14, Definition 3.4-3.6,Proposition 3.7] for the precise definitions of the regularity conditions and the construction of this bundle). Then $\bar{\partial}$ can be considered as a section, $\bar{\partial} : \mathcal{B}_{\mathcal{I}} \to \mathcal{E}$, and with respect to this section the moduli space $\mathcal{M}_I$ is the preimage of the zero section, $\mathcal{M}_I = \bar{\partial}^{-1}(0)$, while $T\mathcal{M}_I \cong \text{Ker}(D\bar{\partial})$. We write j for the inclusion $j : \mathcal{B}_0 \to \mathcal{B}_I$ given by $j(u) = (u, 0)$, and consider the pullback of $\mathcal{E}$ along this map. The linearized $\bar{\partial}$ operators under consideration are defined as:

$$D\bar{\partial} : T\mathcal{B}_I \to T\mathcal{E} \xrightarrow{\sim} T\mathcal{B}_I \oplus \mathcal{E} \to \mathcal{E}$$

and

$$D(\bar{\partial}|_{\mathcal{B}_0}) : T\mathcal{B}_0 \to T(j^*\mathcal{E}) \xrightarrow{\sim} T\mathcal{B}_0 \oplus j^*\mathcal{E} \to j^*\mathcal{E}$$

Here the splittings $T\mathcal{E} \xrightarrow{\sim} T\mathcal{B}_I \oplus \mathcal{E}$ and $T(j^*\mathcal{E}) \xrightarrow{\sim} T\mathcal{B}_0 \oplus j^*\mathcal{E}$ depend on a choice of connection on TW (see [20, Section 3.1] for the details of this construction). Fix a splitting $j^*T\mathcal{B}_I \cong T\mathcal{B}_0 \oplus \mathbb{R}$ so $(D\bar{\partial})|_{\mathcal{B}_0} = [D(\bar{\partial}|_{\mathcal{B}_0}) \;\; C]$ for some C.

We may think of the linearized $\bar{\partial}$ operators as giving us parametrized collections of Fredholm maps

$$(D\bar{\partial})|_{\mathcal{B}_0} : \mathcal{B}_0 \to \bigcup_{x \in \mathcal{B}_0} \mathrm{Fred}(T\mathcal{B}_I|_x \to \mathcal{E}|_{\bar{\partial}(x)})$$

and

$$D(\bar{\partial}|_{\mathcal{B}_0}) : \mathcal{B}_0 \to \bigcup_{x \in \mathcal{B}_0} \mathrm{Fred}(T\mathcal{B}_0|_x \to \mathcal{E}|_{\bar{\partial}(x)})$$

These give rise to virtual bundles $\mathrm{ind}((D\bar{\partial})|_{\mathcal{B}_0})$, $\mathrm{ind}(D(\bar{\partial}|_{\mathcal{B}_0})) \in K(\mathcal{B}_0)$ (see e.g [21, Appendix 1]). Note that $\mathcal{B}_0$ is not compact, and so $K(\mathcal{B}_0)$ has a few possible interpretations. For us, $K(Y)$ will always indicate the Grothendieck group of isomorphism classes of vector bundles on Y. When Y is not compact, this group does not have some of the properties one often enjoys in their favorite notion of topological K-theory, but it will suffice for our purposes here.

Remark 2.9.14. It seems plausible that one could show $\mathcal{B}_t$ and $\mathcal{B}_I$ have the homotopy type of CW complexes, by arguments similar to those used by Milnor to show certain continuous function spaces do [22]. If this were the

case, a natural choice would be to define $K(\mathcal{B}_0)$ to be the inverse limit of the K-theories of the finite subcomplexes of $\mathcal{B}_0$. We will not however pursue this direction here.

We have for each $t \in I$ a line bundle $\mathcal{L}_t$ over $\mathcal{B}_t$, namely the determinant bundle of the virtual index bundle $\mathrm{ind}(D(\bar{\partial}|_{\mathcal{B}_t})) \in K(\mathcal{B}_t)$. These fit together to form a smooth vector bundle $\widetilde{\mathcal{L}_I} := \bigcup_{t\in I} \mathcal{L}_t$ over $\mathcal{B}_I$. Similarly, the index bundles themselves fit together to form a bundle $\widetilde{\mathrm{ind}} := \bigcup_{t\in I} \mathrm{ind}(D(\bar{\partial}|_{\mathcal{B}_t})) \in K(\mathcal{B}_{\mathcal{I}})$. We will compare $\mathcal{L}_I$ to $\widetilde{\mathcal{L}_I}$ and show that

$$\mathcal{L}_I|_X \cong (\widetilde{\mathcal{L}_I} \otimes \mathbb{R})|_X \tag{2.7}$$

for each compact $X \subset \mathcal{B}_I$. To see this it will suffice to prove that the two corresponding index bundles satisfy

$$\mathrm{ind}(D\bar{\partial})|_X = (\widetilde{\mathrm{ind}} \oplus \mathbb{R})|_X \in K(X) \tag{2.8}$$

for each compact $X \subset \mathcal{B}_I$. Indeed, with equation (2.8) understood, we just take the determinant line bundles of the virtual index bundles to obtain equation (2.7). We now assume equation (2.8), and relegate its proof to Lemma 2.9.15 and Remark 2.9.16 below.

Consider now the compactified matched moduli space $\overline{\mathcal{M}_I}$. The ends of $\mathcal{M}_I$ correspond to the boundary components of $\overline{\mathcal{M}_I}$. Fix a collar neighborhood $N \cong \partial\overline{\mathcal{M}_I} \times [0,1)$ of $\overline{\mathcal{M}_I}$. Then $\overline{\mathcal{M}_I} \setminus N \subset \mathcal{B}_I$ is compact, as it is closed in $\overline{\mathcal{M}_I}$ compact. By equation (2.7) the line bundles $\mathcal{L}_I$ and $\widetilde{\mathcal{L}_I}$ thus satisfy $\mathcal{L}_I \cong \widetilde{\mathcal{L}_I} \otimes \mathbb{R}$ on $\overline{\mathcal{M}_I} \setminus N$. In fact, we can extend the bundles $\mathcal{L}_I$, $\widetilde{\mathcal{L}_I} \otimes \mathbb{R}$ over all of $\overline{\mathcal{M}_I}$ since $\iota : \overline{\mathcal{M}_I} \setminus N \hookrightarrow \overline{\mathcal{M}_I}$ is a deformation retraction.

Furthermore, by homotopy invariance of induced bundles and the fact that ι is a deformation retraction, we have

$$r^*\mathcal{L}_I \cong r^*(\widetilde{\mathcal{L}_I} \otimes \mathbb{R}) \tag{2.9}$$

as bundles over $\overline{\mathcal{M}_I}$, where r is any retraction for ι. We note that on $\mathcal{M}_I$ we may assume these extensions in fact agree with the originally defined bundles

$$r^*\mathcal{L}_I|_{\mathcal{M}_I} \cong \mathcal{L}_I|_{\mathcal{M}_I} \text{ and } r^*(\widetilde{\mathcal{L}_I} \otimes \mathbb{R})|_{\mathcal{M}_I} \cong \widetilde{\mathcal{L}_I} \otimes \mathbb{R}|_{\mathcal{M}_I}.$$

Indeed, by our hypotheses on the choice of almost complex structure the moduli space $\overline{\mathcal{M}_I}$ is a smooth 1 manifold with boundary, so the collar is a disjoint union of arcs and there is a unique choice of extension for each bundle over the collar. We thus conclude

$$\mathcal{L}_I|_{\mathcal{M}_I} \cong \widetilde{\mathcal{L}_I} \otimes \mathbb{R}|_{\mathcal{M}_I}. \tag{2.10}$$

Fix now a trivialization $\mathfrak{o}_{\mathcal{M}_I}$ of $\mathcal{L}_I$ over $\mathcal{M}_I$, which is possible by Lemma 2.9.10. Given any section $\mathfrak{o}_{\mathbb{R}}$ of $\mathcal{M}_I \times \mathbb{R}$, equation (2.10) specifies a section $\widetilde{\mathfrak{o}}$ of $\widetilde{\mathcal{L}_I}$ over $\mathcal{M}_I$. This specifies sections $\widetilde{\mathfrak{o}_0}$ of $\widetilde{\mathcal{L}_I}|_{\mathcal{M}_0} = \mathcal{L}_0$ and $\widetilde{\mathfrak{o}_1}$ of $\widetilde{\mathcal{L}_I}|_{\mathcal{M}_1} = \mathcal{L}_1$, which by construction satisfy

$$(\mathfrak{o}_{\mathcal{M}_I})|_{\mathcal{M}_0} = \widetilde{\mathfrak{o}_0} \otimes \mathfrak{o}_{\mathbb{R}}|_{\mathcal{M}_0} \tag{2.11}$$

and

$$(\mathfrak{o}_{\mathcal{M}_I})|_{\mathcal{M}_1} = \widetilde{\mathfrak{o}_1} \otimes \mathfrak{o}_{\mathbb{R}}|_{\mathcal{M}_1} \tag{2.12}$$

Setting $\mathfrak{o}_{\mathcal{M}_0} := -\widetilde{\mathfrak{o}_0}$ and $\mathfrak{o}_{\mathcal{M}_1} := \widetilde{\mathfrak{o}_1}$, we have thus verified there are orientation systems $\mathfrak{o}_{\mathcal{M}_0}$, $\mathfrak{o}_{\mathcal{M}_1}$ and $\mathfrak{o}_{\mathcal{M}_I}$ satisfying the restriction conditions as in the lemma statement. We now turn to verifying that the preceding construction allows for the simultaneous coherence of the orientation systems $\mathfrak{o}_{\mathcal{M}_I}$, $\mathfrak{o}_{\mathcal{M}_0}$ and $\mathfrak{o}_{\mathcal{M}_1}$.

By the same argument used to prove [14, Lemma 10.10], we may arrange for the initially fixed orientation system $\mathfrak{o}_{\mathcal{M}_I}$ in the preceding paragraph to be enlarged to a coherent system in the sense of Definition 2.9.12. We remark that doing so entails enlarging the orientation data to include both the section $\mathfrak{o}_{\mathcal{M}_I}$ of $\mathcal{L}_I$ over $\mathcal{M}_I$ guaranteed by orientability of $\mathcal{M}_I$, but also a collection of sections $(\mathfrak{o}_{\mathcal{M}_I})_{\text{strips}} := \{\mathfrak{o}_I^A\}$ of the determinant bundles $\mathcal{L}$ over the (unmatched) configuration spaces $\mathcal{B}^A$ in all homology classes of strips, A, in the three associated Heegaard double diagrams. The coherence of this data then says that all possible pregluing maps of two strips, and all possible pregluing maps of triangles with strips, respect the orientations.

More precisely, consider the Heegaard triple diagram in question, $\mathcal{T}_0 = (\Sigma_0, \boldsymbol{\alpha}_0', \boldsymbol{\alpha}_0, \boldsymbol{\beta}_0)$, and the associated double diagrams $\mathcal{H}_{\boldsymbol{\alpha}_0', \boldsymbol{\alpha}_0}$, $\mathcal{H}_{\boldsymbol{\alpha}_0, \boldsymbol{\beta}_0}$ and $\mathcal{H}_{\boldsymbol{\alpha}_0', \boldsymbol{\beta}_0}$. Let $\boldsymbol{x}$, $\boldsymbol{y}$ and $\boldsymbol{z}$ be intersection points (also referred to as I-chord collections in the cylindrical setting) in the respective double diagrams.

For all homology classes of triangles $\psi_0 \in \pi_2(\boldsymbol{x}, \boldsymbol{y}, \boldsymbol{z})$ and homology classes of strips $A \in \pi_2(\boldsymbol{z}, \boldsymbol{z}')$ (with $\boldsymbol{z}'$ also an intersection point on $\mathcal{H}_{\boldsymbol{\alpha}_0', \boldsymbol{\beta}_0}$),

there are pregluing maps, covered by linearized preglueing maps on the determinant bundles, fitting into the diagram below:

$$\begin{array}{ccc} \mathcal{L}_I^{\psi_0} \times \mathcal{L}^A & \xrightarrow{\natural_*} & \mathcal{L}_I^{\psi_0+A} \\ \downarrow & & \downarrow \\ \mathcal{B}_I^{\psi_0} \times \mathcal{B}^A & \xrightarrow{\natural} & \mathcal{B}_I^{\psi_0+A} \end{array} \tag{2.13}$$

The coherence condition for $\mathfrak{o}_{\mathcal{M}_I}$ regarding glueing triangles to strips says that in all such diagrams, we have $\natural_*(\mathfrak{o}_{\mathcal{M}_I}^{\psi_0} \times \mathfrak{o}^A) = +\mathfrak{o}_{\mathcal{M}_I}^{\psi_0+A}$. Of course, the analogous statements must hold for homology classes of strips $A \in \pi_2(\boldsymbol{x}, \boldsymbol{x}')$ and $A \in \pi_2(\boldsymbol{y}, \boldsymbol{y}')$ as well.

For the condition regarding glueing strips to strips, we consider homology classes of strips $A \in \pi_2(\boldsymbol{x}, \boldsymbol{x}')$ and $A' \in \pi_2(\boldsymbol{x}', \boldsymbol{x}'')$ associated with the diagram $\mathcal{H}_{\boldsymbol{\alpha}_0', \boldsymbol{\alpha}_0}$. Then we have a diagram given by the pregluing maps:

$$\begin{array}{ccc} \mathcal{L}^A \times \mathcal{L}^{A'} & \xrightarrow{\natural_*} & \mathcal{L}^{A+A'} \\ \downarrow & & \downarrow \\ \mathcal{B}^A \times \mathcal{B}^{A'} & \xrightarrow{\natural} & \mathcal{B}^{A+A'} \end{array} \tag{2.14}$$

Here the coherence condition on $\mathfrak{o}_{\mathcal{M}_I}$ says that for all such diagrams, $\natural_*(\mathfrak{o}_I^A \times \mathfrak{o}_I^{A'}) = +\mathfrak{o}_I^{A+A'}$. The analogous statements for the other Heegaard double diagrams must also hold.

We want to show that the orientation systems $\mathfrak{o}_{\mathcal{M}_0}$ and $\mathfrak{o}_{\mathcal{M}_1}$ defined above satisfy these same coherence conditions. We show this is true for $\mathfrak{o}_{\mathcal{M}_0}$, as the other case is identical.

Let us define the data $(\mathfrak{o}_{\mathcal{M}_0})_{\text{strips}} = \{\mathfrak{o}_0^A\} = \{-\mathfrak{o}_I^A\}$ of orientations for homology classes of strips in the three double diagrams to be the negation of that used for the coherent system into which $\mathfrak{o}_{\mathcal{M}_I}$ fits. Then we note that the coherence of the orientation systems $\mathfrak{o}_{\mathcal{M}_0}$ with respect to preglueings of strips to strips follows immediately; since $\mathfrak{o}_{\mathcal{M}_I}$ was chosen to be coherent we have $\natural_*(\mathfrak{o}_I^A \times \mathfrak{o}_I^{A'}) = +\mathfrak{o}_I^{A+A'}$.

To check the coherence of glueing triangles to strips, fix classes $\psi_0 \in \pi_2(\boldsymbol{x}, \boldsymbol{y}, \boldsymbol{z})$ and $A \in \pi_2(\boldsymbol{z}, \boldsymbol{z}')$ and consider the corresponding orientations over them: $\mathfrak{o}_{\mathcal{M}_0}^{\psi_0}$, $\mathfrak{o}_0^A$ and $\mathfrak{o}_{\mathcal{M}_0}^{\psi_0+A}$. By equation (2.11), we have $(\mathfrak{o}_{\mathcal{M}_I})|_{\mathcal{M}_0} = -\mathfrak{o}_{\mathcal{M}_0} \otimes (\mathfrak{o}_{\mathbb{R}}|_{\mathcal{M}_0})$. Coherence of $\mathfrak{o}_{\mathcal{M}_I}$ then yields:

$$
\begin{aligned}
\natural_*(\mathfrak{o}_{\mathcal{M}_I}^{\psi_0} \times \mathfrak{o}_I^A) = +\mathfrak{o}_{\mathcal{M}_I}^{\psi_0+A} &\implies \natural_*(\mathfrak{o}_{\mathcal{M}_I}^{\psi_0} \times \mathfrak{o}_I^A)|_{\mathcal{M}_0} = +\mathfrak{o}_{\mathcal{M}_I}^{\psi_0+A}|_{\mathcal{M}_0} \\
&\implies (\mathfrak{o}_{\mathcal{M}_I}^{\psi_0} \wedge \mathfrak{o}_I^A)|_{\mathcal{M}_0} = -\mathfrak{o}_{\mathcal{M}_0}^{\psi_0+A} \wedge \mathfrak{o}_{\mathbb{R}} \\
&\implies (-\mathfrak{o}_{\mathcal{M}_0}^{\psi_0} \wedge \mathfrak{o}_{\mathbb{R}} \wedge \mathfrak{o}_I^A) = -\mathfrak{o}_{\mathcal{M}_0}^{\psi_0+A} \wedge \mathfrak{o}_{\mathbb{R}} \\
&\implies (\mathfrak{o}_{\mathcal{M}_0}^{\psi_0} \wedge \mathfrak{o}_I^A \wedge \mathfrak{o}_{\mathbb{R}}) = -\mathfrak{o}_{\mathcal{M}_0}^{\psi_0+A} \wedge \mathfrak{o}_{\mathbb{R}} \\
&\implies -(\mathfrak{o}_{\mathcal{M}_0}^{\psi_0} \wedge \mathfrak{o}_0^A \wedge \mathfrak{o}_{\mathbb{R}}) = -\mathfrak{o}_{\mathcal{M}_0}^{\psi_0+A} \wedge \mathfrak{o}_{\mathbb{R}} \\
&\implies -\natural_*(\mathfrak{o}_{\mathcal{M}_0}^{\psi_0} \times \mathfrak{o}_0^A) \wedge \mathfrak{o}_{\mathbb{R}} = -\mathfrak{o}_{\mathcal{M}_0}^{\psi_0+A} \wedge \mathfrak{o}_{\mathbb{R}} \\
&\implies \natural_*(\mathfrak{o}_{\mathcal{M}_0}^{\psi_0} \times \mathfrak{o}_0^A) = +\mathfrak{o}_{\mathcal{M}_0}^{\psi_0+A}
\end{aligned}
$$

We have thus shown the orientation systems $\mathfrak{o}_{\mathcal{M}_0}$, $\mathfrak{o}_{\mathcal{M}_1}$, and $\mathfrak{o}_{\mathcal{M}_I}$ we have defined can be taken to be simultaneously coherent, which completes the proof of the lemma. □

The following lemma can be used to establish equation (2.8) in the preceding argument.

Lemma 2.9.15. *Let X be a compact topological space, H_1 and H_2 be Banach bundles over X, $B : H_1 \to H_2$ be a bundle map over X which is Fredholm on each fiber, $V = \mathbb{R}^n$ be a finite dimensional Banach space, and $C : V \times X \to H_2$ be a linear bundle map. Then the index of $\begin{bmatrix} B & C \end{bmatrix} : H_1 \oplus V \to H_2$ satisfies*

$$ind(\begin{bmatrix} B & C \end{bmatrix}) = ind(B) + [V] \in K(X)$$

Proof. To fix notation and terminology, we very briefly recall the definition of the index bundle associated with a map such as B. For more details of the construction, see [21, Appendix] for the general idea in the context of Fredholm operators on seperable Hilbert spaces, and [20, Appendix A.2] for the necessary modifications needed to carry out the same constructions for Fredholm maps between Banach spaces.

Fix $x \in X$ and consider B restricted to the fiber over x, $B_x : H_1|_x \to H_2|_x$.

- If $\operatorname{coker}(B_x) = 0$, one can show that $\operatorname{coker}(B_y) = 0$ and $\operatorname{ind}(B_x) = \operatorname{ind}(B_y)$ for all y sufficiently close to x (where here we use $\operatorname{ind}(B_x)$ to denote the numerical index of the Fredholm map B_x). Denote such a neighborhood of x by U. Then the kernels fit together into a well-defined honest vector bundle, $\bigcup_{y \in U} \ker(B_y)$, over U.
- Otherwise, choose a finite dimensional space W and a linear map $\pi_x : W \to H_2|_x$ such that $B_x \oplus \pi_x : H_1|_x \oplus W \to H_2|_x$ is surjective

and Fredholm. Choose continuously the analogous data for all y in a neighborhood U of x, i.e. maps $\pi_y : W \to H_2|_y$. Via the same construction described in the preceding paragraph, $\bigcup_{y\in U} \ker(B_y \oplus \pi_y)$ has the structure of a vector bundle over U.

We note that the first case may be subsumed into the second case by taking W, and thus the auxiliary data, to be trivial. For the remainder of the proof we will refer to the local data necessary to define the bundle of kernels in the second case above, i.e the collection $\{(W, \pi_y)|y \in U\}$, as *auxiliary data for B on the neighborhood U*.

Given two collections of auxiliary data on neighborhoods U and V, we can enlarge the data to a single set of auxiliary data on $U \cup V$, at the cost of potentially increasing the dimension of W if the cokernel of B changes dimension from U to V. That one can do so continuously is verified in e.g. [21, Appendix] and [20, Appendix A.2], in the cases of Fredholm maps on Hilbert spaces and Fredholm maps on Banach spaces respectively. For a compact base one can then ensure there exists a choice of a single finite dimensional space W and a continous family of linear maps $\pi_z : W \to H_2|_z$ so that $\ker(B \oplus \pi) := \bigcup_{z\in X} \ker(B_z \oplus \pi_z)$ has the structure of a vector bundle.

The index bundle of B is then defined via this construction as

$$\mathrm{ind}(B) = [\ker(B \oplus \pi)] - [W \times X] \in K(X)$$

and one readily checks that any other choice of global auxiliary data gives rise to the same element in K-theory. This completes our summary of the construction of the index bundle associated to the map B.

To prove the lemma, we will compare the results of applying this construction to B and to $\begin{bmatrix} B & C \end{bmatrix}$.

Fix $x \in X$. Then we have $\dim(\text{coker}(\begin{bmatrix} B_x & C_x \end{bmatrix})) + k = \dim(\text{coker}(B_x))$ for some $0 \leq k \leq \dim(V)$. Fix any choice of auxiliary data (W, π) for B on a neighborhood U of x. Then because $\text{im}(B_x) \subset \text{im}(\begin{bmatrix} B_x & C_x \end{bmatrix})$ for all x in U, (W, π) also serves as auxiliary data for $\begin{bmatrix} B & C \end{bmatrix}$ on U. The bundles $\ker(\begin{bmatrix} B & \pi \end{bmatrix})$ and $\ker(\begin{bmatrix} B & C & \pi \end{bmatrix})$ are therefore both well-defined on U, and we will now show that $\ker(\begin{bmatrix} B & \pi \end{bmatrix}) \oplus V \cong \ker(\begin{bmatrix} B & C & \pi \end{bmatrix})$. Indeed, consider the exact sequences:

$$0 \to \ker(B) \to \ker(\begin{bmatrix} B & \pi \end{bmatrix}) \to \pi^{-1}(\text{im}(B)) \to 0$$

and

$$0 \to \ker(\begin{bmatrix} B & C \end{bmatrix}) \to \ker(\begin{bmatrix} B & C & \pi \end{bmatrix}) \to \pi^{-1}(\text{im}(\begin{bmatrix} B & C \end{bmatrix})) \to 0$$

Here the first map in the top sequence is given by $a \mapsto (a, 0)$ and the second map is given by $(b, c) \mapsto c$, with the second sequence defined similarly. The cokernels differ in dimension by k, and we have $\ker(\begin{bmatrix} B & C \end{bmatrix}) \cong \ker(B) \oplus \mathbb{R}^{\dim(V)-k}$. Furthermore since $H_2 = \text{im}(B) + \text{im}(\pi)$ we have isomorphisms $\text{cok}(B) = H_2/\text{im}(B) \cong W/\pi^{-1}(\text{im}(B))$ and $\text{cok}(\begin{bmatrix} B & C \end{bmatrix}) = H_2/\text{im}(\begin{bmatrix} B & C \end{bmatrix}) \cong W/\pi^{-1}(\text{im}(\begin{bmatrix} B & C \end{bmatrix}))$, so $\pi^{-1}(\text{im}(\begin{bmatrix} B & C \end{bmatrix})) \cong \pi^{-1}(\text{im}(B)) \oplus \mathbb{R}^k$. Thus since the sequences split we have $\ker(\begin{bmatrix} B & \pi \end{bmatrix}) \oplus V \cong$

$\ker(\begin{bmatrix} B & C & \pi \end{bmatrix})$. To summarize, we have shown that on a neighborhood U of x, any choice of auxiliary data (W, π) for B yields $\ker(\begin{bmatrix} B & \pi \end{bmatrix}) \oplus V \cong \ker(\begin{bmatrix} B & C & \pi \end{bmatrix})$ as vector bundles over U.

Finally, we need to show that the index bundles are globally equivalent in $K(X)$. To do this, it suffices to show that there are constants k_1 and k_2 and global choices of auxiliary data (W, π) and (W', π') for B and $\begin{bmatrix} B & C \end{bmatrix}$ respectively such that there are (now global) isomorphisms of vector bundles $\ker(\begin{bmatrix} B & C & \pi' \end{bmatrix}) \oplus \mathbb{R}^{k_1} \cong \ker(\begin{bmatrix} B & \pi \end{bmatrix}) \oplus V \oplus \mathbb{R}^{k_2}$ and $W' \oplus \mathbb{R}^{k_1} \cong W \oplus \mathbb{R}^{k_2}$.

In fact, this follows immediately from the observations above. Fix once and for all a finite open cover $\bigcup_i U_i$ of X, and a collection of local auxiliary data $\{(W_i, \pi_i)\}$ for B on the U_i. To construct $\mathrm{ind}(B)$, we use the collection of local data to produce global auxiliary data (W, π) for B on X. By the observations made earlier, $\mathrm{ind}(\begin{bmatrix} B & C \end{bmatrix})$ can be constructed from the same finite collection of local auxiliary data, which will give rise to the same global auxiliary data (W, π) for $\begin{bmatrix} B & C \end{bmatrix}$. Finally, we have observed above that for such global auxiliary data (W, π), the two (honest) vector bundles $\ker(\begin{bmatrix} B & C & \pi \end{bmatrix})$ and $\ker(\begin{bmatrix} B & \pi \end{bmatrix})$ on X will satisfy

$$\ker(\begin{bmatrix} B & C & \pi \end{bmatrix})|_{U_i} \cong_{f_i} (\ker(\begin{bmatrix} B & \pi \end{bmatrix}) \oplus V)|_{U_i}$$

for each U_i. Furthermore, the isomorphisms agree across charts in the sense that $f_i|_{U_i \cap U_j} = f_j|_{U_i \cap U_j}$, so we have a global isomorphism of vector bundles on X

$$\ker(\begin{bmatrix} B & C & \pi \end{bmatrix}) \cong \ker(\begin{bmatrix} B & \pi \end{bmatrix}) \oplus V$$

We thus have

$$\begin{aligned}\operatorname{ind}(\begin{bmatrix} B & C \end{bmatrix}) &= [\ker(\begin{bmatrix} B & C & \pi \end{bmatrix})] - [W \times X] \\ &= [\ker(\begin{bmatrix} B & \pi \end{bmatrix}) \oplus V] - [W \times X] \\ &= \operatorname{ind}(B) + [V] \in K(X),\end{aligned}$$

as desired. □

Remark 2.9.16. Equation (2.8) in the proof of Lemma 2.9.13 now follows from applying Lemma 2.9.15 to any compact subset $X \subset \mathcal{B}_I$, with $H_1 = \bigcup_{t\in I} T\mathcal{B}_t$, $H_2 = \mathcal{E}$, $V = \mathbb{R}$, $B = \coprod_{t\in I} D(\bar{\partial}|_{\mathcal{B}_t\cap X})$ and $C = \coprod_{t\in I}((D\bar{\partial})|_{\mathcal{B}_t\cap X})|_{0\oplus\mathbb{R}\subset T\mathcal{B}_t\oplus\mathbb{R}}$.

Having discussed the smooth manifold structure and a particular construction of coherent orientations on the matched moduli spaces of triangles on a triple diagram, we now state a glueing result from [3] which will allow us to relate these matched moduli spaces of triangles on the diagram $\mathcal{T}_0$ to the triangles on $\mathcal{T}\#\mathcal{T}_0$ we seek to count. We consider homology classes of triangles ψ on an arbitrary pointed triple diagram $\mathcal{T} = (\Sigma, \boldsymbol{\alpha}', \boldsymbol{\alpha}, \boldsymbol{\beta}, p)$ and ψ_0 on the pointed diagram $\mathcal{T}_0 = (\Sigma_0, \boldsymbol{\alpha}'_0, \boldsymbol{\alpha}_0, \boldsymbol{\beta}_0, p_0)$. We form the connected sum of the diagrams at the points p and p_0, and consider the resulting homology class $\psi\#\psi_0$:

Proposition 2.9.17 (Proposition 9.49 in [3])**.** *Let u and u_0 be holomorphic triangles representing homology classes ψ and ψ_0 in $\Sigma \times \Delta$ and $\Sigma_0 \times \Delta$ respectively. Let $k = n_p(\psi) = n_{p_0}(\psi_0)$, and suppose $\mu(u) = 0$, $\mu(u_0) = 2k$, and $\rho^p(u) = \rho^{p_0}(u_0) \in Sym^k(\Delta) \setminus Diag^k(\Delta)$. Suppose further that*

$\mathcal{M}(\psi)$ and $\mathcal{M}(\psi_0, \rho^p(u))$ are transversely cut out near u and u_0. Then there is a homeomorphism h between $[0,1)$ and a neighborhood of (u, u_0) in the compactified 1-dimensional moduli space

$$\overline{\bigcup_T \mathcal{M}_{J(T)}(\psi \# \psi_0)}$$

such that $h(u, u_0) = \{0\}$

Finally, the following three facts will also be useful in the proof of the triangle count of Proposition 2.9.1, so we state them here as lemmas for convenience in referencing.

Lemma 2.9.18 (Lemma 9.50 in [3])**.** *Consider the triple diagram $\mathcal{T}_0 = (\Sigma_0, \boldsymbol{\alpha'_0}, \boldsymbol{\alpha_0}, \boldsymbol{\beta_0})$. If $\boldsymbol{x} \in \mathbb{T}_{\alpha'_0} \cap \mathbb{T}_{\alpha_0}$ and $\psi_0 \in \pi_2(\boldsymbol{x}, \boldsymbol{a}, \boldsymbol{b})$, then*

$$\mu(\psi_0) = 2n_{p_0}(\psi_0) + \mu(\boldsymbol{x}, \boldsymbol{\Theta}) \tag{2.15}$$

Lemma 2.9.19. *The differential on $\widehat{CF}(\Sigma_0, \boldsymbol{\alpha'_0}, \boldsymbol{\alpha_0}, p_0, \mathfrak{o}_{\boldsymbol{\alpha}'_0, \boldsymbol{\alpha}_0})$, defined with respect to the coherent orientation system $\mathfrak{o}_{\boldsymbol{\alpha}'_0, \boldsymbol{\alpha}_0}$ specified in Lemma 2.7.2, vanishes.*

Proof. By [1, Lemma 9.4] $\operatorname{rank}_{\mathbb{Z}}(\widehat{HF}(\Sigma_0, \boldsymbol{\alpha'_0}, \boldsymbol{\alpha_0}, p_0, \mathfrak{o}_{\boldsymbol{\alpha}'_0, \boldsymbol{\alpha}_0})) = 4$. By inspection $\operatorname{rank}_{\mathbb{Z}}(\widehat{CF}) = 4$, so the differential must vanish. □

Lemma 2.9.20. *The map*

$$\Psi_{\beta_0}^{\alpha_0 \to \alpha'_0} : \widehat{CF}(\Sigma_0, \boldsymbol{\alpha_0}, \boldsymbol{\beta_0}, p_0) \to \widehat{CF}(\Sigma_0, \boldsymbol{\alpha'_0}, \boldsymbol{\beta_0}, p_0)$$

satisfies $\Psi_{\beta_0}^{\alpha_0 \to \alpha'_0}(\boldsymbol{a}) = \pm \boldsymbol{b}$.

Proof. By Lemma 2.7.4, $\Psi_{\beta_0}^{\alpha_0 \to \alpha_0'}$ is a quasi-isomorphism. Since the two complexes in question are trivial of rank one over $\mathbb{Z}$, the quasi-isomorphism must be an isomorphism between trivial, rank one complexes over $\mathbb{Z}$, of which there are precisely two. □

Counting Triangles

We are now in position to prove the main triangle count, and conclude the proof of handleswap invariance.

Proof of Proposition 2.9.1. As we did in Sections 2.7 and 2.8, we will consider the case of the chain complexes CF^- in what follows in order to fix definitions, however we note that the proof carries over equally well for all variants CF°.

For an almost complex structure J which achieves transversality we have, by definition,

$$\mathcal{F}_{\mathcal{T}\#\mathcal{T}_0}((\boldsymbol{x} \times \boldsymbol{\Theta}) \otimes (\boldsymbol{y} \times \boldsymbol{a})) = \sum_{\boldsymbol{z}} \sum_{\substack{A \in \pi_2(\boldsymbol{x} \times \boldsymbol{\Theta}, \boldsymbol{y} \times \boldsymbol{a}, \boldsymbol{z} \times \boldsymbol{b}) \\ \mu(A) = 0}} (\#\mathcal{M}_J(A)) U^{n_p(A)} \cdot \boldsymbol{z} \times \boldsymbol{b}$$

and

$$\mathcal{F}_{\mathcal{T}}(\boldsymbol{x} \otimes \boldsymbol{y}) \times \boldsymbol{b} = \left(\sum_{\boldsymbol{z}} \sum_{\substack{A \in \pi_2(\boldsymbol{x}, \boldsymbol{y}, \boldsymbol{z}) \\ \mu(A) = 0}} (\#\mathcal{M}_J(A)) U^{n_p(A)} \cdot \boldsymbol{z} \right) \times \boldsymbol{b}$$

To obtain the result we will count Maslov index 0 holomorphic triangles in the homology class A, for each generator $\boldsymbol{z} \in \mathbb{T}_{\boldsymbol{\alpha'}} \cap \mathbb{T}_{\boldsymbol{\beta}}$ and class $A \in \pi_2(\boldsymbol{x} \times \boldsymbol{\Theta}, \boldsymbol{y} \times \boldsymbol{a}, \boldsymbol{z} \times \boldsymbol{b})$.

Consider two homology classes of triangles $\psi \in \pi_2(\boldsymbol{x}, \boldsymbol{y}, \boldsymbol{z})$ on $\mathcal{T} = (\Sigma, \boldsymbol{\alpha'}, \boldsymbol{\alpha}, \boldsymbol{\beta}, p)$ and $\psi_0 \in \pi_2(\boldsymbol{\Theta}, \boldsymbol{a}, \boldsymbol{b})$ on $\mathcal{T}_0 = (\Sigma_0, \boldsymbol{\alpha'_0}, \boldsymbol{\alpha_0}, \boldsymbol{\beta_0}, p_0)$. If $n_p(\psi) = n_{p_0}(\psi_0)$, so the classes match across the connect sum point, then the homology classes can be combined to give a class $\psi \# \psi_0 \in \pi_2(\boldsymbol{x} \times \boldsymbol{\Theta}, \boldsymbol{y} \times \boldsymbol{a}, \boldsymbol{z} \times \boldsymbol{b})$. Conversely, it is clear that any class $A \in \pi_2(\boldsymbol{x} \times \boldsymbol{\Theta}, \boldsymbol{y} \times \boldsymbol{a}, \boldsymbol{z} \times \boldsymbol{b})$ can be written uniquely as a connect sum of suitable classes with this matching condition.

So for any such homology class $A = \psi \# \psi_0$ with $\mu(A) = 0$, we aim to count Maslov index zero holomorphic representatives as we stretch the neck, i.e to count $\#\mathcal{M}_{J(T_i)}(\psi \# \psi_0)$, where $J(T_i)$ is a sequence of almost complex structures being stretched along the neck. To do so, suppose u_{T_i} is a sequence of $J(T_i)$-holomorphic triangles representing $\psi \# \psi_0$, where $\mu(\psi \# \psi_0) = 0$. We note here that by [23, Theorem 4.1] and Lemma 2.9.18 we have $\mu(\psi \# \psi_0) = \mu(\psi) + \mu(\psi_0) - 2n_p(\psi_0) = \mu(\psi) + \mu(\boldsymbol{\theta}, \boldsymbol{\theta}) = \mu(\psi)$. Hence $\mu(\psi) = 0$, and $\mu(\psi_0) = 2n_{p_0}(\psi_0)$.

By Proposition 2.9.6, there is a subsequence of u_{T_i} which converges to a triple (U, V, U_0) where U is a broken holomorphic triangle in $\Sigma \times \Delta$ representing ψ, U_0 is a broken holomorphic triangle in $\Sigma_0 \times \Delta$ representing ψ_0, and V is a collection of holomorphic curves mapping into the neck regions that are asymptotic to (possibly multiply covered) Reeb orbits of the form $S^1 \times \{d\}$.

The proof will now proceed in steps as follows:

1. We will show U consists of a single holomorphic triangle u with Maslov index zero, with u satisfying (M1)-(M8), and potentially some number of constant holomorphic curves.

2. We then show that U_0 consists of a single Maslov index $2n_{p_0}(\psi_0)$ triangle u_0', with u_0' satsisfying (M1)-(M8) and $\rho^p(u) = \rho^{p_0}(u_0)$, and potentially some number of constant holomorphic curves.

3. We rule out the possibility of constant curves occurring in steps 1 and 2, and show that V consists of a collection of trivial holomorphic cylinders.

4. Using this knowledge of (U, V, U_0) and the glueing result, we reduce the proof to showing Lemma 2.9.21 below.

In fact, the proofs of steps (1) through (3) given in [3] carry over exactly as they are stated there, so we will only carry out step (4).

Step 4 By steps (1)-(3), a sequence u_{T_i} of $J(T_i)$-holomorphic triangles representing $\psi\#\psi_0$ converges to a broken holomorphic triangle (U, V, U_0), where $U = u$ is a single holomomorphic triangle satisfying $\mu(u) = 0$, V is a collection of trivial holomorphic cylinders, U_0 is a single holomorphic triangle u_0 satisfying $\mu(u_0) = 2n_p(\psi)$, and $\rho^p(u) = \rho^{p_0}(u_0)$. By Proposition 2.9.17, there is therefore a homeomorphic identification h between a neighborhood of (u, u_0) in the compactified 1 dimensional moduli space

$$\overline{\bigcup_{T_i} \mathcal{M}_{J(T_i)}(\psi\#\psi_0)}$$

and the interval $[0,1)$, such that $h(u,u_0)=\{0\}$. This yields an identification

$$\mathcal{M}_{J(T_i)}(\psi\#\psi_0)\cong\{(u,u_0)\in\mathcal{M}(\psi)\times\mathcal{M}(\psi_0)|\rho^p(u)=\rho^p(u_0)\}$$

for sufficiently large T_i. We now fix J_{T_i} for such a sufficiently large value of T_i, and drop this choice of almost complex structure from our notation.

Given coherent orientation systems $\mathfrak{o}_{\mathcal{T}}$ over $\mathcal{T}$ and $\mathfrak{o}_{\mathcal{T}_0}$ over $\mathcal{T}_0$, there is a coherent orientation system $\mathfrak{o}_{\mathcal{T}\#\mathcal{T}_0}$ with respect to which the signed count of the 0 dimensional moduli space $\mathcal{M}(\psi\#\psi_0)$ is given by

$$\#\mathcal{M}(\psi\#\psi_0)=\#\{(u,u_0)\in\mathcal{M}(\psi)\times\mathcal{M}(\psi_0)|\rho^p(u)=\rho^p(u_0)\}.$$

Indeed, given two homology classes of triangles ψ on $\mathcal{T}$ and ψ_0 on $\mathcal{T}_0$, the glueing map $\natural$ (see [14, Appendix A, page 1082] for the definition) used to identify the two moduli spaces is covered by a map of determinant lines $(\natural)_\#$ which can be used to produce an orientation $\mathfrak{o}^{\psi\#\psi_0}_{\mathcal{T}\#\mathcal{T}_0}$ over $\mathcal{M}(\psi\#\psi_0)$ from orientations $\mathfrak{o}^{\psi}_{\mathcal{T}}$ over $\mathcal{M}(\psi)$ and $\mathfrak{o}^{\psi_0}_{\mathcal{T}_0}$ over $\mathcal{M}(\psi_0)$. Similarly, for two homology classes of strips A on $\mathcal{T}$ and A_0 on $\mathcal{T}_0$, the same procedure can be used to determine an orientation $\mathfrak{o}^{A\#A_0}_{\mathcal{T}\#\mathcal{T}_0}$ from $\mathfrak{o}^{A}_{\mathcal{T}}$ and $\mathfrak{o}^{A_0}_{\mathcal{T}_0}$. The fact that homology classes of strips and triangles on $\mathcal{T}\#\mathcal{T}_0$ are in bijective correspondence to pairs of homology classes of strips on $\mathcal{T}$ and $\mathcal{T}_0$ ensures that the coherent orientation systems $\mathfrak{o}_{\mathcal{T}}$ and $\mathfrak{o}_{\mathcal{T}_0}$ thus determine a single orientation system $\mathfrak{o}_{\mathcal{T}\#\mathcal{T}_0}$ over all classes of strips and triangles in the connect summed diagram (i.e. the determinations for a particular class of triangle or strip on the summed diagram are not overspecified). That this induced orientation is coherent follows from the coherence of the two constituent orientations,

along with the fact that glueing map $(\natural)_{\#}$ above commutes with the map $(\natural)_*$ appearing in Definition 2.9.12. More precisely, the coherence follows from these facts as

$$\begin{aligned}
\mathfrak{o}_{\mathcal{T}\#\mathcal{T}_0}^{(\psi+A)\#(\psi_0+A_0)} &:= (\natural)_{\#}(\mathfrak{o}_{\mathcal{T}}^{\psi+A} \times \mathfrak{o}_{\mathcal{T}_0}^{\psi_0+A_0}) \\
&= (\natural)_{\#}((\natural)_*(\mathfrak{o}_{\mathcal{T}}^{\psi} \times \mathfrak{o}_{\mathcal{T}}^{A}) \times (\natural)_*(\mathfrak{o}_{\mathcal{T}_0}^{\psi_0} \times \mathfrak{o}_{\mathcal{T}_0}^{A_0})) \\
&= (\natural)_*((\natural)_{\#}(\mathfrak{o}_{\mathcal{T}}^{\psi} \times \mathfrak{o}_{\mathcal{T}_0}^{\psi_0}) \times (\natural)_{\#}(\mathfrak{o}_{\mathcal{T}}^{A} \times \mathfrak{o}_{\mathcal{T}_0}^{A_0})) \\
&=: (\natural)_*(\mathfrak{o}_{\mathcal{T}\#\mathcal{T}_0}^{\psi\#\psi_0} \times \mathfrak{o}_{\mathcal{T}\#\mathcal{T}_0}^{A\#A_0})
\end{aligned}$$

where the second equality is the definition of coherence for the orientation systems $\mathfrak{o}_{\mathcal{T}}$ and $\mathfrak{o}_{\mathcal{T}_0}$, and the third equality is the statement of the commutativity of the two induced glueing maps referenced above. This commutativity follows from the fact that the two glueing maps can be viewed as taking place in a small neighborhood of the curves being glued, and can thus be performed in either order, or simultaneously, via the construction in [14, Appendix A]. This establishes coherence of the system $\mathfrak{o}_{\mathcal{T}\#\mathcal{T}_0}$.

For $u \in \mathcal{M}(\psi)$ let

$$\mathcal{M}_{(\boldsymbol{\Theta},\boldsymbol{a},\boldsymbol{b})}(\rho^p(u)) = \coprod_{\substack{\psi_0 \in \pi_2(\boldsymbol{\Theta},\boldsymbol{a},\boldsymbol{b}) \\ \mu(\psi_0)=2n_p(\psi)}} \mathcal{M}(\psi_0, \rho^p(u)).$$

With respect to a coherent orientation system $\mathfrak{o}_{\mathcal{T}\#\mathcal{T}_0}$ on $\mathcal{T}\#\mathcal{T}_0$ determined from any coherent systems $\mathfrak{o}_{\mathcal{T}}$ and $\mathfrak{o}_{\mathcal{T}_0}$ as above, the triangle map in question can then be written as

$$\mathcal{F}_{\mathcal{T}\#\mathcal{T}_0}((\boldsymbol{x}\times\boldsymbol{\Theta})\otimes(\boldsymbol{y}\times\boldsymbol{a})) =$$

$$= \sum_{\boldsymbol{z}} \sum_{\substack{\psi\in\pi_2(\boldsymbol{x},\boldsymbol{y},\boldsymbol{z})\\ \psi_0\in\pi_2(\boldsymbol{\Theta},\boldsymbol{a},\boldsymbol{b})\\ \mu(\psi\#\psi_0)=0}} \#\{(u,u_0)\in\mathcal{M}(\psi)\times\mathcal{M}(\psi_0)|\rho^p(u)=\rho^p(u_0)\}U^{n_p(\psi)}\cdot\boldsymbol{z}\times\boldsymbol{b}$$

$$= \sum_{\boldsymbol{z}} \sum_{\substack{\psi\in\pi_2(\boldsymbol{x},\boldsymbol{y},\boldsymbol{z})\\ \mu(\psi)=0}} \sum_{\substack{\psi_0\in\pi_2(\boldsymbol{\Theta},\boldsymbol{a},\boldsymbol{b})\\ \mu(\psi_0)=2n_p(\psi)}} \#\{(u,u_0)\in\mathcal{M}(\psi)\times\mathcal{M}(\psi_0)|\rho^p(u)=\rho^p(u_0)\}U^{n_p(\psi)}\cdot\boldsymbol{z}\times\boldsymbol{b}$$

$$= \sum_{\boldsymbol{z}} \sum_{\substack{\psi\in\pi_2(\boldsymbol{x},\boldsymbol{y},\boldsymbol{z})\\ \mu(\psi)=0}} \sum_{\substack{\psi_0\in\pi_2(\boldsymbol{\Theta},\boldsymbol{a},\boldsymbol{b})\\ \mu(\psi_0)=2n_p(\psi)}} \sum_{u\in\mathcal{M}(\psi)} \#\left(u\times\mathcal{M}(\psi_0,\rho^p(u))\right)U^{n_p(\psi)}\cdot\boldsymbol{z}\times\boldsymbol{b}$$

$$= \sum_{\boldsymbol{z}} \sum_{\substack{\psi\in\pi_2(\boldsymbol{x},\boldsymbol{y},\boldsymbol{z})\\ \mu(\psi)=0}} \sum_{u\in\mathcal{M}(\psi)} \#\left(u\times\mathcal{M}_{(\boldsymbol{\Theta},\boldsymbol{a},\boldsymbol{b})}(\rho^p(u))\right)U^{n_p(\psi)}\cdot\boldsymbol{z}\times\boldsymbol{b}$$

We will show in Lemma 2.9.21 below that there is a coherent orientation system $\mathfrak{o}_{\mathcal{T}_0}$ on $\mathcal{T}_0$ for which either

$$\#\mathcal{M}_{(\boldsymbol{\Theta},\boldsymbol{a},\boldsymbol{b})}(\rho^p(u)) = 1$$

for all ψ with $\mu(\psi)=0$ and all $u\in\mathcal{M}(\psi)$, or

$$\#\mathcal{M}_{(\boldsymbol{\Theta},\boldsymbol{a},\boldsymbol{b})}(\rho^p(u)) = -1$$

for all ψ with $\mu(\psi)=0$ and all $u\in\mathcal{M}(\psi)$. Then we will have

$$
\begin{aligned}
&\mathcal{F}^{-}_{\mathcal{T}\#\mathcal{T}_0}((\boldsymbol{x}\times\boldsymbol{\Theta})\otimes(\boldsymbol{y}\times\boldsymbol{a})) = \\
&= \sum_{\boldsymbol{z}} \sum_{\substack{\psi\in\pi_2(\boldsymbol{x},\boldsymbol{y},\boldsymbol{z}) \\ \mu(\psi)=0}} \sum_{u\in\mathcal{M}(\psi)} \#\left(u\times\mathcal{M}_{(\boldsymbol{\Theta},\boldsymbol{a},\boldsymbol{b})}(\rho^p(u))\right) U^{n_p(\psi)}\cdot\boldsymbol{z}\times\boldsymbol{b} \\
&= \pm\sum_{\boldsymbol{z}} \sum_{\substack{\psi\in\pi_2(\boldsymbol{x},\boldsymbol{y},\boldsymbol{z}) \\ \mu(\psi)=0}} \#\mathcal{M}(\psi) U^{n_p(\psi)}\cdot\boldsymbol{z}\times\boldsymbol{b} \\
&= \pm\left(\sum_{\boldsymbol{z}} \sum_{\psi\in\pi_2(\boldsymbol{x},\boldsymbol{y},\boldsymbol{z}),\mu(\psi)=0} (\#\mathcal{M}(\psi)) U^{n_p(\psi)}\cdot\boldsymbol{z}\right)\times\boldsymbol{b} \\
&= \pm\mathcal{F}^{-}_{\mathcal{T}}(\boldsymbol{x}\otimes\boldsymbol{y})\times\boldsymbol{b}
\end{aligned}
$$

This completes the proof of the proposition, modulo Lemma 2.9.21. □

Lemma 2.9.21. *For $\boldsymbol{d}\in Sym^k(\Delta)\setminus Diag(\Delta)$ and a generic choice of almost complex structure J, the moduli space $\mathcal{M}_{(\boldsymbol{\Theta},\boldsymbol{a},\boldsymbol{b})}(\boldsymbol{d})$ is a smoothly cut out 0-manifold. For such J, there is a coherent orientation system $\mathfrak{o}_{\mathcal{T}_0}$ on $\mathcal{T}_0$ for which the signed count of points in the moduli space is*

$$\#\mathcal{M}_{(\boldsymbol{\Theta},\boldsymbol{a},\boldsymbol{b})}(\boldsymbol{d}) = \pm 1$$

where the constant is independent of $\boldsymbol{d}$.

Proof. The proof is again carried out in steps:

1. We show the moduli space is transversely cut out for generic J.
2. We show that for generic $\boldsymbol{d}\in \mathrm{Sym}^k(\Delta)\setminus\mathrm{Diag}(\Delta)$, the signed count $\#\mathcal{M}_{(\boldsymbol{\Theta},\boldsymbol{a},\boldsymbol{b})}(\boldsymbol{d})$ is independent of $\boldsymbol{d}$.
3. We find one choice of $\boldsymbol{d}$ giving the desired count.

In fact, the proof of step (1) given in [3] carries over exactly as it is stated there, so we will only prove steps (2) and (3).

Step 2 Let $p : I \to \mathrm{Sym}^k(\Delta)$ be a path from $\boldsymbol{d_0}$ to $\boldsymbol{d_1}$, where the image of p satisfies the conditions of Lemma 2.9.9. We consider the moduli space

$$\bigcup_{t\in I} \mathcal{M}_{(\boldsymbol{\Theta},\boldsymbol{a},\boldsymbol{b})}(p(t))$$

which by Proposition 2.9.9 and Lemma 2.9.10 is a smooth, orientable 1 manifold. From orientability, we know that the signed count of the ends of the moduli space above is zero. We now describe all contributions to the count of the ends. We begin by making considerations which will hold for any choice of coherent orientation system satisfying the property appearing in Lemma 2.9.13.

The ends of $\bigcup_{t\in I} \mathcal{M}_{(\boldsymbol{\Theta},\boldsymbol{a},\boldsymbol{b})}(p(t))$ fall into three classes. They arise from $\mathcal{M}_{(\boldsymbol{\Theta},\boldsymbol{a},\boldsymbol{b})}(\boldsymbol{d_0})$, $\mathcal{M}_{(\boldsymbol{\Theta},\boldsymbol{a},\boldsymbol{b})}(\boldsymbol{d_1})$, and degenerations of holomorphic triangles to broken holomorphic triangles in the compactification. Let $u_i : S_0 \to \Sigma_0 \times \Delta$ be a sequence of holomorphic triangles in $\bigcup_{t\in I} \mathcal{M}_{(\boldsymbol{\Theta},\boldsymbol{a},\boldsymbol{b})}(p(t))$. As shown in [3, Lemma 9.58], the only degenerations that can occur correspond to "strip breaking". In particular, if u_i converges to a broken holomorphic triangle

$$U = (u_1, v_1, \ldots, v_n, w_1, \ldots, w_m)$$

(in the sense of Definition 2.9.5), then in fact $U = (u_1, v_1, \ldots, v_n)$ where the v_i are holomorphic strips. We note that the argument used to rule out other types of degenerations has nothing to do with orientations. Furthermore, we will see presently that among degenerations corresponding to strip breaking,

the only ones which can occur yield broken triangles U consisting of a triangle u_1 of index $2k-1$ which matches a divisor $p(t)$ for some $t \in I$, as well as a single curve $v_1 : S \to \Sigma_0 \times I \times \mathbb{R}$ with index 1.

To see this, note that if U is genuinely broken then $U = (u_1, v_1, \ldots, v_n)$ with u_1 a holomorphic triangle representing a class in $\pi_2(\boldsymbol{x}, \boldsymbol{a}, \boldsymbol{b})$ and v_i holomorphic curves in $\pi_2(\boldsymbol{y}_i, \boldsymbol{z}_i)$ for some $\boldsymbol{y}_i, \boldsymbol{z}_i \in \mathbb{T}_{\alpha'} \cap \mathbb{T}_{\alpha}$.We now analyze what contributions to the ends can occur for the four possible intersection points $\boldsymbol{x} \in \mathbb{T}_{\alpha'} \cap \mathbb{T}_{\alpha}$.

Suppose $\boldsymbol{x} = \boldsymbol{\Theta}$. Then by applying Lemma 2.9.18 to u_1 we obtain $\mu(u_1) = 2n_{p_0}(u_1)$. Since u_1 satisfies a matching condition with $p(t)$ for some $t \in I$, we have $2n_{p_0}(u_1) = |\rho^p(p(t))| = k = 2n_{p_0}(\psi_0) = \mu(\psi_0)$. Thus $\mu(u_1) = \mu(\psi_0)$. Since the total homology class of U must be ψ_0, we therefore must have $\mu(v_i) = 0$ and $n_{p_0}(v_I) = 0$ for all i. Since the v_i satisfy $(M1)$ and $(M3)$-$(M6)$, the only possibility for such curves is that each is a collection of constant components. Indeed, if any v_i were locally nonconstant, it would satisfy $(M2)$, hence by [3, Corollary 7.2] the dimension of the relevant moduli space containing it would be negative. Thus $U = (u_1)$ (plus potentially some constant curves) is in the interior of $\bigcup_{t \in I} \mathcal{M}_{(\boldsymbol{\Theta}, \boldsymbol{a}, \boldsymbol{b})}(p(t))$, and so contributes nothing to the signed count of the ends.

Next we consider the cases $\boldsymbol{x} = \theta_1^+\theta_2^-, \theta_1^-\theta_2^+$. In these cases Lemma 2.9.18 yields that the index of the triangle must be $\mu(u_1) = 2n_{p_0}(u_1) - 1 = 2n_{p_0}(\psi_0) - 1$, so the remaining curves must have indices which sum to 1. Similarly, $0 = n_{p_0}(\psi_0) - n_{p_0}(u_1) = \sum_i n_{p_0}(v_i)$, so v_i must have multiplicity 0 at the basepoint for each i. The only possibility in this case is that there

is a single Maslov index 1 strip v_1. Thus in this case, we have additional contributions to the ends coming from:

$$\bigcup_{\substack{t\in I\\ \boldsymbol{x}\in\{\theta_1^+\theta_2^-,\theta_1^-\theta_2^+\}}} \bigcup_{\substack{\phi\in\pi_2(\boldsymbol{\Theta},\boldsymbol{x})\\ n_{p_0}(\phi)=0}} \mathcal{M}_{(\boldsymbol{x},\boldsymbol{a},\boldsymbol{b})}(p(t)) \times \widehat{\mathcal{M}}(\phi)$$

Fix $\boldsymbol{x} \in \{\theta_1^+\theta_2^-, \theta_1^-\theta_2^+\}$. Then by Lemma 2.9.19 we know that

$$\sum_{\substack{\phi\in\pi_2(\boldsymbol{\Theta},\boldsymbol{x})\\ n_{p_0}(\phi)=0}} \#\widehat{\mathcal{M}}(\phi) = 0$$

Thus

$$\begin{aligned}
&\#\Big(\bigcup_{\substack{t\in I\\ \boldsymbol{x}\in\{\theta_1^+\theta_2^-,\theta_1^-\theta_2^+\}}} \bigcup_{\substack{\phi\in\pi_2(\boldsymbol{\Theta},\boldsymbol{x})\\ n_{p_0}(\phi)=0}} \mathcal{M}_{(\boldsymbol{x},\boldsymbol{a},\boldsymbol{b})}(p(t)) \times \widehat{\mathcal{M}}(\phi)\Big) \\
&= \sum_{\substack{t\in I\\ \boldsymbol{x}\in\{\theta_1^+\theta_2^-,\theta_1^-\theta_2^+\}}} \sum_{\substack{\phi\in\pi_2(\boldsymbol{\Theta},\boldsymbol{x})\\ n_{p_0}(\phi)=0}} \#(\mathcal{M}_{(\boldsymbol{x},\boldsymbol{a},\boldsymbol{b})}(p(t)) \times \widehat{\mathcal{M}}(\phi)) \\
&= \sum_{\substack{t\in I\\ \boldsymbol{x}\in\{\theta_1^+\theta_2^-,\theta_1^-\theta_2^+\}}} \sum_{\substack{\phi\in\pi_2(\boldsymbol{\Theta},\boldsymbol{x})\\ n_{p_0}(\phi)=0}} (\#\mathcal{M}_{(\boldsymbol{x},\boldsymbol{a},\boldsymbol{b})}(p(t))) \cdot (\#\widehat{\mathcal{M}}(\phi)) = 0
\end{aligned}$$

Here we have used in the last equality the fact that we have endowed the orientable manifold $\bigcup_{t\in I} \mathcal{M}_{(\boldsymbol{\Theta},\boldsymbol{a},\boldsymbol{b})}(p(t))$ with some coherent orientation system. This implies in particular that the orientation induced on the compactification agrees with the product orientation at ends such as those above. So we see these cases also contribute nothing to the count of signed ends of the moduli space.

Lastly, we consider the case $\boldsymbol{x} = \theta_1^-\theta_2^-$. For any $\psi_0 \in \pi_2(\theta_1^-\theta_2^-, \boldsymbol{a}, \boldsymbol{b})$ we have by lemma 2.9.18 $\mu(psi_0) = 2n_{p_0}(\psi_0) - 2 = 2k - 2$. By proposition 2.9.9,

for a generic choice of almost complex structure J, and a fixed source S, the matched moduli space $\mathcal{M}(\psi_0, S, p(I))$ is a smooth manifold of dimension

$$\mathrm{ind}(\psi_0, S) - \mathrm{codim}(p(I)) = \mathrm{ind}(\psi_0, S) - (2k-1) \leq \mu(\psi_0) - (2k-1) = -1$$

Here the fact being used to establish the inequality is that for any holomorphic triangle u in the homology class A (not necessarily embedded), the index of the linearized $\bar{\partial}$ operator at u satisfies $\mathrm{ind}(A, S) = \mu(A) - 2\mathrm{sing}(u)$, and in particular $\mathrm{ind}(A, S) \leq \mu(A)$. This is [3, Equation 9.46], which comes from adapting [24, Proposition 5.69]. This shows that for a generic choice of J, the broken triangle U can not in fact contain a triangle u_1 in such a class ψ_0.

To summarize, we have shown that the ends of $\bigcup_{t\in I} \mathcal{M}_{(\boldsymbol{\Theta},\boldsymbol{a},\boldsymbol{b})}(p(t))$ correspond to $\mathcal{M}_{(\boldsymbol{\Theta},\boldsymbol{a},\boldsymbol{b})}(\boldsymbol{d_0})$, $\mathcal{M}_{(\boldsymbol{\Theta},\boldsymbol{a},\boldsymbol{b})}(\boldsymbol{d_1})$, and to degenerations of triangles into broken triangles containing one triangle and one strip, and that the last types of ends contribute nothing to the total signed count of the ends. Since we have chosen a collection of orientation systems satisfying the conclusion of Lemma 2.9.13, we see that the signed count of the ends of $\bigcup_{t\in I} \mathcal{M}_{(\boldsymbol{\Theta},\boldsymbol{a},\boldsymbol{b})}(p(t))$ is given by:

$$\#\mathcal{M}_{(\boldsymbol{\Theta},\boldsymbol{a},\boldsymbol{b})}(\boldsymbol{d_1}) - \#\mathcal{M}_{(\boldsymbol{\Theta},\boldsymbol{a},\boldsymbol{b})}(\boldsymbol{d_0}) = 0.$$

This concludes step 2.

We note that by Lemma 2.9.13, a coherent orientation system on $\mathcal{M}_{(\boldsymbol{\Theta},\boldsymbol{a},\boldsymbol{b})}(p(0))$ induces a coherent orientation system over

$\bigcup_{t\in I} \mathcal{M}_{(\boldsymbol{\Theta},\boldsymbol{a},\boldsymbol{b})}(p(t))$ and $\mathcal{M}_{(\boldsymbol{\Theta},\boldsymbol{a},\boldsymbol{b})}(p(1))$ satisfying the conclusion of the lemma. We thus see that if we can find a single divisor $\mathbf{d}$ and a coherent orientation system $\mathfrak{o}$ over $\mathcal{M}_{(\boldsymbol{\Theta},\boldsymbol{a},\boldsymbol{b})}(\mathbf{d})$ giving the desired count, then the argument of step 2 shows that there are induced coherent orientations over all divisors $\mathbf{d}'$ in the same path component as $\mathbf{d}$ for which the counts are the same. We will construct such a divisor in step 3 below.

Step 3 To construct a divisor $\mathbf{d} \in \mathrm{Sym}^k(\Delta) \setminus \mathrm{Diag}(\Delta)$ giving the desired count, we consider a path of divisors subject to constraints, and evaluate the asymptotics of the moduli spaces of triangles matched to divisors in this path. Our argument is an explication of that in [3], which is in turn based on an analogous argument in [25, pg. 653] which deals with holomorphic strips. Our goal in summarizing these proofs is to make explicit the dependence of all statements on signs and orientations.

We consider any path $p : [1,\infty) \to \mathrm{Sym}^k(\Delta) \setminus \mathrm{Diag}(\Delta)$ for which each point in $p(t)$ is at least a distance of t away from all other points in $p(t)$, with respect to a metric on Δ for which the corners are infinite strips in $\mathbb{C}$ (see Figure 24). We further require that the points in $p(t)$ smoothly approach the vertex $v_{\alpha_0\beta_0}$ of Δ as $t \to \infty$. For such a path of divisors, we have as before a matched moduli space

$$\mathcal{M}_{(\boldsymbol{\Theta},\boldsymbol{a},\boldsymbol{b})}(p) = \bigcup_{t\in[1,\infty]} \mathcal{M}_{(\boldsymbol{\Theta},\boldsymbol{a},\boldsymbol{b})}(p(t)).$$

By the same arguments used in step 2, the ends of this moduli space corresponding to degenerations of triangles at finite values of t, with $t \neq 1$, will contribute nothing to the signed count of the ends, for any choice of coherent orientation system. Consider any coherent orientation system

$\mathfrak{o}$ satisfying the properties of that furnished by Lemma 2.9.13; then with respect to such an orientation system the signed count $\#\mathcal{M}_{(\boldsymbol{\Theta},\boldsymbol{a},\boldsymbol{b})}(p(1))$ must agree with the signed count of the ends of $\mathcal{M}_{(\boldsymbol{\Theta},\boldsymbol{a},\boldsymbol{b})}(p)$ coming from degenerations of triangles as $t \to \infty$. So we now count these ends.

We claim that as $t \to \infty$, the only broken triangles which can occur in the limit consist of a single genuine triangle τ of index 0 on $(\Sigma_0, \boldsymbol{\alpha}_0', \boldsymbol{\alpha}_0, \boldsymbol{\beta}_0)$, along with k index 2 curves on $(\Sigma_0, \boldsymbol{\alpha}_0, \boldsymbol{\beta}_0)$ which satisfy matching conditions with some collection of divisors $c_i \in [0,1] \times \mathbb{R}$. To see this, we note that each point in the path p consists of k distinct points in Δ, and the fact that these k points separate and approach the vertex $v_{\alpha_0\beta_0}$ in the limit necessitates that the limiting broken triangle must contain k strips satisfying matching conditions. To see the index of each of these curves must be 2, we make some simple observations about the diagram $(\Sigma_0, \boldsymbol{\alpha}_0, \boldsymbol{\beta}_0)$ for S^3.

First, note that the only homology classes of discs supporting holomorphic representatives are $\{\boldsymbol{e_a} + s[\Sigma_0]\}$ for nonnegative integers s, where $\boldsymbol{e_a}$ is the constant disk at $\boldsymbol{a}$. The Maslov indices for such classes are $\mu(\boldsymbol{e_a} + s[\Sigma_0]) = 2s$. The fact that each strip satisfies a matching condition implies we must have $s \geq 1$ for each homology class. Since the total index of each holomorphic triangle in the moduli space $\mathcal{M}_{(\boldsymbol{\Theta},\boldsymbol{a},\boldsymbol{b})}(p)$ is $2k$, the limiting broken holomorphic triangle must have index $2k$, so the only possibility is that each of the k curves has index 2 (i.e. has s=1), and the triangle τ has index 0. By counting multiplicities and noting positivity of intersections, we see that the triangle τ must satisfy $n_{p_0}(\tau) = 0$. Using the same arguments

as in the preceding proposition, we have that all of the curves in the broken triangle must satisfy $(M1)-(M8)$.

Applying the glueing result of Lipshitz [14, Appendix A, Proposition A.1], we see that we can obtain the signed count of the ends ocurring as degenerations as $t \to \infty$, or equivalently the count $\#\mathcal{M}_{(\boldsymbol{\Theta},\boldsymbol{a},\boldsymbol{b})}(p(1))$, as:

$$\#\mathcal{M}_{(\boldsymbol{\Theta},\boldsymbol{a},\boldsymbol{b})}(p(1)) = (\#\mathcal{M}_{(\boldsymbol{a},\boldsymbol{a})}(c))^k \cdot \sum_{\substack{\psi \in \pi_2(\boldsymbol{\Theta},\boldsymbol{a},\boldsymbol{b}) \\ n_{p_0}(\psi)=0}} \#\mathcal{M}(\psi)$$

where c is a divisor in $[0,1] \times \mathbb{R}$ and $\mathcal{M}_{(\boldsymbol{a},\boldsymbol{a})}(c)$ is the moduli space of index 2 strips on $(\Sigma_0, \boldsymbol{\alpha}_0, \boldsymbol{\beta}_0)$ with $\rho^p(u) = c$. Here the counts are occurring with respect to any coherent orientation system $\mathfrak{o}_{\mathcal{T}_0} = \{\mathfrak{o}_{\boldsymbol{\alpha}_0',\boldsymbol{\alpha}_0,\boldsymbol{\beta}_0}, \mathfrak{o}_{\boldsymbol{\alpha}_0,\boldsymbol{\beta}_0}, \mathfrak{o}_{\boldsymbol{\alpha}_0',\boldsymbol{\alpha}_0}, \mathfrak{o}_{\boldsymbol{\alpha}_0',\boldsymbol{\beta}_0}\}$ on $\mathcal{T}_0$ and the compatible orientation system $\mathfrak{o}_{\boldsymbol{\alpha}_0,\boldsymbol{\beta}_0}$ included in the data $\mathfrak{o}_{\mathcal{T}_0}$. The sum on the right hand side is precisely the count occurring in the triangle map in Lemma 2.9.20, and is thus ± 1. Thus to finish this step it suffices to show that there is a coherent orientation system $\mathfrak{o}_{\mathcal{T}_0}$ for which

$$\#\mathcal{M}_{(\boldsymbol{a},\boldsymbol{a})}(c) = \pm 1.$$

Consider the standard diagram $\mathcal{H}_{S^1\times S^2}$ for $S^1 \times S^2$, twice stabilized via the diagram $(\Sigma_0, \boldsymbol{\alpha}_0, \boldsymbol{\beta}_0)$ as shown in Figure 26. The figure depicts this genus 3 diagram for $S^1 \times S^2$, along with a choice of basepoint z. Both bigons in $\mathcal{H}_{S^1\times S^2}$ for $S^1 \times S^2$ admit a single holomorphic representative. We consider a choice of coherent orientation system on $\mathcal{H}_{S^1\times S^2}$ for which the the bigons cancel, and the resulting Floer homology is $\widehat{HF} \cong \mathbb{Z}^2$. By invariance of $\widehat{HF}$, the twice stabilized bigon in the twice stabilized diagram must also have a

single holomorphic representative. As in the proof of stabilization invariance in [14], this implies via a neck stretching argument that there is a coherent orientation system $\mathfrak{o}_{\boldsymbol{\alpha}_0,\boldsymbol{\beta}_0}$ on $(\Sigma_0, \boldsymbol{\alpha}_0, \boldsymbol{\beta}_0)$ for which

$$\#\mathcal{M}_{(\boldsymbol{a},\boldsymbol{a})}(c) = \pm 1.$$

By [1, Lemma 8.7], this coherent orientation system can be extended to a coherent orientation system $\mathfrak{o}_{\mathcal{T}_0}$ for which the same condition holds. This completes step 3, and the proof of the lemma.

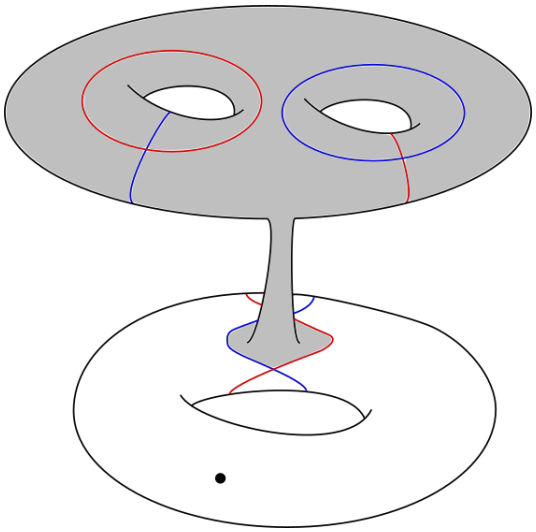

FIGURE 26 The diagram $\mathcal{H}_{S^1\times S^2}$ on the bottom of the figure is twice stabilized via a connect sum with $(\Sigma_0, \boldsymbol{\alpha}_0, \boldsymbol{\beta}_0)$. Shaded in grey is a domain on the genus 3 diagram, the "twice stabilized bigon", which arises from one of the bigons in $\mathcal{H}_{S^1\times S^2}$.

□

This concludes the payment of all unpaid debts that were needed for the proofs of our theorems. Having established our naturality results, we will proceed in the subsequent chapter to investigate applications, and attempt to provide some answers the question "What is it all good for?".

CHAPTER III

FURTHER DIRECTIONS AND APPLICATIONS

We now point out some applications and potential generalizations of the naturality results established in the previous chapter. The work in this chapter has been submitted for publication to the Journal of Topology. Given two based 3-manifolds (Y_1, z_1) and (Y_2, z_2), a cobordism W between them decorated with a choice of path in W from z_1 to z_2, and a choice of $\mathfrak{t} \in \mathrm{Spin}^c(W)$, Ozsváth and Szabó constructed in [2] cobordism maps:

$$F^{\circ}_{W,\mathfrak{t}} : HF^{\circ}(Y_1, z_1, \mathfrak{t}|_{Y_1}) \to HF^{\circ}(Y_2, z_2, \mathfrak{t}|_{Y_2}).$$

(The choice of path is not made explicit in [2]). In [5] Zemke extended the results in [3] to show that over $\mathbb{F}_2$ these maps are well-defined and natural with respect to composition of decorated cobordisms. We expect that our results can be used in a similar way to establish such naturality over $\mathbb{Z}$, up to an overall sign. Furthermore, in [2] Ozsváth and Szabó showed how naturality of the Heegaard Floer invariants with respect to decorated cobordisms can be used to define the so called mixed invariants of closed 4-manifolds. Given a closed 4-manifold X and a choice of $\mathfrak{t} \in \mathrm{Spin}^c(X)$, these take the form of maps

$$\Phi_{X,\mathfrak{t}} : \Lambda^*(H_1(X; \mathbb{F}_2)/\mathrm{Tors}) \otimes_{\mathbb{F}_2} \mathbb{F}_2[U] \to \mathbb{F}_2.$$

These share many of the features of the Seiberg-Witten invariants, and serve as powerful tools in detecting subtle smooth information. If one can

establish naturality with respect to cobordisms over $\mathbb{Z}/\pm$, we would obtain corresponding mixed invariants

$$\Phi_{X,\mathfrak{t}} : \Lambda^*(H_1(X;\mathbb{Z})/\text{Tors}) \otimes_{\mathbb{Z}} \mathbb{Z}[U] \to \mathbb{Z}/\pm$$

which we expect would provide fruitful extra information. In fact, before the gap in the literature was noticed, the integral mixed invariants had already been extensively studied in papers including [26], [27] and [28], so establishing naturality with respect to cobordisms over $\mathbb{Z}$ would immediately prove useful, and would likely also be useful for computations and applications in the future.

A second application of our work comes from involutive Heegaard Floer homology, defined by Hendricks and Manolescu in [29]. To describe it, fix a closed 3-manifold Y and $\mathfrak{s} \in \text{Spin}^c(Y)$. Given a pointed Heegaard diagram $\mathcal{H} = (\Sigma, \boldsymbol{\alpha}, \boldsymbol{\beta}, z)$ for (Y, z), there is a conjugate diagram $\overline{\mathcal{H}} = (-\Sigma, \boldsymbol{\beta}, \boldsymbol{\alpha}, z)$ for (Y, z) given by reversing the orientation on the surface and switching the role of the α and β curves. Under suitable admissibility hypotheses, there is a chain isomorphism

$$\eta_{\mathcal{H}\to\overline{\mathcal{H}}} : CF^\circ(\mathcal{H}, \mathfrak{s}) \to CF^\circ(\overline{\mathcal{H}}, \overline{\mathfrak{s}})$$

given by mapping intersection points to themselves [7, Theorem 2.4]. Using the results in [3], Hendricks and Manolescu showed that the $\mathbb{F}_2$ analog of Corollary 1.3.5 holds: the modules $CF^\circ(\mathcal{H}, \mathfrak{s})$ fit into a transitive system in the homotopy category of chain complexes of $\mathbb{F}_2[U]$-modules with respect to the maps induced by the Heegaard moves appearing in Corollary 1.3.5.

Thus, since $\mathcal{H}$ and $\overline{\mathcal{H}}$ represent the same 3-manifold, there is a chain homotopy equivalence

$$\Phi(\overline{\mathcal{H}}, \mathcal{H}) : CF^\circ(\overline{\mathcal{H}}, \overline{\mathfrak{s}}) \to CF^\circ(\mathcal{H}, \overline{\mathfrak{s}})$$

of complexes of $\mathbb{F}_2[U]$-modules which is well defined up to homotopy. Using these maps, they consider the map $\iota := \Phi(\overline{\mathcal{H}}, \mathcal{H}) \circ \eta_{\mathcal{H} \to \overline{\mathcal{H}}}$, which is well defined up to homotopy, and which is shown to be a homotopy involution in [29, Lemma 2.5]. They then use it to construct an invariant of Y as follows.

There is a $\mathbb{Z}/2\mathbb{Z}$ action on $\mathrm{Spin}^c(Y)$ given by conjugation. Let $[\mathrm{Spin}^c(Y)]$ denote the set of orbits in $\mathrm{Spin}^c(Y)$ under this action. Given an orbit $\overline{\omega} \in [\mathrm{Spin}^c(Y)]$, let

$$CF^\circ(\mathcal{H}, \overline{\omega}) = \bigoplus_{\mathfrak{s} \in \overline{\omega}} CF^\circ(\mathcal{H}, \mathfrak{s}).$$

The authors investigate the map $(1 + \iota)$, considered as a chain map between complexes of $\mathbb{F}_2[U]$-modules, and consider its cone

$$CFI(\mathcal{H}, \overline{\omega}) := \mathrm{Cone}(1+\iota) = \left(CF^\circ(\mathcal{H}, \overline{\omega})[-1] \oplus CF^\circ(\mathcal{H}, \overline{\omega}), \partial_{\mathrm{cone}} = \begin{pmatrix} \partial & 0 \\ 1 + \iota & -\partial \end{pmatrix} \right).$$

Here $CF^\circ(\mathcal{H}, \overline{\omega})[-1]$ indicates the shifted chain complex, whose degree n piece is given by $(CF^\circ(\mathcal{H}, \overline{\omega})[-1])_n = CF^\circ(\mathcal{H}, \overline{\omega})_{n-1}$. They then introduce a formal variable Q of degree -1 satisfying $Q^2 = 0$, and rewrite the map being coned over as

$$CF^\circ(\mathcal{H}, \overline{\omega}) \xrightarrow{Q \cdot (1+\iota)} Q \cdot CF^\circ(\mathcal{H}, \overline{\omega})[-1].$$

As one can readily check, the cone and its differential can then be rewritten as

$$\mathrm{Cone}(1+\iota) = \left(CF^\circ(\mathcal{H},\overline{\omega})[-1] \otimes \mathbb{F}_2[Q]/(Q^2), \partial + Q(1+\iota)\right).$$

Considered in this way, it is a complex of modules over the ring $\mathcal{R} = \mathbb{F}_2[Q,U]/(Q^2)$. The authors then show that the quasi-isomorphism class of the complex $CFI(\mathcal{H},\overline{\omega})$ of $\mathcal{R}$-modules thus defined is an invariant of $(Y,\overline{\omega})$.

We now explain how Corollary 1.3.5 can be used to construct a version of such an invariant defined over $\mathbb{Z}$. Fix again a 3-manifold Y, and diagrams $\mathcal{H}$ and $\overline{\mathcal{H}}$ representing Y as above. Since $\mathcal{H}$ and $\overline{\mathcal{H}}$ represent the same 3 manifold, we obtain from Corollary 1.3.5 (at most) two homotopy classes of chain homotopy equivalences

$$\pm\Psi(\overline{\mathcal{H}},\mathcal{H}) : CF^\circ(\overline{\mathcal{H}},\mathfrak{s}) \to CF^\circ(\mathcal{H},\mathfrak{s})$$

associated to sequences of Heegaard moves relating the two diagrams. The set $\{\pm\Psi(\overline{\mathcal{H}},\mathcal{H})\}$ is well defined up to chain homotopy. We thus obtain two homotopy classes of maps $\pm\iota := \pm\Psi(\overline{\mathcal{H}},\mathcal{H}) \circ \eta_{\mathcal{H}\to\overline{\mathcal{H}}}$. The same argument used in [29, Lemma 2.5] to show that ι is a homotopy involution over $\mathbb{F}_2$ now shows that $\pm\iota$ both have order at most 4 (up to homotopy) over $\mathbb{Z}$. We define

$$CFI_\pm(\mathcal{H},\overline{\omega}) := \mathrm{Cone}(1 \pm \iota),$$

where now both complexes are considered as complexes of $\mathbb{Z}[U]$-modules. While we can no longer conclude the maps $\pm\iota$ are homotopy involutions, we still obtain that the collection of the two quasi-isomorphism classes of the

complexes of $\mathbb{Z}[U]$-modules that we obtain is an invariant of the underlying 3-manifold.

Theorem 3.0.1. *The unordered pair of quasi-ismorphism classes determined by the complexes*

$$CFI_{\pm}(\mathcal{H}, \overline{\omega})$$

(considered as complexes of $\mathbb{Z}[U]$-modules) is an invariant of $(Y, \overline{\omega}, z)$.

Proof. The proof is essentially the same as that in [29], but we include a sketch of it here for the reader's convenience.

Fix $(Y, z, \overline{\omega})$, and consider a diagram $\mathcal{H}$ and its conjugate $\overline{\mathcal{H}}$ as above. As we noted earlier, for the fixed diagram $\mathcal{H}$ the collection of the two chain homotopy equivalences $\{\pm\Psi(\overline{\mathcal{H}}, \mathcal{H})\}$ is well defined up to chain homotopy by Corollary 1.3.5. Thus so too is the collection $\{\pm\iota\}$. We conclude that the set of the two cones $\{CFI_{\pm}(\mathcal{H}, \overline{\omega})\}$ associated to $(\mathcal{H}, \overline{\omega})$ is well defined up to chain homotopy equivalence.

Next, we consider the dependence on the choice of diagram. Consider a different diagram $\mathcal{H}'$ for (Y, z) and its conjugate $\overline{\mathcal{H}'}$. We obtain corresponding collections $\{\pm\Psi(\overline{\mathcal{H}'}, \mathcal{H}')\}$ and $\{\pm\iota'\}$ which are both well defined up to homotopy, and $\{CFI_{\pm}(\mathcal{H}', \overline{\omega})\}$ well defined up to homotopy equivalence. Choose some fixed sequence of Heegaard moves connecting $\mathcal{H}$ to $\mathcal{H}'$, and consider either of the (at most two) corresponding chain homotopy equivalences $\pm\Psi(\mathcal{H}, \mathcal{H}')$ furnished by Corollary 1.3.5. We denote our choice by $\Psi(\mathcal{H}, \mathcal{H}')$. Consider the following diagram involving the four

cone complexes in question

$$\begin{array}{ccc} CF^\circ(\mathcal{H},\overline{\omega})[-1] & \xrightarrow{1\pm\iota} & CF^\circ(\mathcal{H},\overline{\omega}) \\ \downarrow{\scriptstyle \Psi(\mathcal{H},\mathcal{H}')} & & \downarrow{\scriptstyle \Psi(\mathcal{H},\mathcal{H}')} \\ CF^\circ(\mathcal{H}',\overline{\omega})[-1] & \xrightarrow{1\pm\iota'} & CF^\circ(\mathcal{H}',\overline{\omega}) \end{array}$$

We claim that for a fixed choice in $\{\pm\iota\}$, the diagram commutes up to homotopy for at least one of the two choices in $\{\pm\iota'\}$. We denote our choice of the fixed homotopy class in the top row by ι. To establish the claim, we need to show that

$$\Psi(\mathcal{H},\mathcal{H}')\circ\Psi(\overline{\mathcal{H}},\mathcal{H})\circ\eta_{\mathcal{H}\to\overline{\mathcal{H}}}\sim\pm\Psi(\overline{\mathcal{H}'},\mathcal{H}')\circ\eta_{\mathcal{H}'\to\overline{\mathcal{H}'}}\circ\Psi(\mathcal{H},\mathcal{H}').$$

We note that

$$\eta_{\mathcal{H}'\to\overline{\mathcal{H}'}}\circ\Psi(\mathcal{H},\mathcal{H}')\circ\eta_{\overline{\mathcal{H}}\to\mathcal{H}}\sim\pm\Psi(\overline{\mathcal{H}},\overline{\mathcal{H}'}).$$

To see this, observe that $\Psi(\mathcal{H},\mathcal{H}')$ is a map induced by some sequence of Heegard moves. The map resulting from precomposing and postcomposing this map with the isomorphisms η can be realized as the map induced on $CF^\circ(\overline{\mathcal{H}})$ by the same set of Heegaard moves giving rise to $\Psi(\mathcal{H},\mathcal{H}')$ (recall the maps η have no effect on the attaching curves). Thus the conjugated map is homotopic to $\pm\Psi(\overline{\mathcal{H}},\overline{\mathcal{H}'})$ by Corollary 1.3.5. We thus conclude that

$$\begin{aligned}\Psi(\overline{\mathcal{H}'},\mathcal{H}')\circ\eta_{\mathcal{H}'\to\overline{\mathcal{H}'}}\circ\Psi(\mathcal{H},\mathcal{H}')&\sim\pm\Psi(\overline{\mathcal{H}'},\mathcal{H}')\circ\Psi(\overline{\mathcal{H}},\overline{\mathcal{H}'})\circ\eta_{\mathcal{H}\to\overline{\mathcal{H}}}\\&\sim\pm\Psi(\mathcal{H},\mathcal{H}')\circ\Psi(\overline{\mathcal{H}},\mathcal{H})\circ\eta_{\mathcal{H}\to\overline{\mathcal{H}}}\end{aligned}$$

where the last two maps being homotopic up to a sign is again guaranteed by Corollary 1.3.5. Having established that the diagram with ι in the top row commutes up to chain homotopy for at least one choice of $\{\pm\iota'\}$ in the bottom row, the argument in [29] now applies directly to establish that $\mathrm{Cone}(1+\iota)$ is quasi-isomorphic to at least one of the cones $\mathrm{Cone}(1\pm\iota')$. This concludes the proof. □

Finally, we will address a final line of potential future applications in the subsequent chapter.

CHAPTER IV

ORIENTATION REVERSING DIFFEOMORPHISMS

In this chapter, we will set out to address a potential application of Heegaard Floer homology to the study of nonorientable 3-manifolds, and more generally to the study of orientation reversing diffeomorphisms on 3-manifolds. In fact, this line of research was the original motivation for understanding the naturality results presented earlier. At this stage, all of the results in this chapter are preliminary and exploratory, in the sense that we are still working out how the theory might be applied, and how best to form the theory given the interests and questions at hand. We provide our partial progress here nontheless, as we hope it may prove to be a useful resource for others who wish to investigate related questions.

4.1. Heegaard Splittings for Nonorientable Manifolds

We begin by recalling again the fundamental notion of a splitting of a 3-manifold into handlebodies. A *handlebody* is a three manifold with boundary containing pairwise disjoint properly embedded discs such that the manifold resulting from cutting along these discs is a 3-ball. A *Heegaard splitting* of a closed 3-manifold is a decomposition into two handlebodies which are identified along their boundary. As is well known, closed, orientable 3-manifolds admit Heegaard splittings:

Lemma 4.1.1. *Every closed, connected, orientable 3-manifold Y admits a Heegaard splitting $Y = H_1 \cup_\Sigma H_2$.*

We note that this notion need not be restricted to the orientable case, and indeed the same lemma holds in the nonorientable context:

Lemma 4.1.2. *Every closed, connected, nonorientable 3-manifold M admits a Heegaard splitting $M = H_1 \cup_\Sigma H_2$ into (possibly nonorientable) handlebodies H_1, H_2.*

Proof. The two lemmas can be proved simultaneously. In the smooth category, choose any self indexing Morse function $f : M \to \mathbb{R}$. It then follows from standard results in Morse theory that $M = f^{-1}[0, 3/2] \cup_{f^{-1}(3/2)} f^{-}[3/2, 3]$, and that $H_1 = f^{-1}[0, 3/2]$ and $H_2 = f^{-1}[3/2, 3]$ are handlebodies (See e.g. [30]).

Alternatively, in the PL category, consider a regular neighborhood of the 1-skeleton $M^1 \hookrightarrow M$. This is a handlebody. Now observe that the complement of the closure of the neighborhood has a collection of disks (given by the interiors of the 2 dimensional faces), such that cutting along the disks yields a disjoint collection of balls. This implies the complement is a handlebody (See e.g. [10]). □

Notation 4.1.3. Throughout this chapter, Y will always denote an orientable 3-manifold, while we will use M to denote a 3-manifold which is not necessarily orientable.

Lemma 4.1.4. *Let M be a 3-manifold, and $\alpha \in H_2(M; \mathbb{Z}/2\mathbb{Z})$ a nonzero homology class. Then α can be represented by a closed, connected, embedded surface $i : K \hookrightarrow M$.*

Proof. Consider the Poincare dual of α, $P.D.(\alpha) \in H^1(M; \mathbb{Z}/2\mathbb{Z}) \cong [M, \mathbb{R}P^\infty]$. Let $f : M \to \mathbb{R}P^4$ be a smooth map in this homotopy class which

is transverse to the submanifold $j : \mathbb{R}P^3 \hookrightarrow \mathbb{R}P^4$. Let $K = f^{-1}(\mathbb{R}P^3)$. After attaching tubes along arcs connecting the various components, we obtain a homologous connected representative (note here that this operation is always a homology over $\mathbb{Z}/2\mathbb{Z}$). □

We now investigate the normal bundles of such representatives.

Definition 4.1.5. We will say a smoothly embedded surface $S \hookrightarrow M$ is *locally one sided* if its normal bundle $N_{S\hookrightarrow M}$ is nontrivial, and that it is *locally two sided* otherwise. We will say the surface is *nonseparating* if $M \setminus S$ is connected, and that it is *separating* otherwise.

Lemma 4.1.6. *Let M be a closed, non-orientable, connected 3 manifold, and $\alpha = P.D.(w_1(TM)) \in H_2(M; \mathbb{Z}/2\mathbb{Z})$. Then α has a connected, embedded, nonseparating representative S if and only if it has a connected, embedded representative K for which $w_1(TM)|_K \neq 0$.*

Proof. Let K be a connected, embedded representative for α. If $w_1(TM)|_K \neq 0$, there exists a class $[\gamma] \in H_1(K)$ satisfying $\langle w_1(TM), [\gamma]\rangle = [\gamma] \cdot [K] = 1 \in \mathbb{Z}/2\mathbb{Z}$. Thus there is a representative loop γ in K, and a generic pushoff $\tilde{\gamma}$ of γ in M, so that $\tilde{\gamma}$ intersects K an odd number of times transversely.

Do surgery on K by attaching a tube along an arc of $\tilde{\gamma}$ whose interior misses K. This produces a new surface K' with $[K] = [K']$, and $|K \cap \tilde{\gamma}|$ reduced by 2. Repeating this procedure, one obtains a surface K'' homologous to K which intersects the closed loop $\tilde{\gamma}$ exactly once. This shows K'' is nonseparating. See Figure 27 for a depiction of this process.

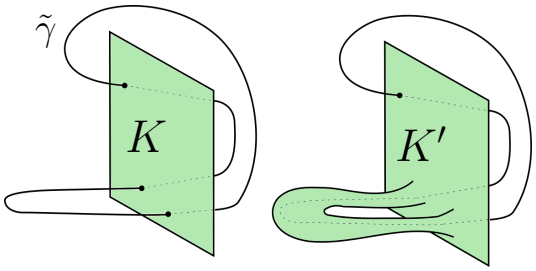

FIGURE 27 Performing surgery on K along an arc in the curve $\tilde{\gamma}$ to reduce geometric intersection.

Suppose S is a connected, embedded representative for α which is nonseparating.

1. If S is locally one sided, then the normal bundle $N_{S\hookrightarrow M}$ is nontrivial. So there is a loop γ in S which has a generic pushoff which intersects S an odd number of times geometrically. Thus $\langle w_1(TM), [\gamma]\rangle = [\gamma] \cdot [S] = 1$, so $w_1(TM)|_S \neq 0$.

2. If S is locally two sided, then $w_1(N_{S\hookrightarrow M}) = 0$, so $w_1(TS) = w_1(TM)|_S$. Thus if S is non-orientable, $w_1(TM)|_S \neq 0$ and we are done. If S is nonseparating, locally two sided, and orientable, choose a path γ from one side of S to the other, and attach a tube along γ to obtain S' homologous to S which is nonseparating, locally one sided, and nonorientable. See Figure 28 for a depiction of this process. Then $w_1(TM)|_{S'} \neq 0$ by step (1).

□

Lemma 4.1.7. *Let M be a closed, connected, nonorientable 3 manifold, and $\alpha = P.D.(w_1(TM)) \in H_2(M; \mathbb{Z}/2\mathbb{Z})$. Then α has an embedded, nonorientable, and nonseparating representative.*

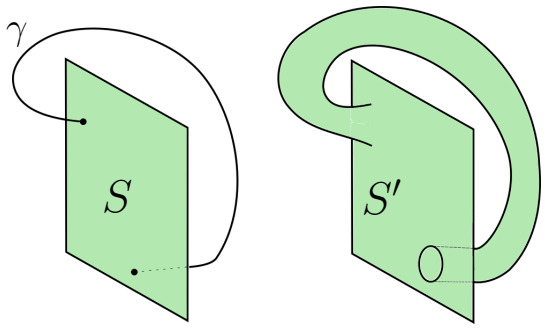

FIGURE 28 Performing surgery on S along the curve γ to produce a locally one-sided, nonrientable, homologous surface.

Proof. Suppose every closed, embedded representative for α is separating. Fix a closed embedded representative K for α, which is possible by Lemma 4.1.4.

Let $\nu(K)$ be a tubular neighborhood of K, and consider the Mayer Vietoris sequence for $M = \overline{\nu(K)} \cup (M \setminus \nu(K))$. Since K is separating, $\overline{\nu(K)} \cap (M \setminus \nu(K)) \cong K \amalg K$. We also note that the map

$$H^0(K) \oplus H^0(M \setminus K) \to H^0(K \amalg K)$$

appearing in the Mayer Vietoris sequence is surjective, since k is separating. One then has:

$$0 \to H^1(M) \to H^1(K) \oplus H^1(M \setminus K) \to H^1(K \amalg K)$$

By Lemma 4.1.6, K must satisfy $w_1(TM)|_K = 0$. By definition of K, $w_1(TM)|_{M \setminus K} = 0$. Thus $w_1(TM) = 0$ by exactness, contradicting nonorientability of M. This shows α has a closed, embedded, nonseparating representative.

If this representative is orientable, add a tube as in the proof of the last part of Lemma 4.1.6 to obtain a surface K' representing α; this is now closed, embedded, non orientable, and nonseparating. □

Using the previously established facts, we will now prove the existence of certain "equivariant" Heegaard splittings for orientation double covers. This line of thought follows ideas presented in [31], where Rubinstein constructs one sided Heegaard splittings of orientable 3-manifolds.

Theorem 4.1.8. *Given a closed, nonorientable 3-manifold M, there is a Heegaard splitting of the orientation double cover $\widetilde{M} = H_1 \cup H_2$ such that the nontrivial deck transformation $\tau : \widetilde{M} \to \widetilde{M}$ exchanges the handlebodies. i.e. $\tau(H_1) = H_2$, $\tau(H_2) = H_1$.*

Proof. Fix a closed, nonseparating, non orientable representative K for the class $\alpha = P.D.(w_1(TM)) \in H_2(M; \mathbb{Z}/2\mathbb{Z})$. Such a representative exists by Lemma 4.1.7. Let $p : \widetilde{M} \to M$ be the orientation double cover. The preimage of K in the orientation double cover, $\widetilde{K} = p^{-1}(K) \hookrightarrow \widetilde{M}$, is an orientable surface preserved by τ.

We claim that the surface $\widetilde{K}$ is separating in $\widetilde{M}$. To see this, consider τ-translates $\widetilde{q}$ and $\tau(\widetilde{q})$ in $\widetilde{M} \setminus \widetilde{K}$, and let γ be a path from $\widetilde{q}$ to $\tau(\widetilde{q})$ transverse to $\widetilde{K}$. Then $p(\gamma)$ is a loop in M based at $q = p(\widetilde{q})$. Furthermore, since this loop lifts to a path, it is an orientation reversing loop and therefore must satisfy $[K] \cdot [p(\gamma)] \neq 0$. In particular, $K \cap p(\gamma)$ is non-empty. Thus there exist points $l \in \gamma$ and $l' \in \widetilde{K}$ such that $p(l) = p(l')$. Since $\widetilde{K}$ is preserved by τ, this implies $\gamma \cap \widetilde{K}$ is non-empty. Hence $\widetilde{M} \setminus \widetilde{K}$ is not path connected, and $\widetilde{K}$ is separating. To summarize, the lift $\widetilde{K}$ is a separating,

orientable, surface in $\widetilde{M}$ which is preseved by τ. Note that this argument also shows that if H_1 and H_2 are the closures of the components of $\widetilde{M} \setminus \widetilde{K}$, with $\widetilde{M} = H_1 \cup_{\widetilde{K}} H_2$, then $\tau(H_1) = H_2$.

We will now alter the decomposition $\widetilde{M} = H_1 \cup_{\widetilde{K}} H_2$ so that it becomes a Heegaard splitting while remaining τ-equivariant. Fix a Morse function $f_1 : H_1 \to \mathbb{R}$ which has a unique index 0 critical point, no index 3 critical points, and which has $\partial H_1 = \widetilde{K}$ as a level set (corresponding the to the largest regular value with a nonempty level set). This is possible by standard results in Morse theory (see e.g. [32]). The interior of H_1 will contain a single index 0 critical point, and some number of index 1 and index 2 critical points. Consider the ascending manifolds of the index 2 critical points. These intersect the boundary $\partial H_1 = \widetilde{K}$ in some collection of points $P = \{p_i\} \subset \widetilde{K}$. By performing a suitable perturbation of f_1 if necessary, we may assume $P \cap \tau(P) = \emptyset$. Use a suitable translate of f_1 to define a Morse function $f : \widetilde{M} \to \mathbb{R}$ by using (a suitable translate of) f_1 to define f on H_1, and then enforcing $f(x) = -f(\tau(x))$ for all $x \in \widetilde{M}$. Then f will have a unique index 3 critical point, as well as some number of index 1 and 2 critical points in the interior of H_2. The descending manifolds of the index 1 critical points in H_2 will intersect $\widetilde{K}$ in the collection of points $\tau(P)$. A schematic illustrating this situation is depicted in Figure 29.

Now consider small open tubular neighborhoods $N(A)$ and $N(B)$ of these ascending and descending manifolds respectively, with $N(B) = \tau(N(A))$. Since $P \cap \tau(P) = \emptyset$, we may arrange for these neighborhoods to satisfy $N(A) \cap N(B) = \emptyset$. Let $H_1' = (H_1 \setminus N(A)) \cup \overline{N(B)}$ and $H_2' = (H_2 \setminus N(B)) \cup \overline{N(A)}$. These are both handlebodies, as the restriction

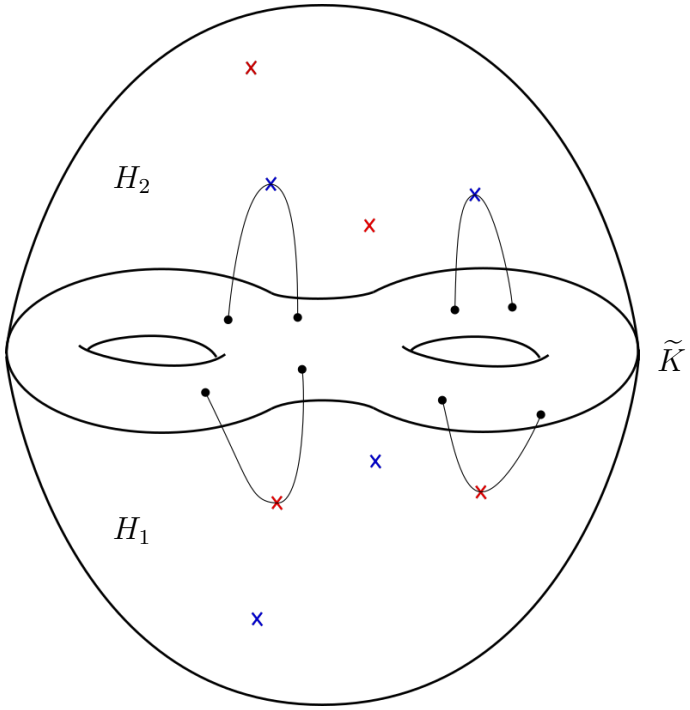

FIGURE 29 A schematic of the decomposition $\widetilde{M} = H_1 \cup_{\widetilde{K}} H_2$ with a Morse function. Index 1 critical points are labeled with blue crosses, while index 2 critical points are labeled with red crosses. Some ascending and descending manifolds are drawn.

of f to these spaces is either a Morse function with only index 0 and index 1 critical points, or a Morse function with only index 3 and 2 critical points. Furthermore, $\widetilde{M} = H_1' \cup_{\partial H_1' = \partial H_2'} H_2'$ and $\tau(H_1') = H_2'$ by construction. (A depiction of this alteration of the decomposition $\widetilde{M} = H_1 \cup_{\widetilde{K}} H_2$ is depicted in Figure 30.) This completes the proof.

□

Given an orientation double cover $\widetilde{M} \to M$, we will call a Heegaard splitting $\widetilde{M} = H_1 \cup_\Sigma H_2$ satisfying the property in Theorem 4.1.8 an *equivariant Heegaard splitting (EHS) of* $\widetilde{M}$. We note that an EHS gives rise to a Heegaard diagram which respects the action by τ:

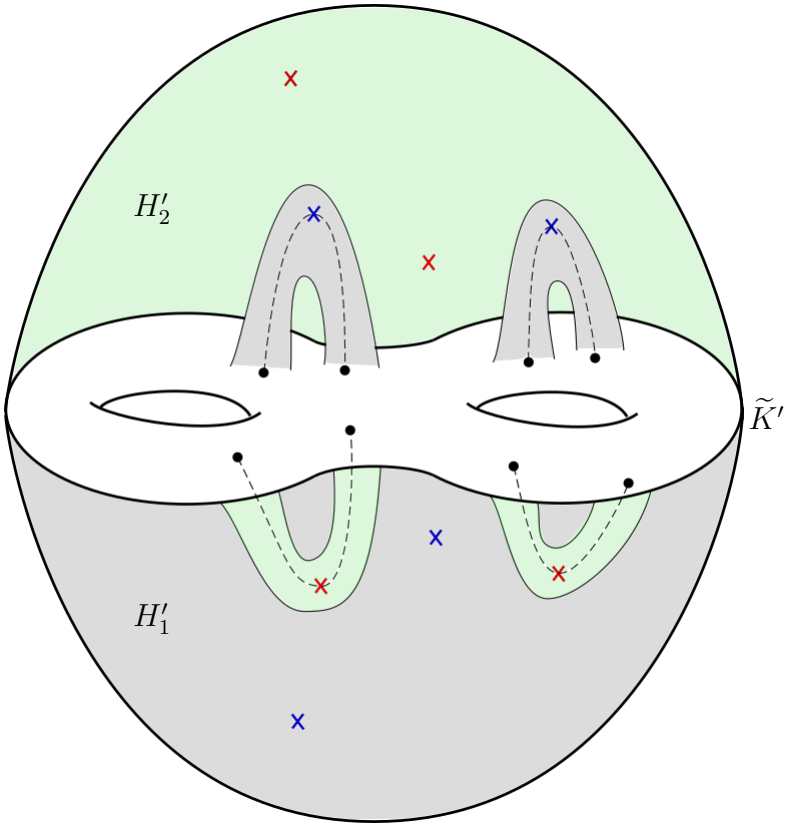

FIGURE 30 An alteration of the decomposition from Figure 29 into a Heegaard splitting $\widetilde{M} = H_1' \cup_{\widetilde{K}'} H_2'$. The handlebody H_1' is depicted in gray and the handlebody H_2' is depicted in green.

Corollary 4.1.9. *A closed, orientable 3-manifold Y which is an orientation double cover admits a* τ-equivariant Heegard diagram*: that is, a Heegaard diagram $(\Sigma, \boldsymbol{\alpha}, \boldsymbol{\beta})$ satisfying $\tau(\boldsymbol{\alpha}) = \boldsymbol{\beta}$.*

We now provide some examples of equivariant Heegaard splittings.

Example 4.1.10. Consider the orientation double cover $p : S^1 \times S^2 \to S^1 \times \mathbb{R}P^2$. We construct a EHS of $S^1 \times S^2$ corresponding to this cover. The class $\alpha := \text{P.D.}(w_1(T(S^1 \times \mathbb{R}P^2))) \in H_2(S^1 \times \mathbb{R}P^2)$ is nonzero. We note that representatives for this class can be identified in practice in several ways, such as:

1. By work of Halperin and Toledo [33], if one considers the union of all two simplices in the 1st barycentric subdivision of any triangulation of $S^1 \times \mathbb{R}P^2$, this chain represents α.

2. Any 2-cycle S satisfying $[S] \cdot [\gamma] = 0 \in \mathbb{Z}/2\mathbb{Z}$ for all orientation preserving loops γ, and $[S] \cdot [\delta] = 1 \in \mathbb{Z}/2\mathbb{Z}$ for all orientation reversing loops δ, represents α.

Using the second characterization, we construct an embedded representative for α as follows. Let us represent $S^1 \times \mathbb{R}P^2$ as

$$(S^1 \times D)/\sim$$

where $(x, e^{i\theta}) \sim (x, e^{i(\theta+\pi)})$ for $(x, e^{i\theta}), (x, e^{i(\theta+\pi)}) \in S^1 \times \partial D$. Consider the subspace defined by

$$K = \{(e^{i\theta}, re^{i\theta/2}) | r \in [-1, 1], \theta \in [0, 2\pi]\}.$$

We illustrate a schematic for our model of $S^1 \times \mathbb{R}P^2$ as well as the subspace K in Figure 31.

Note that K is an embedded submanifold, is nonseparating, and satisfies the second characterization of the class α. Thus K is an embedded, nonseparating representative for α. It is not difficult to see that K is nonorientable.

To finish constructing a EHS for $S^1 \times S^2$ corresponding to this cover, we lift K to the orientation double cover, and make alterations to the lift as in the proof of Theorem 4.1.8 if necessary. In fact, K lifts to a torus T

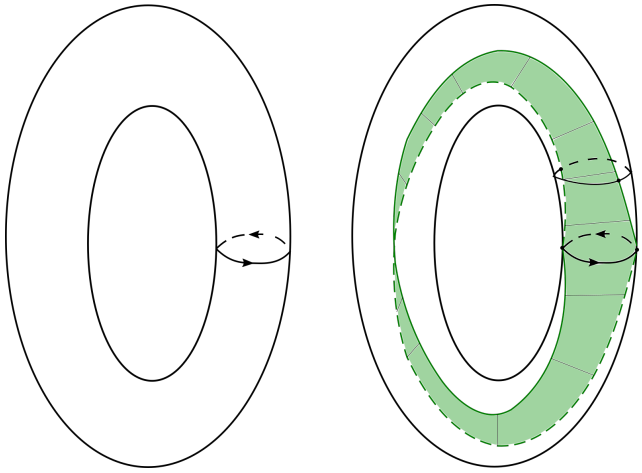

FIGURE 31 On the left is a schematic for $S^1 \times D$. Quotienting $\{p\} \times \partial D$ by the antipodal map for all p in S^1 yields $S^1 \times \mathbb{R}P^2$. On the right, the subspace K is illustrated. It represents the Poincare dual of the first Stiefel-Whitney class in $S^1 \times \mathbb{R}P^2$.

in $S^1 \times S^2$, and the the complement can be seen to consist of the union of two handlebodies. Thus no alterations are necessary. One can check that a resulting τ-equivariant Heegaard diagram coming from this splitting is that given in Figure 32. The action of τ on this diagram is realized as rotation by π in the vertical direction.

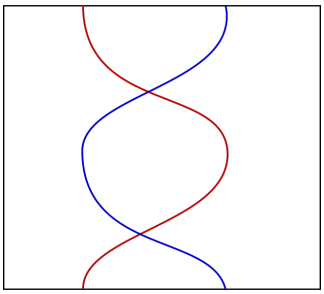

FIGURE 32 An equivariant diagram for $S^1 \times S^2$ corresponding to the orientation double cover over $S^1 \times \mathbb{R}P^2$. The sides of the square should be identified to produce a torus as the Heegaard surface.

Example 4.1.11. Consider the orientation double cover $p : S^1 \times S^1 \times S^1 \to S^1 \times K$ where K is the Klein bottle. We construct a EHS of $S^1 \times$

$S^1 \times S^1$ corresponding to this cover. First, we construct a closed, embedded representative $S \to S^1 \times K$ for the homology class $P.D.(w_1(T(S^1 \times K)) \in H_2(S^1 \times K, \mathbb{F}_2)$. In Figure 33 we depict $S^1 \times K$ as a quotient of a solid cube. An orientation reversing loop γ is depicted in the identification space, and an embedded surface S homeomorphic to $S^1 \times S^1$ is depicted. One can verify that S represents $\alpha := \text{P.D.}(w_1(T(S^1 \times K)))$. As a particular consequence, we have $[S] \cdot [\gamma] = 1$. The surface S is an embedded, orientable,

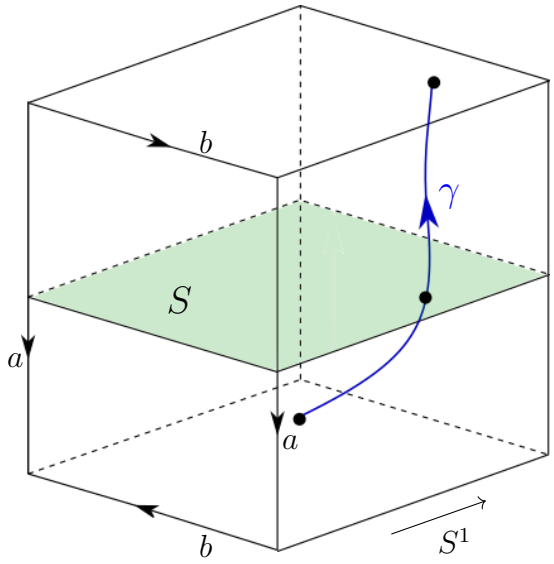

FIGURE 33 A model for $S^1 \times K$. The embedded surface S is a torus representing the Poincare dual of the first Stiefel-Whitney class. It has odd algebraic intersection with every orientation reversing loop in $S^1 \times K$, and in particular with γ.

nonseparating surface representing α. We alter the surface by a homology to obtain a new surface S' which is an embedded, nonorientable, nonseparating surface representing α, as in the last step of the proof of Lemma 4.1.7. A depiction of this altered surface is illustrated in Figure 34.

To finish constructing a EHS for $S^1 \times S^1 \times S^1$ corresponding to this cover, we lift S' to the orientation double cover, and make alterations to the

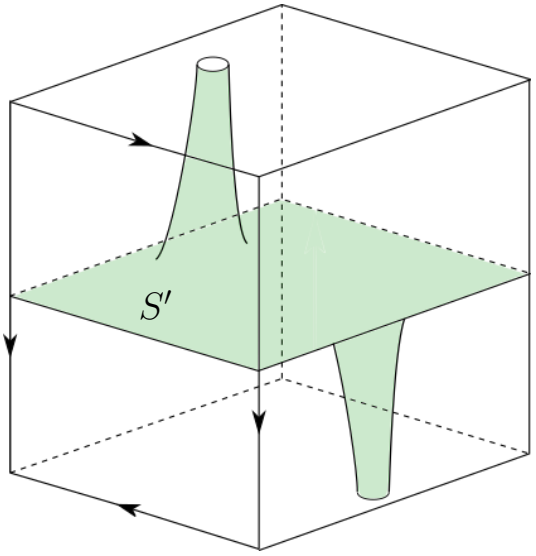

FIGURE 34 The result of performing surgery on S to obtain a homologous surface S' which is nonorientable.

lift as in the proof of Theorem 4.1.8 if necessary. In this case the covering map is easy to understand via understanding of the double cover of the Klein bottle by the torus. We depict an illustration of a quotient of a solid cube representing $S^1 \times S^1 \times S^1$, as well as a lift of the surface S' to this space, in Figure 35.

The nontrivial deck translation τ in this schematic is given by vertical translation through half the cube and reflection in a vertical plane which divides the front (labeled) face and the opposite face in half. In this case, we see that the lift $\widetilde{S}'$ is already τ equivariant, and its complement consists of two handlebodies. We have thus constructed a EHS. Finally, we note that one can use this EHS to construct a τ-equivariant diagram for $S^1 \times S^1 \times S^1$. For example, one such diagram is depicted in Figure 36.

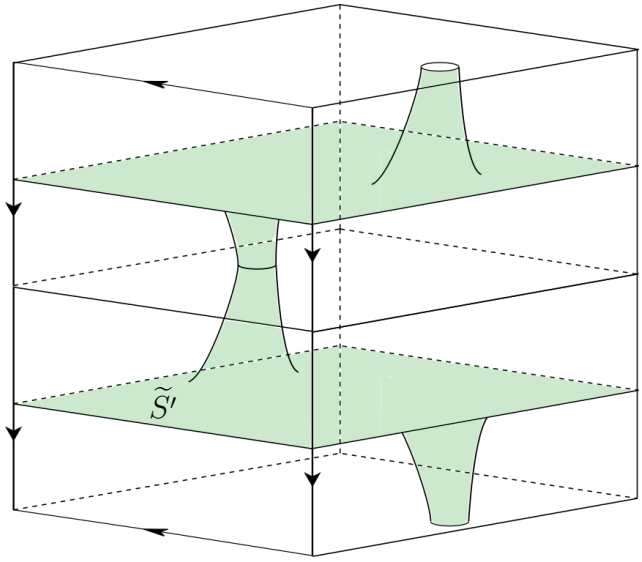

FIGURE 35 A schematic for $S^1 \times S^1 \times S^1$ with the lift $\widetilde{S}'$ of the surface S' from Figure 34.

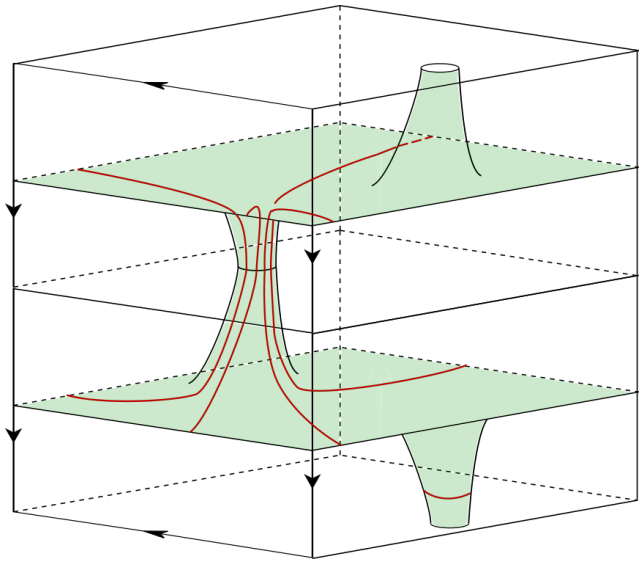

FIGURE 36 A collection of closed curves $\boldsymbol{\alpha} = (\alpha_1, \alpha_2, \alpha_3)$ on the Heegaard surface from Figure 35 which bound disks in one of the handlebodies. Applying τ to the collection would yield a collection $\boldsymbol{\beta}$ bounding disks in the other handlebody, and in this way the the figure depicts a Heegaard diagram.

4.2. A Pairing on Heegaard Floer Homology

In this section we consider the Heegaard Floer invariants $\widehat{HF}(Y)$ of orientation double covers Y. We work throughout this section over $\mathbb{F}_2$ unless otherwise stated.

Given a nonorientable 3-manifold M, we consider the orientation double cover $Y \to M$, and fix some basepoint $p \in Y$. The cover comes equipped with an orientation reversing involution

$$\tau : (Y, p) \xrightarrow{\sim} (-Y, q).$$

By work of Juhász, Thurston and Zemke, this diffeomorphism induces a map on Heegaard Floer homology:

Theorem 4.2.1. *[3, Theorem 1.5] There is a natural isomorphism $\tau_* : \widehat{HF}(Y, p) \xrightarrow{\sim} \widehat{HF}(-Y, q)$ associated to the diffeomorphism τ.*

Since the diffeomorphism reverses the orientation on Y, the induced map lands in the Floer homology of $-Y$. However, as investigated by Ozsvàth and Szabò, there is a chain isomorphism which can be used to identify this Floer homology with the Floer cohomology of Y.

Lemma 4.2.2. *[7] Given a Heegaard diagram $\mathcal{H} = (\Sigma, \boldsymbol{\alpha}, \boldsymbol{\beta}, p)$ for (Y, p), let $-\mathcal{H} = (-\Sigma, \boldsymbol{\alpha}, \boldsymbol{\beta}, p)$ be the same diagram with the orientation on the Heegaard surface reversed, representing $(-Y, p)$. There is a chain isomorphism*

$$\Phi_{rev} : \widehat{CF}_*(-\mathcal{H}) \xrightarrow{\sim} \widehat{CF}^*(\mathcal{H}).$$

Thus there is an induced isomorphism

$$\Phi_{rev} : \widehat{HF}_*(-Y, p) \xrightarrow{\sim} \widehat{HF}^*(Y, p).$$

By the universal coefficient theorem, we also have:

Lemma 4.2.3. *There is an isomorphism* $\Psi : \widehat{HF}^*(Y,p) \xrightarrow{\sim} Hom_{\mathbb{Z}/2\mathbb{Z}}(\widehat{HF}_*(Y,p), \mathbb{Z}/2\mathbb{Z})$.

We will now use Lemmas 4.2.1, 4.2.2 and 4.2.3 to define a pairing on the Floer homology of an orientation double cover.

Definition 4.2.4. Let M be a nonorientable 3-manifold, Y it's orientation double cover, and τ the nontrivial deck translation of Y. Fix a basepoint $p \in Y$, and let $q = \tau(p)$. We write

$$P_\tau : \widehat{HF}_*(Y,p;\mathbb{Z}/2\mathbb{Z}) \times \widehat{HF}_*(Y,q;\mathbb{Z}/2\mathbb{Z}) \to \mathbb{Z}/2\mathbb{Z} \tag{4.1}$$

for the $\mathbb{Z}/2\mathbb{Z}$ bilinear pairing given by $P_\tau(x,y) = (\Psi \circ \Phi_{rev} \circ \tau_*(x))(y)$. We will interchangeably use the notation $\langle , \rangle_\tau$ for the pairing.

Remark 4.2.5.

1. While our main interest thus far has been in orientation double covers, the pairings above are defined for any closed, orientable manifold Y with an orientation reversing, involutive diffeomorphism $\tau : Y \to -Y$.

2. If Y is a closed, orientable manifold with an orientation preserving, involutive diffeomorphism $\psi : Y \to Y$, the formula above yields the more familiar trace pairing studied in [34] (with a twist coming from a basepoint moving map):

$$P_\tau : \widehat{HF}_*(Y,p;\mathbb{Z}/2\mathbb{Z}) \times \widehat{HF}_*(-Y,q;\mathbb{Z}/2\mathbb{Z}) \to \mathbb{Z}/2\mathbb{Z}.$$

3. We can use a path γ from p to q, and the corresponding basepoint moving isomorphism:

$$\gamma_{\#} : \widehat{HF}_*(Y, p; \mathbb{Z}/2\mathbb{Z}) \xrightarrow{\sim} \widehat{HF}_*(Y, q; \mathbb{Z}/2\mathbb{Z})$$

to turn the pairing in Equation (4.1) into a bilinear form

$$P_{\tau,\gamma} : \widehat{HF}_*(Y, p; \mathbb{Z}/2\mathbb{Z}) \times \widehat{HF}_*(Y, p; \mathbb{Z}/2\mathbb{Z}) \to \mathbb{Z}/2\mathbb{Z}.$$

Explicitly, one has the bilinear form:

$$P_{\tau,\gamma}(x, y) := P_\tau(x, \gamma_{\#} y).$$

4. By Corollary 4.1.9, we can always find a diagram $\mathcal{H}$ so that $\mathcal{H} = -\tau(\mathcal{H})$.

We say a bilinear pairing $\phi : A \times B \to R$ is *nondegenerate* if the resulting maps $A \to \mathrm{Hom}_R(B, R)$ and $B \to \mathrm{Hom}_R(A, R)$ are isomorphisms.

Lemma 4.2.6. *P_τ and $P_{\tau,\gamma}$ are non-degenerate*

Proof. This is immediate from the definitions of the pairings, as all maps involved are isomorphisms. □

Lemma 4.2.7. *Let P_τ be as above, and*

$$\widetilde{P}_\tau : \widehat{HF}_*(Y, p; \mathbb{Z}/2\mathbb{Z}) \times \widehat{HF}_*(Y, q; \mathbb{Z}/2\mathbb{Z}) \to \mathbb{Z}/2\mathbb{Z}$$

be the pairing obtained from reversing the roles of the factors. That is,

$$\widetilde{P}_\tau(x, y) := (\Psi \circ \phi_{rev} \circ \tau_*^{-1})(y)[x]$$

where $\tau_*^{-1} : \widehat{HF}_*(Y,q;\mathbb{Z}/2\mathbb{Z}) \to \widehat{HF}_*(-Y,p;\mathbb{Z}/2\mathbb{Z})$ *and* $\phi_{rev} : \widehat{HF}_*(-Y,p;\mathbb{Z}/2\mathbb{Z}) \to \widehat{HF}^*(Y,p;\mathbb{Z}/2\mathbb{Z})$.

Then

$$P_\tau(x,y) = \widetilde{P}_\tau(x,y).$$

Proof. The map $\Psi \circ \phi_{rev} \circ \tau_*^{-1}$ appearing in the definition of $\widetilde{P}_\tau$ is in fact the dual of the map appearing in the definition of P_τ,

$$\Psi \circ \phi_{rev} \circ \tau_*^{-1} = (\Psi \circ \phi_{rev} \circ \tau_*)^\vee.$$

This is a straightforward consequence of the fact that $\tau^2 = \mathrm{id}$, and the result follows. □

In some cases the bilinear form $P_{\tau,\gamma}$ is a symmetric. We now investigate when this can occur by studying the effect of certain basepoint moving maps on Floer homology.

Lemma 4.2.8. *Let* γ *be an embedded path from* p *to* q. *Then* $\tau_* \circ \gamma_\# = \tau(\gamma)_\# \circ \tau_*$, *i.e. the following diagram commutes:*

$$\begin{array}{ccc} \widehat{HF}(Y,p) & \xrightarrow{\tau_*} & \widehat{HF}(-Y,q) \\ \downarrow{\scriptstyle \gamma_\#} & & \downarrow{\scriptstyle \tau(\gamma)_\#} \\ \widehat{HF}(Y,q) & \xrightarrow{\tau_*} & \widehat{HF}(-Y,p) \end{array}$$

Proof. This follows from consideration of the graph cobordism functors defined in [5]. There Zemke showed that there are functors which naturally associate to an equivalence class of graph coborism (W,Γ) from a multi-

based 3-manifold $(Y, \vec{p})$ to a multibased 3-manofld $(Y', \vec{p}')$ a map

$$F_{(W,\Gamma)} : \widehat{HF}_*(Y, \vec{p}) \to \widehat{HF}_*(Y', \vec{p}')$$

One can describe $\tau_* \circ \gamma_\#$ and $\tau(\gamma)_\# \circ \tau_*$ as the images under the functor of the two graph cobordisms depicted in Figure 37.

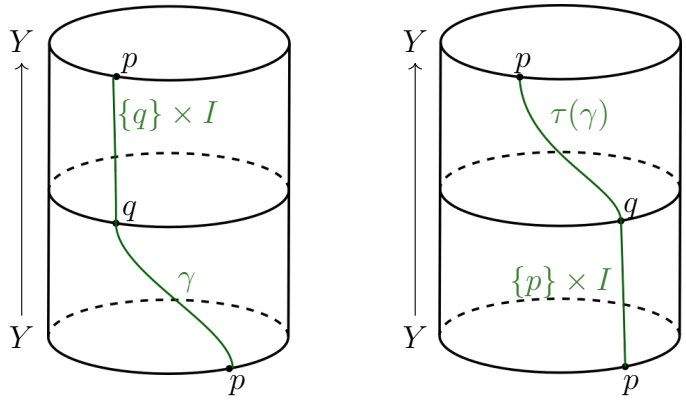

FIGURE 37 A schematic for the graph cobordisms (W_1, Γ_1) and (W_2, Γ_2).

Here the graph cobordism (W_1, Γ_1) yielding the map $\tau_* \circ \gamma_\#$ has underlying 4-manifold given by concatenating the product cobordism $Y \times I$ to the mapping cylinder Cylinder(τ) of the diffeomorphism τ, while the graph cobordism (W_2, Γ_2) yielding the map $\tau_* \circ \gamma_\#$ has underlying 4-manifold given by concatenating the mapping cylinder Cylinder(τ) to the product cobordism $-Y \times I$. The graph Γ_1 is obtained by concatenating γ and $\{q\} \times I \subset$ Cylinder(τ), and the graph Γ_2 is obtained by concatenating $\{p\} \times I \subset$ Cylinder(τ) and $\tau(\gamma)$.

These graph cobordisms are in fact equivalent in the sense of [5], hence induce the same maps on Floer homology. □

Consider now the embedded curve $\gamma \cdot \tau(\gamma)$, and consider $(\gamma \cdot \tau(\gamma))_*$, the map given by the $\pi_1(Y,p)$ action on $\widehat{HF}_*(Y,p;\mathbb{Z}/2\mathbb{Z})$. In what follows we write $(\gamma_\#)^\vee$ for the map dual to the basepoint moving map $\gamma_\#$,

$$(\gamma_\#)^\vee : \mathrm{Hom}_{\mathbb{Z}/2\mathbb{Z}}(\widehat{HF}_*(Y,q),\mathbb{Z}/2\mathbb{Z}) \to \mathrm{Hom}_{\mathbb{Z}/2\mathbb{Z}}(\widehat{HF}_*(Y,p),\mathbb{Z}/2\mathbb{Z}).$$

Corollary 4.2.9. *If $(\gamma \cdot \tau(\gamma))_* = 1$, then $P_{\tau,\gamma}$ is symmetric.*

Proof. We have $(\gamma \cdot \tau(\gamma))_* = \gamma_\# \circ \tau(\gamma)_\# = 1$, so $\tau(\gamma)_\# = \gamma_\#^{-1}$. We compute:

$$\begin{aligned}
P_{\tau,\gamma}(x,y) &= P_\tau(x,\gamma_\# y) \\
&= (\Psi \circ \Phi_{rev} \circ \tau_*(x))[\gamma_\# y] \\
&= ((\gamma_\#)^\vee \circ \Psi \circ \Phi_{rev} \circ \tau_*(x))[y] \\
&= (\Psi \circ \Phi_{rev} \circ \gamma_\#^{-1} \circ \tau_*(x))[y] \text{ (by Lemma 4.3.12)} \\
&= (\Psi \circ \Phi_{rev} \circ \tau(\gamma)_\# \circ \tau_*(x))[y] \\
&= (\Psi \circ \Phi_{rev} \circ \tau_* \circ \gamma_\#(x))[y] \text{ (by Lemma 4.2.8)} \\
&= \widetilde{P}_\tau(y,\gamma_\# x) \\
&= P_\tau(y,\gamma_\# x) \text{ (by Lemma 4.2.7)} \\
&= P_{\tau,\gamma}(y,x)
\end{aligned}$$

Here we have used commutativity of a certain diagram involving $\Psi \circ \Phi_{\mathrm{rev}}$ and the basepoint moving maps in the fourth equality. This commutativity will follow from the proof of Lemma 4.3.12 appearing in the next section, but we postpone a disussion of that proof, as it will take us too far astray from our

current goals. We invite the interested reader to skip ahead and investigate the relevant square. □

In [5], the author establishes a formula which can be used to compute the $\pi_1(Y,p)$ action on $\widehat{HF}_*(Y,p;\mathbb{Z}/2\mathbb{Z})$. For a strongly admissible Heegaard diagram, the infinity version of the Heegaard Floer complex associated to a 3-manifold Y is a $\mathbb{Z}/2\mathbb{Z}[U,U^{-1}]$-module, whose differential ∂^∞ can be decomposed as

$$\partial^\infty = \partial + \partial_1 U + \partial_2 U^2 + \dots.$$

The map ∂_1 induces a map on $\widehat{HF}(Y,p)$ which we denote by $(\partial_1)_*$ in what follows. For more details about this map and relevant context, see [5].

Theorem 4.2.10. *[5] If $\delta \in \pi_1(Y,p)$ is an embedded curve, δ_* denotes the π_1 action on $\widehat{HF}_*(Y,p;\mathbb{Z}/2\mathbb{Z})$, $[\delta]$ denotes the $\Lambda(H_1(Y)/Tors)$ action on $\widehat{HF}_*(Y,p;\mathbb{Z}/2\mathbb{Z})$, and $(\partial_1)_*$ denotes the map induced by ∂^∞ on $\widehat{HF}_*(Y,p;\mathbb{Z}/2\mathbb{Z})$, then*

$$\delta_* = 1 + (\partial_1)_*[\delta] = 1 + [\delta](\partial_1)_*.$$

We have thus far been unable to characterize nonorientable 3-manifolds with orientation double covers which admit a symmetric form $P_{\tau,\gamma}$. However Corollary 4.2.9 coupled with Theorem 4.2.10 yields two cases in which the form will be symmetric on an orientation double cover Y. We will see that there exists an embedded curve γ from p to q for which $P_{\tau,\gamma}$ is symmetric if either:

1. $(\partial_1)_* = 0$ on $\widehat{HF}(Y,p)$

or

2. There is a curve γ from p to q such that $[\gamma \cdot \tau(\gamma)] \in \mathrm{Tors}(H_1(Y;\mathbb{Z}))$.

The fact that these criteria yield a symmetric form is immediate from Corollary 4.2.9 and Theorem 4.2.10. We explain the second criterion as a condition on the nonorientable manifold M in the next lemma.

Lemma 4.2.11. *Let M be a nonorientable 3-manifold. Given a class $\bar{\gamma} \in$ Tors$(H_1(M;\mathbb{Z}))$ with $w_1(M)[\bar{\gamma}] \neq 0$, let γ be the unique lift of $\bar{\gamma}$ beginning at p. Then $P_{\tau,\gamma}$ is a symmetric bilinear form.*

Proof. Let $p : Y \to M$ be the orientation double cover, and $T : H_1(M;\mathbb{Z}) \to H_1(Y;\mathbb{Z})$ be the transfer map. If τ is the nontrivial deck transformation of p, we have $T(\bar{\gamma}) = [\gamma \cdot \tau(\gamma)]$, by definition of the transfer map. Since $\bar{\gamma}$ is torsion, so too is $T(\bar{\gamma}) = [\gamma \cdot \tau(\gamma)]$, and thus the latter acts by zero under the $\Lambda(H_1(Y)/\mathrm{Tors})$ action. By Theorem 4.2.10, the π_1 action is thus $(\gamma \circ \tau(\gamma))_* = 1$, so the result follows by Corollary 4.2.9. □

Example 4.2.12. Let $N_h \cong (\mathbb{R}P^2)^{\#h}$ be the closed, nonorientable surface of genus h. Then $H_1(S^1 \times N_h;\mathbb{Z}) \cong \mathbb{Z}^h \oplus \mathbb{Z}/2\mathbb{Z}$.

For $h = 1$, the torsion class is represented by an orientation reversing loop γ in $\mathbb{R}P^2$ which satisfies $w_1(S^1 \times \mathbb{R}P^2)[\gamma] = 1$. Lemma 4.2.11 thus yields that the Heegaard Floer homology of the orientation double cover $S^1 \times S^2$ with deck translation τ admits a symmetric bilinear form $P_{\tau,\gamma}$.

For $h = 2$, the torsion class in $H_1(S^1 \times N_h;\mathbb{Z})$ is not represented by an orientation reversing loop, so this construction fails.

We now seek to characterize the first criterion in a slightly different, perhaps more familiar, way. First, we note that $(\partial_1)_*$ can be interpreted as

arising from the long exact sequence relating the minus and hat variants of Heegaard Floer homology.

Lemma 4.2.13. *The map $(\partial_1)_*$ is given by the composite $f \circ g$ of the maps appearing in the exact sequence*

$$HF^-(Y,p) \xrightarrow{\cdot U} HF^-(Y,p) \xrightarrow{f} \widehat{HF}(Y,p) \overset{g}{\curvearrowleft}$$

Proof Sketch. This follows from a straightforward application of the snake lemma, and the definition of ∂^∞. We leave the details to the reader. □

In the next two lemmas, we use the previous lemma to provide two characterizations of the kernel of $(\partial_1)_* = f \circ g$.

Lemma 4.2.14. *The composition $f \circ g$ is identically zero if and only if there are no height one towers (i.e. summands of the form $\mathbb{F}_2[U]/(U)\langle \boldsymbol{x} \rangle$) in $HF^-(Y,p)$.*

Proof. For a fixed Spin^c-structure we have

$$HF^- \cong \mathbb{F}_2[U]^{\oplus n} \oplus \mathbb{F}_2[U]/(U)^{\oplus n_1} \oplus \left(\bigoplus_{k>1} \mathbb{F}_2[U]/(U^k)^{\oplus n_k} \right).$$

By exactness $\ker(f) = \mathrm{im}(\cdot U)$, so $f \circ g = 0$ if and only if $\mathrm{im}(g) \subset \mathrm{im}(\cdot U)$. Analysis of the snake lemma shows that im(g) is precisely the bottom of all finite towers. Thus $f \circ g = 0$ if and only if there are no height one towers.

□

Consider the short exact sequence of $\mathbb{F}_2[U]$-modules given by

$$0 \to \mathbb{F}_2 \to \mathbb{F}_2[U]/(U^2) \to \mathbb{F}_2 \to 0$$

where the first map is $(1 \mapsto U)$, the second map takes $(1 \mapsto 1)$ and $(U \mapsto 0)$, and $\mathbb{F}_2$ is considered as the $\mathbb{F}_2[U]$-module where U acts by zero. Tensoring over $\mathbb{F}_2[U]$ with CF^- yields a short exact sequence

$$0 \to CF^- \otimes_{\mathbb{F}_2[U]} \mathbb{F}_2 \to CF^- \otimes_{\mathbb{F}_2[U]} \mathbb{F}_2[U]/(U^2) \to CF^- \otimes_{\mathbb{F}_2[U]} \mathbb{F}_2 \to 0$$

which can be easily seen to be equivalent to

$$0 \to \widehat{CF} \to CF^-/(U^2 \cdot CF^-) \to \widehat{CF} \to 0.$$

We thus obtain a Bockstein morphism $\beta : \widehat{HF} \to \widehat{HF}$. Another way to characterize the kernel of the map $(\partial_1)_*$ is as the kernel of this Bockstein:

Lemma 4.2.15. *The Bockstein β satisfies $\beta = f \circ g = (\partial_1)_*$, where f and g are the maps from Lemma 4.2.13.*

Proof sketch. This also follows from a straightforward application of the snake lemma, and the definition of $f \circ g$. We leave the details to the reader. □

We end this subsection by making some general remarks about the bilinear pairing we have been considering, and its application to studying nonorientable 3-manifolds.

Remark 4.2.16. Suppose a connected orientable 3-manifold Y admits a fixed point free, orientation reversing involution τ. By the Lefschetz fixed point theorem,

$$\sum_{i\geq 0}(-1)^i tr(\tau_*|_{H_i(Y;\mathbb{Q})}) = 0$$

which becomes

$$1 - tr(\tau_*|_{H_1(Y;\mathbb{Q})}) + tr(\tau_*|_{H_2(Y;\mathbb{Q})}) + 1 = 0.$$

This indicates we won't find examples of orientation double covers which are rational homology 3-spheres.

We also note that nondegenerate, symmetric bilinear forms over $\mathbb{F}_2$ do not contain much information:

Lemma 4.2.17 ([35])**.** *Let $R(x,y) = xy$ be the trivial bilinear form of rank 1, and $H = \left(\begin{smallmatrix} 0 & 1 \\ 1 & 0 \end{smallmatrix}\right)$. Then any symmetric and nondegenerate bilinear form over $\mathbb{F}_2$ is isometric to one of:*

1. $H^{\oplus n}$
2. $R \oplus H^{\oplus n}$
3. $R \oplus R \oplus H^{\oplus n}$

Corollary 4.2.18. *Two odd, symmetric and nondegenerate forms over $\mathbb{F}_2$ are isometric if and only if they have the same rank. Two even, symmetric and nondegenerate forms over $\mathbb{F}_2$ are isometric if and only if they have the same rank.*

With these results in mind, we had hoped to characterize when the form $P_{\tau,\gamma}$ is even, however we have been unable at this stage to establish such a characterization.

4.3. The Pairing on the Chain Level

We now set out to describe how the pairing we have been investigating arises on the chain level. In this section we always work over $\mathbb{Z}$ unless otherwise stated.

First, we note that an orientation reversing diffeomorphism τ still gives rise to an induced map at the level of chain complexes, and over $\mathbb{Z}$:

Lemma 4.3.1. *Let Y be a closed, connected, oriented and based 3-manifold, and τ be an orientation reversing diffeomorphism on Y. Fix a strongly $\mathfrak{s}$-admissible diagram $\mathcal{H} = (\Sigma, \boldsymbol{\alpha}, \boldsymbol{\beta}, z)$ for (Y, z), and let $\tau(\mathcal{H}) = (\tau(\Sigma), \tau(\boldsymbol{\alpha}), \tau(\boldsymbol{\beta}), z' = \tau(z))$ be the induced diagram for $(-Y, z')$. Then for appropriate choices of almost complex structures there is a $\mathbb{Z}[U]$-module chain isomorphism:*

$$\tau_* : CF^-(\Sigma, \boldsymbol{\alpha}, \boldsymbol{\beta}, z, \mathfrak{s}) \to CF^-(\tau(\Sigma), \tau(\boldsymbol{\alpha}), \tau(\boldsymbol{\beta}), \tau(z), \tau(\mathfrak{s}))$$

The fact that diffeomorphisms induce such isomorphisms on the Heegaard Floer chain complexes with coefficients in either $\mathbb{F}_2$ or $\mathbb{Z}$ is straightforward; one simply pushes forward all intersection points, the complex structure choices, and holomorphic disks via the diffeomorphism restricted to the Heegaard surface. More details can be found in [3].

As before, we also have a chain isomorphism corresponding to reversing the orientation of a Heegaard diagram. However, this isomorphism mixes the invariants CF^- and CF^+.

Lemma 4.3.2 ([7, Proposition 2.5]). *Let $\mathcal{H} = (\Sigma, \boldsymbol{\alpha}, \boldsymbol{\beta}, z)$ be a strongly $\mathfrak{s}$-admissible diagram for (Y, z) and $-\mathcal{H} := (-\Sigma, \boldsymbol{\alpha}, \boldsymbol{\beta}, q)$ be the reversed diagram for $(-Y, z)$. Then there is a $\mathbb{Z}[U]$-module chain isomorphism*

$$\phi_{rev} : CF^-(\Sigma, \boldsymbol{\alpha}, \boldsymbol{\beta}, z, \mathfrak{s}) \to Hom_{\mathbb{Z}}(CF^+(-\Sigma, \boldsymbol{\alpha}, \boldsymbol{\beta}, z, \mathfrak{s}), \mathbb{Z})$$

.

As noted in [34], this isomorphism can also be interpreted as an unmixed duality on the invariant CF^- as follows:

Lemma 4.3.3 ([34, Lemma 2.3]). *Let $\mathcal{H} = (\Sigma, \boldsymbol{\alpha}, \boldsymbol{\beta}, z)$ be a strongly $\mathfrak{s}$-admissible diagram for (Y, z) and $-\mathcal{H} := (-\Sigma, \boldsymbol{\alpha}, \boldsymbol{\beta}, z)$ be the reversed diagram for $(-Y, z)$. Then there is a $\mathbb{Z}[U]$-module chain isomorphism:*

$$\phi_{rev} : CF^-(\Sigma, \boldsymbol{\alpha}, \boldsymbol{\beta}, z, \mathfrak{s}) \to Hom_{\mathbb{Z}[U]}(CF^-(-\Sigma, \boldsymbol{\alpha}, \boldsymbol{\beta}, z, \mathfrak{s}), \mathbb{Z}[U]).$$

Remark 4.3.4. The map

$$\phi_{rev}([\boldsymbol{x}, i]) \in \mathrm{Hom}_{\mathbb{Z}[U]}(CF^-(-\mathcal{H}), \mathbb{Z}[U])$$

in Lemma 4.3.3 is given explicitly by

$$\phi_{rev}([\boldsymbol{x},i])([\boldsymbol{y},k]) = \begin{cases} U^{-i-k-2} & \boldsymbol{x}=\boldsymbol{y} \\ 0 & \boldsymbol{x}\neq\boldsymbol{y}. \end{cases}$$

We note that $-i-k-2 \geq 0$, as CF^- is generated by $[\boldsymbol{x},i]$ with $i<0$.

Notation 4.3.5. We note that the map $\phi_{rev}([\boldsymbol{x},i])$ appearing in Lemma 4.3.3 is a $\mathbb{Z}[U]$-module map, so it is uniquely specified by its values on elements of the form $[\boldsymbol{y},-1]$. With this in mind, we will sometimes denote $\phi_{rev}([\boldsymbol{x},i])$ by $(\boldsymbol{x} \mapsto U^{-1-i})$ or by $\boldsymbol{x}^\vee$, abusing notation to indicate $\boldsymbol{x} := [\boldsymbol{x},-1]$.

We are now in position to introduce the invariant at the chain level, which will be defined with respect to the composition

$$\Psi := \phi_{\text{rev}} \circ \tau_* : CF^-(\Sigma,\boldsymbol{\alpha},\boldsymbol{\beta},z,\mathfrak{s}) \to \text{Hom}_{\mathbb{Z}[U]}(CF^-(-\tau(\Sigma),\tau(\boldsymbol{\alpha}),\tau(\boldsymbol{\beta}),\tau(z),\tau(\mathfrak{s})),\mathbb{Z}[U]).$$

We note that if the diffeomorphism τ preserves the oriented Heegaard surface Σ, this composition is a map

$$\Psi := \phi_{\text{rev}} \circ \tau_* : CF^-(\Sigma,\boldsymbol{\alpha},\boldsymbol{\beta},z,\mathfrak{s}) \to \text{Hom}_{\mathbb{Z}[U]}(CF^-(-\Sigma,\tau(\boldsymbol{\alpha}),\tau(\boldsymbol{\beta}),\tau(z),\tau(\mathfrak{s})),\mathbb{Z}[U]).$$

Definition 4.3.6. Let Y be a closed, connected, oriented and based 3-manifold, and τ be an orientation reversing diffeomorphism on Y. Fix a strongly $\mathfrak{s}$-admissible diagram $\mathcal{H} = (\Sigma,\boldsymbol{\alpha},\boldsymbol{\beta},z)$. We denote by

$$\langle , \rangle_\tau : CF^-(\Sigma,\boldsymbol{\alpha},\boldsymbol{\beta},z,\mathfrak{s}) \times CF^-(-\tau(\Sigma),\tau(\boldsymbol{\alpha}),\tau(\boldsymbol{\beta}),\tau(z),\tau(\mathfrak{s})) \to \mathbb{Z}[U]$$

the pairing defined by $\langle a, b\rangle_\tau = \Psi(a)[b]$.

Remark 4.3.7. The pairing in Definition 4.3.6 obviously depends on the diagrams (even the chain complexes do), however we often suppress this dependence unless it is explicitly needed. As we shall justify in what follows, this map will end up being independent of the diagrams chosen to represent it, up to an appropriate notion of homotopy.

Lemma 4.3.8. *$\langle , \rangle_\tau$ is $\mathbb{Z}[U]$-bilinear.*

Proof. Linearity in both factors follows from the definitions. For the first factor, ϕ_{rev} and τ_* are both chain isomorphisms of complexes of $\mathbb{Z}[U]$-modules, so their composition Ψ is $\mathbb{Z}[U]$-linear in its argument. For the second factor,

$$\phi_{rev} \circ \tau_*(a) \in \text{Hom}_{\mathbb{Z}[U]}(CF^-(-\tau(\Sigma), \tau(\boldsymbol{\alpha}), \tau(\boldsymbol{\beta}), z', \tau(\mathfrak{s}))), \mathbb{Z}[U])$$

for any $a \in CF^-(\Sigma, \boldsymbol{\alpha}, \boldsymbol{\beta}, z, \mathfrak{s})$, so $\phi_{rev} \circ \tau_*(a)$ is a $\mathbb{Z}[U]$-module map. □

Lemma 4.3.9. *Consider $\mathbb{Z}[U]$ as the chain complex with one copy of $\mathbb{Z}$ in every non-negative grading, and with differential $\delta = 0$. Then the map*

$$\langle , \rangle_\tau : CF^-(\Sigma, \boldsymbol{\alpha}, \boldsymbol{\beta}, z, \mathfrak{s}) \otimes_{\mathbb{Z}[U]} CF^-(-\tau(\Sigma), \tau(\boldsymbol{\alpha}), \tau(\boldsymbol{\beta}), \tau(z), \tau(\mathfrak{s})) \to \mathbb{Z}[U]$$

induced by the map given in Definition 4.3.6 is a chain map.

Proof. Let ∂ be the differential on $CF^-(\mathcal{H})$, ∂' be the differential on $CF^-(-\tau(\mathcal{H}))$, $(\partial')^\vee$ be the induced differential on $\text{Hom}_{\mathbb{Z}[U]}(CF^-(-\tau(\mathcal{H})), \mathbb{Z}[U])$, and $d = \partial \otimes \text{id} - \text{id} \otimes \partial'$ be the differential on $CF^-(\mathcal{H}) \otimes CF^-(-\tau(\mathcal{H}))$. As $\delta \circ \langle , \rangle_\tau = 0$, we need to show that $\langle , \rangle_\tau \circ d = 0$.

For $[\boldsymbol{x}, i] \otimes [\boldsymbol{y}, j] \in CF^-(\mathcal{H}) \otimes CF^-(-\tau(\mathcal{H}))$ we have:

$$\begin{aligned}
\langle , \rangle_\tau \circ d([\boldsymbol{x}, i] \otimes [\boldsymbol{y}, j]) &= \langle \partial[\boldsymbol{x}, i], [\boldsymbol{y}, j] \rangle_\tau - \langle [\boldsymbol{x}, i], \partial'[\boldsymbol{y}, j] \rangle_\tau \\
&= \Psi(\partial[\boldsymbol{x}, i])[\boldsymbol{y}, j] - \Psi([\boldsymbol{x}, i])[\partial'[\boldsymbol{y}, j]] \\
&= (\partial')^\vee \Psi([\boldsymbol{x}, i])[\boldsymbol{y}, j] - \Psi([\boldsymbol{x}, i])[\partial'[\boldsymbol{y}, j]] \\
&= \Psi([\boldsymbol{x}, i])[\partial'[\boldsymbol{y}, j]] - \Psi([\boldsymbol{x}, i])[\partial'[\boldsymbol{y}, j]] \\
&= 0
\end{aligned}$$

Here the third equality follows from the fact that $\Psi = \phi_{rev} \circ \tau_*$ is a chain map according to Lemmas 4.3.1 and 4.3.3. □

Notation 4.3.10. We will sometimes use the notation P_τ (P for pairing) to denote the map

$$\langle , \rangle_\tau : CF^-(\mathcal{H}) \otimes CF^-(-\tau(\mathcal{H})) \to \mathbb{Z}[U].$$

Theorem 4.3.11. *Let $\mathcal{H}$, $\widetilde{\mathcal{H}}$ be two Heegaard diagrams for the based 3-manifold (Y, z), and $-\tau(\mathcal{H})$, $-\tau(\widetilde{\mathcal{H}})$ be the diagrams for $(Y, \tau(z))$ obtained by reversing $\tau(\mathcal{H})$ and $\tau(\widetilde{\mathcal{H}})$. Then there is a chain homotopy equivalence of the form*

$$G = g_1 \otimes g_2 : CF^-(\mathcal{H}) \otimes CF^-(-\tau(\mathcal{H})) \to CF^-(\widetilde{\mathcal{H}}) \otimes CF^-(-\tau(\widetilde{\mathcal{H}}))$$

such that the diagram below commutes up to chain homotopy (up to an overall sign).

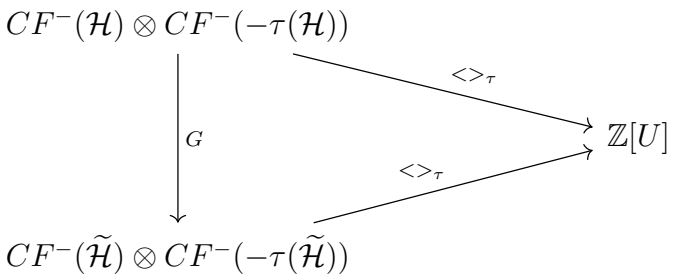

Before proving Theorem 4.3.11, we will establish the following fact about the map $\Psi = \phi_{\text{rev}} \circ \tau_*$.

Lemma 4.3.12. *Let $\mathcal{H} = (\Sigma, \boldsymbol{\alpha}, \boldsymbol{\beta}, z)$ and $\widetilde{\mathcal{H}} = (\widetilde{\Sigma}, \widetilde{\boldsymbol{\alpha}}, \widetilde{\boldsymbol{\beta}}, \widetilde{z})$ be two Heegaard diagrams representing the same 3-manifold. Fix a homotopy equivalence*

$$g : CF^-(\mathcal{H}) \to CF^-(\widetilde{\mathcal{H}})$$

fitting into the transitive system of [36, Corollary 1.5], and let

$$f : CF^-(\widetilde{\mathcal{H}}) \to CF^-(\mathcal{H})$$

be the homotopy inverse given by applying the same sequence of Heegaard moves in reverse. Let

$$\tau(g) : CF^-(\tau(\mathcal{H})) \to CF^-(\tau(\widetilde{\mathcal{H}}))$$

be the corresponding homotopy equivalence resulting from applying τ to the sequence of Heegaard moves defining g. Finally, let

$$\overline{\tau(f)} : CF^-(-\tau(\widetilde{\mathcal{H}})) \to CF^-(-\tau(\mathcal{H}))$$

be the homotopy equivalence resulting from the same sequence of Heegaard moves defining $\tau(f)$ applied to the reversed diagram. Then the diagram below commutes up to chain homotopy (up to an overall sign.)

$$\begin{array}{ccccc}
CF^-(\mathcal{H}) & \xrightarrow{\tau_*} & CF^-(\tau(\mathcal{H})) & \xrightarrow{\phi_{rev}} & Hom_{\mathbb{Z}[U]}(CF^-(-\tau(\mathcal{H})), \mathbb{Z}[U]) \\
\downarrow{\scriptstyle g} & & \downarrow{\scriptstyle \tau(g)} & & \downarrow{\scriptstyle \overline{\tau(f)}^{\vee}} \\
CF^-(\widetilde{\mathcal{H}}) & \xrightarrow{\tau_*} & CF^-(\tau(\widetilde{\mathcal{H}})) & \xrightarrow{\phi_{rev}} & Hom_{\mathbb{Z}[U]}(CF^-(-\tau(\widetilde{\mathcal{H}})), \mathbb{Z}[U])
\end{array}$$

Proof. The first square commutes up to an overall sign by the work in [3] (see [36] for the case of $\mathbb{Z}$ coefficients), where it is shown that the diffeomorphism maps commute with the homotopy equivalences induced by Heegaard moves.

For the second square, it will suffice to establish commutativity for the homotopy equivalences determined by each of the three types of Heegaard moves. We provide a proof for the case when g is a homotopy equivalence induced by a handleslide relating $\mathcal{H}$ and $\widetilde{\mathcal{H}}$, and leave the other moves as an exercise for the reader.

Suppose g is a homotopy equivalence induced by a handleslide relating $\mathcal{H} = (\Sigma, \boldsymbol{\alpha}, \boldsymbol{\beta}, z)$ and $\widetilde{\mathcal{H}} = (\Sigma, \boldsymbol{\alpha}, \boldsymbol{\gamma}, z)$. Then for $\boldsymbol{x} \in \mathbb{T}_{\boldsymbol{\alpha}} \cap \mathbb{T}_{\boldsymbol{\beta}}$, the homotopy

equivalence g will act on $[\boldsymbol{x}, i]$ by counting certain holomorphic triangles emanating from $\boldsymbol{x}$:

$$g([\boldsymbol{x}, i]) = \sum_{\boldsymbol{y} \in \mathbb{T}_{\boldsymbol{\alpha}} \cap \mathbb{T}_{\boldsymbol{\gamma}}} \sum_{\substack{\phi \in \pi_2(\boldsymbol{x}, \boldsymbol{\Theta}, \boldsymbol{y}) \\ \mu(\phi) = 0}} \#\mathcal{M}(\phi) \cdot [\boldsymbol{y}, i - n_z(\phi)].$$

We recall that $\boldsymbol{\Theta} \in \mathbb{T}_{\boldsymbol{\beta}} \cap \mathbb{T}_{\boldsymbol{\gamma}}$ is the unique (up to sign) generator in the diagram $(\Sigma, \boldsymbol{\beta}, \boldsymbol{\gamma}, z)$ with highest relative grading. In the cylindrical setting, the holomorphic triangles being counted in this sum are holomorphic maps $u : S \to \Sigma \times \Delta$ from Riemann surfaces satisfying certain boundary conditions and asymptotics near the corners of the triangle Δ (See [14]). A schematic of such a triangle, and the asymptotic and boundary conditions it must satisfy, is displayed on the left hand side of Figure 38.

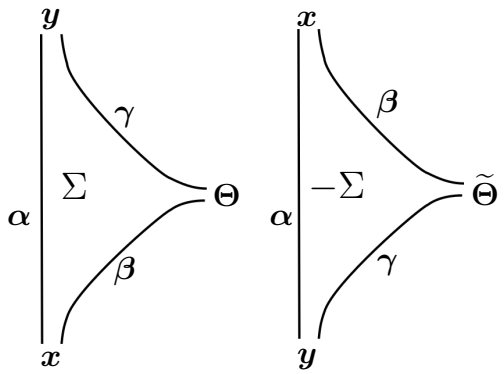

FIGURE 38 Schematics of holomorphic triangles. On the left is a triangle representing a class $\phi \in \pi_2(\boldsymbol{x}, \boldsymbol{\Theta}, \boldsymbol{y})$ on the diagram $(\Sigma, \boldsymbol{\alpha}, \boldsymbol{\beta}, \boldsymbol{\gamma})$ and on the right is a triangle representing a class $\widetilde{\phi} \in \pi_2(\boldsymbol{y}, \widetilde{\boldsymbol{\Theta}}, \boldsymbol{x})$ on the diagram $(-\Sigma, \boldsymbol{\alpha}, \boldsymbol{\gamma}, \boldsymbol{\beta})$.

On the other hand, the homotopy inverse $\overline{f}$ induced by the same handleslide viewed in reverse, and taking place on $-\Sigma$, takes the form

$$\overline{f}([\boldsymbol{y}, i]) = \sum_{\boldsymbol{x}} \sum_{\substack{\phi \in \pi_2(\boldsymbol{y}, \widetilde{\boldsymbol{\Theta}}, \boldsymbol{x}) \\ \mu(\phi) = 0}} \#\mathcal{M}(\phi) \cdot [\boldsymbol{x}, i - n_z(\phi)]$$

for $\boldsymbol{y}$ in $\mathbb{T}_{\boldsymbol{\alpha}} \cap \mathbb{T}_{\boldsymbol{\gamma}}$. The triangles being counted here are holomorphic maps $u : S \to -\Sigma \times \Delta$, with the role of the boundary conditions altered slightly. Again, see Figure 38 for a depiction of the situation. We note that a homotopy class $\phi \in \pi_2(\boldsymbol{x}, \boldsymbol{\Theta}, \boldsymbol{y})$ specifies a homotopy class $\widetilde{\phi} \in \pi_2(\boldsymbol{y}, \widetilde{\boldsymbol{\Theta}}, \boldsymbol{x})$ by vertical reflection, and note that in fact there is an identification of the moduli spaces $\mathcal{M}(\phi) \cong \mathcal{M}(\widetilde{\phi})$ for an appropriate choice of complex structure data. Indeed, given a fixed Riemann surface (S, j), an almost complex structure J on $\Sigma \times \Delta$ (satisfying the usual conditions, see e.g. [14]), and a J-holomorphic triangle $u : S \to \Sigma \times \Delta$ in the class ϕ, one can postcompose u with a vertical reflection of Δ to obtain a triangle $\widetilde{u}$ representing $\widetilde{\phi}$ which is $\widetilde{J}$-holomorphic, where $\widetilde{J} = \overline{J}$ is the conjugate structure to J. The identification of these two moduli spaces implies that if

$$g(\boldsymbol{x}) = \sum_{\boldsymbol{y}} n_{\boldsymbol{xy}} \cdot \boldsymbol{y}$$

then

$$\overline{f}(\boldsymbol{y}) = \sum_{\boldsymbol{x}} n_{\boldsymbol{xy}} \cdot \boldsymbol{x}.$$

But this in turn ensures that

$$\overline{f}^{\vee}(\boldsymbol{x}^{\vee}) = \sum_{\boldsymbol{y}} n_{\boldsymbol{xy}} \cdot \boldsymbol{y}^{\vee}.$$

Returning to the second square in the diagram in question, we thus have

$$\phi_{\text{rev}} \circ g(\sum_{\boldsymbol{x}} a_{\boldsymbol{x}} \cdot \boldsymbol{x}) = \sum_{\boldsymbol{x}} \sum_{\boldsymbol{y}} a_{\boldsymbol{x}} n_{\boldsymbol{xy}} \boldsymbol{y}^{\vee}$$

while

$$\overline{f}^{\vee} \circ \phi_{\text{rev}}(\sum_{\boldsymbol{x}} a_{\boldsymbol{x}} \cdot \boldsymbol{x}) = \sum_{\boldsymbol{x}} \sum_{\boldsymbol{y}} a_{\boldsymbol{x}} n_{\boldsymbol{xy}} \boldsymbol{y}^{\vee}.$$

This completes the proof.

□

With this result in hand, we proceed with the proof of the theorem.

Proof of Theorem 4.3.11. Let g, $\tau(g)$ and $\overline{\tau(g)}$ be homotopy equivalences as in Lemma 4.3.12. We will prove that the triangle in the theorem statement commutes up to homotopy with respect to the map $\mathrm{G} = g \otimes \overline{\tau(g)}$. We have

$$P_{\tau}(\boldsymbol{x} \otimes \boldsymbol{y}) = (\phi_{rev} \circ \tau_*)(\boldsymbol{x})[\boldsymbol{y}]$$

and

$$(\widetilde{P}_{\tau} \circ G)(\boldsymbol{x} \otimes \boldsymbol{y}) = (\phi_{\text{rev}} \circ \tau_* \circ g)(\boldsymbol{x})[\overline{\tau(g)}(\boldsymbol{y})].$$

By Lemma 4.3.12, we also know that

$$\phi_{rev} \circ \tau_* \circ g_1 \sim \overline{\tau(f)}^{\vee} \circ \phi_{rev} \circ \tau_*.$$

Thus $(\widetilde{P}_{\tau} \circ G)$ is homotopic to the map given by

$$(\overline{\tau(f)}^{\vee} \circ \phi_{\text{rev}} \circ \tau_*)(\boldsymbol{x})[\overline{\tau(g)}(\boldsymbol{y})] = (\phi_{\text{rev}} \circ \tau_*)(\boldsymbol{x})[(\overline{\tau(f)} \circ \overline{\tau(g)})(\boldsymbol{y})].$$

Since $\overline{\tau(f)}$ and $\overline{\tau(g)}$ are homotopy inverses, this map is homotopic to

$$(\phi_{rev} \circ \tau_*)(\boldsymbol{x})[\boldsymbol{y}] = P_\tau(\boldsymbol{x} \otimes \boldsymbol{y}),$$

as desired.

□

Properties

We collect here some properties of the chain map P_τ analogous to those discussed in the case of the pairing defined at the level of homology. Fix diagrams $\mathcal{H} = (\Sigma, \boldsymbol{\alpha}, \boldsymbol{\beta}, z)$ and $-\tau(\mathcal{H}) = (-\tau(\Sigma), \tau(\boldsymbol{\alpha}), \tau(\boldsymbol{\beta}), \tau(z))$ related by the orientation reversing diffeomorphism τ and reversal of the Heegaard surface as above.

We first investigate a notion of symmetry for the pairing.

Lemma 4.3.13.

$$P_\tau([\boldsymbol{x}, i] \otimes [\boldsymbol{y}, j]) = P_\tau([\tau(\boldsymbol{y}), j] \otimes [\tau(\boldsymbol{x}), i])$$

Proof. Note first that for $[\boldsymbol{x}, i] \in CF^-(\mathcal{H})$ and $[\boldsymbol{y}, j] \in CF^-(-\tau(\mathcal{H}))$, we have $[\tau(\boldsymbol{x}), i] \in CF^-(-\tau(\mathcal{H}))$ and $[\tau(\boldsymbol{y}), j] \in CF^-(\mathcal{H})$.

We compute

$$\begin{aligned} P_\tau([\boldsymbol{x}, i] \otimes [\boldsymbol{y}, j]) &= \phi_{rev} \circ \tau_*([\boldsymbol{x}, i])[\boldsymbol{y}, j] \\ &= \phi_{rev}([\tau(\boldsymbol{x}), i])[\boldsymbol{y}, j] \\ &= (\tau(\boldsymbol{x}) \mapsto U^{-i-1})[\boldsymbol{y}, j] \\ &= \begin{cases} 0 & \boldsymbol{y} \neq \tau(\boldsymbol{x}) \\ U^{-i-j-2} & \boldsymbol{y} = \tau(\boldsymbol{x}) \end{cases} \end{aligned}$$

and

$$\begin{aligned} P_\tau([\tau(\boldsymbol{y}), j] \otimes [\tau(\boldsymbol{x}), i]) &= \phi_{rev} \circ \tau_*([\tau(\boldsymbol{y}), j])[\tau(\boldsymbol{x}), i] \\ &= \phi_{rev}([\tau^2(\boldsymbol{y}), j])[\tau(\boldsymbol{x}), i] \\ &= (\boldsymbol{y} \mapsto U^{-j-1})[\tau(\boldsymbol{x}), i] \\ &= \begin{cases} 0 & \boldsymbol{y} \neq \tau(\boldsymbol{x}) \\ U^{-i-j-2} & \boldsymbol{y} = \tau(\boldsymbol{x}) \end{cases} \end{aligned}$$

where the second from last equality uses $\tau^2 = id$. □

Question 4.3.14. What notions of symmetry, even-ness, or other computable properties of the pairing are preserved by our notion of equivalence/homotopy?

We note that by Theorem 4.3.11, the chain maps given by

$$P_\tau : CF^-(\mathcal{H}) \otimes CF^-(-\tau(\mathcal{H})) \to \mathbb{Z}[U]$$

specify a well-defined chain homotopy class associated to a 3-manifold Y with an orientation reversing diffeomorphism. We thus obtain $P_\tau \in (CF^-(\mathcal{H}) \otimes CF^-(-\tau(\mathcal{H})))^\vee$ in the cochain complex. In fact, this is an element of the cohomology of the tensor chain complex:

Lemma 4.3.15. *$P_\tau \in H^*(CF^-(\mathcal{H}) \otimes CF^-(-\tau(\mathcal{H}))$ and the cohomology class is independent of the Heegaard diagram used to define P_τ.*

Proof. Let d be the differential on $CF^-(\mathcal{H}) \otimes CF^-(-\tau(\mathcal{H}))$. We have $d^\vee \circ P_\tau(a) = P_\tau \circ d(a)$ for all a. By 4.3.9, P_τ is zero on the image of d, hence P_τ is a cocycle. If P_τ and P'_τ are the pairings defined with respect to the same diffeomorphism, but with respect to different Heegaard diagrams $\mathcal{H}$ and $\widetilde{\mathcal{H}}$, they are chain homotopic when both are viewed as maps $CF^-(\mathcal{H}) \otimes CF^-(-\tau(\mathcal{H})) \to \mathbb{Z}[U]$, by Lemma 4.3.11. Thus $P_\tau - P'_\tau = K \circ d = d^\vee(K)$. Hence the two pairings define cohomologous cocyles in $(CF^-(\mathcal{H}) \otimes CF^-(-\tau(\mathcal{H}))^\vee$. □

Question 4.3.16. Can we characterize when $P_\tau \in H^*(CF^-(\mathcal{H}) \otimes CF^-(-\tau(\mathcal{H}))$ is nontrivial?

In [7] the authors describe a quasi-isomorphism

$$\Psi : (CF^-(\mathcal{H}) \otimes CF^-(-\tau(\mathcal{H}))^\vee \to CF^-(\mathcal{H}\# - \tau(\mathcal{H}))^\vee.$$

In fact, this map is further elucidated in [37, Proposition 5.2], where it is shown to be the map induced by a graph cobordism in the sense of [5]. The graph cobordism which induces this map has underlying 4-manifold given by the standard cobordism from $Y \coprod Y$ to $Y\#Y$, and is sketched in Figure 39 below.

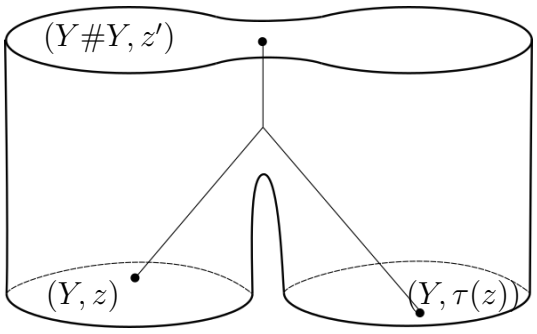

FIGURE 39 A graph cobordism from $Y \coprod Y$ to $Y\#Y$.

We therefore obtain $\Psi(P_\tau) \in CF^-(\mathcal{H}\#\tau(\mathcal{H})')^\vee$. At the level of homology, this yields a well defined element $\Psi(P_\tau) \in (HF^-)^*(\mathcal{H}\# - \tau(\mathcal{H}))$. We have yet to investigate this element of homology in depth, however we hope that it may prove useful in investigating our homotopical notion of equivalence, and in studying involutions on 3-manifolds.

4.4. Examples and Computations

In this section we examine the construction of the invariants we have defined in the context of specific examples of orientation reversing diffeomorphisms.

Example 4.4.1. We compute the form for the orientation double cover $\widetilde{M}$ of $M = S^1 \times \mathbb{R}P^2$. Consider the pointed Heegaard diagram $\mathcal{H} = (\Sigma, \boldsymbol{\alpha}, \boldsymbol{\beta}, z)$ we obtained for the orientation double cover $\widetilde{M}$ in Example 4.1.10. We reproduce this diagram in Figure 40.

Recall that the nontrivial deck translation τ of the orientation double cover $p : S^1 \times S^2 \to \mathbb{R}P^2$ acts on this Heegaard surface by a rotaton of π in

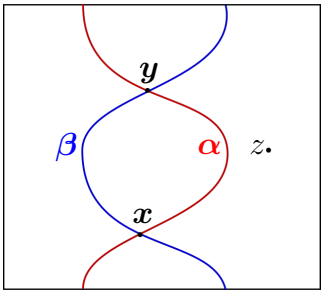

FIGURE 40 A pointed diagram for $S^1 \times S^2$.

the vertical direction. The Heegaard Floer chain complex is given by

$$CF^-(\mathcal{H}) = (\mathbb{Z}[U]\langle \boldsymbol{x}, \boldsymbol{y} \rangle, \partial)$$

with $\partial = 0$. Note that this diagram is equivariant, in the sense that $(\Sigma, \boldsymbol{\alpha}, \boldsymbol{\beta}) = (\tau(\Sigma), \tau(\boldsymbol{\beta}), \tau(\boldsymbol{\alpha}))$. Thus the Floer homology of the diagram $\tau(\mathcal{H})$ may be computed as:

$$CF^-(-\tau(\Sigma), \tau(\boldsymbol{\alpha}), \tau(\boldsymbol{\beta}), z') = CF^-(-\Sigma, \tau(\boldsymbol{\alpha}), \tau(\boldsymbol{\beta}), z') = CF^-(\Sigma, \boldsymbol{\alpha}, \boldsymbol{\beta}, z').$$

Thus the Heegaard Floer chain complex for the reversed diagram is given by

$$CF^-(-\tau(\mathcal{H})) = (\mathbb{Z}[U]\langle \boldsymbol{x}, \boldsymbol{y} \rangle, \partial)$$

where again $\partial = 0$. Note that

$$\langle \boldsymbol{x}, \boldsymbol{y} \rangle_\tau = \tau(\boldsymbol{x})^\vee(\boldsymbol{y}) = \boldsymbol{y}^\vee(\boldsymbol{y}) = 1,$$

and similarly

$$\langle \boldsymbol{y}, \boldsymbol{x} \rangle_\tau = 1,$$

while

$$\langle \boldsymbol{x}, \boldsymbol{x} \rangle_\tau = \langle \boldsymbol{y}, \boldsymbol{y} \rangle_\tau = 0.$$

The pairing is determined by these relations, and we see that with respect to the $\mathbb{Z}[U]$-basis $\{\boldsymbol{x}, \boldsymbol{y}\}$ for CF^-, it is given by $\left(\begin{smallmatrix} 0 & 1 \\ 1 & 0 \end{smallmatrix}\right)$. We remark that of course it is at this stage only the homotopy class (in the sense of Theorem 4.3.11) of this pairing

$$\langle , \rangle_\tau : CF^-(\mathcal{H}) \otimes CF^-(-\tau(\mathcal{H})) \to \mathbb{Z}[U]$$

which we know to be an invariant of the cover $(S^1 \times S^2, \tau)$.

Example 4.4.2. Fix any closed, connected, oriented, 3-manifold Y. Then we may form the connect sum $Y\# - Y$. This manifold comes equipped with an orientation reversing diffeomorphism τ which exchanges the two factors, regardless of whether or not Y admits an orientation reversing diffeomorphism. This diffeomorphism is not free, however we may still consider the bilinear pairing from Definition 4.3.6. In the following computations we fix the basepoint to lie in the connected sum region and to be τ-invariant, and suppress it from our notation.

To see the effect of the pairing, we consider the chain isomorphisms

$$\tau_* : CF^-(Y\# - Y) \to CF^-(-Y\#Y)$$

and

$$\phi_{\text{rev}} : CF^-(-Y\#Y) \to CF^-(Y\# - Y)^\vee.$$

The orientation reversing diffeomorphism τ acts on $Y\#-Y$ by swapping the factors, and with respect to the identification

$$CF^-(Y\#-Y) \cong CF^-(Y) \otimes_{\mathbb{Z}[U]} CF^-(-Y)$$

the two chain maps take the form

$$\tau_*(\boldsymbol{x} \otimes \boldsymbol{y}) = \boldsymbol{y} \otimes \boldsymbol{x}$$

and

$$\phi_{\mathrm{rev}}(\boldsymbol{y} \otimes \boldsymbol{x}) = (\boldsymbol{y} \otimes \boldsymbol{x})^\vee.$$

Thus according to Definition 4.3.6, we have

$$\langle \boldsymbol{x} \otimes \boldsymbol{y}, \boldsymbol{z} \otimes \boldsymbol{w} \rangle_\tau = (\boldsymbol{y} \otimes \boldsymbol{x})^\vee(\boldsymbol{z} \otimes \boldsymbol{w}) = \boldsymbol{y}^\vee(\boldsymbol{z}) \cdot \boldsymbol{x}^\vee(\boldsymbol{w}) \in \mathbb{Z}[U].$$

We note for the interested reader that we can rephrase this computation in terms of the trace maps

$$\mathbf{tr} : CF^-(Y) \otimes CF^-(-Y) \to \mathbb{Z}[U]$$

introduced in [34]. From the definition of the trace map, our computation above is equivalent to the statement

$$\langle \boldsymbol{x} \otimes \boldsymbol{y}, \boldsymbol{z} \otimes \boldsymbol{w} \rangle_\tau = \mathbf{tr}(\boldsymbol{x} \otimes \boldsymbol{w}) \cdot \mathbf{tr}(\boldsymbol{z} \otimes \boldsymbol{y}).$$

This is equivalent to the statement that the pairing is the map induced by the graph cobordism depicted in Figure 41 below.

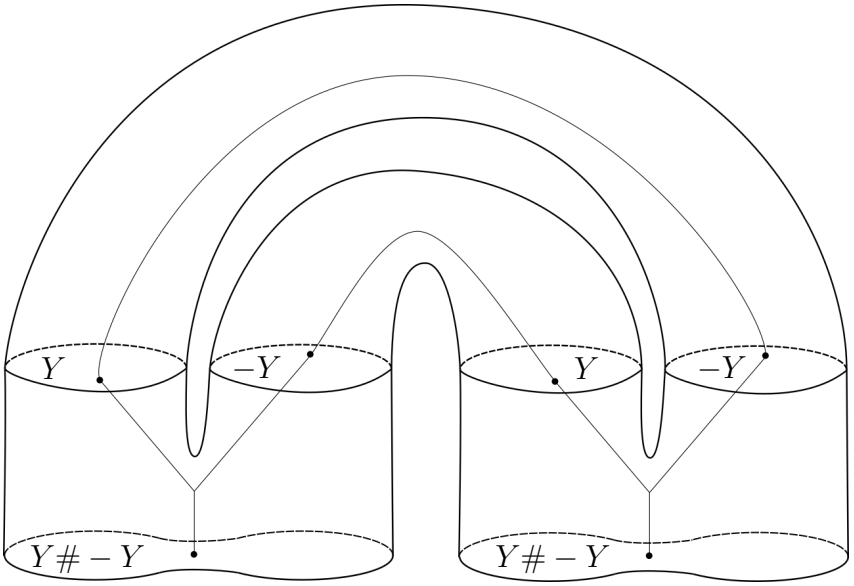

FIGURE 41 A null graph cobordism of $(Y\# - Y) \coprod (Y\# - Y)$.

Fix a $\mathbb{Z}[U]$-basis $\{\boldsymbol{x}_i\}$ for $CF^-(Y)$ coming from the intersection points in a fixed admissible Heegaard diagram. Then $\{\boldsymbol{x}_i\}$ also serves as a $\mathbb{Z}[U]$-basis for $CF^-(-Y)$ (since it corresponds to the intersection points in the reversed diagram). With respect to the basis on the tensor product obtained from these two bases, we have

$$\langle \boldsymbol{x}_i \otimes \boldsymbol{x}_j, \boldsymbol{x}_k \otimes \boldsymbol{x}_l \rangle_\tau = \begin{cases} 1 & \text{if } \boldsymbol{x}_i = \boldsymbol{x}_l \text{ and } \boldsymbol{x}_j = \boldsymbol{x}_k \\ 0 & \text{else.} \end{cases}$$

Thus if n is the $\mathbb{Z}[U]$ rank of $CF^-(Y)$, with respect to the basis $\{\boldsymbol{x}_i \otimes \boldsymbol{x}_j\}$ for $CF^-(Y) \otimes CF^-(-Y)$ the bilinear form can be expressed as a direct sum of an $n \times n$ identity block (where n is the rank of $CF^-(Y)$) coming from the

terms

$$\langle \boldsymbol{x}_i \otimes \boldsymbol{x}_i, \boldsymbol{x}_i \otimes \boldsymbol{x}_i \rangle_\tau = 1,$$

and $\binom{n}{2}$ blocks of the form $\left(\begin{smallmatrix} 0 & 1 \\ 1 & 0 \end{smallmatrix}\right)$ coming from the terms

$$\langle \boldsymbol{x}_i \otimes \boldsymbol{x}_j, \boldsymbol{x}_j \otimes \boldsymbol{x}_i \rangle_\tau = 1.$$

Summarizing, the bilinear form for $Y\# - Y$ with its obvious orientation reversing involution can be presented on a $\mathbb{Z}[U]$-basis by :

$$\langle , \rangle_\tau \cong (1)^{\oplus n} \oplus \left(\begin{smallmatrix} 0 & 1 \\ 1 & 0 \end{smallmatrix}\right)^{\oplus \binom{n}{2}}.$$

Since we suppressed the explicit dependence of the above computation on a choice of Heegaard data into one or two sentences, we now provide an actual example of the model computation given above to make this dependence more clear.

Example 4.4.3. Consider $(S^1 \times S^2)\#(-S^1 \times S^2)$ with the orientation reversing diffeomorphism τ switching the two factors. We consider the Heegaard diagram $\mathcal{H} = (\Sigma, \boldsymbol{\alpha}, \boldsymbol{\beta}, z)$ for $(S^1 \times S^2)\#(-S^1 \times S^2)$ in Figure 42 below, where the action of τ on the diagram is given by the reflection taking α_1 to α_2.

We fix the $\mathbb{Z}[U]$-basis for $CF^-(\mathcal{H})$ given by the intersection points labeled in the diagram: $\boldsymbol{a} = \{x_1, y_2\}$, $\boldsymbol{b} = \{x_1, x_2\}$, $\boldsymbol{c} = \{y_1, y_2\}$ and $\boldsymbol{d} = \{y_1, x_2\}$. We have

$$CF^-(\mathcal{H}) = (\mathbb{Z}[U]\langle \boldsymbol{a}, \boldsymbol{b}, \boldsymbol{c}, \boldsymbol{d} \rangle, \partial)$$

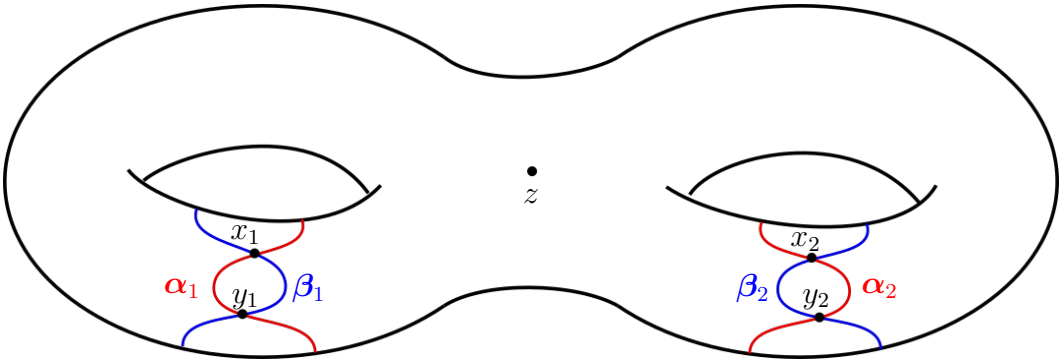

FIGURE 42 The pointed diagram $\mathcal{H}$ for $(S^1 \times S^2)\# - (S^1 \times S^2)$.

where the differential takes the form

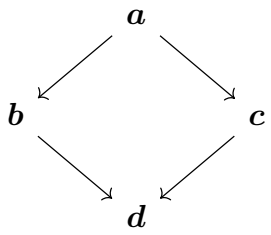

We note that the diagram $\mathcal{H}$ is actually the connect sum of the genus 1 diagram on the left with its reverse $-\mathcal{H}_1$: if $\mathcal{H}_1 = (\Sigma_1, \alpha_1, \beta_1, z)$ is the left diagram and $-\mathcal{H}_1 = (-\Sigma_1, \alpha_1, \beta_1, z)$ then $\mathcal{H} = \mathcal{H}_1\# - \mathcal{H}_1$. We have

$$CF^-(\mathcal{H}) = CF^-(\mathcal{H}_1) \otimes_{\mathbb{Z}[U]} CF^-(-\mathcal{H}_1).$$

where $CF^-(\mathcal{H}_1) = (\mathbb{Z}[U]\langle x_1, y_1\rangle, \partial x_1 = y_1)$. With respect to this identification, x_2 and y_2 are respectively just x_1 and y_1 in the second tensor factor, and we may rewrite

$$CF^-(\mathcal{H}) = (\mathbb{Z}[U]\langle x_1 \otimes x_1, x_1 \otimes y_1, y_1 \otimes x_1, y_1 \otimes y_1\rangle, \partial)$$

where the differential takes the form

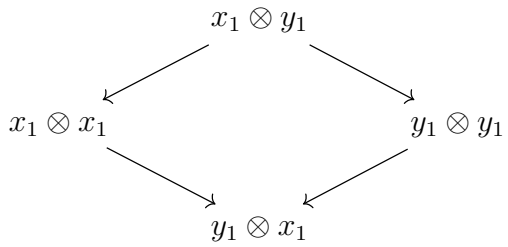

We now want to compute the action of the chain maps τ_* and ϕ_{rev}. Note that the diagram

$$\tau(\mathcal{H}) := (\tau(\Sigma), \tau(\boldsymbol{\alpha}), \tau(\boldsymbol{\beta}), \tau(z)) = (-\Sigma, \boldsymbol{\alpha}, \boldsymbol{\beta}, z)$$

is the diagram $-\mathcal{H}$. We thus have

$$\tau_* : CF^-(\mathcal{H}) \to CF^-(\tau(\mathcal{H})) = CF^-(-\mathcal{H}).$$

Any basis for $CF^-(\mathcal{H})$ is also a basis for $CF^-(-\mathcal{H})$, and with respect to the $\mathbb{Z}[U]$-basis

$$CF^-(\mathcal{H}) = (\mathbb{Z}[U]\langle x_1 \otimes x_1, x_1 \otimes y_1, y_1 \otimes x_1, y_1 \otimes y_1\rangle, \partial),$$

this map takes the form

$$\tau_*(a \otimes b) = b \otimes a.$$

Note that while $CF^-(\mathcal{H})$ and $CF^-(-\mathcal{H})$ share a basis, the relative gradings of elements in this basis are different in the two chain complexes; in particular, this remark should be considered to reconcile that the formula

for τ_* given above determines a chain isomorphism which preserves relative grading, as it must.

The chain map ϕ_{rev} has the straightforward effect:

$$\phi_{\text{rev}}(b \otimes a) = (b \otimes a)^{\vee}.$$

We thus see that

$$\langle x_1 \otimes x_1, x_1 \otimes x_1 \rangle_\tau = \langle y_1 \otimes y_1, y_1 \otimes y_1 \rangle_\tau = 1.$$

and

$$\langle x_1 \otimes y_1, y_1 \otimes x_1 \rangle_\tau = \langle y_1 \otimes x_1, x_1 \otimes y_1 \rangle_\tau = 1.$$

while all other pairings between basis elements are zero. Finally, all other possible pairings are determined by $\mathbb{Z}[U]$-bilinearity. We thus see that the pairing can be presented on a $\mathbb{Z}[U]$-basis by :

$$\langle , \rangle_\tau \cong (1)^{\oplus 2} \oplus \left(\begin{smallmatrix} 0 & 1 \\ 1 & 0 \end{smallmatrix}\right)$$

which agrees with the model computation from the previous example.

This concludes our exploration of orientation reversing diffeomorphisms viewed from the context of Heegaard Floer theory. We hope the investigations discussed in this chapter may prove useful in further study of orientation reversing involutions in this context, and on the study of orientation double covers in their own right.

REFERENCES CITED

[1] Peter Ozsváth and Zoltán Szabó. Holomorphic disks and topological invariants for closed three-manifolds. *Ann. of Math. (2)*, 159(3): 1027–1158, 2004. ISSN 0003-486X. doi: 10.4007/annals.2004.159.1027. URL https://doi.org/10.4007/annals.2004.159.1027.

[2] Peter Ozsváth and Zoltán Szabó. Holomorphic triangles and invariants for smooth four-manifolds. *Adv. Math.*, 202(2):326–400, 2006. ISSN 0001-8708. doi: 10.1016/j.aim.2005.03.014. URL https://doi.org/10.1016/j.aim.2005.03.014.

[3] András Juhász, Dylan P. Thurston, and Ian Zemke. Naturality and mapping class groups in heegaard floer homology, 2012. arXiv:1210.4996.

[4] Sucharit Sarkar. Moving basepoints and the induced automorphisms of link Floer homology. *Algebr. Geom. Topol.*, 15(5):2479–2515, 2015. ISSN 1472-2747. doi: 10.2140/agt.2015.15.2479. URL https://doi.org/10.2140/agt.2015.15.2479.

[5] I. Zemke. A graph tqft for hat heegaard floer homology, 2015. arXiv:1503.05846.

[6] Peter Ozsváth and Zoltán Szabó. Heegaard Floer homology and contact structures. *Duke Math. J.*, 129(1):39–61, 2005. ISSN 0012-7094. doi: 10.1215/S0012-7094-04-12912-4. URL https://doi.org/10.1215/S0012-7094-04-12912-4.

[7] Peter Ozsváth and Zoltán Szabó. Holomorphic disks and three-manifold invariants: properties and applications. *Ann. of Math. (2)*, 159(3): 1159–1245, 2004. ISSN 0003-486X. doi: 10.4007/annals.2004.159.1159. URL https://doi.org/10.4007/annals.2004.159.1159.

[8] James Singer. Three-dimensional manifolds and their Heegaard diagrams. *Trans. Amer. Math. Soc.*, 35(1):88–111, 1933. ISSN 0002-9947. doi: 10.2307/1989314. URL https://doi.org/10.2307/1989314.

[9] Martin Scharlemann and Abigail Thompson. Heegaard splittings of (surface) $\times$ I are standard. *Math. Ann.*, 295(3):549–564, 1993. ISSN 0025-5831. doi: 10.1007/BF01444902. URL https://doi.org/10.1007/BF01444902.

[10] Jesse Johnson. Notes on heegaard splittings. URL https://users.math.yale.edu/ jj327/notes.pdf.

[11] Kurt Reidemeister. Zur dreidimensionalen Topologie. *Abh. Math. Sem. Univ. Hamburg*, 9(1):189–194, 1933. ISSN 0025-5858. doi: 10.1007/BF02940644. URL https://doi.org/10.1007/BF02940644.

[12] Andreas Floer. Morse theory for Lagrangian intersections. *J. Differential Geom.*, 28(3):513–547, 1988. ISSN 0022-040X. URL http://projecteuclid.org/euclid.jdg/1214442477.

[13] Peter Ozsváth and Zoltán Szabó. An introduction to Heegaard Floer homology. In *Floer homology, gauge theory, and low-dimensional topology*, volume 5 of *Clay Math. Proc.*, pages 3–27. Amer. Math. Soc., Providence, RI, 2006.

[14] Robert Lipshitz. A cylindrical reformulation of Heegaard Floer homology. *Geom. Topol.*, 10:955–1096, 2006. ISSN 1465-3060. doi: 10.2140/gt.2006.10.955. URL https://doi.org/10.2140/gt.2006.10.955. Paging previously given as 955–1097.

[15] David Gabai. Foliations and the topology of 3-manifolds. *J. Differential Geom.*, 18(3):445–503, 1983. ISSN 0022-040X. URL http://projecteuclid.org/euclid.jdg/1214437784.

[16] Gregory Arone and Marja Kankaanrinta. On the functoriality of the blow-up construction. *Bull. Belg. Math. Soc. Simon Stevin*, 17(5): 821–832, 2010. ISSN 1370-1444. URL http://projecteuclid.org/euclid.bbms/1292334057.

[17] R. M. Vogt. Homotopy limits and colimits. *Proceedings of the International Symposium on Topology and its Applications (Budva, 1972)*, pages 235–241, 1973.

[18] Kristen Hendricks, Robert Lipshitz, and Sucharit Sarkar. A flexible construction of equivariant Floer homology and applications. *J. Topol.*, 9(4):1153–1236, 2016. ISSN 1753-8416. doi: 10.1112/jtopol/jtw022. URL https://doi-org.libproxy.uoregon.edu/10.1112/jtopol/jtw022.

[19] Mario J. Micallef and Brian White. The structure of branch points in minimal surfaces and in pseudoholomorphic curves. *Ann. of Math. (2)*, 141(1):35–85, 1995. ISSN 0003-486X. doi: 10.2307/2118627. URL https://doi-org.libproxy.uoregon.edu/10.2307/2118627.

[20] Dusa McDuff and Dietmar Salamon. *J-holomorphic curves and symplectic topology*, volume 52 of *American Mathematical Society Colloquium Publications*. American Mathematical Society, Providence, RI, second edition, 2012. ISBN 978-0-8218-8746-2.

[21] M. F. Atiyah. *K-theory*. Advanced Book Classics. Addison-Wesley Publishing Company, Advanced Book Program, Redwood City, CA, second edition, 1989. ISBN 0-201-09394-4. Notes by D. W. Anderson.

[22] John Milnor. On spaces having the homotopy type of a CW-complex. *Trans. Amer. Math. Soc.*, 90:272–280, 1959. ISSN 0002-9947. doi: 10.2307/1993204. URL https://doi.org/10.2307/1993204.

[23] Sucharit Sarkar. Maslov index formulas for Whitney n-gons. *J. Symplectic Geom.*, 9(2):251–270, 2011. ISSN 1527-5256. URL http://projecteuclid.org/euclid.jsg/1309546044.

[24] Robert Lipshitz, Peter S. Ozsvath, and Dylan P. Thurston. Bordered Heegaard Floer homology. *Mem. Amer. Math. Soc.*, 254(1216): viii+279, 2018. ISSN 0065-9266. doi: 10.1090/memo/1216. URL https://doi.org/10.1090/memo/1216.

[25] Peter Ozsváth and Zoltán Szabó. Holomorphic disks, link invariants and the multi-variable Alexander polynomial. *Algebr. Geom. Topol.*, 8(2): 615–692, 2008. ISSN 1472-2747. doi: 10.2140/agt.2008.8.615. URL https://doi.org/10.2140/agt.2008.8.615.

[26] Peter Ozsváth and Zoltán Szabó. Holomorphic triangle invariants and the topology of symplectic four-manifolds. *Duke Math. J.*, 121(1):1–34, 2004. ISSN 0012-7094. doi: 10.1215/S0012-7094-04-12111-6. URL https://doi-org.libproxy.uoregon.edu/10.1215/S0012-7094-04-12111-6.

[27] Stanislav Jabuka and Thomas E. Mark. Product formulae for Ozsváth-Szabó 4-manifold invariants. *Geom. Topol.*, 12(3):1557–1651, 2008. ISSN 1465-3060. doi: 10.2140/gt.2008.12.1557. URL https://doi-org.libproxy.uoregon.edu/10.2140/gt.2008.12.1557.

[28] Lawrence P. Roberts. Rational blow-downs in Heegaard-Floer homology. *Commun. Contemp. Math.*, 10(4):491–522, 2008. ISSN 0219-1997. doi: 10.1142/S0219199708002880. URL https://doi-org.libproxy.uoregon.edu/10.1142/S0219199708002880.

[29] Kristen Hendricks and Ciprian Manolescu. Involutive Heegaard Floer homology. *Duke Math. J.*, 166(7):1211–1299, 2017. ISSN 0012-7094. doi: 10.1215/00127094-3793141. URL https://doi.org/10.1215/00127094-3793141.

[30] J. Milnor. *Morse theory*. Based on lecture notes by M. Spivak and R. Wells. Annals of Mathematics Studies, No. 51. Princeton University Press, Princeton, N.J., 1963.

[31] J. H. Rubinstein. One-sided Heegaard splittings of 3-manifolds. *Pacific J. Math.*, 76(1):185–200, 1978. ISSN 0030-8730. URL http://projecteuclid.org/euclid.pjm/1102807036.

[32] John Milnor. *Lectures on the h-cobordism theorem*. Notes by L. Siebenmann and J. Sondow. Princeton University Press, Princeton, N.J., 1965.

[33] Stephen Halperin and Domingo Toledo. Stiefel-Whitney homology classes. *Ann. of Math. (2)*, 96:511–525, 1972. ISSN 0003-486X. doi: 10.2307/1970823. URL https://doi.org/10.2307/1970823.

[34] I. Zemke. Duality and mapping tori in heegaard floer homology, 2018. arXiv:1801.09270.

[35] A. Adrian Albert. Symmetric and alternate matrices in an arbitrary field. I. *Trans. Amer. Math. Soc.*, 43(3):386–436, 1938. ISSN 0002-9947. doi: 10.2307/1990068. URL https://doi.org/10.2307/1990068.

[36] Mike Gartner. Projective naturality in heegaard floer homology, 2019. arXiv:1908.06237.

[37] Kristen Hendricks, Ciprian Manolescu, and Ian Zemke. A connected sum formula for involutive Heegaard Floer homology. *Selecta Math. (N.S.)*, 24(2):1183–1245, 2018. ISSN 1022-1824. doi: 10.1007/s00029-017-0332-8. URL https://doi.org/10.1007/s00029-017-0332-8.